Western Washington University

Western CEDAR

Fall 2005

The Hydrogeology of North Lummi Island, Washington

William M. (William Martin) Sullivan
Western Washington University

Follow this and additional works at: https://cedar.wwu.edu/wwuet

Part of the Geology Commons

Recommended Citation

THE HYDROGEOLOGY OF NORTH LUMMI ISLAND, WASHINGTON

By

William M. Sullivan

Accepted in Partial Completion

of the Requirements for the Degree

Master of Science

Geology

_____

Moheb A. Ghali, Dean of Graduate School

Advisor Committee

_____

Dr. Robert Mitchell

_____

Dr. R. Scott Babcock
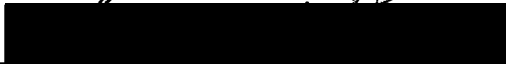
_____

Dr. Douglas Clark

_____

Mr. Douglas J. Kelly

MASTER'S THESIS
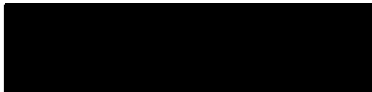
In presenting this thesis in partial fulfillment of the requirements for a master's degree at Western Washington University, I grant to Western Washington University the non-exclusive royalty-free right to archive, reproduce, distribute, and display the thesis in any and all forms, including electronic format, via any digital library mechanisms maintained by WWU.

I represent and warrant this is my original work, and does not infringe or violate any rights of others. I warrant that I have obtained written permissions from the owner of any third party copyrighted material included in these files.

I acknowledge that I retain ownership rights to the copyright of this work, including but not limited to the right to use all or part of this work in future works, such as articles or books.

Library users are granted permission for individual, research and non-commercial reproduction of this work for educational purposes only. Any further digital posting of this document requires specific permission from the author.

Any copying or publication of this thesis for commercial purposes, or for financial gain, is not allowed without my written permission.

William Sullivan
February 16, 2016

THE HYDROGEOLOGY OF NORTH LUMMI ISLAND, WASHINGTON

_____

A Thesis
Presented to the Faculty of
Western Washington University

_____

In Partial Fulfillment
of the Requirements for the Degree
Master of Science

_____

by

William M. Sullivan

October 2005

ABSTRACT

Lummi Island is a 10.8 square mile island in the northern Puget Sound Region, west of Bellingham, Washington. The population of Lummi Island has grown steadily for decades to approximately 900 permanent and 1,500 seasonal residents. The increasing demand for groundwater resources on the island has caused some wells to experience seasonal shortages and seawater intrusion, prompting an assessment of the hydrogeology for growth-management purposes. My study focused on characterizing the hydrogeology of the north half of the island (3.9 square miles) where most residents live and where groundwater is the sole source of potable water.

I examined data collected from up to 130 wells including well logs, seasonal water level measurements, water chemistry, and precise GPS well-head elevations and positions. From these data, I created a three-dimensional bedrock and unconsolidated stratigraphic model using Department of Defense Groundwater Modeling Software. A dramatically undulating bedrock surface is concealed nearly everywhere by mostly fine-grained unconsolidated Pleistocene deposits up to 300 feet thick. Bedrock in the study area is dominated by tightly-folded sandstone, shale, and conglomerate of the Tertiary Chuckanut Formation (sandstone) in the north. This is separated by a deep southeast-northwest trending trough from metamorphosed volcanics of the pre-Tertiary Fidalgo opiolite sequence (greenstone) in the south.

The stratigraphic model and potentiometric data were used to identify and define the extent, volume, and thickness of at least 12 distinct aquifers. The major aquifer is the Sandstone Aquifer, one of two separate bedrock aquifers that occupy the majority of the study area. Half of 130 wells examined are in sandstone and greenstone. Hydraulic properties including horizontal hydraulic conductivity, estimated from well log data, indicate the Sandstone Aquifer is in the upper range of textbook values for fractured sandstone. The Greenstone Aquifer is much smaller and has the lowest hydraulic properties of any in the study area. Seasonal water level fluctuations are greatest in the bedrock aquifers.

Ten Pleistocene aquifers were identified as thin, largely discontinuous coarse-grained (mostly sand) lenses within less permeable, fine-grained silt-clay diamicton. These aquifers fill depressions in the bedrock surface. Seven Pleistocene aquifers lie below sea level and three are perched well above sea level. The Legoe Bay and Nugent aquifers are the largest and most utilized Pleistocene groundwater source, occupying most of the southern half of the study area. These aquifers have the highest hydraulic properties and mostly negligible seasonal water level fluctuations.

Recharge areas identified through the stratigraphic model, potentiometric surfaces, and water chemistry occupy the inland and upper regions of the study area. Infiltration of water through overlying glacial drift into bedrock aquifers is the most important recharge mechanism because of their large areal extent and because many Pleistocene aquifers receive recharge, in part, from where they are in contact with saturated bedrock. The average recharge magnitude, estimated from a site-specific water-mass balance, is 8 inches/year or 24% of average annual precipitation. A chloride-mass balance, performed as a semi-independent estimate, establishes a lower bound for recharge of 4 inches/year or 11% of average annual precipitation.

Water-chemistry data vary among aquifer media. Water chemistry in the Sandstone Aquifer is dominated by sodium ions while most Pleistocene aquifers are dominated by calcium ions. Despite that nearly 80% of all wells that are completed below sea level, wide-spread seawater intrusion is not evident. Only 5 wells were determined to be intruded and, 14 additional wells may be experiencing some degree of intrusion. Occurrences of seawater intrusion are localized and are most common in the Sandstone Aquifer where low storage and fracture flow combine to increase contamination susceptibility.

ACKNOWLEDGEMENTS

Finally, I need to acknowledge the lifetime of love and support that I have received from my mom and dad, Linda and Bill. You are fundamentally responsible for every good thing that has come my way and I will do my best to pass-on the lessons in kindness. My entire family, including my brother, Jim and sister, Debbie and loved ones gained through my marriage to Kris, have been enthusiastic supporters of my endeavors. I will always be grateful to have you in my life.

TABLE OF CONTENTS

LIST OF FIGURES

LIST OF TABLES

LIST OF APPENDICES

1.0 INTRODUCTION

Lummi Island lies 6 miles west of Bellingham, in western Whatcom County, Washington. Situated in the southern end of the Strait of Georgia, it is part of the San Juan Archipelago and is closely related to other islands in the Puget Sound Region and the Gulf Islands of British Columbia in geology, climate, land cover, and human impact (Figure 1). Lummi Island is one of about 25 populated islands in the Puget Sound Region. Originally inhabited by Native Americans as a fishing base, the island was settled in the late 1800s and early 1900s for use in the timber, fishing, and agricultural industries. In recent decades, the scenery of Lummi Island has brought seasonal vacationers, retired persons, and working families looking for an alternative to the suburban lifestyle. A year-round ferry serves the present population of approximately 900 permanent and 1,500 seasonal residents.

Groundwater quantity on islands is limited by finite recharge from local precipitation. Aquifers in such settings can be depleted by increased use as a result of population growth. Increased development and demand on island groundwater resources can also cause the saline contamination of an aquifer, known as seawater intrusion (Washington State Department of Ecology, 1991). Despite these risks, many planning decisions have been made without a clear understanding of the potential effects of development on island groundwater resources. As a result, numerous island aquifers in the Puget Sound are at risk of water shortages, or the related effects of seawater intrusion. Of nearly 300 wells sampled throughout neighboring Island and San Juan Counties, 10-15% showed elevated chloride concentrations indicating the presence of seawater intrusion (Whiteman et al., 1983). A recent study on neighboring Guemes Island found that several near-shore wells were experiencing seawater intrusion (Kahle and Olsen, 1995) and a study on nearby Lopez Island showed that 46% of 185 well-water samples indicated seawater intrusion (Orr, 1997). Results of a seawater intrusion study in Island County, to the south, indicate nearly 10% of 379 samples taken from wells on Camano and Whidbey islands show definite signs of intrusion (Kelly, 2005). The elongated shape of Lummi Island places nearly all wells within ½ mile of the shoreline. Seawater intrusion has been identified on Lummi Island along the northeast shore south of Migley Point and in the

area east of Village Point (Walters, 1971; Dion and Sumioka, 1984). Chloride concentrations from 12% of 75 wells sampled during various studies over a seven-year period from 1984 to 1993 may also indicate seawater intrusion on north Lummi Island (Whatcom County, 1994).

There has been no comprehensive hydrogeologic study of Lummi Island so it remains unclear how much groundwater is available for future growth and development on the island. The effects of population growth on seawater intrusion are also poorly understood. As Lummi Island continues to develop, water resources will be a crucial in shaping the island's future. Understanding the groundwater resources of Lummi Island will allow the community to better manage future development.

In contrast to the north half of the island, most residents on the south half of Lummi Island obtain their domestic water from surface sources. Therefore, this study will focus on the north half of the island where the majority of the population lives. The term "Study Area" will refer to the north half of Lummi Island (Figure 1). To be consistent with other water resource studies in the region, elevations given in this study are in feet. Elevations are referenced to mean sea level (MSL) using North American Vertical Datum, 1988 (NAVD 88).

2.0 BACKGROUND

2.1 Geologic Setting

2.1.1 Bedrock Geology

The bedrock geology of Lummi Island is dominated by rocks of the Decatur terrane that consists of two terranes (Brandon et al., 1988; Garver, 1988) and the Tertiary Chuckanut Formation (Mclellan, 1927; Calkin, 1959; Easterbrook, 1971; Johnson, 1982; Carroll, 1980).   One of the Decatur terranes consists of rocks of mid-oceanic origin including ribbon chert, metagreywacke, and pillow basalts (Brandon et al., 1988; Burmester et al., 2000). The other is the Fidalgo ophiolite of island-arc origin (Brown, 1977; Brown et al., 1979; Gusey and Brown, 1989). The Fidalgo ophiolite terrane is structurally underlain by the oceanic terrane at Lummi Island (Blake, 2002). Rocks of the Decatur terrane are often referred to by locals and well drillers as greenstone. These rocks will be collectively referred to as greenstone throughout this study.

The north and south halves of Lummi Island are geologically different and are separated by an east-west trending normal fault that roughly parallels the southern boundary of the study area (Figure 1) and dips ~60° to the north (Blake, 2002). The south half of the island lies in the footwall of this fault. The exposed bedrock topography of the south half of Lummi Island is steep with a maximum elevation of 1692 feet. The south half of the island is primarily composed of Jurassic oceanic sediments of the Decatur terrane (Brandon et al., 1988; Garver, 1988).   On south Lummi Island, these rocks are metamorphosed sandstone, siltstone, and greywacke (Easterbrook, 1971; Carroll, 1980; Blake, 2002).

The north half of Lummi Island comprises 3.87 square miles of relatively gentle topography reflecting undulating bedrock draped with a mantle of unconsolidated glacial drift. Maximum elevation is 362 feet. The bedrock geology of the north half of the study area (northern quarter of Lummi Island) is primarily composed of the Padden Member of the Tertiary Chuckanut Formation (McClellan, 1927; Johnson, 1982; Lapen, 2000). The

3

Padden Member is the youngest in the Chuckanut Formation, deposited during a colder climate than the previous members (Johnson, 1982). The Padden Member is cross-bedded arkosic sandstone with thin interbeds of mudstone, shale, and cemented conglomerate within coal beds that originated as alluvial floodplain deposits (Easterbrook, 1971). In the study area, these rocks are slightly metamorphosed (Caulkin, 1959; Carroll, 1980). The thickness of the Chuckanut Formation on Lummi Island is estimated to be ~330 feet (Carroll, 1980). Preliminary examinations of well-log data indicate that this member is well fractured in most locations and is the predominant bedrock unit underlying the glacial drift mantle. The Chuckanut Formation of northern Lummi Island has few faults, veins, and cleavages (Carroll, 1980). Exposures of the Chuckanut Formation are common throughout the north half of the study area (Easterbrook, 1971, Lapen, 2000), with resistant conglomerate forming almost half of the outcrops, especially the steeper and topographically higher regions (Caulkin, 1959). No shale facies are known to outcrop on north Lummi Island (Caulkin, 1959) but preliminary examinations of well log data indicate the presence of shale within the Chuckanut Formation at various locations throughout the study area.

Fidalgo ophiolite crops out in the south half of the study area (Lapen, 2000; Blake, 2002). The Fidalgo ophiolite on Lummi Island consists of metamorphosed volcanics including basalts, pillow basalts, gabbro and diorite (Caulkin, 1959; Easterbrook, 1971; Carroll, 1980; Blake, 2002). Small exposures of basalts and overlying sediments, including a basal conglomerate that is about 3 feet thick, occur at Lovers Bluff in the middle of the study area and along the northeastern shoreline from Migley Point to just north of Lummi Point, also known as Lane Spit (Figure 1). These rocks unconformably underlie Chuckanut sandstone to form the upper unit of the Fidalgo ophiolite sequence on Lummi Island (Caulkin, 1959; Carroll, 1980; Blake, 2002), and are possibly underlain by an intrusive gabbro and diorite sequence of the Fidalgo ophiolite dated at 160 Ma (Blake, 2002). Rocks of the Fidalgo ophiolite are inferred to underlie all of northern Lummi Island (Carroll, 1980). Two outcrops of the gabbro and diorite unit exist at the south end of the study area. Small exposures of pillow basalts and chert occur in the southeast corner of the study area (Blake, 2002).

In the north half of the study area, several tightly-folded, northwest plunging (up to 50°) anticline/syncline pairs have generally sub-parallel axes and steeper southern limbs that produce bedding dips in the Chuckanut formation in excess of 80° (Caulkin, 1959; Carroll, 1980). Underlying rocks of the Fidalgo Ophiolite may have been folded as a unit with the Chuckanut as reflected in Fidalgo rocks that outcrop at Lover's Bluff and near Migley Point (Caulkin, 1959).

2.1.2 Pleistocene Geology

2.1.2.1 Glacial Drift

Unconsolidated sediments deposited during the continental Fraser Glaciation are common throughout western Whatcom County and the San Juan Islands (Easterbrook, 1971; Dethier et al., 1996; Dragovich et al., 2002).   During the Fraser Glaciation, the Puget lobe of the Cordilleran ice sheet advanced and retreated through the Puget Sound lowland. This massive glaciation resulted in land surface depression. Subsequent land surface rebound and rising sea levels caused by warmer global temperatures combined to produce complex changes in relative sea level and patterns of sedimentation that are reflected in the local geology.

The Fraser Glaciation is divided into the Vashon Stade, Everson Interstade, and Sumas Stade (Armstrong et al., 1965).   The weight of the ice sheet, estimated at up to 6000 feet thick in the vicinity of Whatcom County, caused crustal depression of the land surface during the Vashon Stade 13-18 thousand years ago (ka) (Easterbrook, 1971; Kovanen and Easterbrook, 2001). Sediment deposited ahead of the advancing ice sheet formed broad plains of advance outwash on a grade below present day sea level (Easterbrook, 1971; Dethier et al., 1996). Till deposited during the Vashon Stade (Vashon till) underlies most of the lowland in western Whatcom County and comprises most of the sediment exposed in the San Juan Islands (Easterbrook, 1971; Pessl, 1988; Easterbrook, 1992; Kovanen and

Easterbrook, 2001; Dethier et al., 1996). Striations and grooves in bedrock indicate that basal ice at Lummi Island flowed southwesterly over the north half and southeasterly over the south half of the island (Caulkin, 1959).

Most of the sediment exposed in western Whatcom County was deposited during the Everson Interstade (Easterbrook, 1971; Lapen, 2000). The Everson Interstade (11.3-13.6 ka); (Dethier et al., 1995) marks a period of warming. As the ice sheet retreated north, it thinned allowing seawater to invade depressed topography of the Puget lowland creating a shallow sea that covered most of western Whatcom County and the San Juan Islands. Sediment laden ice in contact with seawater rapidly melted, depositing massive volumes of glaciomarine drift on the floor of a shallow sea (Easterbrook, 1962; Armstrong et al., 1965). These deposits range from well-sorted sands, gravels, silts, and clays to diamictic combinations of silt, clay, sand, gravel, and boulders (Easterbrook, 1971; Dethier et al., 1996; Lapen, 2000). With the weight of the ice sheet removed, isostatic rebound subsequently caused the land surface to rise to its present elevation. As relative sea level decreased, wave action reworked glaciomarine drift forming coarse-grained emergence beach deposits.

2.1.2.2 Published Interpretations of Regional Glacial Drift Geology

Different interpretations exist for the depositional environments during the Everson Interstade. Two interpretations are described below.

Interpretation A. In western Whatcom County, deposits related to the Everson Insterstade have been divided into three units: Kulshan and younger Bellingham glaciomarine drift, separated by an intermediate terrestrial fluvial unit, the Deming Sand (Armstrong et al., 1965; Easterbrook, 1963, 1966b; Easterbrook, 1971). In this interpretation, the Kulshan Glaciomarine Drift (15-25 ft thick) formed early in the Everson Interstade from melting ice in contact with seawater of a shallow sea.

6

Widespread deposition of unsorted fine-grained material and localized, discontinuous lenses of sand and gravel occurred where sediments within the floating ice sheet and icebergs melted out and fell to the sea floor as diamictic glaciomarine drift. Following isostatic rebound, the Deming Sand (thickness about 30 ft) unit was deposited over a broad area, in a terrestrial fluvial environment extending from the Cascade foothills west to about Bellingham Bay, approximately six miles east of Lummi Island. Late in the Everson Interstade, a second marine deposition occurred, dominated by clean clays comprising the overlying Bellingham Glaciomarine Drift (maximum thickness 70 ft). The maximum combined thickness of the fine-grained Kulshan and Bellingham glaciomarine drift package is 95 ft (Easterbrook, 1971). When combined with underlying Vashon till, maximum thickness of the fine-grained package is 125 feet.

Interpretation B. A recent interpretation is that one episode of crustal depression and rebound is responsible for the coeval deposition of the diamictic glaciomarine drift, clean clays, and lenses of sand and gravel (Dethier et al., 1995; Dethier et al., 1996; Dragovich and Grisamer, 1998; Dragovich et al., 1998, 1999; Lapen, 2000). The glaciomarine drift is largely interpreted as a single unit having subunits that vary in texture corresponding to Bellingham and Kulshan glaciomarine drift units of Interpretation A, respectively.

These authors believe the outwash units were deposited as submarine and local terrestrial outwashes, deltas, and turbidites that underlie and are interbedded with glaciomarine drift. This interpretation suggests that the glaciomarine drift and coarse interbed package are as thick as 295 feet. To support the argument for a single rebound event, Dragovich et al. (1998) note that the texture of the single glaciomarine drift unit generally fines-upward. Coarse recessional marine outwash grades into a diamictic glaciomarine drift subunit that is overlain by a clay glaciomarine drift subunit. According to Dragovich et al. (1998) this trend reflects the northward retreat of the ice sediment source. Thicker sequences of glaciomarine drift and some localized interbeds of coarse sediments within the glaciomarine drift are explained as resulting from localized regions of stagnant or slowly retreating ice. The authors believe that large remnant blocks of ice became stranded on bedrock highlands such as San Juan Island and Anderson Mountain in the

Alger 7.5 minute quadrangle (Dethier et al., 1996; Dragovich and Grisamer, 1998; Dragovich et al., 1998, 1999). These stranded ice blocks acted as a sediment source after the main ice sheet had retreated north, creating locally thicker sequences of marine and terrestrial outwash, up to 230 feet thick, especially near the foothills of the Cascade Mountains. The authors do not believe a single fluvial coarse-grained sand unit, such as Deming Sand, was deposited over most of western Whatcom County and describe coarse-grained interbeds within glaciomarine drift as marine outwash units.

Interpretations A and B. Both interpretations describe widespread emergence beach deposits. The maximum elevation at which Everson Interstade marine deposits have been reported (marine limit) is about 300 feet in the western San Juan Islands (Dethier et al, 1996) and up to 400-600 feet in western Whatcom County (Easterbrook, 1963, 1971; Dethier et al., 1995). Estimates for rates of rebound and changes in relative sea level vary by location, age, and author. In northern Skagit County, southeast of Lummi Island, rebound was significant from 13.5-9 ka, slowing by 11 ka, and giving way to slow submergence as global temperatures warmed and sea level rose achieving the present day sea level at about 8 ka (Dragovich et al., 1998). In the western San Juan Islands, the rate of rebound is estimated at 0.4ft/yr from 13.1-12.5 ka and relative sea level is estimated to have risen by 150 feet over the past 10,000 years (Dethier et al., 1996). One of the goals of my study has been to determine which interpretation of the glacial drift geology best fits the north Lummi Island study area.

2.1.2.3 Glacial Drift Unit Descriptions

The following units are described in various studies of the regional geology and may occur on or below the surface of Lummi Island. With the exception of marine outwash, all units are described in both published interpretations of regional glacial drift geology.

Emergence Beach Deposits. Emergence beach deposits were formed during the Everson Interstade as waves reworked glacial drift, commonly glaciomarine drift, resulting from changes in relative sea level. The sediments are well-sorted, loose sand and sub-rounded to rounded gravel, fine to medium sand with local boulders. Bedding is massive, laminated, or cross-stratified. Deposits usually grade into organic-rich eolian deposits and commonly fill channels in underlying glaciomarine drift. Thickness is from 1-27 feet. These deposits are generally occur at elevations below 200 feet, form terraces, and are often characterized on air photos as linear features (strandlines) that parallel contours. Many outcrops of glaciomarine drift and till are overlain by at least a thin veneer of emergence deposits in the vicinity of Alger 7.5 minute quadrangle, northern Skagit County (Dragovich et al., 1998). This description is from information in Easterbrook (1971); Dethier et al. (1996); Lapen (2000). Lapen (2000) mapped emergence beach deposits on north Lummi Island.

Marine Outwash. In the northern Puget Sound Region, marine outwash sediments were deposited during the Everson Interstade from ice-proximal processes near the terminus of the retreating ice sheet. They consist of outwash, deltaic, turbidite, and alluvial fan deposits and may be interbedded with glaciomarine drift. The sediments are loose, moderately well-sorted to well-sorted, sub-angular to sub-rounded gravelly sand, sandy gravel, and sand with minor interbeds of silt. Grain size generally fines upward and grades into glaciomarine drift. Marine outwash is distinguished from emergence beach deposits by sub-angular to locally angular clasts. Bedding is well-developed and crossbeds are common. Color is brown to gray. Thickness can be as much as 230 feet locally. Deposits occur at elevations below the marine limit. Marine outwash lies beneath marine diamicton units in the western San Juan Islands. Marine outwash is only described in Interpretation B. This description is from information in Dethier et al. (1996), Dragovich et al. (1998), and Lapen (2000).

Glaciomarine Drift. Glaciomarine drift is moderately to poorly indurated till-like deposits formed during the Everson Insterstade as sediment fell out of the retreating ice sheet that was in contact with the waters of a shallow sea.   These sediments are moderately sorted to unsorted diamicton with dropstones and discontinuous lenses of moderately to well-sorted gravel, sand, silt, and clay. Grain size generally fines-up. Bedding is unstratified to poorly-stratified. Color is blue-gray to light olive-gray to gray or brown. These deposits are fossiliferous.   This description is from information in Easterbrook (1971), Dethier et al. (1996), and Lapen (2000). The reported thickness of glaciomarine drift varies by author. Authors of Interpretation A describe two distinct units, Kulshan glaciomarine drift (15-25 feet thick) and Bellingham glaciomarine drift (up to 70 feet thick) often separated by Deming Sand (30 feet thick) in western Whatcom County.   Authors of Interpretation B describe a single unit of glaciomarine drift divided into diamicton and clay subunits with a combined thickness of up to 295 feet in the Alger 7.5 minute quadrangle. Glaciomarine drift drapes topography and mantles bedrock and more commonly till to an elevation of 200 feet in the western San Juans (Dethier et al., 1996) and possibly up to 600 feet in western Whatcom County (Easterbrook, 1971). Glaciomarine drift may locally include units of till, emergence beach deposits, and marine outwash (Lapen, 2000).

Till. Ice-contact till deposits were formed during the Vashon Stade.   Vashon till is dense and unsorted diamicton of clay, silt, sand, and gravel with scattered cobbles and boulders with few lenses of sand and gravel. Bedding is massive and unstratified. Color is dark yellowish brown to brownish gray where oxidized and gray where unoxidized. Thickness ranges from 10-30 feet. This description is from information in Easterbrook (1971), Dethier et al. (1996), and Lapen (2000). Till drapes topography and overlies bedrock and older glacial deposits such as Vashon advance outwash and occurs in the subsurface beneath most of the lowland of western Whatcom County (Easterbrook, 1971; Lapen, 2000) and beneath glaciomarine drift and soil in most areas in the San Juan Islands that lie below the marine limit of 300 feet (Dethier et al., 1996). Till can be difficult to differentiate by density only from dried clay of glaciomarine drift deposits (Lapen, 2000).

Advance Outwash. Advance outwash sediments were deposited ahead of the advancing ice sheet across a broad plain during the Vashon Stade. Vashon advance outwash is moderately indurated and cemented as a result of over-compaction caused by the weight of the overriding ice sheet. Texture is moderately to well-sorted sandy gravel, pebbly sand, medium to coarse with general upward-coarsening from silt and clay with dropstones at its base to coarse sands and gravels in the upper regions.   Bedding is crossbedded with common cut and fill structures. Color is gray to pale yellowish brown. Thickness ranges from 10 to 265 feet.   This description is from information in Easterbrook (1971), Dethier et al. (1996), Dragovich et al. (1998), and Lapen (2000). Exposures of advance outwash are uncommon in western Whatcom County (Lapen, 2000).

Cherry Point Silt.   Cherry Point silt is a fluvial sediment deposited during the Olympia Non-Glacial Interval when the ice sheet terminus was located north of the Canadian border. Texture is dominated by silt and clay with minor lenses of sand and dropstones. Bedding is laminated. Color is blue-brownish gray. Thickness is up to 140-300 feet. Cherry Point silt is fossiliferous and dated at 38 ka (Easterbrook, 1973), prior to the Fraser glaciation. This description is from information in Easterbrook, 1962, 1963, 1971. Exposures of Cherry Point silt occur near sea level on Lummi Peninsula 1-2 miles northeast of the study area (Easterbrook, 1962).

2.2 Soils

Soils affect evapotranspiration, runoff, and infiltration. They also play an important role in groundwater chemistry. Soils in the study area were mapped and classified by the United States Soil Conservation Service (currently Natural Resource Conservation Service), (1980; Figure 2 and Table 1). The dominant soil in the study area is Kickerville siltloam that covers 39% of the study area (Table 1). This Spodosol is moderately thick (3.3 ft) and has an infiltration capacity in its upper horizon of 1.3 in/hr (Soil Conservation Service, 1980). Fifteen other soils make up the remaining soil cover mapped by Soil

Conservation Service and all have nearly the same infiltration capacity in the upper horizon as Kickerville siltloam. Infiltration capacities for all soils in the study area range from .95 to 1.3 in/hr. There are some places in the study area where the soil depth is shallow or bedrock is exposed. Soils data from the Whatcom County Area Soil Survey (Soil Conservation Service, 1980) do not account for this discrepancy.

2.3 Land Cover

Land cover affects evapotranspiration and runoff. Land cover data for north Lummi Island is from Landsat 4 (Figure 3 and Table 2). Slightly more than 50% of land cover in the study area is forest classified as deciduous, coniferous, and mixed deciduous-coniferous. Deciduous trees are primarily red alder with lesser bigleaf maple. Coniferous trees are mostly douglas fir and western hemlock. Western red cedar also occurs. The dominant non-forest land cover is grass that occupies 36% of the study area. Urban area consisting of asphalt, concrete, and buildings comprise less than 1% of the study area. Notably, areas designated as rock equal less than 0.1% of the study area despite several outcrops noted in geologic maps (for example Easterbrook, 1971; Carroll, 1980) and field observations.

2.4 Climate

Lummi Island has a maritime climate characterized by mild temperatures and abundant precipitation. There are no official weather stations on Lummi Island and the closest is a National Weather Service station 8 miles to the northeast at Bellingham International Airport. However, three unofficial precipitation collection stations have been continuously monitored by Lummi Island volunteers for up to 19 years (Figure 1). These stations are 1.5 miles apart. The difference in annual precipitation between these stations is slightly more than 1 inch per year over a 12-year period. Average precipitation at these stations is 33.5 inches (standard deviation of 4.7, over 18 years) for West Shore gauge, 32.5 inches (standard deviation of 4.6, over 12 years) for Tuttle gage, and 33.7 inches (standard deviation of 4.9, over 12 years) Nugent gauge (Marshall et al., written communication, 2004). The vast majority of precipitation is rain. An arithmetic average of these three gauges is 33.2 inches, hereafter referred to as average annual precipitation

for north Lummi Island. This method was chosen because of the relatively flat topography and even spacing of these stations.   For comparison, average annual precipitation over a 55-year period at Bellingham International Airport is 35.4 inches (National Climatic Data Center).

2.5 Hydrologic Features

The north half of Lummi Island has no perennial streams (Figure 4). A stream discharge monitoring study during Water Years (WY) 2003 and 2004 identified and measured discharge from 11 small streams in the study area (Nielson and Armfield, written communication; see Section 5.7.2.1). Two additional streams were identified by Nielson and Armfield, but were not monitored. Most streams stopped flowing or flow became negligible in spring with most showing no flow in April through October of both years. Streams draining larger basins exhibited greater discharge volumes and flowed into early summer during WY 2004. By July, discharge from all streams stopped, or became negligible and remained dry through the summer months. Flow resumed in most streams following the onset of rain in October and November. This pattern demonstrates that there is no there is no sustained baseflow from aquifers to study area streams. Storage of shallow groundwater in soils could explain why some of the larger basins continue to flow through June.

There are no lakes in the study area, although several ponds and wetlands occur. Most ponds are man-made. The largest pond is located in the southeast corner of the study area and feeds a stream that flows along the southern boundary of the study area (Figure 4). According to locals, at least three wetlands have been enhanced by island residents during the early to mid-1900s. The slough that parallels Legoe Bay Rd and discharges into Legoe Bay was created to direct water from uphill sources away from fishery operations and homes along Legoe Bay. Two ponds on the landward side of Legoe Bay Rd. filled with water following gravel mining operations. The wetland northeast of the intersection of South Nugent and Sunrise roads was impounded by a weir that has since been breached, lowering the water level of the swamp. The southern portion of the swamp near Richards Mountain has been excavated to retain surface water through the

summer months. Early in the last century, workers excavated a pit just to south of the western extension of Blizzard Rd. to exploit the shallow groundwater table at this location. Water from this "spring" was piped to Village Point to support the operation of a large cannery.

2.6 Hydrogeologic Setting

This study is limited to the north half of Lummi Island (Figure 1) because the steep exposed bedrock of the south half of Lummi Island does not support significant groundwater resources. Consequently, residents on the south half use surface water for domestic use. The south and north halves of Lummi Island are also likely hydrologically separated by a west-to-east flowing stream that comprises the southern boundary of the study area (Figure 4).   I assume this stream acts as a discharge zone for surface water and some groundwater between the south and north halves of the island. The primary hydrogeologic units in the study area are the Chuckanut sandstone and glacial drift. Preliminary examination of over 90 well logs in the study area indicate that virtually all wells are completed in these two units.

A simplified conceptual model of island hydrogeology shows head distribution and flow direction in a homogeneous unconfined aquifer (Figure 5). Recharge to most island aquifers is from precipitation. Recharge to island aquifers creates a pressure distribution that typically causes hydraulic head to be highest in the middle of the island and lowest near the shoreline. Fresh groundwater in an island usually forms a lens that lies above denser saline groundwater. This lens is thickest in the middle region of the island and thinnest near the shoreline. Groundwater flow direction is typically downward in recharge areas and upward in discharge areas. Under natural conditions, the interface between freshwater and saline groundwater dips at a steep angle beneath an island. In map view, groundwater in homogeneous and isotropic media tends to flow in a radial pattern from the middle of an island.

14

<u>2.6.1 Bedrock</u>

Chuckanut sandstone. Wells completed in the sandstone are most common in the north half of the study area where the depth to bedrock may be shallow. Wells completed in bedrock often do not have casings through the entire depth of the well and are not screened at the bottom. Movement of water within the bedrock is controlled by fractures and is called secondary porosity. In well logs, well drillers describe sandstone locally as soft to medium to hard with fractures. In at least one case, the bedrock near a well has been hydrofractured in an effort to improve well productivity. Hydraulic conductivities vary in sandstone. Textbook values for hydraulic conductivity of fractured sandstone range from 2.8×10^{-5} to 2.8×10^{-1} ft/day (Freeze and Cherry, 1979). Based on a pump test on a local public water system, Willing (1997) estimated that the transmissivity in a confined Chuckanut sandstone aquifer on Lummi Island range from 118 to 225 ft^2/day. Schmidt (1979), not distinguishing between sandstone and greenstone bedrock, noted that wells completed in bedrock have moderate to low yields that, in some cases, are too low to be used for domestic purposes.

Greenstone. A handful of wells in the southeastern region of the study area, are completed in greenstone. Preliminary examination of well-log data indicate that the greenstone unit is much less fractured than Chuckanut sandstone. It is frequently described as hard to very hard by drillers, and is generally less productive than the sandstone. Textbook values for hydraulic conductivity of metamorphic rocks range from 2.8×10^{-3} to 2.8 ft/day (fractured) to 2.8×10^{-8} to 2.8×10^{-5} ft/day (unfractured) (Freeze and Cherry, 1979). No pump test data were available for wells completed in greenstone.

<u>2.6.2 Glacial Drift</u>

Most wells completed in glacial drift are located in the south half of the study area where there seems to be a deep trough in the underlying bedrock that is filled with glacial drift (Schmidt, 1978; Kelly, 1998). According to Schmidt (1978), the glacial drift is

15

estimated to have a higher transmissivity and groundwater storage capacity than the bedrock. The high heterogeneity of the glacial drift unit that includes thin lenses of sand is likely responsible for perched water tables noted by Schmidt and by Washington State Department of Conservation (1960). Textbook hydraulic conductivities for silt and sand range from 2.8 x 10^{-2} to 2,800 ft/day (Freeze and Cherry, 1979). A glacial drift unit consisting of till and glaciomarine drift on Guemes Island (Kahle and Olsen, 1995) is estimated to have a median hydraulic conductivity of 23 ft/day. This relatively high hydraulic conductivity of glaciomarine drift is likely due to the presence of silt or sand lenses.

2.7 Recharge

Aquifer recharge on the island comes from infiltration of precipitation (Schmidt, 1978). Schmidt described and mapped recharge areas where land surface slope is relatively flat and granular soils or marshy areas occur, noting that these are important to recharge of Pleistocene materials. Recharge areas mapped by Schmidt are mostly in low-lying regions. Recharge can be estimated by conducting a water-budget study that quantifies precipitation, evapotranspiration, and runoff. The input data required for a site-specific recharge estimate includes climate, soils, geologic strata, topography, and land cover. For example, aquifer recharge for similar settings is estimated to be 1 in/yr for exposed bedrock in the Puget Sound Lowland (Bauer and Vaccaro, 1987) and 3.9 in/yr for glaciomarine drift on Guemes Island (Kahle and Olsen, 1995). Schmidt (1978) estimated recharge through a crude water-mass balance using only climatic and precipitation data from official weather stations at Bellingham International Airport and Olga on Orcas Island. He reported recharge as ranging from 5 to 9 inches on north Lummi Island.

2.8 Seawater Intrusion

Seawater intrusion is the saline contamination of an aquifer and can be induced by increased groundwater withdrawal resulting from development. Seawater consists of a variety of dissolved constituents that can cause contamination even when significantly diluted by freshwaters (Table 3). The maximum contaminant level (MCL), established by the Washington State Legislature to conform to various federal laws (WAC 246-290-

310, 1988; WAC 173-200-040, 1991), for selected water quality parameters are listed in Table 4. Chloride and sodium are two contaminants commonly associated with the advance of saline waters into an aquifer.

One definition of seawater intrusion is chloride concentrations in groundwater exceeding 100 mg/L (Washington State Department of Ecology, 1991). Seawater intrusion meeting this definition has been observed at several locations on Lummi Island in previous studies (Walters, 1971; Dion and Sumioka, 1984, Whatcom County, 1994). As summarized in the introduction, additional previous works addressing seawater intrusion of islands in the Puget Sound Region include the groundwater resource studies of four San Juan Islands (Whiteman et al., 1983), neighboring Guemes (Kahle and Olsen, 1995) and Lopez islands (Orr, 1997), and Whidbey and Camano islands to the south (Kelly, 2005).

Chloride is commonly used to define the presence of seawater intrusion because it does not occur in great concentrations in freshwater and is non-reactive with aquifer material as it moves inland from the sea (Freeze and Cherry, 1979; Fetter, 1980). Chloride is designated as a secondary (nuisance) contaminant with an MCL of 250 mg/L (WAC 246-290-310, 1988). Concentrations exceeding this level can cause drinking water to taste salty and can corrode metal pipes and well casings. Sources of chloride in groundwater other than seawater intrusion include septic tank effluent, formation waters, leaching of minerals from aquifer media, and airborne sea salts deposited on the land surface as solids or dissolved in precipitation. During seawater intrusion, sodium undergoes cation-exchange with aquifer material. In some cases, sodium concentrations in intruding waters may occur in a smaller ratio with chloride than the ratio of these ions in seawater. In fully intruded aquifers, the ratio of sodium to chloride will approach the ratio in seawater. Sodium is considered a primary contaminant with no MCL, though the United States Environmental Protection Agency has recommended an MCL of 20 mg/L for persons restricted to a low-sodium diet (WAC 246-290-310, 1988).

Specific conductance is proportional to total dissolved solids and can be used as a proxy to detect seawater intrusion because of the extremely high concentrations of dissolved solids in seawater. It provides the advantage that it can be quickly measured in the field.

The density contrast between freshwater and seawater makes it possible to predict the location of the location of the interface between these two fluids at any point where the absolute elevation of the pressure surface in an aquifer is known. This can be accomplished by applying the Ghyben-Herzberg Relation (Figure 6). This relation states that in a steady state, where the specific gravity of seawater is approximately 1.025, the depth of the freshwater/seawater interface is 40 times the height of the freshwater table above sea level. This ratio may be greater than 40:1 locally because waters of the Puget Sound can be less saline than waters of the open ocean (Sapik et al., 1988; Culhane, 1993). Other factors that may cause the actual location of the interface to vary from the predicted location are dynamic flow conditions, shape, orientation, and hydraulic properties of aquifer and confining strata, fracture patterns in bedrock, and confining conditions. Dispersive processes are enhanced by groundwater flow around grains within the aquifer media and by fluctuations in water levels due to seasonal and tidal water level fluctuations and pumping wells. Diffusive processes are driven by ionic concentration gradients between the fresh and sea waters. These processes mix fresh and sea waters at the interface to create a zone of mixing (Freeze and Cherry, 1979). The sharp Ghyben-Herzberg predicted interface is not a realistic representation of actual conditions where the mixing zone is especially thick (Bear, 1979).

Seawater intrusion can be either passive or active. Passive seawater intrusion occurs when there is a decline in fresh groundwater on an aquifer-wide scale due to increased withdrawal, decreased precipitation, or a rise in sea level and generally occurs over long periods of time. This results in the inland and upward migration of the mixing zone. Active seawater intrusion is the result of concentrated groundwater withdrawal due to pumping wells that actually reverses the hydraulic gradient in an aquifer toward shore, inducing seawater intrusion on a relatively short time scale. The cone of depression in

18

freshwater that is associated with a pumping well creates a localized region of lower aquifer head. This results in a localized rise in the freshwater/seawater interface, known as upconing (Figure 6). The decrease in hydraulic head associated with upconing tends to cause seawater to move vertically toward a pumping well. Active intrusion via upconing can occur over a very short period of time. Given that all other conditions are the same, a confined aquifer will tend to be more prone to the effects of upconing than an unconfined aquifer due to lower storage properties that cause larger drawdowns occurring over shorter periods of time. Unlike other types of groundwater contamination, seawater intrusion can be reversed over relatively short periods of time by mitigating the conditions causing intrusion or by increasing freshwater head.

2.9 Limitations of Previous Studies

Previous geologic studies of Lummi Island have not defined the hydrostratigraphy. Although nearly half of the wells in the study area are completed in unconsolidated deposits, little was known about the Pleistocene stratigraphy. Previous mapping efforts were primarily focused on the bedrock geology or were included in larger studies of western Whatcom County. The works of Caulkin (1959), Easterbrook (1971), Carroll (1980), and Blake (unpublished) identified and mapped bedrock outcrops from fieldwork. The mapped extent of bedrock and glacial drift varies among these studies. Kelly (1998) improved upon Schmidt's (1978) depth-to-bedrock mapping by including more data, but did not address glacial stratigraphy. Studies that did describe glacial geology contained insufficient detail to characterize the hydrostratigraphy. Glacial deposits in the study area were described by Caulkin (1959), but not mapped. Easterbrook (1971) mapped glacial deposits as undifferentiated. Subsequent mapping of the glacial drift by Lapen (2000) identified two separate units, glaciomarine drift and emergence beach deposits of the Everson Interstade. Lapen mapped north Lummi Island in reconnaissance by examining air photos and making comparisons to mainland locations having similar glacial drift outcrops, but included little or no field documentation. Because emergence beach deposits overlie older glacial drift sediments and are relatively thin, Lapen's map was of limited use in characterizing the hydrostratigraphy at the depths where aquifers exist.

19

Most previous work examining the hydrogeology of the north half of Lummi Island is qualitative and not based on field data, or is confined to small areas on the island. The report completed for Whatcom County Planning (Schmidt, 1978) is the only study to address the hydrogeology of the entire north Lummi Island and has been the basis for groundwater management decisions on Lummi Island for more than two decades. Unfortunately, Schmidt was unable to identify hydrostratigraphy, delineate aquifers, or provide reliable static water levels. Schmidt used only well-log data to map aquifer surfaces and recharge zones. Although well logs can be effective for depth-to-bedrock mapping (Schmidt, 1978; Kelly, 1998), they are of limited use in mapping groundwater surfaces because the dates of static water-level measurements on well logs can differ by decades. It seems that Schmidt used a topographic map to estimate well-head and aquifer-surface elevations, potentially introducing large errors into his aquifer surface map. Schmidt's mapping of aquifer recharge zones is generalized because he used only data from his aquifer surface map. The water budget conducted by Schmidt is based only on climatic data. Soils, geologic, and land cover data that could be used to better quantify potential evapotranspiration (PET), infiltration, and runoff, were not available.

A brief and qualitative assessment of groundwater occurrences on Lummi Island is contained in a broader report on the water resources of the Nooksack River Basin (Washington State Department of Conservation, 1960). This report mentions that the presence of Chuckanut sandstone near the surface in many places indicates limited groundwater availability. This study states that wells are completed at sea level in glacial drift that fills pockets in the bedrock, comprising the principle source of water in the north half of the island. This study also noted reliance upon shallow dug wells.

The most complete set of hydrogeologic field data from wells on Lummi Island is contained in the report by Whatcom County (1994). This report compiles data from Whatcom County Health Department, Department of Ecology, and a citizen-initiated Centennial Grant study. During the latter effort, water-level data from up to 38 wells

were collected over two years but no well-head elevation data were obtained that would make it possible to map aquifer potentiometric surfaces and wells from which data were collected were not sufficiently mapped. As a result, the County made no hydrogeologic conclusions from this or previous studies. Well logs were not matched to wells or were not available during my study. Chloride analysis results from 75 wells on Lummi Island originating from the sources listed above and collected over a seven-year period are contained in Whatcom County (1994). From these data, Whatcom County examined the number of wells belonging to each of Department of Ecology's seawater intrusion risk levels and some trends in chloride concentrations with regard to time and tidal effects. Willing (1997) examined aquifer properties by conducting pump tests on two wells serving the Isle Aire Beach Water Association. This study provides some hydrologic properties for fractured sandstone and glacial drift material but addresses only one portion of the island.

Previous water-chemistry studies of seawater intrusion on Lummi Island have been limited in scope, or inconclusive. The two statewide surveys addressing seawater intrusion in the region (Walters, 1971; Dion and Sumioka, 1984) were not focused on Lummi Island and only identified that seawater intrusion occurred in some wells. The Whatcom County (1994) study collected the largest set of water-chemistry data including chloride concentrations from 24 wells over two years, but again, made no conclusions.

3.0 RESEARCH OBJECTIVES

My primary objective is to define the physical hydrogeology of north Lummi Island including hydrostratigraphy, groundwater flow (directions and gradients), static groundwater quantity, and recharge. The secondary objective is to assess the impact of seawater intrusion through analysis of groundwater chemistry and physical relationships. The use of new and existing data and tools that were not utilized, or not available, to previous studies such as global positioning systems (GPS), stratigraphic and groundwater modeling software (GMS), and geographic information systems (GIS), makes it possible to quantify the hydrogeology of north Lummi Island. To accomplish these goals, I completed the following tasks:

Select domestic wells, collect well logs, and determine well-head elevations. A total of about 80 wells is necessary to capture the complex heterogeneities in water level, water chemistry, and stratigraphy that were assumed to exist in the study area. A database was constructed to contain well construction, well performance test, and driller's texture description data. Additionally, newly collected field data such as water levels, water chemistry analysis, and observations have been added to the database. Well-head locations and elevations were measured using a survey-grade GPS and added to the database.

Characterize the geologic stratigraphy. A detailed determination of the bedrock and glacial drift stratigraphy is a prerequisite to characterize the hydrogeology of north Lummi Island. An improved depth-to-bedrock map was used as a basis for modeling the complex hydrostratigraphy of overlying glacial deposits. A detailed three-dimensional (3-D) model of the glacial drift stratigraphy enabled identification of subunits with varying hydraulic conductivities such as sand lenses and aquitards.

Define the hydrostratigraphy and identify aquifers. The bedrock and glacial-drift stratigraphic models were used to identify the texture and extent of units of hydrologic significance. The lateral extent, elevations, thickness, volume, confining conditions, and position in regard to sea level were quantified for each aquifer based on the 3-D stratigraphic model.

Determine the hydraulic properties of aquifers. Hydraulic properties of aquifers that are important for estimating groundwater flow, groundwater quantity, and overall productivity of aquifers are well yield, specific capacity, transmissivity, and horizontal hydraulic conductivity.

Identify water level trends and groundwater flow patterns. Characterizing groundwater flow requires mapping potentiometric surfaces in the major aquifers. This required static water-level measurements from over 80 wells during fieldwork to obtain recent water-level measurements. By locating each of these wells with a survey-grade GPS, I was able to measure the elevation of the aquifer surface at every point. The potentiometric surface maps have been used to determine groundwater flow directions and gradients. Trends in water levels were examined from previous (Whatcom County, 1994) and newly collected data.

Estimate total groundwater storage capacity. The total groundwater in storage under static, or steady state conditions assumes that the amount of water entering and leaving the aquifer system is equal. Saturated volumes for each aquifer were quantified using the 3-D stratigraphic model and recent water-level and potentiometric surface data. Static groundwater quantity was calculated using the saturated volumes and hydrologic properties (effective porosity) of the dominant texture for each aquifer. Results have been used to examine how withdrawal affects aquifer head and were checked against other methods for estimating groundwater quantity that examine recharge rates.

Identify recharge/discharge areas. The major recharge and discharge areas for each aquifer have been identified using the 3-D stratigraphic model, potentiometric surface data, and mapped and observed hydrologic features such as springs. When possible, water-chemistry data were used to validate recharge area results.

Estimate aquifer recharge using a water-mass balance. Aquifer recharge rates can be determined by examining input and output variables to estimate a water-mass balance that is also known as a water budget. This yielded an estimate for the total volume of groundwater that is available for withdrawal. The method used to conduct this water budget is similar to the one used for the Guemes Island groundwater study (Kahle and Olsen, 1995).

Estimate aquifer recharge using a chloride-mass balance. The concentrations of chloride ions in groundwater were used as a second means of estimating recharge. This method has been employed to estimate recharge on local islands in San Juan and Island counties (Orr et al., 2002; Sumioka and Bauer, 2003).

Survey water chemistry. General trends in water chemistry were identified through analysis of samples collected from about 80 wells during two seasons.

 Assess the seawater intrusion potential. This has been accomplished primarily through the analysis of groundwater chemistry (chemical approach) and also by defining the location of the Ghyben-Herzberg predicted freshwater/seawater interface (physical approach), then testing the predicted location against water chemistry.

4.0 METHODOLOGY

Below I describe the most important details about the methods that I employed to accomplish the tasks outlined above. For a more detailed discussion regarding methods, assumptions, and sources of error, please refer to Appendix A.

4.1 Domestic Well Database

A total of 130 wells were used in this study (Table 5). A total of 89 wells in the study area were selected for monitoring based on the following criteria: permission from the owner, spatial (lateral and vertical) distribution, well log availability or the probability of locating the well log, and well-head accessibility for water-level measurements and water sampling. An additional 41 well logs (for 130 total wells) were used in the development of the stratigraphic model. Well logs were located for all but 16 (6 dug wells and 10 drilled wells) of 130 wells. The total depths of the ten drilled wells without well logs were measured to create dummy well-logs based on the 3-D stratigraphic model allowing the use of water level and water sample data from these wells.

The well logs (for most wells) were obtained from a variety of resources including well owners, Washington Department of Ecology, Whatcom County Health Department, and in one case, information obtained from a previous study. I used a variety of resources to match a well log with its island location, including information from well owners, previous landowners, neighbors, addresses, public water system names, Washington Department of Ecology Unique Well Identification Numbers, Whatcom County Health Department records, tax and plat history in the Whatcom County Assessor's database and maps, previous studies, well depths measured during fieldwork, and information from well drillers. Well-numbering consists of two digits indicating the section where the well is located followed by one, or sometimes two (for sections having more than 26 wells), randomly selected letters. This system does not follow those in previous studies.

Locations and Elevations

Nearly all of the wells used for water-level measurements and water sample monitoring were located using a Trimble 5700 survey-grade Global Positioning System (GPS). Because there are no official survey benchmarks on Lummi Island, a GPS base station was established in an open field (Figure 1). A benchmark stake was set in the ground at this location to ensure consistency between different field days. A precise location for the base station was obtained from the National Geodetic Online User Positioning Service (OPUS) with horizontal coordinates in the North American Datum 1983 (NAD 83) and elevations in the North American Vertical Datum 1988 (NAVD 88). Vertical precision is generally less than one foot, but is greater at some wells. A rover GPS receiver in post-processing kinematics (PPK) mode was used to survey well locations that were later solved against the position of the base station. All GPS-surveyed positions are in the NAD 83 and NAVD 88 datums. About 1/3 of the 89 wells are located under thick tree cover or in a pump house where a direct GPS measurement could not be made. For these wells, a temporary GPS benchmark was set nearby. In most cases, a total station was used to translate the position of the temporary benchmark to the well, up to a mile in some places. At several wells where the distance between the temporary benchmark and well-head were sufficiently small (less than about 15 feet), a string level, Brunton compass, and measuring tape were used. GPS surveys for 3 of the 89 wells are not available because the temporary benchmarks had been altered or removed. These 4 wells were located from a 10-m DEM overlay on a topographic map using GIS and checked against temporary GPS benchmark positions taken earlier. Thirty-eight of the 41 additional wells used in the stratigraphic model were located using this method. One was located using GPS and two wells (05AA and 05BB) were not precisely located.

4.2 Three-Dimensional Stratigraphic Model

The three-dimensional stratigraphic model (3-D stratigraphic model) was developed in two parts: the bedrock surface elevation model and the Pleistocene stratigraphic model. Data from a total of 111 well logs, (about 29 wells per square mile; Figure 7) surface geologic maps, and fieldwork were used with Department of Defense Groundwater Modeling Software (GMS) to create a 3-D stratigraphic model of the bedrock and Pleistocene units. The base of the stratigraphic model is the bedrock surface.

Bedrock Surface Elevation Model

The surface of the bedrock is concealed nearly everywhere beneath overlying Pleistocene deposits. Input data for the bedrock surface elevation model include geologic maps from Easterbrook (1971) and Lapen (2000), used to delineate the outline of bedrock outcrops and well logs for wells that penetrate to bedrock. Additionally, well logs from some of the deeper wells completed in unconsolidated deposits were used to establish a maximum bedrock elevation in areas where no wells penetrate to bedrock. These data were used as 3-D vertices for a series of iterative triangle irregular networks (TINs) created in GMS (Appendix A) to represent the elevation of the bedrock surface at any point in the study area. The region below the bedrock surface was filled to a constant elevation of –300 feet. Data from well logs and published geologic reports were used to derive the location of the contact between sandstone and greenstone.

Pleistocene Stratigraphic Model

The bedrock surface elevation model served as a base to model the stratigraphy of the overlying Pleistocene sediments. Well log data indicated that fine-grained material dominate the Pleistocene subsurface environment. Therefore, the overall strategy for modeling Plesitocene stratigraphy was focused on defining the three-dimensional extent of lenses of coarse-grained material interbedded with the fine-grained material. Driller's descriptions of the textures of Pleistocene strata encountered during well drilling are noted in well logs. From these descriptions, I interpreted the texture of strata at each well

27

(Appendix B). Coarse-grained deposits were interpreted to have hydraulic properties that are dominated by sand. Therefore, coarse-grained units are referred to as sand units. The majority of fine-grained deposits are variations of poorly sorted mixtures of clay, silt, sand, gravel, and cobbles. These deposits were interpreted to have hydraulic properties dominated by silt and are therefore referred to as silt-clay diamicton. These interpreted textures were imported into GMS as well logs. Preliminary cross sections between these well logs were manually constructed using fundamental geologic concepts. Relationships between sand lenses, ascertained from the preliminary cross sections, were used to create top and bottom elevation TINs for each lens. The regions between these TINs were filled to create sand unit solids. The greater region surrounding the sand unit solids was modeled as a single silt-clay diamicton solid, extending from land surface to the modeled bedrock surface. The sand, silt-clay diamicton, and bedrock solids form the stratigraphic model for north Lummi Island. This model was validated against additional well logs, existing geologic maps, soil descriptions from on-site sewage disposal applications, and field observations. The stratigraphic model was used to create a revised geologic map and interpretation as well as numerous cross sections that display relationships between sand, silt-clay diamicton, and bedrock units.

4.3 Hydrostratigraphy and Aquifer Identification

The foundation for defining hydrostratigraphy and identifying aquifers is the 3-D stratigraphic model. Water bearing sand and bedrock units were identified through well-log data. Water bearing units with wells screened in them were designated as aquifers. The stratigraphic model and water-level data were used to delineate confining conditions in each aquifer.   From this, the volume, thickness, and position with regards to sea level of the saturated regions of each aquifer were calculated using GMS.

4.4 Hydraulic Properties

Properties of aquifers that are important for estimating groundwater flow, groundwater quantity, and overall productivity of aquifers are well yield and specific capacity, effective porosity, transmissivity, horizontal hydraulic conductivity of aquifer media, and hydraulic head distributions. Well yield and specific capacity were quantified from well performance testing data in the majority of well logs.   An average effective porosity, the pore space available for fluid flow, was estimated for each aquifer by determining the dominant texture and assigning values from published reports for similar geologic material.   Transmissivity was estimated from specific capacity data then combined with screened or saturated open interval (bedrock wells) data to estimate horizontal hydraulic conductivity at each well. Methods used to determine hydraulic head distributions are discussed in Section 4.5.

4.5 Water Level Trends and Groundwater Flow Patterns

Water Level Trends

Static water levels were collected from a total of 87 wells. Most of these wells (77) were measured during fall 2002 and spring 2003 with the intent to capture water levels during the low and high water periods, respectively. Water-level data were used to create potentiometric maps for three of the largest aquifers. Well hydrographs were produced from monthly water levels collected from March 1991 through January 1993 as part of an earlier Lummi Island groundwater study (Whatcom County, 1994). The well hydrographs were compared to precipitation patterns during the same time period to determine the magnitude, timing, and distribution of seasonal water level fluctuations. Water levels in wells used in the Whatcom County study and this study were examined for long-term trends. Well-head elevations were measured using a survey-grade GPS to find the absolute elevation of water-level data (total head) collected in this study.

Groundwater Flow Patterns

Groundwater flow patterns (direction and magnitude) were determined from water-level measurements, the stratigraphic model, and hydraulic properties of each aquifer. Groundwater flow directions were primarily determined from water-level data collected in fall 2002 and spring 2003. These data were used to create potentiometric maps for three of the largest aquifers. Groundwater divides in three aquifers were identified from the potentiometric maps. The groundwater contours from these potentiometric maps give an indication of flow directions. For aquifers with limited water-level data, groundwater flow directions were estimated using three-point problem methods and the 3-D stratigraphic model. Groundwater flow magnitudes (average linear velocity) were estimated for the aquifers with potentiometric surfaces maps by incorporating head gradient, average effective porosity, and estimated horizontal conductivities of aquifer material.

4.6 Estimate Total Groundwater Storage Capacity (steady state)

The total groundwater storage capacity of study area aquifers was estimated by multiplying the saturated volume of each aquifer by the average effective porosity of each aquifer. Aquifers were modeled and their respective saturated volumes were calculated using GMS and water-level data (Section 4.3). The average effective porosity was estimated for each aquifer (Section 4.4). This method assumes static (steady state) conditions. A steady state groundwater quantity estimate represents a snapshot of the groundwater occurring in the aquifer system at a given time.

4.7 Identify Recharge/Discharge Areas

Primary and secondary recharge areas were identified by examining the stratigraphic model, potentiometric maps, groundwater flow directions, land surface topography, surface geology, and soils data. The stratigraphic model was used to trace out potential recharge strata in three dimensions. Potentiometric maps were used to identify generalized groundwater flow directions, groundwater highs, and groundwater divides.

Potential recharge areas were checked against topography, soil type, geology, and water-chemistry data. Sources of recharge for each aquifer were also identified in this manner.

Primary and secondary discharge areas were identified by examining potentiometric surfaces, groundwater flow directions, bedrock and glacial-drift stratigraphic models, surface topography, hydrologic features such as surface water and springs, and soils. A bathymetric surface TIN was imported into GMS and examined against the stratigraphic model to identify aquifers that extend beyond the shoreline to discharge offshore (see Section 5.7.1). Groundwater divides were used to differentiate primary and secondary discharge areas.   Aquifers that discharge at land surface were identified at places where the aquifers and potentiometric surfaces intersect topography. These were validated against hydrologic features such as surface water and springs from topographic maps and field observations.

4.8 Recharge Estimate Using a Water-Mass Balance

Recharge to north Lummi Island aquifers was estimated for water years (WY) 2001-2004 by quantifying the input and output variables for a simple water-mass balance equation. The input variable is precipitation and the output variables are evapotranspiration, runoff, and recharge. Precipitation was quantified from data collected by volunteers on Lummi Island (Marshall et al., written communication, 2004). Data used to quantify potential evapotranspiration and runoff were obtained from a variety of sources. Climatic and land cover data (National Climatic Data Center; Landsat 4) were used to estimate evapotranspiration. Discharge data collected by volunteers from study area basins for WY 2004 (Nielson and Armfield, written communication) were used to estimate runoff. Ranges for maximum and minimum evapotranspiration and runoff were established. Recharge was estimated as a range of values from the annual average during WY 2001-2004.

4.9 Recharge Estimate Using a Chloride-Mass Balance

A chloride-mass balance approach to estimating recharge was employed as a second, mostly independent method to estimate aquifer recharge. This method has been used as a secondary means of estimating recharge in studies of local islands in San Juan and Island Counties (Orr et al., 2002; Sumioka and Bauer, 2003). Application of this method in the current study follows these previous works.

4.10 Survey Groundwater Chemistry and Assess Seawater Intrusion

Physical Approach

The total head at each well with water-level data was used to predict the location of the freshwater/seawater interface using the Ghyben-Herzberg Relation. The location of this predicted interface represents a sharp boundary that was used to identify wells that are completed at depths below or close to the interface.

Chemical Approach

A survey groundwater sampling program was conducted to assess general seawater intrusion conditions, establish background values for parameters associated with seawater intrusion, and to increase the understanding of the overall hydrogeochemical setting. Groundwater chemistry was analyzed for selected parameters for a total of 80 wells, 71 of which were sampled in fall (September-October) 2002 and spring (May-June) 2003. Samples were analyzed in the field and in the laboratory for selected parameters and constituents. These include chloride, sodium, and calcium ion concentrations, specific conductance, total dissolved solids, pH, and redox potential.   Several diagnostic methods were used to identify wells potentially showing seawater intrusion. Chloride concentrations were compared to well completion elevations. Seasonal changes in chloride concentrations were examined. Ratios of concentrations of sodium to chloride were compared to ratios that occur in seawater. Values for chloride and specific conductance were plotted and were also used to develop a method for estimating chloride concentrations using a conductivity meter. Five wells with suspect water chemistry were selected for additional groundwater sampling. A major ion analysis was conducted on

samples collected from these wells in winter 2005 in an effort to delineate the source of elevated chlorides for wells having high chloride concentrations or otherwise unusual water chemistry. Results were plotted on Piper and Stiff diagrams and compared with results from other island settings in the Puget Sound Region.

5.0   RESULTS AND DISCUSSION

5.1   Geologic Setting

5.1.1 Bedrock

A model of the bedrock surface of the north half of Lummi Island was produced using Groundwater Modeling Software (GMS) and data from well logs, surficial geologic maps, field observations, and discussions with geologists that have studied Lummi Island bedrock (Blake, personal communication, 2002; Blake and Engebretsen, personal communication, 2004; Figure 8). The bedrock surface model was validated against previous depth-to-bedrock mapping efforts (Schmidt, 1978; Kelly, 1998), additional well logs, and the anticline/syncline pairs of Caulkin (1959) and Carroll (1980).

The anticline/syncline pairs generally match the location and orientation of depressed and elevated regions of the modeled bedrock surface indicating that the dramatic relief of this surface is controlled structurally through high amplitude folding (Figure 8). The southern-most syncline was extrapolated beyond its previously mapped extent and indicates that the deep northwest-southeast trending bedrock trough in the middle of the study area is a part of this syncline. Consistent with Caulkin and Carroll's observations, this syncline has a steeper southern limb.   This trough is the deepest and most extensive depression in the bedrock surface, extending from Hale Passage northwest to Sunny Hill Lane, and possibly further as indicated by a log for an un-located well (05BB) that lies to the northeast of Village Point (Figure 8).

The contact between the Chuckanut Formation and Fidalgo ophiolite units is modeled as trending northwest-southeast, roughly parallel to the extrapolated axis of the southern-most syncline (Figure 8). The contact is depicted as a relatively sharp interface between Chuckanut and Fidalgo rocks. However, data from some well logs to the south of this contact and along Seacrest Drive indicate the presence of a thin veneer of sandstone (about 20 feet thick) overlying Fidalgo ophiolite rocks. It is not clear whether these

34

descriptions of sandstone are Chuckanut or a clastic member of the Fidalgo ophiolite, possibly the Deception Pass sandstone (Blake and Engebretsen, personal communication, 2004). Interpreting these descriptions of sandstone as Chuckanut and incorporating them into the bedrock surface model would produce a more jagged and irregular Chuckanut/Fidalgo contact than shown in Figure 8. This contact may be an unconformable contact instead of a fault bounded contact as evidenced by its parallel orientation with the axes of mapped and projected anticline-syncline pairs and the presence of a thin layer of sandstone over greenstone south of the contact.

Most of the bedrock is covered by a veneer of soil and glacial drift, exposed bedrock outcrops are not extensive. Caulkin (1959) noted that bedrock outcrops are not common on north Lummi Island. Although two geologic maps (Easterbrook, 1971; Lapen, 2000) show relatively extensive sandstone outcrops in the north half of the study area, these studies did not include significant fieldwork. A geologic map constructed by Carroll (1980) did include significant fieldwork. This map presents the outcrops as inferred contacts, obscured by thin sediments in most places. My field observations validate the latter.

The Chuckanut sandstone is described as having a thickness of approximately 330 feet on Lummi Island and unconformably overlies older rocks of the Fidalgo ophiolite (Carroll, 1980). Rocks of the underlying Fidalgo ophiolite may be folded with the Chuckanut sandstone in the north half of the study area (Caroll, 1980) possibly creating irregular depths to Fidalgo rocks beneath the Chuckanut. Data from the deepest well log (05C) indicate that greenstone underlies Chuckanut sandstone near the middle of the study area at an elevation of –261 feet. Another log for an unlocated well (05BB) suggests the presence of greenstone at a slightly shallower depth in the area northeast of Village Point. Along the northeastern shore of Lummi Island, several workers have mapped Fidalgo rocks underlying Chuckanut sandstone at sea level. It is likely that the sandstone-greenstone contact beneath the north half of the study area occurs at variable elevations. However, because no well log data were found to quantify this, I chose the base of the

sandstone to be at a constant elevation of –261 feet because greenstone is encountered at –261 feet in well 05C, the deepest known well. Choosing this elevation as the base of the sandstone is roughly consistent with a cross section in Carroll (1980).

5.1.2 Pleistocene Sediments

Nearly half of all wells in the study area are completed in coarse units of glacial drift. The majority of these wells are located in the south half of the study area where large depressions in the bedrock surface have been filled with up to 300 feet of Pleistocene sediments (Figures 7 and 8). A solid model representing the total of all undifferentiated Pleistocene deposits was created by filling in the region between a land surface TIN and the modeled bedrock surface.

Preliminary examinations of well logs imported into GMS showed a highly heterogeneous environment dominated by fine-grained diamictic material with discontinuous coarse-grained lenses of varying thickness. These lenses are dominantly composed of sand or mixtures of sand and gravel. Lenses of clean gravel are rare. Because the hydraulic conductivity of the coarse-grained material will be dominated by the smallest abundant texture, in this case it is sand, the coarse-grained units in the study area are identified as sand.

 The strategy employed was to trace the top and bottom surfaces of the coarse lenses between wells to create solid models for major sand lenses, then to fill the intermediary regions with fine-grained material. Using the three-dimensional features in GMS facilitated this effort. The stratigraphic modeling effort was enhanced with the release of GMS 5.0, which provided more robust 3-D capabilities. GMS is designed to model the subsurface environment from user-assigned strata identifiers called "horizons". However, the complex subsurface glacial drift and bedrock on north Lummi Island prohibited the use of this feature. Attempts to use the horizons approach yielded a

stratigraphic model that violated geologic constraints with sand and clay units undulating more dramatically than one would expect under natural conditions.

Instead, a more time-consuming manual approach was used by creating preliminary cross sections between all wells and tracing out sand units as described in the methods section. This manual approach likely has a great deal more accuracy because it forced me to make frequent decisions based on geologic constraints that are ultimately reflected in the final 3-D stratigraphic model. The stratigraphic model identifies the extent of major sand lenses in three dimensions, hereafter referred to as sand units (SU).

Sand units represent layers of coarse materials sharing common textures and similar elevations with respect to data available from well logs. Some may actually be composites of different geologic units that do not share the same origin or age, but are modeled as physically connected. The method used to delineate sand units was conducted without regard to a particular geologic interpretation, largely because it was unclear which interpretation might apply. This proved to be advantageous because it forced me to model sand units based solely on the application of fundamental geologic constraints rather than trying to make the model fit a preconceived geologic picture.

A total of 29 major sand units were identified and modeled into solids using GMS. The properties of each are summarized in Table 6. The largest sand unit, SU-6, is located in the southern part of the study area and has an area of 0.38 square miles and a volume of 1.46×10^7 cubic yards. The estimated mean thickness of sand units throughout the study area ranges from 2-23 ft. The total volume of sand units is estimated to be 6.94×10^7 cubic yards (19% of the total volume of glacial drift).

The dominant grain size of coarse-grained units is sand. Of 29 coarse-grained units identified in the stratigraphic model, 19 are primarily composed of a mixture of sand and gravel, 9 are primarily composed of sand, and 1 is primarily composed of gravel (Table

7c). Medium-grained sand seems to be the dominant sand texture. Units that are primarily composed of a mixture of sand and gravel generally lie above present sea level. Units containing fine sand generally lie at or below present sea level.

The material surrounding sand units was designated as silt-clay diamicton based on examination of well logs, fieldwork, conversations with well drillers experienced on Lummi Island, and published geologic reports. Diamictons are mixtures of clay, silt, sand, and larger clasts such as pebbles, cobbles, and boulders. Though driller's descriptions on well logs in the study area frequently list clay as the only texture occurring in some strata, clean clay is very rare, unlike other regions of western Whatcom County (Livermore and Boulton, personal communication, 2004). Fine-grained samples collected in the field from shoreline bluffs all met the defining criteria for diamicton.

Most of the diamicton occurring on north Lummi Island have fine fractions dominated by silt size particles, not clay. Clay soils are defined under the Unified Soil Classification as generally having more than 20% clay size particles (Selby, 1993). The abundance of clay-size particles in this material likely varies and may be relatively low at most locations. Local cable tool well drillers typically determine the presence of clay based on whether the borehole sluffs-in ahead of the casing, not necessarily by examination of the material at the surface. This method of determining texture is based on material cohesion and is not exclusive to clay. Silt (and possibly indurated sands) would yield the same results. Additionally, particle size analysis of the fine fraction of 7 samples taken from shoreline exposures of diamictic material (Figure 9) indicates less than 5% clay by volume in all but one sample. Although most of the island is mantled in glaciomarine drift, surface runoff is relatively low (Section 5.7) and recharge to bedrock through overlying sediments is relatively high. Permanent standing water is limited to a few wetland areas. Subsoil textures described in 16 on-site sewage disposal applications obtained from Whatcom County Health Department are dominated by sand and loam (Table 24). Loams are dominated by silt and contain from 7-27% clay (Brady and Weil, 2000). Finally, only one well log examined through the course of this study noted the

presence of silt, suggesting that local drillers might be using the term "clay" rather loosely, lumping silt and clay together, on the basis of borehole cohesion.

The presence of "hardpan" in a well log corresponds to glacial till in other studies within the region (Easterbrook, 1973; Dragovich et al., 1998). Thirty of the well logs used to create the stratigraphic model contain descriptions of hardpan. Correlations between strata containing hardpan were difficult to determine from available data as thickness topographic elevations vary. However, where hardpan is described, it is generally thin and most commonly within about 50 feet of the surface. Thickness ranges from approximately 2-50 feet. Hardpan does occur at depths below present sea level in at least 4 wells (for example 15D, 16B) and lies directly on sandstone in the eastern half of the center of the study area (for example 04AA, 05T). Occurrences of hardpan are included in the overall silt-clay diamicton unit in the stratigraphic model.

Combining the stratigraphic model with specific interpretations of driller's notes from 111 well logs (Appendix C), and fieldwork allowed me to make detailed observations regarding the Pleistocene stratigraphy. I consider the following observations to be significant in facilitating my effort to interpret the greater geologic setting on north Lummi Island:

- Fine-grained deposits dominate the subsurface environment.

- Coarse-grained deposits are thicker and more common above present sea level.

- Coarse-grained deposits are mostly comprised of poorly sorted mixtures of sand and gravel and are especially common at land surface.

- Where they occur, clean sands and fine sands are more common at depths below present sea level.

- Considering all textures, there is an overall fining-up of Pleistocene deposits in the south half of the study area.

- Considering all textures, there is an overall coarsening-up of Pleistocene deposits in the middle of the study area in vicinity of the east-west trending bedrock trough.

- Considering only fine textures, there is a coarsening-up at most locations with silt-clay diamicton as the most common texture.

- "Hardpan" (possibly correlated to till) occurs in 30 well logs (23%) throughout the study area. Nearly all of these logs show hardpan within 50 feet of the surface. Hardpan thickness ranges from 2-50 ft. Driller's descriptions of hardpan have been correlated to till in local geologic studies (for example, Dragovich and Grisamer, 1998).

- Hardpan is largely discontinuous. Concentrations of hardpan lie directly on sandstone in the vicinity of wells 04N, 05T and over Pleistocene deposits in the south half of the study area. Hardpan is largely absent from the region overlying the east-west trending bedrock trough.

- Fine-grained sequences close to 200 feet thick occur, especially in the middle of the study area over the east-west trending bedrock trough (for example 09G, 09T, 10A).

- Coarse-grained sequences over 100 feet thick occur in the upland region south of the east-west trending bedrock trough (for example 09B, 09V).

- Silt appears to be the dominant texture of fine material.

5.1.3 Revised Geologic Interpretation

Revising the geologic interpretation of north Lummi Island was not one of the objectives
of this study, however it became one of the outcomes. To better understand the
hydrostratigraphic environment, it became necessary to make my own interpretation of
local Pleistocene geology based on one of two published interpretations of the regional
geology. These published interpretations are discussed in Section 2.1.2.2.   It is
important to designate one or the other as being more applicable to aid in drawing
conclusions about the hydraulic properties of and to establish a naming convention for
Pleistocene stratigraphy in the study area.   Choosing one of these interpretations to apply
to north Lummi Island affects my interpretation of the study area geology because each
offers a different thickness for the glaciomarine drift that lies at land surface. The
combined thickness of the two glaciomarine drift units described in Interpretation A is
much less than the thickness of the single glaciomarine drift unit described in
Interpretation B.

After analyzing both published interpretations of regional geology, I believe that my
stratigraphic model best fits the geologic interpretation presented as Interpretation A.
Possible correlations of modeled sand units to units in published geologic studies of
Interpretation A are listed in Table 8. Evidence supporting a correlation to the units in
Interpretation A is listed:

- The majority of the study area is mantled by silt-clay diamicton that seems to
  correlate to undifferentiated Vashon till and glaciomarine drift. The thickness of this
  diamicton mantle falls within the maximum combined thickness of the till and
  glaciomarine drift (125 feet); (Easterbrook, 1971).
- Hardpan, which I interpret as Vashon till, occurs within 50 feet of the surface in many
  areas, suggesting the underlying materials are pre-Everson deposits.

- Sand and gravel units (SU-3, SU-6, SU-7) that underlie the mantle of silt-clay diamicton might correlate to Vashon advance outwash. Some well logs completed in these units describe cemented sands. The thicknesses of these coarse units fall within published thicknesses for Vashon advance outwash.

- These coarse units are largely underlain by fine-grained material at elevations below present sea level. This material is less diamictic than the silt-clay diamicton mantle, possibly indicating that it correlates to the pre-Vashon Cherry Point silt.

- Cherry Point silt is observed near present sea level at Lummi Peninsula located 1-2 miles to the northeast (Easterbrook, 1963). Silt, not clay, appears to be the dominant texture in fine-grained materials at depth.

- There is an overall coarsening-up of fine-grained materials in most well logs, with diamicton more common at elevations above present sea level. This pattern seems to indicate a transition from Cherry Point silt at or below sea level to till and glaciomarine drift above sea level.

- The overall thickness of coarse units increases with elevation and the overall texture of these units coarsens-up. This pattern seems to indicate a transition from fine sand interbeds within the Cherry Point silt below present sea level through fine, medium, and coarse grained sequences of Vashon advance outwash that lie just below and above sea level. Units with mixtures of sand and gravel at land surface correlate to emergence beach deposits.

Most of the fine-grained deposits mantling the study area seem to correlate to undifferentiated Vashon till and Kulshan and Bellingham glaciomarine drifts (collectively referred to as glaciomarine drift), although the importance of clay in the latter units is de-emphasized in my study. Bellingham glaciomarine drift is probably less common than the more diamictic, stratigraphically lower Kulshan glaciomarine drift. This conclusion is considered reasonable because according to well drillers experienced on Lummi Island, the clean, sticky clays often associated with Bellingham glaciomarine drift in other parts of western Whatcom County are largely absent on north Lummi Island

(Livermore and Boulton, personal communication, 2004). Additionally, the overall coarsening-up of fine grained materials observed in well logs extends to the surface, where the diamicton is most common, favoring presence of the more diamictic Kulshan drift. Finally, widespread, discontinuous occurrences of "hardpan" assumed to be Vashon till lie close to land surface in most places, leaving little room for both Kulshan and Bellingham glaciomarine drifts. Where fine-grained sequences exceed the published thickness of the combined Vashon till and Kulshan and Bellingham glaciomarine drift units (for example 09G, 09T, 10A), Vashon advance outwash is absent and the till and glaciomarine drift is interpreted to lie directly on the older Cherry Point silt.

Deming sand probably does not occur in the study area because of the barrier formed by deep troughs of Bellingham Bay and Hale Passage (Easterbrook, 1962 and 1973). Frequently, Vashon advance outwash is in contact with overlying emergence deposits and underlying sand lenses within Cherry Point silt. The coarse-grained units correlated to Vashon advance outwash are thicker and coarser in the upper and inland regions of the island and thin toward the shoreline where they are deeper and interbedded with fine-grained units (Figure 12g). The decrease in overall thickness and fining of these coarse units down and toward shore may indicate regions near the base of Vashon advance outwash that alternate between fine and coarse modes or are in contact with sand interbeds within the older Cherry Point silt. Thinner and finer interbeds of coarse material located below present sea level within less diamictic silt and clay units seem to correlate to sand subunits of Cherry Point silt. These sand subunits are relatively thin and are commonly comprised of clean and fine sands. Coarse-grained units at land surface are mixtures of sand and gravel that seem to correlate to emergence beach deposits overlying till and glaciomarine drift.

If Interpretation B is applied, then most Pleistocene deposits in the study area can be correlated to the Everson Interstade. The thickness of fine-grained sequences observed in the study area fall within the maximum published thickness for glaciomarine drift (295 ft, Lapen, 2000). Coarse-grained units at various depths can be correlated to marine

outwash, turbidite, and fluvial deposits that are interbedded within the glaciomarine drift. Older units, including Vashon advance outwash, may occur, especially at depth, but were not possible to differentiate from other coarse units of Interpretation B using the methods of this study.

A geologic map, produced from the stratigraphic model, shows my interpretation of the geologic setting (Figure 10). A cross section detailing my geologic interpretation of the subsurface with units of Interpretation A is shown in Figure 11. Cross sections and fence diagrams cut through the stratigraphic model, Figures 12a-12i and 13a-13e, show units that are broadly classified on the basis of texture, not necessarily on their correlations to units in published reports. Because the stratigraphic model was developed, in part, from bedrock outcrops mapped by Easterbrook (1971) and Carroll (1980) outcrops shown in the current map somewhat reflect these earlier works. The distribution of Pleistocene sediments as shown in this geologic map are similar to Lapen (2000);(not shown) that was not used in the development of the stratigraphic model.

5.2 Hydrostratigraphy

The resulting stratigraphic model defines the extent of sandstone, greenstone, silt-clay diamicton, and sand units. These materials have different hydraulic properties and make up the major hydrostratigraphic units in the study area. Hydrostratigraphy was determined by examining the screened interval and the presence of water as noted in well logs and water-level measurements. Based on well logs I examined, the Pleistocene deposits and bedrock support nearly equal numbers of wells.

More than 78% of drilled wells are completed below sea level (Table 9). Completion elevations for all wells range from –289 to 146 feet with a median value of –37 feet and the median completion elevation for wells below sea level is –50 feet (Table 9). Well lengths (total depth) range from shallow dug wells to wells drilled greater than 300 feet (Table 10). Wells completed in bedrock are typically 28% longer than wells completed in glacial drift because the regions where bedrock aquifers occur are the upland topographic highs. Screened and open interval lengths are summarized in Table 11. Wells completed in Pleistocene aquifers typically use screens that are 5 feet long.

Numerous wells are completed within the sandstone and greenstone. Wells completed in bedrock are usually not cased beyond the depth of the overlying glacial sediments or where sediments are thin, beyond the regulatory 18 feet. These open boreholes collect water from unsaturated and saturated regions of bedrock over a long open interval. Groundwater flow in fractured bedrock is mostly through secondary porosity, along structurally controlled and bedding plane fractures. A more complete discussion of porosity and other hydraulic properties of each hydrostratigraphic unit follows in Section 5.4.

The degree of fracturing in rocks of the Chuckanut Formation is not clear, but is likely high. Carroll (1980) stated that while these rocks are well-bedded, they contain few faults, veins, and cleavages. However, many wells logs describe fractured, soft, or decomposed sandstone and hydraulic properties (Section 5.4) indicate a high degree of fracturing in sandstone. Most wells in the Chuckanut Formation are completed in the

sandstone facies. The hydraulic significance of conglomerate and shale facies is not clear. These facies are likely less productive than the more common sandstone and few wells are completed in them. The conglomerate is largely cemented and resistant to groundwater flow.   The anisotropic nature of shale bedding can cause these units to limit groundwater flow. However, the steeply dipping bedding of the Chuckanut Formation as mapped by Carroll (1980) may allow significant groundwater to flow along fractures and between shale bedding planes. Vertical groundwater flow through sandstone within the study area is probably concentrated along fractures and steeply dipping bedding planes that lie perpendicular to the axes of the anticline-syncline pairs mapped by Carroll (1980).   Horizontal groundwater flow is probably concentrated along regional fractures. The vast majority of sandstone is mantled by glaciomarine drift that may serve as a confining unit forcing groundwater to flow through fractures in the bedrock. There may also be significant groundwater flow along the interface between bedrock and overlying glaciomarine drift. Evidence of this was observed along the northeastern shoreline of the island south of Migley Point (Figure 14). It is also possible that the bedrock is saturated and confined by the overlying glaciomarine drift, causing water to seep from below, visible where the contact between these materials is exposed.

Due to the low primary porosity of the greenstone (Section 5.4.3), I assumed that some fracturing exists within these rocks because there are several wells completed in this unit. Well log data indicate that greenstone is often hard and sometimes decomposed or fractured, especially near the top of the bedrock. Hydraulic properties (Section 5.4) indicate greenstone is much less fractured than sandstone. As with the sandstone, groundwater flow through greenstone is likely along fractures. However, the degree and direction of fracturing of greenstone rocks is not specifically noted in any literature and probably has few fractures that have not been partially filled through metamorphic or hydrothermal processes. With the exception of the east-west trending fault south of the study area, greenstone rocks in the south half of the study area are not known to incorporate any large structural features. As with the sandstone, the vast majority of greenstone is mantled by glaciomarine drift that may serve as a confining unit, forcing

groundwater flow through fractures in the bedrock and/or along the interface between bedrock and overlying glaciomarine drift.

Fifteen of the 29 sand units identified in the stratigraphic model support completed wells (Table 6). Most of these water bearing sand units are at or below sea level. The texture of water bearing sand units is mostly poorly sorted mixtures of sand and gravel with the hydraulic conductivity dominated by sand (Table 7c). The sand texture ranges from fine to coarse with fine sand more common below sea level and medium to coarse sand more common at higher elevations. Three water bearing sand units lie completely above sea level with average top elevations ranging from 59 to 133 feet (Table 6). These are relatively thin interbeds of sand and gravel within the glaciomarine drift.

Confining layers are materials with finer textures and lower hydraulic conductivites than the coarse materials they bound. The primary confining unit is the silt-clay diamicton of glaciomarine drift. The secondary confining unit is bedrock. Because silt-clay diamicton is the dominant Pleistocene sediment in the study area (estimated to be 81% of the volume of all unconsolidated sediments) and water bearing sand units are interfingered throughout the finer Pleistocene deposits, it is not possible to delineate individual confining units. Instead, the silt-clay diamicton is modeled as a single confining unit that bounds water-bearing sand units.

An aquitard is defined as a less permeable bed in a stratigraphic sequence that may transmit water but is not sufficiently permeable to support wells with adequate yields (Freeze and Cherry, 1979). The silt-clay diamicton and bedrock serve as aquitards. The fine fraction of most silt-clay diamicton is dominated by silt, allowing leakage of water from above and below the aquifer but creating enough of a contrast in hydraulic conductivity to form a confining layer. The same applies to locations where sand units are in contact with bedrock. The majority of wells are in confined regions (Appendix B). Confining conditions were difficult to determine for some wells in bedrock. They draw

water from long open intervals and, unlike many Pleistocene well logs, lack pronounced changes in lithology that indicate the depth were water-bearing strata were encountered. An aquiclude is defined as a saturated unit that is incapable of transmitting significant quantities of water (Freeze and Cherry, 1979). Given that the fine fraction of most of the glaciomarine drift appears to be dominated by silt, not clay, it is probable that aquicludes are a less common confining layer in the study area than aquitards. Leakage through confining layers is probably common, but was not quantified. Therefore, many of the aquifers described as being confined may actually be semi-confined.

Numerous shallow dug wells occur throughout the study area and six were included my analysis. Most of these wells seem to be dug into thin beach emergence deposits overlying silt-clay diamicton of the glaciomarine drift. Some may also be completed in thin permeable lenses within the upper portion of glaciomarine drift.

5.3 Aquifers

An aquifer is defined as a geologic unit or part of a geologic unit that is saturated and sufficiently conductive to transmit economic quantities of water to a well or spring (Fetter, 1980). A total of 12 aquifers including 10 Plesitocene and 2 bedrock aquifers were modeled in north Lummi Island (Table 12). One additional Plesitocene aquifer (Village Point Aquifer) was identified but not modeled because of insufficient data. Several of the 15 sand units supporting completed wells were combined because they were determined to be connected. Some Pleistocene aquifers support only one or two study wells. Most of these aquifers are bounded by the modeled bedrock surface and their presence was validated by additional wells that were examined but not included in the study. The Village Point Aquifer was not included in the stratigraphic model because its presence is inferred from logs for wells that were not precisely located. The distribution of modeled aquifers, extent of each, and unconfined/confined regions of the Pleistocene aquifers were established (Figure 15). An orthographic view of these aquifers further illustrates their spatial relationships (Figure 16). Top elevations of the Pleistocene aquifers were mapped (Figures 17a –17c). Of 130 wells incorporated in this study, 101 (78%) are completed in four aquifers: Sandstone, Greenstone, Legoe Bay, and Nugent. For ease of referring to aquifers, I named the aquifers based on their geographic location or matrix material. Examination of additional well-log data and hydraulic testing is required to confirm that all are actually separate aquifers.

5.3.1 Bedrock Aquifers

Sandstone. The Sandstone Aquifer is defined as the saturated region within the Chuckanut Formation in the north half of the study area (Figure 15). The Sandstone Aquifer occupies 2.2 square miles of north half of the study area. It is the largest and most utilized aquifer on Lummi Island, providing water for nearly all homes in the north half of the study area (49 of 130 study wells). The Sandstone Aquifer hosts several

public water systems. This aquifer is comprised of folded sandstone, shale and conglomerate of the Chuckanut Formation, collectively referred to here as sandstone.

The Sandstone Aquifer is laterally bounded by the sea on all sides except in the south where it is bounded by glacial sediments that fill a deep bedrock trough assumed to be a large synclinal structure (Figures 8, 15 and 16). The lateral extent of the Sandstone Aquifer encloses all wells known to be completed in sandstone (Figures 7 and 15). However, this aquifer may extend beyond the region shown, beneath glacial drift in the vicinity of Loganita, West Shore, Lane Spit, Nugent, and Legoe Bay Aquifers, although no wells are known to be completed in sandstone in these regions (Figures 7 and 15). The sandstone beneath these areas is probably water bearing but wells are typically completed in the overlying Pleistocene deposits. Few wells are completed in the Sandstone Aquifer where the surface of the bedrock lies below sea level, probably because coarse units in the overlying glacial drift are more productive and less expensive to exploit.

The thickness of the Chuckanut Formation in the study area is estimated to be about 330 ft (Carroll, 1980) and is unconformably underlain by rocks of the Fidalgo ophiolite referred to as greenstone (for example Carroll, 1980; Blake, unpublished). Greenstone comprises the bottom boundary of the Sandstone Aquifer (Figure 11). The bottom contact likely has an irregular surface as the greenstone is probably folded with the sandstone. For the purposes of this study, the lower boundary of the Sandstone Aquifer is estimated to be at a constant elevation of –261 ft, the depth of greenstone under sandstone in the deepest well known to have been drilled through the sandstone and completed in greenstone. The overall bottom elevation of the sandstone likely increases to the north where greenstone rocks outcrop at sea level.

The Sandstone Aquifer is bounded everywhere above by a mantle of Pleistocene deposits, mainly glacial drift, except where sandstone crops-out at land surface (Figure

10). Most of the bounding glacial drift is silt-clay diamicton that thickens toward shore and in bedrock depressions (Figures 13a, 13c, and 13e). The silt-clay diamicton overlying sandstone serves as an aquitard, creating confining conditions within the sandstone at most places below about 150 feet (land surface elevation). In these lower reaches, aquifer head frequently exceeds the height of bedrock and the entire thickness of the sandstone seems to be saturated. The aquifer may also be confined by less fractured facies of the Chuckanut Formation and near the axes of synclines mapped by Carroll (1980); (Figure 8). About 20 well logs have driller's notes that describe the depth where water was encountered (Appendix C). At most of these wells, the measured aquifer head lies above the depth where driller encountered water, suggesting that confining layers occur within the Chuckanut Formation. Due to heterogeneities of facies and structure, insufficient data exist to accurately map potential confining conditions caused by less permeable strata within the Chuckanut Formation. Using the results of a pump test, Willing (1997) concluded that wells correlating to 32M and 32Q are in confined regions of the Sandstone Aquifer. The estimated average saturated thickness of the Sandstone Aquifer is 312 ft and the unsaturated thickness is estimated to range from 50-80 ft (Table 12).

Complex bedrock structures and varying facies of the Chuckanut Formation make the fractured sandstone a highly heterogeneous medium for groundwater flow. Well log data indicate usable quantities of water were most frequently encountered above sea level during drilling, however, the majority of wells in this aquifer (61%) are completed below sea level. Several logs show that usable quantities of water were only encountered below sea level (for example, 04Z, 05P) or not at all (for example 04X, 05Q). Usable quantities of water were noted in well logs for wells with completion elevations ranging from –38 feet (08O) to about 190 feet (32X). Wells are completed at various elevations in the Sandstone Aquifer with no clear pattern, probably due to the previously mentioned heterogeneities. Well completion elevations range from –289 to 141 feet with a median value of –21 feet (Table 9). The top elevation of the sandstone ranges from elevations less than –200 feet to greater than 300 feet. I estimated the base of this aquifer to be at an elevation of –261 feet.

Greenstone Aquifer. The Greenstone Aquifer occupies 0.41 square miles of the southeastern region of the study area (Figure 15). It is the main source of water for homes along the middle stretch of Seacrest Drive and for some homes in the less densely populated upland region west of this road. Thirteen of 130 wells are completed in this aquifer. The Greenstone Aquifer is comprised of metamorphosed volcanics and marine sediments of the Fidalgo ophiolite that have an undetermined degree of fracturing.

The Greenstone Aquifer is laterally bounded by the sea to the east and by glacial drift that fill depressions in the bedrock surface on all other sides. As with the Sandstone Aquifer, the lateral extent of the Greenstone Aquifer as shown, encloses all wells known to be completed in greenstone (Figures 7 and 15). Saturated greenstone may occur at depth beneath glacial drift outside of the boundary as shown beneath Legoe Bay and Nugent aquifers. The lower boundary of the Greenstone Aquifer is undetermined and thickness is unknown. The aquifer was modeled to a depth of –300 feet, greater than the known depth of any well completed in greenstone.   Except where small bedrock outcrops are occur on Hill 275 (Figure 10), the Greenstone Aquifer is bounded everywhere above by a mantle of silt-clay diamicton that thickens toward shore (Figures 13a and 13b). Most of the aquifer seems to be confined with aquifer head exceeding the elevation of the bedrock surface below about 150 ft (bedrock elevation)/180 ft (land surface elevation).

Completion elevations for wells in greenstone range from –89 to 52 feet with a median value of –18 feet (Table 9). Well log data indicate the presence of usable water at elevations above sea level for most wells. Two well logs, 15H and 15U, did not indicate the presence of usable water. The top elevation of this aquifer ranges from approximately sea level to greater than 150 feet, though limited data make it difficult to determine accurate aquifer top elevations.

5.3.2 Pleistocene Aquifers

Nugent Aquifer. The Nugent Aquifer occupies 0.6 square miles of the southwest region of the study area and is the largest Pleistocene Aquifer (Figure 15). The Nugent aquifer is the main water source for homes in the south half of the study area, especially along the west side of the island. Twenty of 130 wells are completed in this aquifer. The Nugent Aquifer is likely in Vashon advance outwash and is comprised of sand units SU-4, SU-6, and SU-7.   The upper and inland portion of this aquifer is a thick sequence of sand and gravel (up to 92 feet) that grades to two thinner lenses of sand and fine sand in the lower reaches toward shore (Figures 12e, 12g, and 13a). The lower of these two lenses is thicker and likely more productive, as more wells are screened in it. The majority of wells are completed in the two interconnected thin lenses of sand and fine sand, close to shore where housing density is greater.

The Nugent Aquifer is bounded by greenstone bedrock to the east (and probably to the south although it is not modeled beyond the stream that forms the southern boundary of the study area), to the west by the Rosario Strait, and to the north by greenstone in the lower portion (Figures 15 and 16) and silt-clay diamicton in the upper portion. It is possible that Nugent Aquifer is connected to coarse units comprising the Legoe Bay Aquifer along its northern boundary just to the south of the eastern stretch of Legoe Bay Rd. In the southeast corner, the aquifer may extend further north than modeled (Figure 15). Here, it may extend in a narrow band along Seacrest Drive to include well 15O. The lower boundary is silt-clay diamicton associated with the base of Vashon advance outwash or possibly Cherry Point silt. The aquifer abuts greenstone along its northern, eastern, and southern interior boundary and may be underlain by bedrock at these locations (Figures 12e, 12g and 16). The upper boundary is silt-clay diamicton glaciomarine drift. The upper reaches of Nugent Aquifer are unconfined in the vicinity of 09V and to a lesser extent near 15A. The estimated average saturated thickness is 39 ft and unsaturated thicknesses range from 2 to 55 feet (Table 12).

Most of the aquifer lies below sea level (91% of saturated volume). Well completion elevations range from –118 to –1 feet with a median value of –29 feet (Table 9). The top elevation of the Nugent Aquifer is highest in the center of the island and slopes to below sea level near shore (Figures 12d, 17b, and 17c). Top elevation ranges from –39 near the east shore to 35 feet in the center of the island (Figure 12d).

Legoe Bay Aquifer. This relatively large aquifer occupies 0.40 square miles in the middle part of the study area, over the deep southeast-northwest trending bedrock trough (Figures 8 and 15). Legoe Bay Aquifer is the main source of water for homes in the middle of the study area and hosts several public water systems. Twenty-two of 130 wells are completed in this aquifer. The Legoe Bay Aquifer is in Vashon advance outwash and is comprised of sand units SU-2, SU-3, and SU-5. As with the Nugent Aquifer, the upper and inland reaches of Legoe Bay Aquifer are relatively thick (up to 107 feet) continuous sequences of sand and gravel and the lower portion of the aquifer is two thinner lenses of sand and gravel and fine sand interbedded within silt-clay diamicton (Figures 12f, 13c and 13d). These lenses are interconnected in places and the lower lens is likely more productive, as more wells are screened in it. Unlike the Nugent Aquifer, the top of Legoe Bay Aquifer probably breaches land surface, northwest of the intersection of Legoe Bay Rd and Tuttle Ln where it is overlain by emergence beach deposits (Figure 15).

The lateral extent of Legoe Bay Aquifer is shown in Figure 15 and may be related to the Village Point Aquifer that is possibly a discontinuous section of SU-3 to the west (not shown). Legoe Bay Aquifer is bounded to the west by Rosario Strait, to the east by Hale Passage, to the south by greenstone bedrock and silt-clay diamicton, and to the north by sandstone bedrock. It is possible that Legoe Bay Aquifer is connected to Nugent Aquifer along its southern boundary and probably extends a short distance offshore at Legoe Bay (Figures 15 and 26). The lower boundary is silt-clay diamicton associated with the base of Vashon advance outwash or possibly Cherry Point silt and sandstone along the northern boundary, where it abuts bedrock. The upper boundary of the aquifer is

glaciomarine drift. Most of Legoe Bay Aquifer is confined. Unconfined regions of the aquifer lie north of Legoe Bay Rd and east of Tuttle Ln (Figure 15) at land surface elevations above about the 50 to 100 foot contour line, where emergence deposits comprise the some of upper portion of Legoe Bay Aquifer. The estimated average saturated thickness is 11 ft and unsaturated thicknesses range from 2 feet near sea level to 65 feet at 05O (Table 12).

Legoe Bay Aquifer lies mostly below sea level (53% of saturated volume).   Well completion elevations range from –102 to 15 feet with a median value of –50 feet (Table 9). The top elevation of the aquifer is highest in the center of the island and slopes down to below sea level toward shore (Figures 12f , 17b, and 17c). Top elevation ranges from –28 feet in the west and –40 feet in the east to 18 feet inland near the center of the island.

Hilltop Deep Aquifer. This narrow aquifer occupies 0.13 square miles of the bottom of the east-west trending bedrock trough in the middle of the study area (Figures 8, 15, and 16). Five of 130 wells are completed in the Hilltop Deep Aquifer. This aquifer is in coarse lenses within pre-Vashon Cherry Point silt or other Olympia-age deposits and is comprised of sand unit SU-1. The aquifer is probably comprised of laterally discontinuous, relatively thin (about 4-35 feet) interconnected layers of sand and gravel and fine sand interbedded within silt and clay at various elevations (Figure 12f). Hilltop is the deepest Pleistocene aquifer. It is bounded to the north and south by sandstone, to the west by Legoe Bay, and to the east by Hale Passage. The upper and lower boundaries are silt and clay, likely Cherry Point silt or fine sediments at the base of Vashon advance outwash. The lower boundary might also be formed by bedrock. This aquifer is confined. Well completion elevations range from -228 to –171 feet with a median value of –174 feet (Table 9). Hilltop Deep Aquifer lies well below sea level with top elevations ranging from -223 feet to –165 feet (Figures 12d and 12f).

Centerview Aquifer. This small aquifer near Centerview Rd occupies 0.09 square miles of the northeast portion of the study area (Figure 15). Some adjacent wells that are not included in this study may also be screened in this aquifer.   One of 130 wells is completed in the Centerview Aquifer. The aquifer seems to be comprised, in part, by coarse sand and gravel that have filled a portion of a nearly closed depression in the bedrock surface (Figures 12c and 13e). This aquifer is likely in Vashon advance outwash or in the remnants of coarse deposits left over from older Pleistocene events.   The Centerview Aquifer is comprised of sand unit SU-22.

The presence of this aquifer is defined by only one well so its lateral extent is largely unknown.   The coarse-grained unit supporting completion of well 04Y was extrapolated to the bedrock surface on all sides and the bottom (Figures 12c and 16). Overlying till and glaciomarine drift form the upper boundary. The entire aquifer is confined with aquifer head at 04Y consistent with the head of the surrounding Sandstone Aquifer. Aquifer thickness is as much as 45 feet. Well completion elevation is 44 feet, based on 04Y (Table 9). The top elevation was modeled at a constant 59 feet, the top of the coarse-grained unit that 04Y is completed in (Figure 17a).

Blizzard Aquifer.   This small, shallow aquifer occupies 0.015 square miles south of Blizzard Rd in the northeastern portion of the study area (Figure 15). Some adjacent wells that are not included in this study may also be screened in this aquifer. One of 130 wells is completed in the Blizzard Aquifer. This aquifer is probably a sandy interbed within the glaciomarine drift and is comprised of sand unit SU-21.

The presence of this aquifer is defined by only one well so its lateral extent is largely unknown. The coarse-grained unit supporting completion of well 04H was extrapolated to the bedrock surface and to where it intersects land surface that slopes downward to the east and south (Figures 12c, 13a and 16). The aquifer is bounded to the north and west by sandstone.   To the east and south, the upper, unsaturated region intersects land surface. The lower, saturated region it is bounded by silt-clay diamicton glaciomarine drift. Upper and lower boundaries for the Blizzard Aquifer are formed by fine layers

within the glaciomarine drift. Aquifer thickness is as much as 25 ft. The aquifer is unconfined. The estimated average saturated thickness is 17 ft (Table 12) and unsaturated thickness is 6 ft at 04H. Well completion elevation is 108 feet, based on 04H. The aquifer lies entirely above sea level. The top elevation was modeled at a constant elevation of 133 feet from stratigraphic information observed in log 04H (Figure 17a).

Constitution Aquifer. This thin, shallow aquifer occupies 0.05 square miles near the eastern stretch of Constitution Rd in the southeastern portion of the study area (Figure 15). Two of 130 wells are completed in the Consititution Aquifer. One dug well, 10F, might also be completed in this aquifer, downhill from the other two wells where aquifer depth is near land surface. The Constitution Aquifer is likely in coarse interbeds within the glaciomarine drift (Figures 13b-13d). It may include Vashon advance outwash. The well log for a well that penetrates, but is not completed in this aquifer describes cemented sands.   The aquifer is comprised of sand unit SU-9. The aquifer likely contains several thin interconnected lenses of sand and gravel interbedded with thin layers of silt and clay. The aquifer is bounded on all sides by silt-clay diamicton, except along the western boundary where it abuts greenstone (Figure 13b). The aquifer may extend further to the east than modeled, intersecting land surface along the steep slope uphill from Seacrest Dr. The upper boundary is silt-clay diamicton, except along the south and western edges where portions of the aquifer are modeled to lie directly on bedrock (well 10C). The lower boundary is silt and clay. The aquifer is confined.   Aquifer thickness is from 26 ft in the upper reaches including interbeds of silt-clay layers (well 10E) to about 2 ft in the lower reaches (well 10X). Well completion elevations range from 109 to 11 feet (Table 9). The aquifer lies entirely above sea level with a top surface that slopes down to the north (Figure 17b). Top elevations range from 135 (well 10E) in the south to 113 ft in the north (well 10X).

Lane Spit and Lane Spit Deep Aquifers. These two overlapping aquifers lie in the eastern part of the study area (Figures 13a and 15). Two layers of coarse material are separated by 40-100 ft of silt-clay diamicton over 0.06 square miles at Lane Spit (Figures 12b and 13e). Five of 130 wells are completed in these two, moderately sized aquifers that support a relatively high density of wells. More wells are completed in the Lane Spit Aquifer than the underlying Lane Spit Deep Aquifer. The upper aquifer is likely in Vashon advance outwash. The lower aquifer is probably in a coarse unit within the Cherry Point silt.

The Lane Spit Aquifer is comprised of sand units SU-24 and SU-26 that are made up of clean, fine sands. The aquifer is more laterally extensive than the underlying Lane Spit Deep Aquifer because it abuts sandstone further inland (Figures 12b and 15). This aquifer probably extends some distance offshore beneath Hale Passage, especially to the north and east, where bathymetry slopes gently (Figure 26). The upper boundary is silt-clay diamicton till and glaciomarine drift. In the southwest corner, the overlying silt-clay diamicton thins to about 3 feet and the aquifer nearly breaches land surface (Figure 13e). Aquifer thickness is 40 feet in most places but thickens in the southwest corner to about 75 feet. The aquifer is confined except in the southwest corner where aquifer thickness is greater. The estimated average saturated thickness is 17 ft (Table 12). Unsaturated thickness is approximately 3 feet at 04A. Well completion elevations range from –66 to –35 feet (Table 9). The aquifer lies below sea level. The top surface slopes down steeply to the east and north (Figure 17a). Top elevations range from –121 feet in the north and east to 6 feet in the southwest corner near 04A.

The Lane Spit Deep Aquifer is comprised of sand unit SU-23 that is probably made up of a mixture of sand and gravel bounded by silt and clay. The presence of this aquifer is defined by only one well. The coarse-grained unit supporting completion of well 33F was extrapolated inland to the bedrock surface to the and to the surrounding shoreline (Figure 13e). As modeled, the aquifer is bounded by Hale Passage on three sides and sandstone to the west, but probably extends some distance offshore due to the shallow

bathymetry in Hale Passage (Figure 26). The lower boundary is a silt-clay diamicton, likely associated with the Cherry Point silt. The upper boundary is silt, clay and sand associated with either Cherry Point silt or the fine-grained base of Vashon advance outwash. Aquifer thickness is estimated to be 14 feet based on log 33F. The Lane Spit Deep Aquifer is confined. Well completion elevation is –196, based on 33F. The entire aquifer lies below sea level with a top elevation of –181 feet, based on log 33F.

Loganita and West Shore Aquifers. These two small aquifers occupy depressions in the bedrock surface in the northeast portion of the study area (Figure 15). Two of 130 wells are completed in the Loganita Aquifer and one is completed in the West Shore Aquifer. These two aquifers are in Vashon advance outwash. Loganita Aquifer has an area of less than 0.04 square miles, is sand and gravel and comprised of sand units SU-28 and SU-29. West Shore Aquifer has an area of less than 0.04 square miles, is fine to coarse sand and comprised of sand unit SU-27.

The coarse-grained units supporting completion of wells 32P, 32R, and 32H were extrapolated to the bedrock surface to the and to the shoreline (Figures 12a and 15). These aquifers are laterally bounded by Rosario Strait to the west, where they probably terminate very near shore due to steep bathymetry (Figure 26). On all other sides, they are bounded by sandstone. They are bounded above by silt-clay diamicton till and glaciomarine drift. The lower boundary of the Loganita Aquifer is a mixture of silt, clay, and sand likely associated with Cherry Point silt. The lower boundary of the West Shore Aquifer is sandstone.

The Loganita Aquifer is comprised of two overlapping sand lenses that are separated by a layer of silt-clay diamicton. These sand lenses converge toward the shoreline in the southern portion of the aquifer. The upper lens is unsaturated (Figure 12a) with an average thickness of 20 ft (Table 12). The lower lens is saturated with a thickness of 14 feet at 32R. The estimated average saturated thickness is 21 ft (Table 12). The Loganita

59

Aquifer is thickest in the south where the two sand lenses converge. Aquifer thickness in this region is approximately 40 feet. Loganita Aquifer is confined except where the overlying unsaturated sand unit converges with the lower saturated unit in the southern part of the aquifer. The West Shore Aquifer is thickest (75 feet) at 32P, where it is projected to be in contact with the modeled bedrock surface (Figure 12a). This aquifer is confined.

These aquifers lie mostly below sea level. For the Loganita Aquifer, 100% of the saturated volume lies below sea level. For the West Shore Aquifer, 55% of the saturated volume lies below sea level. Well completion elevations are –47 feet for Loganita and –2 feet for West Shore aquifers (Table 9). The top surface of these aquifers slopes down to the north (Figure 17a). The top elevation of Loganita Aquifer ranges from –44 feet to 25 feet. The top elevation West Shore Aquifer is 13 feet at well 32P.

Village Point Aquifer. This aquifer was not modeled due to limited well log and well location data. Few wells exist in the vicinity of Village Point. The presence of this aquifer is based on descriptions from well logs 05AA, 08G, and 08W. From these logs, it appears that there is a lens of coarse-grained material that extends east from Village Point (Figure 15). The lateral extent of the aquifer is unknown. It is probably bounded by the sea to the west and south and by bedrock to the north and east to near well 08O. The texture of the Village Point Aquifer ranges from clean gravel to fine sand with thin silt-clay interbeds. This aquifer is confined. Well completion elevation is –84 feet, based on 08G. The top surface of this aquifer has an elevation of approximately -90 feet. The location and estimated top elevation of this aquifer suggest that this is related to the lower sand unit of the Legoe Bay Aquifer (SU-3). It is separated from Legoe Bay Aquifer by a buried ridge of sandstone near well 08O.

Glaciomarine Drift and Emergence Deposits. Numerous dug wells exist on Lummi Island. The prevalence of dug wells in the study area warrants brief discussion. Most dug wells are no longer used for drinking water because they are highly susceptible to seasonal water level fluctuations and contamination from surface sources. According to residents, seawater intrusion forced the abandonment of several dug wells dug into beach gravels along the southern shoreline of Lane Spit. Six dug wells were included in this study. These wells are mostly in thin coarse sand and sand and gravel deposits overlying glaciomarine drift. These coarse deposits are emergence deposits or perhaps a combination of emergence deposits and Holocene beach gravels, as seen along the southern shoreline of Lane Spit. However, 3 of 6 dug wells used in this study (10D, 10F, 33X) may be drawing water from thin sand lenses within the glaciomarine drift confining unit.

5.4 Hydraulic Properties

Properties of hydrostratigraphic units that are important in understanding the hydrogeology of the study area are well yield, specific capacity, effective porosity, transmissivity, and hydraulic conductivity. Well logs for about 80 wells contained sufficient well performance and screened interval data to estimate values for most of these hydraulic properties at each well (Tables 13a and 13b). The hydraulic properties at each well were combined with data from published reports and the results of the stratigraphic model and revised geologic interpretation to estimate the hydraulic properties of each aquifer.

5.4.1 Well Yield

Well yield is commonly used to predict the productivity of a newly drilled well and to a lesser extent, can be used to qualitatively assess the relative productivity of an aquifer. Well yield is generally measured by drillers during well performance testing and recorded on well logs (also known as the pumping rate). In theory, these data represent the maximum sustainable pumping rate that a given well will support, irrespective of drawdown. Well yield results are dependant on well construction, aquifer productivity, and well performance testing methods.

Well yields for 101 study wells range from 0.5-60 gpm with a median value of 10 gpm (Table 14). The same range applies to wells completed in bedrock with a median value of 8 gpm. The lowest yield of any aquifer is for wells completed in the Greenstone Aquifer. They ranged from 0.5-35 gpm with a median value of 2 gpm. Wells completed in Pleistocene aquifers had higher yields than bedrock. Their yields ranged from 1-30 gpm with a median value of 10 gpm. The wells in the Legoe Bay Aquifer had the lowest yields for Pleistocene deposits that ranged from 1-20 gpm with a median value of 6.5 gpm. Relatively low well yields likely explain why numerous sites were observed to use storage tanks.

5.4.2 Specific Capacity

The specific capacity of a well is an expression of well construction and aquifer productivity. It is a function of well construction and aquifer properties, and can be used to estimate aquifer properties such as transmissivity. Water-well drillers typically conduct a water well performance test at the time of drilling. During a well performance test, water is withdrawn from the new well at a constant rate, usually with a bailer on Lummi Island, until the water level reaches a nearly static state. The pumping rate, pumping duration, and "static" water levels before and after pumping are recorded in the well log. These data can be used to estimate the specific capacity, expressed in units of gallons per minute per foot of drawdown (gpm/ft), for a well using the equation found in Section 5.4.2. Nine well logs indicated zero drawdown during well performance testing and were not used to calculate specific capacity because the pumping rate was insufficient to stress the aquifer (Table 16). Zero drawdown might be caused by errors during well performance testing or could indicate strata that are highly productive.

The specific capacity for 83 wells ranged from 0.01 to 12 gpm/ft with a median value of 0.17 gpm/ft (Table 15). The specific capacity for wells completed in bedrock are lower than wells completed in Pleistocene deposits. Wells in the Greenstone Aquifer display the lowest specific capacity values that range from .01 to 0.44 gpm/ft with a median value of 0.06 gpm/ft. Wells completed in the Nugent Aquifer display the highest specific capacity values that range from 0.04 to 7.5 gpm/ft with a median value of 0.65 gpm/ft.

The median specific capacity values for wells in Pleistocene deposits are comparable to values in similar geologic material examined during other studies of hydrogeology in the region. For example, a perched aquifer system comprised of Vashon advance outwash deposits on Bainbridge Island showed specific capacity values that range from 0.2 to 16

63

gpm/ft with a median value of 0.5 gpm/ft (Warren, 2000). He also estimated specific capacity values in Tertiary sedimentary rocks to be less than .1 gpm/ft. This value is close to median values for bedrock that I derived during this study. Using results of a pump test, Willing (1997) concluded that the specific capacity of a well completed in glacial drift, correlating to 32P, is 0.94 gpm/ft. Willing's estimate for specific capacity of this well is 55% lower than my estimate (Table 13b). He also stated that a well completed in sandstone, correlating to 32N, has a specific capacity of 1.7 gpm/ft (I did not estimate specific capacity for this well due to insufficient well performance test data in the well log). Most sources of error associated with estimating specific capacity that apply to my study will cause bias favoring overestimation (Appendix A).

5.4.3 Porosity

Total porosity, referred to as porosity, is the percentage of the total volume of an earth material that is not occupied by solids and is defined by the following equation (Freeze and Cherry, 1979):

$$n = V_v/V_t$$

where n = porosity (expressed as a portion of total volume)
V_v = volume of void space
V_t = total volume of geologic material (volume of solids + volume of void space)

The porosity of sand ranges from 25-50% (Freeze and Cherry, 1979). The porosity of silt is 35-50% and the porosity of clay is 40-70%. The porosity of the silt-clay diamicton of glaciomarine drift probably lies somewhere within the average of these ranges. However, the poorly-sorted diamicton contains numerous larger clasts such as pebbles and cobbles. These decrease overall porosity. Assuming that the fraction of clasts larger than 2mm (sand-size) in glaciomarine drift is approximately 40% (Easterbrook, 1962),

64

the overall porosity of glaciomarine drift ranges from 21-30% for diamicton dominated by silt, and 24-42% for diamicton dominated by clay.

Primary porosity represents the interstitial void space between grains of unconsolidated material or bedrock. Porosity is higher for unconsolidated materials than for bedrock (Freeze and Cherry, 1979). Diagenetic processes (cementation of grains during the lithification of sediments) reduce the primary porosity in rocks. Primary porosity is low for sandstone, 5-30%, (Freeze and Cherry, 1979) and for rocks comprising greenstone, near zero for metamorphic rocks, and 1-12% for basalt (Fetter, 1980). However, post-lithification stresses on rocks and the preferred orientation of bedding planes formed during the deposition of sedimentary rocks create discontinuities, fissures, joints, and fractures that increase overall porosity. This is described as secondary porosity. Groundwater flow in hard rocks is a function of secondary porosity.

Effective porosity is defined as the amount of interconnected pore space available for fluid flow and is usually less than total porosity (Fetter, 1980). Groundwater flow is inhibited by dead-end pores and frictional resistance on the surfaces of aquifer media. Average effective porosities were estimated by comparing dominant textures to published values for each sand unit (Tables 7a-7c). Values for sand units that comprise aquifers were used to assign average effective porosity to each aquifer (Table 22).

5.4.4 Transmissivity

Transmissivity is the rate at which water is transmitted through a unit width of aquifer (Fetter, 1980). It is defined as the product of hydraulic conductivity and aquifer thickness. Values for transmissivity were calculated from well performance test data in well logs (Appendix A). Transmissivity values for 77 wells ranged from 0.5 to 2146 ft^2/day with a geometric mean of 40.2 ft^2/day (Table 17). The transmissivity for wells completed in Pleistocene deposits are much higher than wells completed in bedrock. Wells in the Greenstone Aquifer display the lowest transmissivity values that ranged from 0.7 to 22.8 ft^2/day with a geometric mean of 3.7 ft^2/day. Transmissivity values for

wells in the Nugent Aquifer are among the highest.   These values ranged from 9 to 2146 ft^2/day with a geometric mean of 132 ft^2/day.

The geometric mean of transmissivity values for wells in Pleistocene aquifers are comparable to values in similar geologic material examined during other studies of hydrogeology in the region.   For example, a perched aquifer system comprised of Vashon advance outwash deposits on Bainbridge Island showed transmissivity values that range from 44 to 2746 ft^2/day with a median value of 372 ft^2/day (Warren, 2000). Warren estimated transmissivity values in a glaciomarine drift aquifer range from 1.7 to 401 ft^2/day with a median value of 23.4 ft^2/day. Willing (1997) used a pump test to determine transmissivity in 4 wells completed in sandstone on north Lummi Island. These values ranged from 118 to 225 ft^2/day. Most sources of error associated with estimating transmissivity that apply to this study will cause bias favoring overestimation (Appendix A).

5.4.5 Horizontal Hydraulic Conductivity

 Hydraulic conductivity is the rate at which water can move through a permeable medium (Fetter, 1980).   Transmissivity estimates for 77 wells were used to determine horizontal hydraulic conductivity (Kh) values that ranged from <0.01 to 429.2 ft/day with a geometric mean of 1.87 ft/day (Table 18). As with transmissivity, Kh values for wells completed in Pleistocene deposits are much greater than wells completed in bedrock. Wells in the Greenstone Aquifer display the lowest Kh values that range from <0.01 to 0.3 ft/day with a geometric mean of 0.04 ft/day.   Horizontal hydraulic conductivity values for wells completed in the several small Pleistocene aquifers are highest. Values for Kh at wells in the Loganita, Village Point, and West Shore aquifers ranged from 51.4 to 94.9 ft/day. However, these values were determined from only one well in each aquifer. Values for Kh in the Nugent Aquifer are among the highest and are based on 17 wells. These ranged from 0.4 to 429.2 ft/day with a geometric mean of 12 ft/day.

The geometric mean of Kh values for wells in Pleistocene aquifers, 9 ft/day (Table 18) are comparable to values in similar geologic material examined during other studies of hydrogeology in the region. For example, a perched aquifer system comprised of Vashon advance outwash deposits on Bainbridge Island showed Kh values that range from 2 to 3481 ft/day with a median value of 36 ft/day (Warren, 2000). Warren estimated Kh values in a glaciomarine drift aquifer range from 0.2 to 80 ft/day with a median value of 2 ft/day. The geometric mean for all wells completed in glacial drift correlates to textbook values for material ranging from silty sands to clean sands (Freeze and Cherry, 1979; Watson and Burnett, 1995). The Kh values that I have estimated tend to lie closer to text book values for clean sands. Pleistocene aquifers that likely correlate to Vashon advance outwash have higher Kh values than ones that likely correlate to coarse-grained interbeds within glaciomarine drift (Blizzard and Consitution aquifers), further validating the stratigraphic model.

The geometric mean of Kh values for wells in the Sandstone Aquifer (Table 18) lie in the upper range of textbook values for fractured sandstone (Freeze and Cherry, 1979). This indicates that water bearing strata within the Chuckanut Formation is probably highly-fractured. This conclusion is supported by Kh values derived by Willing (1997). Willing did not directly estimate Kh for wells completed in sandstone. However, from transmissivity values in his report and saturated open intervals for two wells that are also included in my study (32Q and 32M), I determined Kh ranged from 1.4 to 2.4 ft/day, respectively. In his report on the hydrogeology of Bainbridge Island, Warren (2000) estimated Kh values in Tertiary sedimentary rocks to be less than 10 ft/day. The geometric mean of Kh values for the Greenstone Aquifer (Table 18) lies within the range of textbook values for fractured metamorphic rocks (Freeze and Cherry, 1979). Most sources of error associated with estimating horizontal hydraulic conductivity that apply to this study will cause bias favoring overestimation (Appendix A).

5.5 Water Level Trends and Groundwater Flow Patterns

5.5.1 Water Levels

Static water-level data representing total aquifer head were collected from study wells in fall 2002 and spring 2003. These periods were chosen to approximately coincide with the low and high water levels, respectively. Precipitation during 2002 was below average (Section 2.4 and 5.7.2) so water levels measured during the fall of 2002 should represent some of the lowest levels that can be expected.

Differences in water levels between fall 2002 and spring 2003 vary by aquifer and are small for most of the 78 wells measured during both periods (Table 19). For all wells, changes in water levels range from less than 0.02 to 26.6 feet with a median value of 0.2 feet (Table 20).   Water level changes between the two measuring periods are greatest for wells in the bedrock aquifers and small for most wells in Pleistocene aquifers (Figure 18). The changes in water levels for the Sandstone Aquifer range from less than 0.02 to 26.6 feet with a median value of 1.5 feet. Water levels in the Greenstone Aquifer were lower in spring than fall, ranging from -0.4 to –15.2 feet with a median value of -1.9 feet. The greatest water level changes, 26.6 feet (33M), 23.4 feet (32S), -15.2 feet (09C), are outliers with magnitudes twice that of other wells in bedrock (Table 19). Owner's notes indicate that 33M dried-up in September, 1994. Although water level fluctuations recorded during a previous study (Whatcom County, 1994) exceed these magnitudes, further study is required to confirm that error is not responsible for these outliers. Water levels in similar bedrock in the Gulf Islands of British Columbia have been observed to vary dramatically with seasons (Allen, personal communication, 2005). Water level changes for all wells completed in Pleistocene deposits range from 0.1 to –2.4 with a median value of -0.2 feet. Dug wells have greater water level changes than wells drilled into the Pleistocene aquifers (Table 20 and Figure 18).

The cause of greater fluctuations in water levels between measuring periods in the bedrock aquifers is likely due to much lower storage, making the bedrock more sensitive to seasonal changes in water input and withdrawal than the Pleistocene aquifers. Water level changes between fall 2002 and spring 2003 within the bedrock aquifers were positive in places and negative in others. In the Sandstone Aquifer, the greatest water level changes were positive (water levels higher in spring) and occurred in the north part of the aquifer, where topography and relief are highest (Figure 18). Negative water level changes were less common with most occurring in the southern part of the Sandstone Aquifer, where a cluster of 4 wells in the vicinity of the intersection of Sunny Hill and Tuttle Lanes all showed negative changes. The cause of negative changes in water levels during spring 2003 compared to fall 2002 is unknown, but could due to the influence of nearby pumping wells, especially because wells showing the greatest negative water level changes are in bedrock. Low storage in bedrock aquifers causes water levels to be more susceptible to the influence of nearby pumping wells.

Water level fluctuations in Pleistocene aquifers between fall 2002 and spring 2003 are a muted reflection of the greater water level changes that occur within the bedrock. Most Pleistocene aquifers lie below sea level. Although several may be in hydraulic continuity with saturated regions of the bedrock, they are located well below the range of water level fluctuations in the bedrock aquifers. Long flow paths from recharge areas to Pleistocene aquifers induce head losses caused by friction. This, and the increased storage of Pleistocene aquifers likely explain why water level fluctuations within these aquifers are much smaller than in bedrock. Water levels in Pleistocene aquifers are probably more affected by long-term precipitation and withdrawal trends than seasonal fluctuations.

Some island residents have reported that their wells dry-up, especially in late summer. This problem is likely limited to wells that are completed in shallow or isolated water-bearing strata. In bedrock, this is probably caused by wells that are drilled too shallow and are completed in the upper region of the aquifer, within the range of seasonal water

level fluctuations that can be exacerbated by nearby pumping wells. In the Pleistocene aquifers, where seasonal water level fluctuations are small, some wells may go dry because they are completed in shallow, discontinuous sand lenses. Others may go dry due to the influence of nearby pumping wells. During the course of this study, one public water system well pumped continuously for approximately 18 months due to a leak in the water distribution system. In at least one case, the cause of a public water system well "drying-up" turned out to be fouling of the well screen or pump intake by fine sediments or bacterial growth.

Examination of Previous Water Level Monitoring

Monthly water levels were measured by volunteers between March 1991 and January 1993 (Whatcom County, 1994) and 7 wells with complete water-level data sets correlate to wells that I monitored during my study (Table 21). Water-level data from these wells were used to create hydrographs (Figure 19). Data from wells that do not correlate to ones used in my study were used to develop 8 additional hydrographs (Figure 20). The scales on these two sets of hydrographs are different because the well-head elevations for the 8 additional wells were not measured. Therefore, depth-to-water measurements from Whatcom County, 1994 could not be converted to elevations for the 8 additional wells. A hyetograph that spans the 1991-1993 monitoring period was created from precipitation data collected by volunteers on Lummi Island (Figure 21; Whatcom County, 1994).

The lag time between a significant change in precipitation patterns and response within the aquifers is from 1-2 months. Lag times are shorter and water level response is greater for wells with higher water level elevations in bedrock aquifers. These water levels closely mimic precipitation patterns, indicating that the wells are in unconfined and recharge regions of the aquifer. Water levels are highest in March and decline slowly until late spring. June 1991 and June 1992 show a marked decline that generally continues until late fall. The lowest water levels are from October through November. The marked decline in June of both years is probably in response to exceptionally dry months of May rather than the influx of seasonal residents and increased irrigation that commence in late May. Seasonal water level changes recorded during the 1991-1993

monitoring period are comparable to changes that I observed during 2002-2003. Water level changes in the Sandstone Aquifer range from 1.7 to 22.4 feet. Maximum seasonal water level changes in two Pleistocene aquifers are 1.1 feet and 0.9 feet for the Legoe Bay and Nugent aquifers, respectively. For the wells in Table 21, the differences in water levels between 1991-1993 and 2002-2003 range from –5.5 to 0.3 feet with a median value of -0.7 feet. I do not consider this slight decrease to be a significant indication of long-term water level trends because it is based on data from only 7 wells and lies within the range of water level fluctuations for all aquifers (Table 20).

5.5.2 Groundwater Flow Patterns

In homogeneous, isotropic media, groundwater flows from regions of higher to lower hydraulic head. The change in hydraulic head over a distance is the hydraulic gradient. The hydraulic head distribution across an aquifer is called a potentiometric surface (imaginary hydraulic pressure surface). The potentiometric surface is equal to the water table (depth where water is encountered) for unconfined areas and can lie above the top of the aquifer or land surface in semi-confined and confined areas. The potentiometric surface is represented as a contour map that is created from water-level measurements (representing total head) at wells scattered across an aquifer (potentiometric map). Horizontal groundwater flow is perpendicular to the contour lines (from high head to low head) in potentiometric maps. The vertical component of groundwater flow can be important, especially near recharge and discharge areas and areas of higher topographic relief. Estimates for vertical groundwater flow directions are difficult to make except where water levels are measured in closely spaced wells that share the same aquifer and have different completion depths.

Groundwater flow patterns (direction and hydraulic gradient) were estimated from water-level data for the largest aquifers. Because overall variation in water levels was negligible between fall 2002 and spring 2003, potentiometric maps were constructed from the spring water-level data. Groundwater flow directions in some smaller aquifers

with limited water-level data points were estimated using the three-point technique to gain a general understanding of the direction of groundwater flow.

Hydraulic gradient decreases with increased transmissivity. Horizontal hydraulic conductivity varies greatly between bedrock and Plesitocene aquifers. Geometric mean Kh values for all wells in bedrock is 0.2 ft/day and for all wells in Pleistocene aquifers is 9 ft/day (Table 18). The steepest hydraulic gradients occur in the bedrock aquifers. Aquifer thickness varies considerably across the unconsolidated Nugent (2-92 feet; SU-4) and Legoe Bay (2-107 feet; SU-5) aquifers (Table 6). Where relatively thick regions of the aquifer occur, total head values and hydraulic gradient are lower than surrounding, thinner regions. Areas where aquifer head is relatively low tend to coincide with parts of the aquifer that have been modeled as being thicker, further validating the stratigraphic model (Figures 22b and 22c).

Sandstone Aquifer Groundwater Flow Patterns

A potentiometric map for the Sandstone Aquifer was created from 38 water-level measurements taken at wells completed in sandstone in spring, 2003 (Figure 22a). The shoreline serves as the outer perimeter boundary for this potentiometric map. Overall groundwater flow direction in the Sandstone Aquifer is from the topographically higher inland region toward shore in a radial pattern. Groundwater flow in the Sandstone Aquifer generally follows the topography of the bedrock surface. To a lesser extent, it also follows land surface topography that is largely controlled by the bedrock. Three groundwater divides create three groundwater flow regions.

Groundwater flow patterns derived from a potentiometric map do not account for heterogeneities within the aquifer media such as varying orientations of fractures and bedding due to local geologic structures or less permeable facies. This may cause local flow directions to differ from those indicated by the potentiometric map. If there is preferential groundwater flow along the oriented bedding planes, then groundwater flow

directions may reflect the geologic structures (anticline-syncline pairs) occurring in the north half of the study area (Figure 8). The effect of these structures on groundwater flow is unknown, but they likely greatly increase the degree of fracturing. If the anticline-syncline pairs have a substantial effect on groundwater flow directions, it might cause groundwater to diverge from the axes of anticlines and converge along the axes of synclines. Groundwater flow would then be along the axes of the synclines toward regions of lower hydraulic head. One region where geologic structure may control groundwater flow is in the southwest corner of the Sandstone Aquifer, near Village Point. A hypothesis is that groundwater flow converges along the axis of the southern-most syncline north of Village Point and follows the center of this structure to discharge into the sea to the northwest and into coarse units that fill a deep bedrock trough to the southeast (Figures 8 and 22a). If this is the case, the synclinal structure might act as a barrier to flow, isolating the area north to the Village Point from the broader flow of groundwater within the Sandstone Aquifer. Water-level data in this region are too scarce to confirm this hypothesis.

One hypothesis for groundwater movement in the Chuckanut Formation is that flow is controlled by fractures within the sandstone. Another is that flow is controlled by closely-spaced fractures in the fine-grained facies. In the Gulf Islands of British Columbia, Allen et al. (2001) and Allen and Matsuo (2002) used hydrochemistry and borehole geophysical data to support a hypothesis that groundwater flow in sedimentary rocks that are similar to the Chuckanut Formation is concentrated along fractures that are most abundant in fine-grained facies such as mudstone and shale. They estimate that the fine-grained facies have closer fracture spacing than sandstone and serve as aquifers while the sandstone serves as an aquiclude/aquitard. Additionally, they note that most wells in the Gulf Islands are completed in fine-grained bedrock facies. Although insufficient data exist to determine which hypothesis is dominant, water chemistry results from my study (Section 5.8.1) suggest that flow is concentrated in the fine-grained facies. It is likely that a combination of flow in fine-grained and sandstone facies is occurring.

Total head elevations range from 1 feet (08O) to 223 feet (32W). The hydraulic gradient in the Sandstone Aquifer ranges from 0.08 (424 ft/mile) in the north, to less than 0.035 (183 ft/mile) in the southeast. The hydraulic gradient is greatest where the surface of the sandstone is steep and overlain by glacial drift. Hydraulic gradient is less in the southeast and center regions of the sandstone where the bedrock surface is not as steep and overlying glacial drift is relatively thin. Estimated average linear velocities range from 0.062 ft/day in the southeast to 0.089 ft/day in the north. In the Gulf Islands, travel times in sedimentary aquifers are estimated to be as little as 6 months (Allen, personal communication).

Nugent Aquifer Groundwater Flow Patterns

A potentiometric map was created for the Nugent Aquifer using water-level measurements taken from 15 wells screened in the aquifer during spring 2003 (Figure 22c). The shoreline serves as the outer perimeter boundary for this potentiometric map. Two groundwater divides separate the aquifer into three flow regions. In the northern region, groundwater flows from the center of the island to the east, perpendicular to shore. It is possible that the Nugent and Legoe Bay Aquifers are connected at the northern part of the Nugent Aquifer (Figure 15). Head values for each aquifer are similar in the area where these aquifers lie adjacent to each other. Therefore, a portion of groundwater flow may also be to the north, into the Legoe Bay Aquifer. Aquifer thickness likely controls groundwater flow in the middle and southern regions of Nugent Aquifer. In these regions, groundwater flow is largely sub-parallel to shore through the thicker inland portions of the aquifer (Figures 12g, 13a, 13d, and 22c) . This flow converges and discharges to sea where the aquifer thickens near the shoreline in the vicinity of 09G and 16K (Figures 13b and 22c). Groundwater flow in the southern-most portion of the aquifer along Sunrise Rd is from east to west. The report by Schmidt, 1978, indicates similar groundwater flow directions in the aquifer parallel to Sunrise Rd. Total head elevations range from 4 feet (16V) to 18 feet (09J). The hydraulic gradient in Nugent Aquifer is uniform throughout the aquifer and has a magnitude of 0.0044 (23 ft/mile). Estimated average linear velocity is 0.196 ft/day.

Legoe Bay Aquifer Groundwater Flow Patterns

The potentiometric map created for the Legoe Bay Aquifer using 13 wells illustrates a groundwater divide that separates the aquifer into two flow regions (Figure 22b). The shoreline serves as the outer perimeter boundary for this potentiometric map. In the eastern region, groundwater flows east and southeast into Hale Passage. In the western region, groundwater flows south and west into Legoe Bay. Total head elevations range from 15 feet to 7 feet. The hydraulic gradient in Legoe Bay Aquifer is uniform throughout the aquifer and has a magnitude of 0.0028 (15 ft/mile). Estimated average linear velocity is 0.65 ft/day.

Greenstone Aquifer Groundwater Flow Patterns

Water-level data was insufficient to create a reliable potentiometric map for the Greenstone Aquifer. Water levels from only 4-5 wells completed in the Greenstone Aquifer were measured during this study. Water levels taken at the time of drilling were used from 4 additional wells to create a rough potentiometric map (not shown).

A northwest-southeasterly trending groundwater divide seems to follow the crest of the greenstone bedrock surface (Figures 8 and 15) and separates groundwater flow into two regions. In the eastern region, groundwater flow is primarily to the east into Hale Passage. However, a distinctive groundwater low occurs in the middle of the eastern region defined by wells 10B, 10J, and 10Y. Groundwater may converge into this low as it flows toward Hale Passage. Flow is also to the northeast, into the deep east-west trending bedrock trough in the middle of the study area. In the western region, groundwater flow is primarily to the west, passing beneath Pleistocene sediments that fill a depression in the bedrock surface, into Rosario Strait. Total head elevations range from 167 ft (10P) to 55ft (10J). The estimated hydraulic gradient within the Greenstone Aquifer (0.095 or 500 ft/mile) is steeper than gradients in the Sandstone Aquifer.

Aquifers with Limited Water-Level Data Groundwater Flow Patterns

Insufficient water-level data are available to support water level contour mapping of the smallest aquifers in the study area. Groundwater flow directions for these aquifers were estimated from water levels measured during this study, and to a lesser extent, water levels listed in well logs at the time of drilling. A three-point solution from available data indicates groundwater flow in the Lane Spit Aquifer is to the southeast, perpendicular to the southern limb of Lane Spit. Total head elevations range from 1 ft (33J) to 12 ft (33T) and decrease to the southeast where the aquifer is thicker. Groundwater flow within the Lane Spit Deep Aquifer is undefined and may be similar to the Lane Spit Aquifer. Groundwater flow in the Loganita and West Shore aquifers is estimated to be perpendicular to the shoreline from east to west, primarily through the thicker regions of each aquifer. The Centerview Aquifer occupies a depression within the saturated sandstone surface and is overlain by silt-clay diamicton that creates confining conditions. The one water level measurement for this aquifer is consistent with the head distribution of the surrounding Sandstone Aquifer. Groundwater flow in the Centerview Aquifer is probably in the same direction as the Sandstone Aquifer, which is to the southeast at this location. Groundwater flow within the Blizzard Aquifer is unknown, but probably to the southeast, away from its contact with sandstone, possibly toward a topographic depression that is drained by a southeasterly flowing surface stream. Groundwater flow within the Constitution Aquifer is probably to the north. Total head elevations range from 133 (10E) to 157 feet (10C). The Village Point Aquifer is not included in the stratigraphic model, but several well logs indicate its presence at Village Point. Groundwater flow directions within this aquifer are probably to the south, perpendicular to the shore along Legoe Bay.

5.6 Total Groundwater Storage Capacity (static estimate)

Estimating groundwater quantities is an essential component of this study. One method is to estimate the total groundwater storage capacity of the aquifers from the product of the saturated volume and the average effective porosity of each aquifer. This approach greatly overestimates the volume of water that is available for exploitation. The stratigraphic model created in this study provides an estimate for the total volume of each aquifer. Water-table data from spring 2003 were used to define the saturated volume of each aquifer (Table 12). Well-log data and the stratigraphic model were used to assign average effective porosities to each aquifer (Section 5.4.3).

The resulting total groundwater storage capacity estimate represents all groundwater in aquifer media that is available for fluid flow (Table 22). The total groundwater storage capacity for all aquifers in north Lummi Island is 1.05×10^5 acre-feet. This volume, if spread out over an area equal to that of the study area, would reach a thickness of 42 feet. The aquifer with the greatest amount of groundwater in storage is the Sandstone Aquifer, 8.17×10^4 acre-feet. The sum of the volume of water in storage in all of the Pleistocene aquifers is 7.33×10^3 acre-feet or 9% of the volume of water in storage in the Sandstone Aquifer. Assuming that the entire volume of the silt-clay diamicton is saturated (a saturated volume was not estimated) and assuming a porosity of 0.5 (Table 22), the volume of water in storage in silt-clay diamicton is 9.2×10^4 acre-feet.

The method I used to quantify total groundwater in storage provides a static estimate. Changes in hydraulic head within the aquifers will result in changes of the volume of water held in storage. This method greatly overestimates the volume of water available for exploitation (Appendix A). However, it establishes a baseline groundwater quantity that can be used to validate other methods and for examining long-term trends in groundwater quantity.

5.7 Recharge

Recharge to north Lummi Island aquifers is from precipitation.   One possible exception is on the south end of the study area where a portion of the Nugent Aquifer may receive recharge from the north slope of Lummi Mountain that lies outside of the study area boundary. Recharge probably occurs everywhere except where the slope is steep, along the shoreline and on the eastern slope of Richards Mountain. The contribution of septic effluent was concluded to be small on nearby Guemes Island (Kahle and Olsen, 1995) and is probably small in the study area.

Mechanisms of Recharge

Conditions potentially affecting recharge such as slope, soils, and geology were examined to identify factors controlling recharge. These conditions indicate recharge is largely controlled by evapotranspiration.

A slope analysis of a USGS 10m-DEM using GIS was accomplished. Results indicate that average slope is 5 degrees, with only 4% of the study area having slope greater than 15 degrees (Table 23 and Figure 23). Most steeply sloping areas are along the shoreline. This, and the relatively low land surface gradient implies that slope is not a major factor limiting recharge.

Although recharge can be attenuated by soils with low infiltration capacities, this does not appear to be the case on north Lummi Island. Soils cover bedrock and glacial drift to a depth of 3.3 feet in most places (Soil Conservation Service, 1980). The area-weighted average infiltration capacity of these soils is 1.25 in/hr and rainfall intensities exceeding this value are rare. In their study, Bauer and Mastin (1997) concluded that because soils overlying till are saturated for most of the wet season, recharge rates are dependent on the hydraulic properties of the underlying material. However, given the horizontal hydraulic conductivity of the sandstone that (Section 5.4.5), bedrock will rarely serve to limit recharge. And, recharge is greatly enhanced by glacial sediments overlying bedrock.

Despite the relatively low hydraulic conductivity of bedrock that is much less than glacial drift (Section 5.4.5), most recharge on north Lummi Island probably occurs from infiltration into bedrock (via overlying sediments). The bedrock is mantled by at least a thin veneer of soil and glacial drift (mostly glaciomarine drift) at most places and outcrops are not common (Section 5.1). These sediments assist infiltration by decreasing runoff and providing storage that releases water to the bedrock at a rate comparable to its infiltration capacity.   The Sandstone Aquifer occupies about 56% of the study area and is modeled to be in contact with seven Pleistocene aquifers. Even with a lower capacity to transmit water from the surface, the large area of this aquifer ensures that significant volumes of water reach the water table in sandstone. This process is also responsible for recharge to the Greenstone Aquifer that is modeled to be in contact with two Pleistocene aquifers. Recharge to bedrock aquifers is also important because flow from these aquifers likely provides some recharge to Pleistocene aquifers that are in contact with saturated bedrock. Flow along the bedrock contact with overlying glaciomarine drift (Figure 14) may also be an important mechanism for recharge where this contact intersects coarse-grained Pleistocene deposits.

Infiltration through silt-clay diamicton and coarse-grained lenses near the surface are important mechanisms for recharge of the Pleistocene aquifers. Glaciomarine drift is the most abundant material over the study area (Figure 10) and probably plays a role in recharge, particularly where semi-confined conditions exist. The silt-clay diamicton of glaciomarine drift has a fine fraction dominated by silt-sized particles, not clay (Section 5.1.3). For this reason, the glaciomarine drift is thought to have a hydraulic conductivity that is closer to silt than clay. The hydraulic conductivity of silt can be up to six orders of magnitude higher than clay (Freeze and Cherry, 1979). Subsoil textures described in 16 on-site sewage disposal applications obtained from Whatcom County Health Department show that while infiltration rates of the glaciomarine drift mantle are variable across the study area (Figure 24), all exceed normal rainfall intensities.   Infiltraion rates range from 1-2 inches/hour to > 12 inches/hour (Table 24).   Coarse-grained material occurs on the

surface over much of the study area (Figure 10) that has been designated as emergence beach deposits by Lapen (2000). These sand and gravel mixtures enhance recharge. Through examination of Figures 10 and 24 and Lapen (2000); (not shown), I determined there is a strong relationship between the highest infiltration rates and coarse-grained deposits at land surface. By slowing runoff and storing water, emergence deposits increase infiltration into the underlying silt-clay diamicton. Because emergence beach deposits originated from an erosional process (wave action), they form terraces cut into the underlying glaciomarine drift that mantles much of north Lummi Island. In places, wave erosion was sufficient to penetrate the glaciomarine drift mantle. Where this occurred, emergence deposits unconformably overlie Vashon advance outwash or fractured bedrock, creating a conduit for the vertical migration of water to aquifers. An example of this is in the upper region of the Legoe Bay Aquifer, west of Tuttle Ln.

5.7.1 Recharge/Discharge Areas

Recharge areas were identified by examining potentiometric surfaces and groundwater flow directions, bedrock and glacial-drift stratigraphic models, confining conditions, land surface topography, surface geology, and soils data. In general, highlands serve as recharge areas while lowlands serve as discharge areas (Freeze and Cherry, 1979). The topography of the highlands in north Lummi Island is dominated by the bedrock relief of sandstone and greenstone rocks that are mantled by glacial sediments comprised mostly of silt-clay diamictic glaciomarine drift. Although recharge probably occurs at most places, especially where slope is low, a total of ten regions were identified as providing recharge to various aquifers (Figures 25a and 25b). These recharge areas (RCA) are located in the upper and inland parts of the study area. Recharge areas were designated as having primary or secondary significance to individual aquifers (Table 25). An area was determined to provide primary recharge if it represents the greatest source area for an aquifer. Areas that provide recharge, but only provide recharge to a portion of the aquifer or, where the mechanism of recharge is probably less effective were designated as secondary recharge areas for an aquifer. The most important recharge area is RCA-1 that

serves as the primary recharge for the Sandstone aquifer because it is the major aquifer in the study area. Most Pleistocene aquifers receive recharge, in part, from bedrock. However, the contribution of the Greenstone Aquifer to recharge of Pleistocene aquifers is less because this aquifer is smaller and greenstone is significantly less fractured than sandstone. Results of groundwater chemistry analyses were used to validate recharge area conclusions (Section 5.8.1). Recharge areas are more extensive than ones mapped by Schmidt (1978).

Most discharge is directly to sea. However, equipotential lines in potentiometric maps that are sub-parallel to shore indicate discharge does not necessarily occur at the shoreline (Figures 22a-22c). Where aquifer depth is near the surface and bathymetry is steep (east side of study area);(Figure 26), discharge is likely closer to the shoreline (for example Loganita Aquifer). Some aquifers that may extend beneath Hale Passage, on the western side of the study area, likely discharge some distance offshore (for example Lane Spit and Hilltop Deep aquifers). For some aquifers, a portion of discharge is subterranean to aquifers having lower hydraulic head. For example, the Greenstone and Sandstone Aquifers likely discharge into several Pleistocene aquifers where these aquifers lie in contact with each other. Discharge of some water from two aquifers may be at land surface to wetlands that are drained by streams (for example Blizzard Aquifer). However, there are no perennial streams in the study area, indicating that discharge from aquifers is either sufficiently small that it is evapotranspirated in wetland areas or re-infiltrates into the subsurface or that it is not occurring.

Sandstone Aquifer

Recharge areas for the sandstone aquifer are RCA-1, RCA-3, and RCA-4 (Figure 25a). Closely spaced, tight folds within the sandstone produce steeply dipping beds throughout the broad upland region that occupies the north half of the study area. These steeply dipping bedding planes along with fractures and joints transmit water from the overlying glacial drift and soil to the Sandstone Aquifer. Hydraulic properties of the sandstone indicate a high degree of fracturing (Section 5.4). Steeply dipping discontinuities along

81

bedding planes formed during deposition and fractures resulting from subsequent deformation are likely important mechanisms for recharge to sandstone, especially on the limbs of anticlines, where infiltration could be greatly increased by groundwater flow along these preferential pathways.

Primary recharge to the Sandstone Aquifer (RCA-1) occurs over the upland region above about 150 feet, where the aquifer is mostly unconfined (Figure 25a). Recharge is greatest in this region, where slope is low, overlying glacial drift is relatively thin, and near the axes of steeply dipping anticlines. Secondary recharge areas are in the southeast (RCA-3) and southwest (RCA-4) portions of the Sandstone Aquifer (Figure 25a). Here, overlying glacial drift is relatively thin and the aquifer seems to be unconfined above elevations of 50-100 feet. It is possible that southerly groundwater flow from RCA-1, in the northern half of the Sandstone Aquifer, changes direction where it intercepts the axis of the southern-most syncline and does not reach the southeast corner of the aquifer (Figure 22a). If this were the case, RCA-4, in the southeast corner of the Sandstone Aquifer would serve as the sole source of recharge for sandstone in the vicinity of Village Point. Isolation from the more regional flow of groundwater originating in the primary recharge area and the relatively small size of the RCA-4, near Village Point, might explain why few productive wells have been completed in this area. Discharge of groundwater from the sandstone aquifer is mostly to the offshore regions at Rosario Strait and Hale Passage with some groundwater discharging at sea level along the shoreline at the interface between sandstone and overlying glacial drift (Figure 14). Discharge from the Sandstone Aquifer likely provides recharge to several Pleistocene aquifers such as the Hilltop Deep, Legoe Bay, Loganita, and West Shore aquifers.

Greenstone Aquifer

Recharge areas for the Greenstone Aquifer are RCA-7 and RCA-8 (Figure 25b).   Like the Sandstone Aquifer, recharge to this aquifer is along fractures that transmit water from the overlying sediments. Unlike the Sandstone Aquifer, geologic structures within the greenstone have not been mapped and likely do not have the same control on recharge

because the greenstone does not have depositional bedding planes. Hydraulic properties of the Greenstone Aquifer indicate that it is less fractured than the Sandstone Aquifer (Section 5.4). Given that nearly all greenstone lies under a mantle of glacial drift and soil, recharge to the Greenstone Aquifer is from the overlying glacial drift, especially where these sediments are thin at higher elevations above about 150 feet, where the aquifer seems to be unconfined (RCA-8). Secondary recharge to this aquifer may occur east of the intersection of S. Nugent and Constitution roads (RCA-7). Discharge from the Greenstone Aquifer is offshore at Hale Passage to the east and to the Nugent Aquifer and southern portion of the Legoe Bay Aquifer.

Legoe Bay Aquifer

Recharge areas for Legoe Bay Aquifer are RCA-5, RCA-6, and from the Sandstone Aquifer (Figures 25a and 25b). Primary recharge to Legoe Bay Aquifer is through overlying glacial drift and from bedrock in regions where the aquifer abuts sandstone along its northern boundary (Figures 15 and 16). Recharge through glacial drift is important in two places. One, RCA-5, is in the upper and inland area north of Legoe Bay and mostly west of Tuttle Ln, in the vicinity of wells 05O and 04AA. The other, RCA-6, is in the upper and inland area east of Legoe Bay, in the vicinity of the Fire Station and wells 05O, 09Y, and 09A (well 09Y does not appear to be completed in this aquifer and is likely screened in a smaller coarse lens that was not modeled but seems to lie just above the Legoe Bay Aquifer). These recharge areas contain coarse-grained units at the surface (emergence beach deposits) that transmit water to underlying sand units (advance outwash) of the Legoe Bay Aquifer. Secondary recharge is through silt-clay diamicton of the overlying glaciomarine drift that likely occurs at all locations. The Legoe Bay Aquifer may be hydraulically connected to the Nugent Aquifer along its southern boundary. Groundwater discharge is primarily offshore at Legoe Bay. Discharge of a portion of the groundwater in the upper lens of Legoe Bay Aquifer (SU-5) is evident at land surface at Legoe Bay where groundwater likely daylights, mixing with tidewater in a manmade slough (Figure 4).

Nugent Aquifer

Recharge areas for the Nugent Aquifer are RCA-6, RCA-7, RCA-8, RCA-9, and RCA-10 (Figure 25b). Primary recharge is in the upper and northern portion of the aquifer, RCA-6, that contains a thick, unsaturated sand unit (advance outwash) connected to overlying emergence deposits at the surface, in the vicinity and to the south of well 09B. Another primary recharge area, RCA-9, is through emergence deposits overlying silt-clay diamicton along the western and southern slopes of Hill 275. The aquifer seems to be unconfined in this area, along its contact with bedrock of the Greenstone Aquifer. Significant recharge to Nugent Aquifer is also from greenstone, RCA-8, where it abuts bedrock beneath land surface, at elevations near or below sea level (Figures 12g, 12h, 15, and 16). Recharge from bedrock is probably most important in the middle section of the aquifer, near well 10M. Secondary recharge is through silt-clay diamicton, east of S. Nugent Rd (RCA-10) and east of the intersection of S Nugent and Consititution roads (RCA-7). The southern portion of RCA-10 contains emergence deposits at land surface. Recharge may also come from the south half of Lummi Island, where the aquifer extends south of the study area boundary formed by stream on the southern boundary of the study area and possibly abuts bedrock at the base of Lummi Mountain. Groundwater discharge is primarily offshore to Rosario Strait and, to a lesser extent, to just below sea level at Hale Passage, in the northern region of the aquifer.

Blizzard Aquifer

Recharge to Blizzard Aquifer is primarily from overlying glaciomarine drift (not shown). The top of the aquifer lies about 30 feet beneath the swamp located to the west of Tuttle Ln (Figure 4). A large portion of recharge probably also comes from the north and west where the aquifer abuts sandstone under a mantle of silt-clay diamicton near the southeastern border of RCA-1 (Figure 25a). Discharge from this aquifer is unclear. A portion may discharge to an unidentified coarse unit beneath the surface. The top of the saturated portion of the aquifer likely daylights to the south of 04H, north of Centerview Rd where some discharge may contribute to a small wetland and southeast flowing stream (Figure 4) for at least part of the year. However, because the stream draining

Centerview Basin is not perennial, discharge from the Blizzard aquifer may not occur, or occur only when aquifer water levels are higher in the wet season. Well 04H was correlated as one of the wells monitored during 1991-1993 and did not show significant water level fluctuations during this period (Figure 19).

Hilltop Deep Aquifer

Recharge areas for the Hilltop Deep Aquifer, RCA-1 and RCA3, are shown in Figure 25a. Recharge to Hilltop Deep Aquifer is primarily from sandstone where coarse lenses of the aquifer are in contact with the bedrock and to a lesser extent, from vertical migration of groundwater in the overlying sediments. Discharge is mostly to the west, into Legoe Bay. The aquifer likely extends some distance offshore into Hale Passage where the top elevation of the aquifer is deeper than the bathymetry of Hale Passage (Figure 26).

Centerview Aquifer

The recharge area for the Centerview Aquifer, RCA-1, is shown in Figure 25a. This aquifer occupies a pocket of sandstone and is bounded by bedrock on all sides and above by a glacial drift aquitard. Recharge to the Centerview Aquifer occurs where it abuts bedrock to the north and west. Secondary recharge is from silt-clay diamicton in the overlying glaciomarine drift. Discharge is to the Sandstone Aquifer to the south and east where hydraulic gradient within the bedrock is lower.

Constitution Aquifer

The recharge area for the Constitution Aquifer, RCA-8, is shown in Figure 25b. Recharge to Constitution Aquifer is primarily from overlying silt-clay diamicton of glaciomarine drift and from greenstone where coarse lenses abut bedrock to the west and south. Groundwater discharge from this aquifer is unclear. A portion may discharge to a coarse unit beneath the surface, perhaps SU-4 via a connection that was not identified during stratigraphic modeling. A portion of discharge seems to be to the northeast into a

wetland area north of Seacrest Drive. Here, the lower portion of the aquifer is modeled to intersect a topographic depression that forms a wetland (Figure 4). However, the stream that drains this wetland (Fire Station Basin, Section 5.7.2.1) is not perennial. Groundwater flow direction, estimated from limited water-level data, indicates that this aquifer might also discharge to the east, along a steep slope uphill from Seacrest Drive, though no evidence of groundwater discharge was found here.

Lane Spit and Lane Spit Deep Aquifers

Recharge areas for the Lane Spit and Lane Spit Deep aquifers are shown in Figure 25a. Water chemistry suggests that recharge to the Lane Spit Aquifer, RCA-2, is primarily through coarse-grained emergence deposits uphill from Lane Spit and west of Nugent Rd (Section 5.8.1). Recharge to the Lane Spit Deep aquifer likely also comes from sandstone where the aquifer abuts bedrock along its western boundary. Discharge from both aquifers is to Hale Passage. However, the top elevations of these aquifers are deeper than the bathymetry of Hale Passage (Figure 26), so it is unclear how far offshore these aquifers might extend. This could explain why local residents report that crews conducting exploratory drilling in Hale Passage, during the latter half of the 20th Century, encountered freshwater at depth.

Loganita and West Shore Aquifers

The recharge area for the Loganita and West Shore is RCA-1 (Figure 25a). Recharge to these two aquifers is from sandstone where the aquifers abut bedrock to the east. Discharge is to Rosario Strait at slightly below sea level and can be seen along the beach at low tide.

Village Point Aquifer recharge/Discharge Areas

This aquifer was not modeled in this study but likely receives recharge from the secondary recharge area for the Sandstone Aquifer, RCA-4, (Figure 25a), located northeast of Village Point, where it abuts bedrock along its northern boundary and through overlying glaciomarine drift. Discharge is offshore to Rosario Strait and Legoe Bay.

5.7.2 Estimating Recharge

Two mostly independent methods were used to estimate recharge for north Lummi Island. The first method involves establishing values for the variables of precipitation, evapotranspiration, and runoff variables of the water-mass balance equation to estimate recharge. The second method is a chloride-mass balance that estimates recharge by comparing concentrations of atmospherically deposited chloride on land surface to concentrations of the ion in aquifers. Results from these methods were compared to each other and to results for studies of other local islands.

5.7.2.1 Water Mass-Balance for north Lummi Island

As with most islands, the precipitation that falls on Lummi Island serves as the sole source of aquifer recharge. The water-mass balance is a budget that accounts for the fate of precipitation falling over Lummi Island. Major fates of precipitation on an island are surface runoff to the sea, evaporation and transpiration back to the atmosphere, and recharge into island aquifers. Aquifer recharge can be estimated by a simple mass balance equation:

RCH = PPT – ET – RNF (Freeze and Cherry, 1979)

Where

RCH = aquifer recharge

PPT = precipitation

ET = evapotranspiration

RNF = runoff

Precipitation, the only input variable, is either measured in the study area or at a nearby weather station. Weather stations close to the study area can also provide climatic data for various methods used to estimate evapotranspiration. Runoff can be measured in basins that lie within the study area or estimated by making assumptions about recharge or through use of a hydrologic model, such as USGS Deep Percolation Model (DPM).

Various forms of a water-mass balance have been employed in groundwater studies of local islands such as Lopez, San Juan, and Shaw Islands (Orr et al., 2002), Bainbridge Island (Warren, 2000), and Guemes Island (Kahle and Olsen, 1995). Additionally, Schmidt, 1978 applied a mass balance to estimate groundwater quantity on north Lummi Island by estimating precipitation based on weather stations at Bellingham International Airport, to the east, and Olga on Orcas Island, to the west. He also estimated potential evapotranspiration using a temperature-index method (Thornthwaite method). Because he did not derive values for runoff and recharge, he presented a series of scenarios given various values for these variables as part of his water budget results. The objective of this water-mass balance is to use information not available to Schmidt in an effort to quantify aquifer recharge for north Lummi Island.

In the following sections, variables used to calculate a water-mass balance on north Lummi Island for Water Years (WY) 2001-2004 are presented.

PRECIPITATION

Average annual precipitation for the study area, 33.2 inches, is 2.2 inches less than the 55-year average at Bellingham International Airport (Section 2.4). Average monthly precipitation on north Lummi Island for WY 2001-2004 was established by using an arithmetic average of the three collection stations maintained by volunteers (Table 26).

Monthly precipitation data from these collection stations were averaged to create a hyetograph for the period preceding, during, and following well monitoring in this study, WY 2001-2004 (Figure 27). Precipitation during WY 2001 was 26.5 inches, WY 2002 was 34.9 inches, WY 2003 was 25.1 inches, and WY 2004 was 39.36 inches. These values are 6.7 inches below, 1.6 inches above, 8.1 inches below, and 6.1 inches above average annual precipitation on north Lummi Island, respectively. Lower than average precipitation in the period leading up to the low-water monitoring of this study should ensure that water levels collected during Fall, 2002 represent some of the lowest levels that are expected to be observed under current use.

Hyetographs for Water Years 2001-2004 show little difference among gauges during this period (not shown). Departure from Bellingham International Airport ranged from –1.4 to 4.7 inches with a negligible median of < 0.1 inch for the period WY 2001-2004. The greatest departures during this period occurred in January 2002 and October-November, 2003 when Lummi Island received more precipitation than Bellingham International (Figure 27). North Lummi Island also received more rain than Bellingham International Airport during WY 2002 and WY 2004 (Figure 28).

EVAPOTRANSPIRATION ESTIMATE, PENMAN-MONTEITH EQUATION

Evapotranspiration (evaporation and transpiration) is a term describing all of the processes that return liquid or solid water on or near the earth's surface back to the atmosphere as water vapor. It includes evaporative processes from free-water bodies, bare soil, vegetative surfaces (interception), and transpiration (Dingman, 2002).

Potential Evapotranspiration versus Actual Evapotranspiration

Potential evapotranspiration (PET) is the rate at which evapotranspiration would occur if vegetation had unlimited access to soil water and ignores advection and heat-storage effects (Dingman, 2002). PET is a theoretical maximum for evapotranspiration. Actual evapotranspiration (AET) is the term used to describe the amount of water on the earth's surface that is actually returned to the atmosphere given the conditions that limit evapotranspiration, mainly soil moisture.

In warm and dry climates where advective energy is high and precipitation is low, PET can significantly exceed AET. In humid climates where advective energy is lower and precipitation is higher, AET can approach PET (Dingman, 2002). Under certain conditions, it appears that AET can actually exceed some estimates of PET. In evergreen-forested areas, canopy interception can account for nearly half of annual precipitation and can be larger than any other variable in the water-mass balance equation except precipitation (Bauer and Mastin, 1997). It should be noted that recharge can be limited to nearly zero where soil-moisture holding capacities are large and the root zone is sufficiently deep (Orr et al., 2002). In the Puget Sound Region, cool and wet winter months cause AET to approach PET while warm and dry summer months causes PET to exceed AET. An exception might be an unusually wet summer, when almost all precipitation would be evapotranspirated, causing AET to approach PET.

Understanding the differences between PET and AET is an important step toward quantifying a water-mass balance. For this reason, I have assigned limits to evapotranspiration on north Lummi Island with PET forming the upper bound and AET forming the lower bound. To estimate AET, monthly soil moisture measurements are required but were not collected as part of this study. Actual evapotranspiration was estimated using results of a mass balance study that employed the Distributive Hydrologic-Soils-Vegetation Model (DHSVM) in the nearby Lake Whatcom watershed

90

(Kelleher, personal communication, 2004). DHSVM also uses the Penman-Monteith method but incorporates soil moisture data to produce an estimate for AET. AET in the Lake Whatcom watershed was estimated to be 16 inches, which is comparable to AET, computed from numerous basins in the Puget Sound Region that range from 12 to 21 inches with a mean value of 17 inches (Vaccaro et al., 1998). The value from Kelleher was adopted as the lower bound of evapotranspiration on north Lummi Island.

Penman (1948) developed a mass-transfer and energy-budget approach to estimate evaporation. Monteith (1965) modified Penman's method to estimate evapotranspiration from a vegetative surface (Dingman, 2002). The Penman-Monteith Equation (Appendix E) is the most widely used method for estimating evapotranspiration (Dingman, 2002). One major advantage of this method is the ability to incorporate local climatic data and vegetative land cover characteristics into the model. Input variables to the Penman-Monteith Equation were tailored to the north Lummi Island study area using climatic data from Bellingham International Airport, precipitation data from three north Lummi Island stations, and vegetation distribution using a GIS analysis of Landsat, and vegetative properties from Dingman, 1994 and 2002.

The Penman-Monteith Equation was used to estimate monthly and annual PET for Water Years 2001-2004 (Tables 27a-d). Annual PET ranged from 23.4 inches to 28.4 inches during this period. The highest PET occurred during WY 2004, which also happened to be the year of greatest precipitation. Differences in PET between years are due to Penman-Monteith variables air temperature, wind speed, and dew point and are independent of precipitation. Average annual PET over this period is 25.5 inches. Because PET is a theoretical maximum value, it serves as an upper bound for evapotranspiration on north Lummi Island. In other studies of local islands, PET has been estimated by methods other than the Penman-Monteith. In the San Juan Islands, PET is 25 inches (Russell, 1975) and Guemes Island, PET is 17 inches (Kahle and Olsen, 1995). Schmidt, 1978, estimated PET as 21 inches on north Lummi Island.

RUNOFF

Estimating runoff requires direct discharge measurements of some or all outlet streams or use of a hydrologic model that simulates runoff from numerous other data. I incorporated direct discharge-measurement data obtained from Nielson and Armfield, written communication.

Discharge from intermittent streams that drain eleven Lummi Island basins (Figure 29) was measured by volunteers during Water Years 2003 and 2004 (Nielson and Armfield, written communication). They used a constant volume container (stop watch and bucket) and flow velocity meter for larger streams. Discharge was measured at the outlet of each basin roughly twice a week during the wet season and during and following precipitation events in the dry season after streams stopped flowing in the spring. Nielson and Armfield extrapolated between discharge measurements to estimate monthly discharge for each basin. The characteristics of outlet channels for basins within the study area are conducive to this type of small-scale effort. All channels are diverted through culverts under the roads that line the perimeter of the island leaving little ambiguity of the location of the outlet for each basin. Measurements were taken at the outlets of these culverts that generally lie within 100 feet of shoreline. The basins are small, producing sufficiently low volumes of discharge that can be captured by the constant volume container method. The intermittent and ephemeral nature of these streams makes them responsive to precipitation events. This causes discharge in most channels to be fairly predictable, favoring the measurement routine chosen by Nielson and Armfield. Discharge data measured during WY 2003 were not used because they are less complete and considered to be less reliable than data for WY 2004 (Nielson and Armfield, written communication, 2004).

Basin characteristics and monthly runoff data for WY 2004 are listed in Table 28. Basin areas were calculated using a digital elevation model in GIS (Nielson and Armfield, written communication). One basin, Southeast basin, may drain a larger area than shown in Table 28 and Figure 29 due to a roadside ditch that may incorporate drainage from part

of an adjacent basin. Removing this basin from runoff calculations had little effect on overall runoff estimates so I chose to include it. Monthly precipitation data are from Marhsall et al. (written communication). The dominant geology of each basin (Table 28) was determined from the stratigraphic model (Figure 10) and published reports (Easterbrook, 1971 and Lapen, 2000). The outlet streams monitored by Nielson and Armfield during WY 2004 represent all known surface water channels in the study area with the exception of one. The exclusion of the west-to-east flowing stream at the southern boundary of the study area is considered appropriate because it receives at least half of its water input from a steep bedrock region that lies outside of the study area.

Discharge for all basins measured during WY 2004 range from 1.0 to 16.7 inches with an average value of 5.7 inches. These values represent 2.6%, 42.5%, and 14.5% of precipitation during this period, respectively. The basins for which discharge was measured by Nielson and Armfield comprise 53% (2.05 square miles) of the study area. Runoff from these eleven basins represents the vast majority of runoff from north Lummi Island. Therefore, the averaged value for runoff from these basins of 5.7 inches or 14.5% of precipitation, serves as an upper bound of runoff for the entire study area during WY 2004. Runoff from the 47% of north Lummi Island not covered by the Nielson and Armfield effort is assumed to be very small because no obvious outlet channels (except the one previously mentioned) were identified in these areas. Applying this assumption, I extrapolated the average runoff for 11 basins monitored during WY 2004 by Nielson and Armfield across the study area. The resulting runoff value of 3 inches or 7.7% of precipitation serves as a lower bound for total discharge in the study area during WY 2004.

A concern was that the discharge measurement routine chosen by Nielson and Armfield might overestimate discharge because it is largely focused on capturing flow during and after precipitation events, when discharge is highest, and extrapolating between data points. Generally, data from the Nielson and Armfield discharge study for WY 2004 seem to be reasonable as an approximation for runoff for four reasons:

93

- The range and average values for runoff as a percentage of annual precipitation among north Lummi Island basins (Table 28) are similar to results of other studies of small glacial drift and bedrock basins within the Puget Sound Region. Using a sample set of 35, discharge as a percentage of annual precipitation from these basins measured or simulated in four USGS reports range from 2% to 50% with an average value of 19% (Sumioka and Bauer, 2003; Orr et al., 2002; Bidlake and Payne, 2001; Bauer and Mastin, 1997). This average value is somewhat higher than the average value for basins measured by Nielson and Armfield of 14.5%.

- These studies indicate that basins determined to be bedrock-controlled and larger basins produced more runoff as a percentage of annual precipitation. This trend is also occurs in the runoff data provided by Nielson and Armfield (Figure 30).

- Although WY 2004 was an unusually wet year, a large amount of precipitation (7.7 inches) occurred during the summer months June through September, when evapotranspiration is highest. Subtracting out precipitation that fell during the summer months increased the average amount of runoff as a percentage of precipitation by only 3%.

- Results of a slope analysis indicate that average slope on north Lummi Island is 5 degrees, with only 4% of the study area having a slope greater than 15 degrees (Table 23 and Figure 23). This land surface gradient would seem to favor conditions for lower relative runoff.

There is a fair relationship between runoff and dominant geology of these basins (Table 28). For example, the upper reaches of the Centerview Basin are dominated by sandstone and thin glaciomarine drift. Runoff as a percentage of precipitation was high for this basin. However, the Lummi Point Basin, which is dominated by emergence beach deposits at land surface, also had significant runoff as a percentage of precipitation. Given that emergence beach deposits are thin and underlain by silt-clay diamction, it is

possible that the hydrology of this basin is controlled by the less-permeable silt-clay diamcton. Seepage along the bluff at Lane Spit (well 04A) was observed during field work. In addition, the direct discharge measurement location for this basin is on Lane Spit may be below the high tide mark, causing discharge measurements to be erroneously high.

5.7.2.2 Recharge Estimated using a Water-Mass Balance WY 2001-2004

Variables to the water-mass balance equation were estimated for north Lummi Island (Section 5.7.2.1). Annual recharge from the water mass-balance method for Water Years 2001-2004 is estimated to range from 0 to 20 inches with an average of 8 inches (24% of annual precipitation); (Table 29). Annual recharge during WY 2004 was estimated using the water-mass balance to range from 5.4 to 20.4 inches with an average of 12.9 inches (33% of annual precipitation).

The recharge values that I have estimated are consistent with those from other local studies. Recharge simulated through DPM ranges from 1.5 to 6.8 inches, or 4% to 17% of annual precipitation in south Puget Sound (Bauer and Mastin, 1997), 2.3 inches to 6.4 inches, or 8% to 21% of annual precipitation in Island County (Sumioka and Bauer, 2003), and 1.4 to 2.5 inches, or 5% to 10% of annual precipitation in San Juan County (Orr et al., 2002). Using lines fitted from DPM simulations in the vicinity of Naval Submarine Base Bangor, Kitsap County, annual precipitation of 32 inches corresponds to annual recharge of 8 inches on forested and non-forested vegetation overlying glacial till or fine-grained sediments (Bidlake and Payne, 2001). On Guemes Island in Skagit County, total recharge for an average year was estimated to be 6 inches (27% of annual precipitation; Kahle and Olsen, 1995). On Bainbridge Island in Kitsap County, recharge is estimated to be 13 inches (34-38% of annual precipitation; Warren, 2000).   Recharge in fine grained deposits near Port Townsend in Jefferson County range from 0.15 to 12.5 inches annually and 19.6 inches in coarse grained deposits (Vaccaro et al., 1998).

Finally, the recharge values that I have estimated are consistent with those in Schmidt (1978) that range from 5 to 9 inches for north Lummi Island.

From these other studies, it is clear that recharge estimates vary greatly among areas with climatic, vegetative, and geologic conditions similar to north Lummi Island. Recharge probably varies greatly throughout the study area. Therefore, recharge estimated in the current study is intended to serve as an approximation.

Using an annual recharge value of 8 inches, the volume of annual recharge to the study area (total area of 3.87 square miles) is 1.65×10^3 acre-ft or about 427 acre-ft/square mile. This volume represents less than 2% of the total groundwater storage capacity of all aquifers in north Lummi Island (Section 5.6). The actual amount of recharge that is available for withdrawal is likely much less. To compare, Warren (2000) estimated the volume of annual recharge for Bainbridge Island (total area of 27.5 square miles) to be 1.91×10^4 acre-ft or about 695 acre-ft/square mile.

5.7.2.3 Recharge Estimated using a Chloride-Mass Balance WY 2004

A chloride-mass balance approach was employed as a second, mostly independent method to estimate aquifer recharge. It is not completely independent from the water-mass balance approach because they both use the same runoff estimates. This method has been used as a secondary means of estimating recharge in studies of local islands in San Juan and Island Counties (Orr et al., 2002; Sumioka and Bauer, 2003). Authors of these studies used the chloride-mass balance method to check recharge estimates obtained through DPM. Application of this method in the current study follows these previous works.

The chloride-mass balance approach works on the principle that atmospherically-deposited chloride makes its way into the water table where it occurs in varying

concentrations depending on the amount of evapotranspiration in a given area which can be used to derive recharge. Most atmospheric chloride originates from very small particles of windborne ocean salts. Most are dissolved into and fall with precipitation. Others are deposited as dry particles. The latter process accounts for about 37% of atmospherically deposited chloride (Orr et al., 2002). As water moves downward from the surface, it is taken up by evapotranspiration and the concentration of chloride increases. At sufficient depth where evapotranspirative processes do not occur, chloride in groundwater should reach a uniform concentration. Using the chloride-mass balance method to estimate aquifer recharge assumes that atmospheric deposition is the only source of chloride in groundwater. Sources of chloride in groundwater other than seawater intrusion are discussed in Section 2.8. To eliminate seawater intrusion as a source of chloride, the median chloride concentration for wells completed above sea level was used. An equation for estimating recharge through a chloride-mass balance was developed by Maurer et al., 1996 and Prych, 1998 and modified by Orr et al., 2002 to account for dry deposition:

$$RCH = 0.0394 \times FWD(1-RO/P)/C_g$$

Where

RCH = aquifer recharge (inches)

FWD = total of wet and dry atmospherically deposited chloride (mg/m^2)

RO = runoff (inches)

P = precipitation (inches)

C_g = concentration of chloride in groundwater (mg/L)

I did not measure the variable FWD during my study. A value of 2359 mg/m^2 for the variable FWD was obtained by averaging total wet and dry chloride deposition measured over a two-year period (1997-1998) on neighboring Lopez Island (Orr et al., 2002). Use of this value makes the assumption that FWD on north Lummi Island for any given year

is close to the average of the two years of measured FWD on Lopez Island. For the variable RO, the lower and upper bounds for runoff during WY 2004, 3 to 5.5 inches were used. The variable P was discussed in Section 5.7.2.1. For the variable C_g, the median concentration in groundwater for wells completed above sea level, 19 mg/L, was used to eliminate the possibility of an erroneous recharge estimate due to elevated chlorides resulting from seawater intrusion.

Recharge estimated by using the chloride-mass balance method for WY 2004 ranges from 4.2 inches to 4.5 inches (average of these is 4.3 inches or 11% of annual precipitation) (Table 30). The average annual recharge derived using this method was 0.6 inches on Lopez Island (Orr et al., 2002) and 2.0 inches on Whidbey and Camano Islands (Island County) (Sumioka and Bauer, 2003). The chloride-mass balance equation is most sensitive to changes in the FWD and C_g variables. In the Lopez Island study, values for FWD (average of 2359 mg/m^2) were considerably higher than the Island County study (average of 78 mg/m^2) and C_g was 64 mg/L (a value for C_g of 19 mg/L was used for north Lummi Island). The greatest potential sources of error for the chloride-mass balance recharge value derived in my study is the FWD variable that was not measured, and error associated with runoff estimates. Recharge derived from a chloride mass-balance probably serves as a lower bound that represents from 17-23% of recharge estimated using DPM (Sumioka and Bauer, 2003; Orr et al., 2002).

5.8 Survey Groundwater Chemistry and Assess Seawater Intrusion

Samples were collected and analyzed in an effort to examine groundwater chemistry trends in aquifers and to survey the impact of seawater intrusion. A total of 80 wells were sampled with 74 in fall 2002 and 77 in spring 2003. Seventy-one of these were sampled during both monitoring periods. Results of groundwater sampling for all wells are listed in Appendix D. Tables 31a and 31b list median concentrations of analyzed constituents for the fall 2002 and spring 2003 sampling periods, respectively. Median concentrations of analyzed constituents are summarized by aquifer in Table 32. Five of wells sampled in 2002-2003 were also sampled for major ion chemistry in winter, 2005 (Table 33). The MCL for groundwater and drinking water for selected water quality parameters are listed in Table 4.

Composition of Seawater

The concentration of dissolved solids in seawater is 35,000 mg/L of which 19,350 mg/L is chloride, 10,760 mg/L is sodium, and 400 mg/L is calcium (Table 3). These concentrations may be lower for local seawater that is diluted by a large freshwater input from numerous rivers. Chloride concentrations in seawater of northern Puget Sound range between 14,000 mg/L (Sapik et al., 1988) and 17,500 mg/L (Culhane, 1993). However, both of these studies analyzed seawater in Island County to the south, where the Puget Sound is more enclosed than waters near Lummi Island and therefore subject to increased dilution from freshwater input. Chloride and sodium do not occur in equal proportions because sodium chloride is only one of three major salts in seawater. Other salts include potassium chloride and magnesium chloride. The specific conductance of seawater is about 50,000 μS.

Seawater Ion-Loading During the Pleistocene

During the Everson Interstade of the Fraser Glaciation, the study area was mostly submerged beneath a shallow sea (see Section 2.1.2.2 for estimated marine limits).

Similar conditions occurred to the north, in the Gulf Islands of British Columbia that are largely composed of sandstone, and mudstone and shale of the upper-Cretaceous Nanaimo Group. Allen et al., (2001) and Allen and Matsuo (2002) examined saline groundwater in Saturna and Hornby islands, British Columbia. They concluded that bedrock was submerged for sufficient time to fully saturate pore spaces with seawater (about 500-100 years). This caused groundwater hardening as high concentrations of marine Na^+ replaced terrestrial Ca^{2+} on cation-exchange sites in negatively charged particles of fine-grained bedrock facies. Chloride and sulfate anions also occurred in concentrations proportional to seawater. Following land surface rebound, fresh water recharge began to flush out the ions introduced by Pleistocene marine inundation. The process is on going with shallower regions being flushed out first. Most of the mobile Cl^- and SO_4^{2-} anions were rapidly flushed out. Some residual marine Cl^- and SO_4^{2-} may persist in dead-end pore spaces and serve as a source of anions in modern groundwater. Sodium cations are more difficult to mobilize and may persist in fine-grained facies in sufficient concentrations to provide a sustained source of Na^+ in modern groundwaters on Mayne Island (Dakin et al., 1983). These authors and Allen et al. (2001) concluded that the slower diffusion processes within fine-grained facies are responsible for concentrating Na^+ along fractures in bedrock where they are assimilated into the groundwater flow regime. The cation-exchange mechanism responsible for mobilizing Na^+ is discussed below. They also concluded that shallow bedrock and coarser-grained facies, such as sandstone, have low remaining concentrations of salts because they have experienced greater freshwater circulation and have fewer cation-exchange sites, respectively.

Groundwater Evolution Processes

Three major geochemical processes are responsible for the evolution of groundwater in the Gulf Islands of British Columbia: (1) dissolution of minerals (2) cation-exchange (3) mixing with chloride-rich waters or salinization (Allen and Matsuo, 2002).

Dissolution of minerals in shallow groundwater regimes, is most common in topographically higher regions corresponding to recharge areas. These waters are

100

described as immature composition and occur under open system conditions. They have low specific conductance and are Ca^{2+}/Mg^{2+} - HCO_3^- type fresh waters. Calcium ion concentrations are near saturated conditions (Allen et al., 2001) originating primarily from the dissolution of carbonate minerals (Allen and Matsuo, 2002). These waters plot in the middle-left (fresh water) diamond region of a Piper tri-linear diagram (Figure 31). The dissolution of sodium bearing minerals, such as feldspar, is assumed to be a minor source of Na^+ ions in groundwater of the Gulf Islands (Allen, personal communication, 2005).

Cation-exchange is most common in fine-grained bedrock facies such as mudstone and shale that lie were inundated by a shallow sea during the Everson Interstade. It takes place in intermediate and deeper groundwater regimes, between recharge and discharge areas. These waters are described as chemically more evolved compositions than immature waters and occur under closed system conditions. In this process, calcium-rich immature waters undergo cation-exchange with Na^+ occurring on cation-exchange sites of fine-grained bedrock facies. The cation-exchange capacities of Ca^{2+} and Mg^{2+} are much higher than Na^+. This results in a robust increase of Na^+ and simultaneous decrease in Ca^{2+} and Mg^{2+} concentrations in groundwater. These waters plot on the lower-right diamond region of a Piper diagram (Figure 31). This process is less important in well-flushed shallow bedrock and was noted to be absent in sandstone facies that have few cation-exchange sites. This process is also less important in Pleistocene deposits that have fewer available cation-exchange sites to retain marine ions and have been largely flushed out due to their higher permeability. And, cation-exchange is significantly less important in geologic materials that lie above the Everson marine limit (Section 2.1.2.2) and therefore not subjected to marine inundation.

Groundwater can also mix with chloride-rich seawater in discharge zones. These highly evolved compositions are characterized by increased specific conductance, increased Cl^- and Na^+ concentrations, and decreased Ca^{2+} concentrations. The dominant evolution path of groundwater on Hornby Island, from immature calcium-rich waters followed by

sodium-enriching cation-exchange, is followed by an increase in chlorides, known as salinization. These waters plot on the right side of a Piper diagram diamond, progressing upward toward the middle-right region (seawater) as the concentration of Cl⁻ increases (Figure 31). In some cases, mixing of immature calcium-rich groundwater with saline water occurs in a process called direct-salinization. This process bypasses sodium enriching cation-exchange and can be associated with active seawater intrusion. On a Piper diagram, these waters move directly from the middle-left diamond region (fresh water) to the middle-right diamond region (seawater); (Figure 31). On Saturna Island, most groundwater in shallow regimes undergoes direct-salinization (Allen et al., 2001).

Cation-exchange processes are largely dependent on the number of cation-exchange sites occurring in aquifer media. Clay minerals, a product of chemical weathering, have numerous negatively charged cation-exchange sites. Kelly (1970) concluded that the clay mineralogy of fine-grained siltstone in the basal member of the Chuckanut Formation, at nearby Lake Samish, contained illite, chlorite, and vermiculite, a clay with abundant cation exchange sites. Although these rocks are up to 14 million years older than the Padden member of north Lummi Island, Kelly's results demonstrate the potential for the Chuckanut Formation to contain clay minerals. No information regarding clay mineralogy of the Fidalgo ophiolite was found, but these dominantly mafic rocks are probably highly prone to weathering into clay minerals. Contrary to the bedrock, Pleistocene deposits contain few clay minerals. Instead, relatively abundant clay-size particles in the Pleistocene deposits are mostly finely-ground and uncharged sediments.

North Lummi Island has geologic units and a geologic history that are similar to the Gulf Islands. Therefore, I chose to apply the hypothesis developed by Allen and others to explain trends in groundwater chemistry in the study area.

5.8.1 Survey Groundwater Chemistry

pH

Water in natural near-surface environments usually has a pH between 4 and 9 (Fetter, 1980). On Hornby Island, pH for immature waters range from 6.7 to 7.6 and pH for chemically more evolved waters range from 7.3 to 9.1, and for deep wells range from 8-9 (Allen and Matsuo, 2002). Results of pH for all wells are listed in Appendix D. My measured values for pH range from 6.7 to 9.8 with a median pH of 8.   Error associated with field measurements of pH can sometimes cause measurements to be higher than actual pH due to the escape of CO_2 (Fetter, 1980). For this reason, pH was measured immediately after sample collection.

Wells showing the highest pH during both sampling periods were mostly near the intersection of Tuttle and Sunny Hill Lanes (04D, 04J, 04S). Differences in median pH between aquifers are small (Table 32). The highest median pH is in the Greenstone Aquifer and the lowest is in dug wells completed in emergence deposits and glaciomarine drift. Negligible variation in pH was observed between sampling periods (Tables 31a and 31b). No relationships between pH and well completion depth, or distance from shore were observed.

Specific Conductance

Specific conductance is a measure of the ability of water to conduct electricity at a given temperature due to its electrolytic capacity, which is a function of the type and concentration of ionic species in the solution (Fetter, 1980). It is commonly used in groundwater studies as a proxy for determining ionic concentrations in water (total dissolved solids). On Hornby Island, conductivity (not temperature compensated) values for immature waters range from 106 to 238 μS and for chemically more evolved waters range from 198 to 1568 μS with an average value of 528 μS (Allen and Matsuo, 2001). The ionic concentration of groundwater increases along it flow path within the saturated

zone (Freeze and Cherry, 1979). This trend is observed in study area aquifers as specific conductance generally increases with depth (Figure 32). This trend is likely caused by a combination of increased mineral dissolution, greater cation-exchange in deeper, less-flushed regions of the aquifer, and by the ionic contribution of seawater.

Measured values for specific conductance range from 121.5 to 11,000 μS with a median value of 407 μS (Appendix D). Variation in median specific conductance for all wells between fall 2002 and spring 2003 is small (Tables 31 a and 31b). Differences in median specific conductance between aquifers are moderate (Table 32), though there is considerable variation within some aquifers, such as the Sandstone Aquifer (Figure 32).

The highest median specific conductance is in the Sandstone Aquifer (Table 32). This result was not expected because sandstone is primarily composed of quartz and feldspar, minerals that have little effect on groundwater composition (Freeze and Cherry, 1979). The elevated specific conductance within the sandstone aquifer could be due to a combination of dissolution of other minerals, such as carbonates, and cation-exchange occurring in the shale facies of the Chuckanut Formation, and the ionic contribution of seawater. Elevated specific conductance may also indicate older groundwater. The median specific conductance for wells completed above sea level in sandstone is 441 μS, standard deviation 192, and for wells completed below sea level is 503 μS, standard deviation 2651. Specific conductance in the Greenstone Aquifer is greatly below the median value for all wells. This was expected because ionic concentrations of groundwater in crystalline rocks can be very low (Freeze and Cherry, 1979).

The higher specific conductance in the sandstone is reflected in the Centerview, Hilltop Deep, and Loganita aquifers (Pleistocene deposits), which are bounded by the Sandstone Aquifer on at least one side and a confining layer of silt-clay diamicton above. Specific conductance in both samples from the Centerview Aquifer are equivalent to the median specific conductance of the Sandstone Aquifer. This observation supports the hypothesis

that it is in hydraulic connectivity with sandstone and part of the overall Sandstone Aquifer system. Median specific conductance values in most Pleistocene aquifers (Table 32) are below the median for all wells. The lowest median specific conductance is in the Constitution Aquifer that is relatively shallow. Shallow dug wells completed in emergence deposits and glaciomarine drift also show specific conductance that is greatly below the median for all wells because they are recharged locally. Small variation in specific conductance among all wells was observed between fall 2002 and spring 2003 sampling periods (Tables 31a and 31b).

Specific conductance and chloride concentrations can be used to develop a relationship that allows field measurements of specific conductance to be used as a proxy for the concentration of chloride in groundwater from wells in the same geographic area. This technique has been applied to coastal aquifers in Puget Sound to offer a method for quick and inexpensive monitoring of seawater intrusion conditions using a specific conductance meter (Dion and Sumioka, 1984; Wildrick et al., 2001).   Similar to these studies, a linear regression was fitted to 148 specific conductance-chloride data pairs of samples analyzed during this study with a correlation coefficient of 0.98 (Figure 33a). When the three highest specific conductance-chloride data pairs were removed, the correlation coefficient decreased to 0.48 (Figure 33b). Dion and Sumioka analyzed 37 sample pairs and determined a correlation coefficient of 0.96 for Whatcom County, indicating that the reliability of the relationship between specific conductance and chloride concentration is very good. In their study, correlation coefficients ranged from 0.45 (poor) to 0.98 (very good).

Total Dissolved Solids

Total dissolved solids (TDS) represents the sum of all dissolved minerals occurring in water. Total dissolved solids is most accurately measured by gravimetric analysis in a laboratory. This method was not employed in this study. Though less accurate, field measurements were made using a conductivity dipstick. This method was chosen because this device is relatively inexpensive and easy to use in the field and the results

can be used as a base for future monitoring using similar techniques. A conductivity

dipstick measures electrical conductivity that is a function of ion concentration in the

water. The use of electrical conductivity can misrepresent total dissolved solids because

it does not account for uncharged species dissolved in water (Freeze and Cherry, 1979).

However, relationships between conductivity and TDS have been developed for various

types of solutions.   Conductivity dipsticks convert electrical conductivity to TDS using a

relationship based on an assumed ionic composition of the water, normally NaCl or KCl.

Results of TDS values for all wells using a conductivity dipstick are listed in Appendix

D. Median values for TDS measured with a conductivity dipstick for all wells in fall,

2002 and spring 2003 are listed in Tables 31a and 31b. Values for TDS measured with a

conductivity dipstick during both sampling periods range from 10 to >10,000 mg/L with

a median value of 150 mg/L. Trends of TDS and potential sources of differences among

aquifers are the same as those identified by specific conductance measurements.

Oxidation-Reduction Potential

Oxidation-reduction (redox) reactions involve the transfer of electrons among ions. This

transfer is an electrical current, therefore an oxidation-reduction equation has an electrical

potential (Fetter, 1980). Redox potential (ORP) is a measure of the oxidation potential of

an aqueous solution, also known as Eh. Positive values indicate oxidizing and negative

values indicate reducing conditions. Error associated with field measurements of ORP

can sometimes cause measurements to be higher than actual ORP due to the introduction

of atmospheric oxygen into a sample. To minimize error, ORP was measured

immediately after sample collection. Measurements of ORP taken during this study

provide a general outline of the distribution of redox conditions.

The ORP of rainwater is generally high due to dissolution of atmospheric oxygen and

decreases with along the flow path of water with depth and away from recharge areas

(Freeze and Cherry, 1979; Fetter, 1980). Upon passing through organic rich soil horizons

and regions of the aquifer suitable for growth of aerobic bacteria, ORP declines dramatically and may continue to decline along the groundwater flow path as the result of various geochemical and biochemical processes (Freeze and Cherry, 1979).

Results of ORP for all wells are listed in Appendix D. Measured values for ORP during both sampling periods range from –283 mV to 185 mV with a median value of 90 mV (Tables 31a and 31b). The difference in median ORP between aquifers is large (Table 32) and could be the result of varying flow path lengths that represent relative distances from recharge areas. The highest median ORP is in shallow dug wells completed in emergence deposits and glaciomarine drift. The lowest median ORP is negative, in Lane Spit Aquifer indicating reducing conditions.

In general, values for ORP are higher for inland wells where groundwater flow paths are shorter due to the proximity of recharge zones (Figures 25a and 25b). There is a relationship between negative ORP values and completion depth. Sixteen wells indicate reducing conditions at depth and all but two are completed below sea level. The median completion elevation of these wells is –41 feet. This is deeper than the median completion elevation of all wells of –33 feet (Table 9). Wells with low positive and negative ORP values are generally located close to shoreline implying that flow paths are longer (i.e. recharge occurs farther inland). Of the 16 wells with negative ORP values, most lie within 100 yards of the shoreline. Most notable is the Lane Spit aquifer that has a much lower median redox potential than the others, possibly indicating that groundwater in this aquifer has a long flow path from a recharge area inland, or that other conditions exist in the aquifer that decrease ORP faster than other locations. A small decrease in median ORP between fall 2002 and spring 2003 was observed (Tables 31a and 31b).

An indication of reducing conditions in an aquifer is the presence of hydrogen sulfide gas released from the water due to the reduction of sulfate in the presence of sulfate-reducing

bacteria (Freeze and Cherry, 1979). A sulfur smell was observed at a number of wells during field work and numerous residents complain of this smell, stating that it is most common in late summer. Nineteen of 32 samples where a sulfur smell was detected had an ORP value less than 0 mV, indicating reducing conditions within the aquifer. The remaining samples had very low positive ORP. Sulfate concentrations in two of these wells completed in sandstone were 86 to 216 mg/L (Table 33). Allen (2004) identified sources of SO_4^{2-} in bedrock aquifers of the Gulf Islands as atmospheric SO_4^{2-} from precipitation recharge waters, marine SO_4^{2-} from modern day seawater intrusion or Pleistocene events, and terrestrial SO_4^{2-} in aquifer media. The most important source for bedrock aquifers is atmospheric SO_4^{2-} (Allen, personal communication, 2005). About half of the wells where a sulfur smell was detected are completed in bedrock.

Reducing conditions in the aquifers may be responsible for the dissolution of iron and arsenic-bearing minerals, contributing to elevated iron and arsenic levels in some wells. Numerous wells within the study area exhibit arsenic concentrations exceeding the 0.01 mg/L MCL for drinking water (WAC 246-290-310); (Whatcom County, 1994). Most of these wells are completed in the Sandstone Aquifer.

Calcium

Calcium is among the dominant cations in groundwater of sedimentary and crystalline bedrock and glacial drift environments (Freeze and Cherry, 1979) and is a minor cation in seawater (Table 3). The presence of high concentrations of Ca^{2+} may indicate areas of elevated groundwater hardness. Hardness is the concentration of ions in water that will react with a sodium soap to precipitate an insoluble residue and is determined from the mass of $CaCO_3$ occurring in water (Drever, 1997). Hardness was not directly analyzed as part of this study. Although the primary source of Ca^{2+} is the dissolution of carbonate minerals (Allen and Matsuo, 2002), concentrations of Ca^{2+} are dependent upon several processes, such as sodium-enriching, calcium-depleting cation-exchange. This process occurs in aquifers that experienced marine inundation during the Pleistocene and where modern seawater intrusion has reversed (freshening). Through a reverse exchange

process, Ca^{2+} concentrations increase as they are displaced from cation-exchange sites by high concentrations of Na^+, hardening groundwater in front of seawater that is advancing that is within the aquifer (intrusion). On Hornby Island, Ca^{2+} concentrations in chemically more evolved waters range from 0.8 to 12.9 mg/L (Allen and Matsuo, 2002).

Concentrations of Ca2+ during both sampling periods range from <0.1 mg/L to 568 mg/L with a median concentration of 18.9 mg/L (Appendix D). The variation in median concentration of Ca^{2+} between fall 2002 and spring 2003 is about 26% (Tables 31a and 31b). This difference could be the result of lower water levels in bedrock aquifers during late summer that cause increased Ca^{2+} concentrations because depressed water levels tend to limit the number of bedrock fractures that are available for groundwater flow. This forces late summer flow through less used and less permeable fractures that are poorly flushed and more mineral-rich (Allen, personal communication, 2004). Moreover, depressed water levels and increased well-pumping in summer months can induce active seawater intrusion, creating a groundwater hardening front.

Calcium ion concentrations vary by aquifer (Table 32). All of the aquifers having higher than median concentrations of Ca^{2+} are comprised of unconsolidated materials. The Nugent and Legoe Bay aquifers have the highest concentration of Ca^{2+}. This result was expected because the minerals in unconsolidated aquifer media have greater surface areas in contact with groundwater than bedrock making them more susceptible to dissolution, increasing groundwater hardness. Immature calcium-rich waters on Hornby and Saturna Islands are associated with recharge (Allen et al., 2001). The higher concentrations of Ca^{2+} in Nugent and Legoe Bay aquifers indicate these aquifers receive significant recharge through the glacial drift. The increased concentrations of Ca^{2+} in Nugent and Legoe Bay aquifers and the relatively high number of study wells completed in these aquifers explain why the median Ca^{2+} concentration for all wells sampled in north Lummi Island (18.9 mg/L) is greater than the upper range of more evolved waters on Hornby Island (12.9 mg/L) where bedrock is the dominant aquifer medium. Concentrations of Ca^{2+} in both bedrock aquifers are greatly lower than the median Ca^{2+} concentration for all wells (Table 32). Calcium concentrations in the Greenstone Aquifer

are exceptionally low, as expected. Low Ca^{2+} concentrations in the Sandstone Aquifer were not expected indicating that processes other than the dissolution of carbonate minerals might dominate groundwater chemistry in this aquifer. Calcium ion concentrations in the bedrock aquifers fall within the range of more chemically evolved waters in Hornby Island. Trends in calcium concentrations with depth are included in the discussion on sodium (*Sodium/Calcium Concentrations and Cation-Exchange*), below.

The effect of one mole of Ca^{2+} on specific conductance is twice that of Na^+ (Fetter, 1980). Because of this, the greater Ca^{2+} concentrations in the Nugent and Legoe Bay aquifers may be responsible for the relatively high specific conductance in these aquifers (Table 32).

Although immature waters are associated with recharge, they can be common even at depth in Pleistocene aquifers because of the absence of a significant source of Na^+ (Allen, personal communication, 2004). Some water reaching deeper regions of the bedrock aquifers does not evolve past the immature phase. Some immature waters were observed at depth in bedrock and near shorelines where fractures facilitate rapid migration of water from recharge areas, bypassing the cation-exchange process (Allen, 2004). This may explain why the composition of some samples from deeper wells completed in bedrock aquifers display high Ca^{2+} and low Na^+ concentrations, implying that they are immature waters (for example 04Z, 32M, 32N). These wells lie within the primary recharge area for the Sandstone Aquifer (Figure 25a). Another possibility is that the aquifer near these wells is experiencing groundwater hardening in advance of seawater intrusion, though low chloride concentrations in these wells that are below the median make this very unlikely.

For wells completed below sea level, waters that seem to be immature calcium-rich compositions generally coincide with Cl^- concentrations that are less than 18 mg/L (Figure 34a). The majority of these wells are completed in Pleistocene aquifers.

Sodium-rich waters that seem to be more chemically evolved compositions generally coincide with Cl⁻ concentrations between 18 and 85 mg/L (Figures 34a and 34b). The majority of these wells are in bedrock aquifers. Wells with immature compositions that have Cl⁻ concentrations between 18 and 85 mg/L are in Pleistocene aquifers. Several wells with Cl⁻ concentrations greater than 85 mg/L (04N, 09G, 29C, 32K) have the highest concentrations of Ca^{2+} and relatively low concentrations of Na^+ (Figure 34b). This is the result of either a hardening front caused by seawater intrusion or direct-salinization of immature-waters, that can also be caused by seawater intrusion.

Sodium

Sodium is among the dominant cations in groundwater of sedimentary and crystalline bedrock and glacial drift environments (Freeze and Cherry, 1979) and is the dominant cation in seawater (Table 3). Sources of sodium in groundwater are dissolution of sodium-bearing minerals of soil and aquifer media, formation waters (connate water), and seawater. Sodium from seawater can enter island aquifers from atmospherically deposited sea salts, Pleistocene marine inundation, and seawater intrusion. Sodium that sorbed to cation-exchange sites during Pleistocene marine inundation continues to be a major source in modern groundwaters (for example Dakin et al., 1983 and Allen, 2004). The dominance of sodium in most samples, compared to calcium and chloride (Figures 34a and 34b) offers evidence that this process is the major source of sodium in groundwaters of north Lummi Island and modern seawater intrusion is a lesser source. Salts, such as halite, introduced into aquifer media during marine inundation are assumed to have largely been dissolved and flushed since reemergence. Dissolution of sodium-bearing minerals in sandstone, such as feldspar, is not considered to be a major source because these are relatively stable minerals (Freeze and Cherry, 1979). Other sources of sodium are agriculture and drinking water treatment systems that use sodium chloride, such as water softeners and salt-backwashing arsenic filter systems. Several of these systems are in use on north Lummi Island. In seawater, the concentration of sodium to chloride is a ratio of about 0.56:1 (mixing ratio). The ratio Na:Cl decreases as seawater moves through an aquifer during seawater intrusion because unlike chloride, sodium is

111

not a conservative ion. Despite its low cation-exchange capacity, sodium in sufficient concentrations will displace higher-order cations such as calcium from cation-exchange sites on aquifer media. This hardening process decreases Na^+ and increases Ca^{2+} concentrations in groundwater. Groundwater hardening can occur in front of seawater that is advancing into an aquifer and is often associated with the early stages of seawater intrusion. As seawater intrusion progresses, the ratio Na:Cl will approach the ratio in seawater. During a process known as freshening, an influx of freshwater enters an aquifer that has been previously intruded or subjected to Pleistocene marine inundation. This process causes increased concentrations of Na^+, in the presence of reduced concentrations of Cl-, as Na^+ is displaced from cation-exchange sites by Ca^{2+} and Cl^- is flushed out. On Hornby Island, Na^+ concentrations in chemically more evolved waters range from 14.1 to 400 mg/L (Allen and Matsuo, 2002).

Concentrations of sodium during both sampling periods range from 2 mg/L to 1345 mg/L with a median concentration of 31.7 mg/L (Appendix D). This value lies within the range of Na^+ concentrations in chemically more evolved waters on Hornby Island. The variation in median concentration of Na^+ between fall 2002 and spring 2003 is negligible (Tables 31a and 31b). Sodium ion concentrations vary by aquifer (Table 32). The Sandstone and Greenstone aquifers are probably a source of sodium for study area groundwater. These aquifers exhibit median sodium concentrations over twice the median concentration for all wells and concentrations that are much higher than most Pleistocene aquifers in the Puget Sound Region (for example Kahle and Olsen, 1995). It is possible that the concentration of Na^+ entering Pleistocene aquifers from bedrock may be sufficient to induce cation-exchange, decreasing concentrations of Na^+ and increasing concentrations of Ca^{2+}. Or, the relative contribution to recharge of Pleistocene aquifers from bedrock may be much less than the contribution from recharge through glacial drift. This would dilute the more concentrated Na^+ waters entering Pleistocene aquifers from bedrock aquifers. The latter explanation is most plausible but does not apply to all Pleistocene aquifers (please refer to the discussion on *Sodium/Calcium Concentrations and Recharge*, below). The highest median Na^+ concentrations are in the Centerview (two samples), Sandstone, Greenstone, and Hilltop Deep (two samples) aquifers (Table

32).   High concentrations of Na^+ in the Sandstone Aquifer are likely not caused by the dissolution of sodium-bearing minerals which are largely stable.

For wells completed below sea level, waters that seem to have chemically more evolved sodium-rich compositions generally coincide with wells that had Cl^- concentrations above 18 mg/L (Figures 34a and 34b). Although Na^+ concentrations vary dramatically with respect to Cl^-, there is an overall increase in Na^+ with Cl^- , especially for wells with Cl^- above about 45 mg/L.

Sodium/Calcium Concentrations and Cation-Exchange

Ratios of the concentration of Na^+ to the concentration of Ca^{2+} (Na:Ca) were examined to identify variations in trends of cation-exchange and recharge relative to sea level and among different aquifer media (Table 35a).   The evolution of groundwater from immature calcium-rich waters to chemically more evolved sodium-rich waters through sodium-enriching cation-exchange is apparent in the chemistry of groundwater (Figures 34a and 34b). Sodium occurs in greater concentrations than Ca^{2+} in most wells.   Most wells where Na^+ occurs in much greater concentrations than Ca2+ are in bedrock indicating that sodium-enriching cation-exchange is an important process controlling groundwater chemistry in these bedrock aquifers. This hypothesis assumes that the dissolution of sodium bearing minerals is small. To a lesser extent, sodium-enriching cation-exchange is likely also occurring in deeper regions of the Pleistocene aquifers. Where cation-exchange is an important process in the evolution of groundwater chemistry, one should see an overall increase in Na^+ and decrease in Ca^{2+} concentrations and an increase in the ratio Na:Ca with depth and near shore. These trends were not always evident, indicating that the importance of cation-exchange varies with depth, aquifer media, and distance from major sources of recharge.

The Ca^{2+} concentrations increase and Na^+ concentrations decrease with depth in wells in bedrock that are completed above sea level (Figures 35a and 36a). Additionally, the ratio

Na:Ca decreases with depth in these wells (Figure 36a). These trends imply that some sodium-enriching cation-exchange is occurring at shallow depths in bedrock and becomes less common at intermediate depths. Shallow, local flow systems are subject to significant annual groundwater cycling. Although the concentration of Pleistocene marine Na^+ remaining in well-flushed shallow regions is lower than deeper regions, the higher rate of groundwater cycling can induce modest sodium-enriching cation-exchange (Allen, personal communication, 2005). Intermediate flow systems have also been exposed to significant flushing but are subject to less annual cycling than more shallow regions of the aquifer. Therefore, cation-exchange may be less important at intermediate depths (Allen, personal communication, 2005).

The Ca^{2+} and Na^+ concentrations and the ratio Na:Ca increase with depth in wells completed below sea level in bedrock (Figures 35a, 36a, and 37a). Deeper regions of the aquifer are where most cation-exchange occurs because residual Pleistocene marine Na^+ is greatest due to longer marine inundation and less flushing (Allen, personal communication, 2005). In bedrock, the median concentration of Na^+ for wells completed below sea level (69 mg/L) is much higher than the median concentration of Na^+ for wells completed above sea level (46 mg/L); (Table 34b). However, median concentrations of Ca^{2+} only decrease slightly in wells completed below sea level (29 mg/L) compared with ones completed above sea level (30 mg/L); (Table 34a). This trend does not contradict the presence of sodium-enriching, calcium-depleting cation-exchange in bedrock below sea level. It is likely that the dissolution of Ca^{2+} from carbonate minerals within the aquifer occurs at all depths. This is evident in wells that are completed above and below sea level, where Ca^{2+} increases with depth in both (Figure 35a). In the absence of cation-exchange with Na^+, concentrations of Ca^{2+} would increase greatly with depth due to relatively long groundwater flow paths and extended time for chemical dissolution to take place. However, the median concentration of Ca^{2+} below sea level is nearly the same as above sea level, demonstrating that the dissolution of Ca^{2+} is mitigated by cation-exchange with Na^+. Therefore, the concentration of Na^+ is increasing faster than the concentration of Ca^{2+}. On Hornby Island, Allen and Matsuo (2002) observed that as quickly as Ca^{2+} is dissolved from aquifer media, it is lost to cation-exchange with Na^+.

Examples where this is probably occurring are in wells 04F, 04J, and 04Q. These wells are completed below sea level and have Na^+ concentrations that are two orders of magnitude higher than Ca^{2+} (Appendix D). These trends also demonstrate that the effects of groundwater hardening, in advance of seawater intrusion, reverse sodium-calcium cation-exchange and are probably localized along fractures and overshadowed by the dominant sodium-enriching, calcium-depleting cation-exchange process.

Given that fine-grained bedrock facies are mostly responsible for cation-exchange within the aquifer (Allen and Matsuo, 2002), the shale and siltstone facies of the Chuckanut Formation probably control groundwater chemistry of the Sandstone Aquifer. This might confirm that groundwater flow within the Sandstone Aquifer is primarily through fractures within fine-grained shale and siltstone facies. However, sandstone facies of the Chuckanut Formation generally have higher primary porosities, and therefore higher cation-exchange capacities, than similar facies in the Nanaimo Group of British Columbia (Allen, personal communication, 2005). For this reason, the effect of sandstone on groundwater chemistry and flow through the sandstone facies may be more significant in north Lummi Island than observed in the Gulf Islands.

Cation-exchange within the Pleistocene aquifers is less common than in bedrock because lower residual concentrations of Pleistocene marine Na^+ remain. Though the Gulf Island studies were focused on bedrock because it is the major aquifer media, groundwaters in Pleistocene aquifers on Saturna Island were observed to be immature calcium-rich waters, probably because they have higher recharge rates and more abundant carbonate minerals than bedrock (Allen, personal communication, 2005). This is evident in drilled wells in Pleistocene aquifers that are completed above sea level, though limited data are available because few drilled wells meeting these criteria exist in the study area. Samples from these wells indicate Ca^{2+} and Na^+ concentrations increase with depth (Figures 35b and 36b). The ratio Na:Ca decreases with depth above sea level (Figure 37b). This trend is also evident in the median ratio Na:Ca for dug wells (1.6) that is slightly higher than the median ratio for drilled wells above sea level (1.5); (Table 35a). The increase in Ca^{2+}

with depth and decrease in the ratio Na:Ca indicates cation-exchange in shallow Pleistocene aquifers is limited. Because Pleistocene aquifer media is dominated by sand and clay-size particles are mostly uncharged, it has fewer cation-exchange sites and has received more flushing. Therefore, less Pleistocene marine Na^+ likely remains in Pleistocene aquifers than in bedrock, especially at shallow depths and in coarse-grained deposits.   The median concentration of Na^+ for these Pleistocene wells above sea level (16 mg/L); (Table 34b) is near the median concentration of Cl^- for all wells (19 mg/L). This ratio is nearly 1:1 and might indicate that the source of Na^+ in shallow Pleistocene aquifers is from atmospherically deposited NaCl residing near the surface. The increase of Na^+ with depth above sea level may demonstrate that some sodium-enriching cation-exchange is occurring or it might be the result of recharge to Pleistocene aquifers from sodium-rich waters in bedrock aquifers. An example of the latter explanation is in well 04Y that has the highest Na^+ concentrations of any Pleistocene well completed above sea level. This well is completed in the Centerview Aquifer that is coupled to the Sandstone Aquifer.

For wells in Pleistocene aquifers that are completed below sea level, Ca^{2+} concentrations decrease slightly and Na^+ concentrations increase and with depth (Figures 35b and 36b). Additionally, the ratio Na:Ca increases with depth (Figure 37b). These trends support a sodium-enriching, calcium-depleting cation-exchange process that becomes more common with depth, where fine-grained Pleistocene deposits are more abundant (Section 5.1.2) and less flushing has occurred. Wells in Pleistocene deposits exhibiting signs of sodium-enriching cation-exchange have much greater Na^+ concentrations than Ca^{2+}. Calcium is near zero at some wells (Figures 34a and 34b). These wells (for example 09H, 09R, 09S, 10X, 15A, 15D) are some of the deeper wells in Pleistocene aquifers. Excess Na^+ in these wells is not caused by seawater intrusion because Cl^- concentrations are low. The sodium enriching cation-exchange process in the deeper Plesitocene aquifers is less obvious than in bedrock because there is less residual Pleistocene marine Na^+ in the unconsolidated aquifer media.

In Pleistocene aquifers, the increase in median Na^+ concentrations, from 16 mg/L above sea level to 21 mg/L below sea level (Table 34b), is modest compared to Ca^{2+} that increases from 9 mg/L above sea level to 17 mg/L below sea level (Table 34a). This demonstrates that because there is relatively little marine Na^+ available for cation-exchange, especially at shallower depths, Ca^{2+} concentrations increase faster than they are being exchanged. This also explains why the median ratio Na:Ca for wells completed below sea level (1.3) is less than above sea level (Table 35a).

Sodium/Calcium Concentrations and Recharge

Concentrations of Na^+ and Ca^{2+} were examined to validate recharge area conclusions for Pleistocene aquifers (Section 5.7.1). Recharge may be significant where concentrations of Na^+ and Ca^{2+} and the ratio Na:Ca are below the median values for all wells in Pleistocene aquifers (fresher waters). A total of 8 wells met these criteria. Wells 04G and 09K suggest that a recharge area for the Legoe Bay Aquifer occurs uphill from the intersection of Legoe bay Rd and Tuttle Ln. Well 10C suggests that a recharge area for the Constitution Aquifer occurs near the eastern extension of Constitution Rd. Additionally, the Consitution Aquifer exhibits the lowest concentration of Na+, and therefore, likely receives little recharge from adjacent greenstone. Well 09Q indicates that recharge to the middle region of the Nugent Aquifer may be occurring in the vicinity of Joan's Ln. This is supported by a groundwater divide at this location (Figure 22c). Wells 33F, 33G, 33T, and 04A indicate that recharge to the Lane Spit Aquifer undergoes little chemical interaction with aquifer media. Confined conditions and negative ORP values in this aquifer imply that recharge occurs some distance inland while low concentrations of Ca^{2+} and Na^+ indicate little carbonate mineral dissolution and sodium-enriching cation exchange are occurring along the groundwater flow path. These trends imply that most recharge to the Lane Spit Aquifer may be through coarse sand and gravel emergence deposits uphill from Lane Spit and west of Nugent Rd (Figure 10) and (Lapen, 2000). The same may also apply to several other small Pleistocene aquifers, such as Lane Spit Deep, Loganita, and West Shore aquifers, that have lower than median Na^+ and Ca^{2+} concentrations (Table 32). The higher concentration of Na^+ in the West

117

Shore Aquifer, relative to other small Pleistocene aquifers, may be due to a larger fraction of recharge that comes from bedrock. The Centerview and Hilltop Deep aquifers (Pleistocene deposits) have Na+ and Ca2+ concentrations that are similar to both bedrock aquifers, offering further evidence that these Pleistocene aquifers receive a large fraction of recharge from bedrock.

Chloride

Chloride is the dominant anion in seawater (Table 3) and, with the exception of very old groundwater, is a minor to trace constituent in most sedimentary and crystalline bedrock and glacial drift environments (Freeze and Cherry, 1979). Sources of chloride in island groundwater include seawater intrusion, atmospheric deposition of airborne sea salts from precipitation and dry deposition from wind, septic effluent, irrigation and agricultural operations, discharge from water treatment systems that use NaCl, dissolution of chloride-bearing minerals, and residual chloride trapped in the pore spaces of aquifer media remaining from the deposition of marine Pleistocene deposits (known as formation waters) or introduced during Pleistocene marine inundation of the study area. Due to the high mobility of these ions, it is likely that most Cl$^-$ introduced to the pore spaces of aquifer media during Pleistocene events has been flushed out and is therefore not a major source in groundwater (Allen, personal communication, 2005). However, Allen (2004) used stable isotope data to conclude that localized pockets of Pleistocene saline groundwater may exist in some infrequently used bedrock fractures. Another source of chloride at the individual well scale is the use of chloride, commonly household bleach, as a disinfectant in wells, tanks, and plumbing. Chloride concentrations were not elevated in wells showing the highest nitrate concentrations (also associated with septic effluent) of nearly 400 wells on Whidbey and Camano islands (Kelly, personal communication, 2005). Therefore, septic effluent is probably not a major source of chloride. Agriculture is limited on north Lummi Island and therefore is not considered to be a major source. Water treatment systems that use NaCl are also not considered to be a significant source because few wells having elevated Cl$^-$ display a ratio Na:Cl that is equal to one. Most wells that show definite signs of intrusion have ratios that are closer

118

to the mixing ratio. With the possible exception of Fidalgo ophiolite rocks in the Greenstone Aquifer, the dissolution of chloride-bearing minerals is considered to be a very minor source. Seawater intrusion and atmospherically-deposited sea salts are assumed to be the major sustained sources of Cl$^-$ in the study area. However, Cl$^-$ data from dug wells indicate that atmospherically-deposited sea salts probably do not produce chloride concentrations that are above background values (Table 32). Chloride is a conservative ion that tends to flow through an aquifer with little chemical interaction. As seawater progresses through an aquifer during intrusion, chloride concentrations are largely diminished as a result of dilution with freshwater. Because Cl$^-$ is a conservative ion, highly abundant in seawater relative to fresh groundwater, and relatively scarce in freshwaters of coastal aquifers in Washington, generally 10 mg/L (Dion and Sumioka, 1984), it is the most commonly used indicator of seawater intrusion.

Median concentrations of chloride for all wells in fall 2002 and spring 2003 are listed in Tables 31a and 31b. Concentrations of chloride during both sampling periods range from 5 mg/L to 3578 mg/L with a median concentration of 18 mg/L (Appendix D). This value is comparable to the median chloride value established by Schmidt (1978) for north Lummi Island, 20 mg/L, and other local studies for example Kahle and Olsen (1995) for Guemes Island, 21 mg/L, and Dion and Sumioka (1984) for Whatcom County, 20 mg/L. This value is much lower than the mean Cl$^-$ concentration for wells completed below sea level in Pleistocene deposits on Camano and Whidbey islands, Island County (38.8 mg/L, standard deviation 30.6); (Kelly, 2005).

Wells with the highest chloride concentrations are located within approximately 100 yards of the shoreline (Figures 38a, 38b, and 38c). Chloride concentrations vary moderately by aquifer. Most are near the median for all wells sampled during fall 2002 and spring 2003. The highest median chloride concentrations are in the Centerview (two samples), Hilltop Deep (two samples), and Sandstone aquifers. The Centerview Aquifer lies entirely above sea level. Chloride concentrations in the Centerview and Hilltop Deep aquifers are not considered to be significant because only one well was sampled in each aquifer. The lowest median chloride concentration is in the Constitution Aquifer that lies

119

entirely above sea level. There is considerable variation in chloride concentrations among wells completed in the Sandstone and Nugent aquifers (Table 36) where most wells are completed below sea level.

Chloride data from 18 wells monitored on a bi-monthly basis from March 1991 to January 1992 as part of previous study (Whatcom County, 1994) were plotted to examine seasonal variability. Median chloride concentrations during this period show a small decrease during the late dry season while their standard deviations show the opposite trend (Figure 39). This indicates that variation in chloride concentrations increases during dryer months when water levels are lower (Section 5.5.1) and pumping rates are higher. The variation of chloride concentrations observed in some wells during the 1991-1992 monitoring period might explain why several wells sampled during my study showed much higher chloride concentrations during the low water monitoring period, fall 2002.   A decrease was most common among wells showing large changes in chloride concentration (greater than 15%) between fall 2002 and spring 2003 (Table 39). The median chloride concentration for all wells was only slightly higher in fall 2002 than spring 2003 (Tables 31a and 31b). Considering the 1991-1992 sampling and the sampling conducted during my study, wells experiencing the greatest fluctuations in chloride concentrations throughout the year exhibit much higher chloride levels in late summer. This pattern is likely the result of active seawater intrusion in some wells during dryer months when water levels are low and pumping rates are high. This causes an increase in the variability of chloride concentrations for wells that are prone to intrusion, but has little effect on wells that are not, implying that intrusion is localized. Most wells that experience small fluctuations in chloride exhibit a slight decline in chloride levels during late summer.

Chloride concentrations increase with depth for most aquifers (Figure 40). This result was expected because the major source of Cl^- in groundwater below sea level is assumed to be from seawater intrusion. For wells completed below sea level, median concentrations of Cl^- are about 30% higher in bedrock than Pleistocene deposits (Table

34c). The median Cl⁻ concentration for wells completed above sea level in bedrock is slightly higher than the median Cl⁻ concentration in wells completed below sea level in Pleistocene deposits.

Establishing a background chloride concentration is necessary to identify wells that may be experiencing seawater intrusion and sets a baseline for future monitoring. The background chloride concentration lies between the median value for all wells completed above sea level (19 mg/L) and the highest concentration of any sample taken from a well completed above sea level in Pleistocene deposits, 37 mg/L (04Y, Centerview Aquifer); (A well from Whatcom County, 1994, that is likely completed in the Centerview Aquifer had Cl⁻ equal to 45 mg/L). This criterion for defining the upper limit of background Cl⁻ concentrations was chosen because some wells completed above sea level in bedrock may be influenced, to a very limited extent, by saline water that is pulled up into the well via fracture flow (Section 5.8.2). Using a value near the maximum chloride concentration found above sea level in this study is a conservative approach to identify wells possibly experiencing seawater intrusion. This background value is considered to be effective in screening many wells that may have elevated chloride levels due to sources other than seawater intrusion.

Sodium/Chloride Concentrations and Cation-Exchange

The cation-exchange processes that affect concentrations of sodium and calcium, do not impact concentrations of chloride.   However, they do affect the ratio of sodium to chloride (Na:Cl); (Table 35b). The ratios Na:Cl for dug wells range from 0.0 to 6.5 with a median value of 1.0. The maximum Na:Cl ratio is for 04P, a dug well completed in beach gravels at Lane Spit that had exceedingly high Cl⁻ concentrations. The significance of a median Na:Cl ratio of 1.0 for dug wells was unexpected because the primary source of Na^+ and Cl⁻ ions in these shallow wells is assumed to be from atmospherically deposited sea salts and, therefore, should resemble the ratio in seawater (Table 3). Given this result, it is possible that the primary atmospherically-deposited sea salt is NaCl (ratio of 1.0) or that near-surface groundwater is undergoing minor sodium-enriching cation-

exchange. The former is most likely because little Pleistocene marine Na^+ is assumed to remain in shallow Pleistocene deposits. This is supported by the median ratio Na:Cl in drilled wells completed above sea level in Pleistocene aquifers, 0.9, that is nearly the same as for dug wells. The median ratio Na:Cl for drilled wells completed below sea level in Pleistocene aquifers is 1.2, slightly higher than at shallower depths, indicating increased sodium-enriching cation-exchange in fine-grained Pleistocene deposits at depth.

Sodium-enriching cation-exchange is a more important process in bedrock than in Pleistocene deposits. This explains the large difference in median values of the ratio Na:Cl between wells completed in bedrock and Pleistocene aquifers (Table 35b). The median ratio Na:Cl for wells completed above sea level in bedrock is 2.4 and for wells completed below sea level in bedrock is 2.9, further supporting the importance of sodium-enriching cation-exchange in bedrock.

5.8.2 Assess Seawater Intrusion

Seawater intrusion conditions were evaluated using a physical and chemical approach. The physical approach involved using the Ghyben-Herzberg Relation to predict the location of the freshwater/seawater interface at each well. The chemical approach involved using water-chemistry data to test results of the physical approach by identifying wells experiencing intrusion. Many studies use chloride concentrations as the only method to assess seawater intrusion because it is the major ion in seawater and because sources other than seawater intrusion often do not create high chloride concentrations in an aquifer. However, there are several potential sources of chloride in groundwater other than seawater intrusion, so using chloride as an exclusive diagnostic method can lead to the incorrect characterization of seawater intrusion conditions (Kelly, 2005). For example, Kelly (2005) used major ion chemistry and surveyed water level elevations to determine that elevated chloride concentrations in numerous wells in central Whidbey Island are not caused by seawater intrusion but are associated with very hard

groundwater. Based only on chloride concentrations, previous workers had determined that this region of Whidbey Island is undergoing large-scale seawater intrusion. To minimize the possibility of making incorrect determinations of seawater intrusion on north Lummi Island, I employed several diagnostic methods based on water-chemistry data that I collected. Water chemistry that is indicative of seawater intrusion occurs only after the aquifer has been intruded and cannot be used as a predictive tool (Kelly, 2005). I also employed the physical approach as an additional diagnostic tool and as a limited attempt to identify regions of the study area that may be at higher risk for intrusion.

Physical Approach

The Ghyben-Herzberg Principle is a physical relation based on the density contrast between freshwater and seawater (Section 2.8). Assuming static conditions, it provides a means to predict the location of the freshwater/seawater interface based on the elevation, above sea level, of the potentiometric surface of an aquifer. Total head at each well completed below sea level was used to predict the location of the freshwater/seawater interface (Table 37). This was compared to well completion elevations. Only one well, 08O, is completed below the predicted interface. The median distance from the bottom of each well to the predicted interface is 477 feet (standard deviation 1321); (Table 37). The large difference between the standard deviation and the median indicates a widely dispersed data series that may have limited reliability. The water-level elevation at which the predicted interface will rise to reach the bottom of each well ranges from 0 to 4.9 feet (Table 37). For most wells completed below sea level, this point is reached after a drawdown of about 12 feet. If the water level in a well is depressed for sufficient time, the hydraulic gradient will be reversed and seawater will begin to migrate toward the well. Because most wells, especially ones completed in bedrock, have low specific capacities (Section 5.4.2), they experience large drawdowns in response to pumping. Therefore, water levels in almost all wells completed below sea level frequently exceed the level at which the predicted interface will reach the bottom of the well (Table 37). Despite this, chloride concentrations indicate that most wells are not experiencing seawater intrusion (Appendix D). There are several reasons for this. The actual location

123

of the interface often varies from the predicted location primarily because most systems do not meet static criteria. Under dynamic conditions, water flow pushes the interface seaward. The Ghyben-Herzberg predicted interface assumes a sharp boundary between freshwater and seawater and does not account for mixing (Bear, 1979). The mixing zone is at least 49 feet thick at 08O. Although this well is completed below the predicted interface and has chloride concentrations higher than any well, its water chemistry is more dilute than seawater. Seawater intrusion is largely driven by the static water level in an aquifer. Many pumping wells probably do not draw down water levels for a period of time that is sufficient to cause the complete migration of seawater to the well. In bedrock wells, observed drawdown in a well is caused by the removal of water from the well that may not have a significant affect on static head in the aquifer. Also, many wells near shore may be completed in discharge zones where hydraulic head increases with depth. Finally, Kelly (2005) concluded that the water levels in some wells can be drawn down below sea level and not experience seawater intrusion as long as the potentiometric surface between the pumping well and shoreline (or submarine aquifer outcrop) remains sufficiently above sea level. If sufficiently above sea level, the water level elevation between the pumping well and the shoreline creates a barrier that prevents seawater intrusion by ensuring the freshwater/seawater interface remains below the base of the aquifer. This will be referred to as a protection factor. The pumping well in Figure 41 is in an aquifer that is bounded below by an aquitard. The pumping well has drawn down the local potentiometric surface to below sea level, causing an upward movement of the predicted interface to the bottom of the well (false interface). In this case, the water level elevation is sufficient to prevent seawater from advancing through the aquifer. According to Kelly (2005), if the potentiometric surface in the aquifer (designated as A) decreases, the protection factor decreases. This will result in the upward movement of the predicted interface (designated as B) until it reaches the base of the aquifer (critical rise). At the critical rise, seawater will advance laterally inland through the aquifer and beneath the pumping well over a relatively short period of time, leading to seawater intrusion at the pumping well. For this reason, and because the freshwater lens thickens inland, Kelly (2005) observed that the risk of seawater intrusion decreases with distance from shore in many aquifers.

Chemical Approach

Water chemistry was used to evaluate seawater intrusion using several diagnostic methods.

Chloride Concentrations

The first step to assess seawater intrusion in north Lummi Island was to identify wells having elevated concentrations of Cl^-. The term elevated chloride concentrations is used to refer to concentrations exceeding 19 mg/L, the median for wells completed above sea level and the lower bound for background concentrations of Cl^-. Twenty-three wells completed in bedrock and 14 wells completed in Pleistocene deposits have Cl^- concentrations that exceed 19 mg/L (Appendix D). Most of these wells showed elevated Cl^- concentrations during both sampling periods. Chloride concentrations in 5 wells (08O, 04P, 09G, 04N, 32K) exceed 100 mg/L, a concentration used to define seawater intrusion (Washington State Department of Ecology, 1991). Chloride concentrations in 6 additional wells (32X, 04J, 04F, 04Q, 33D, 09C) not meeting this definition are above the upper bound for background Cl^- and range from 38 to 66 mg/L. Thirteen additional wells that were not sampled during this study had elevated Cl^- concentrations during monitoring in previous studies (Schmidt, 1978; Dion and Sumioka, 1984; Whatcom County, 1994); (Figure 38c).

Chloride Concentration Versus Completion Elevation

Wells experiencing seawater intrusion will generally be completed below sea level. Well completion elevations are listed in Appendix B. Twenty-nine wells with elevated Cl^- are completed below sea level. Although Cl^- concentrations increase with depth (Figure 40), 6 wells that are completed above sea level also have elevated Cl^- concentrations that range from 37 to 953 mg/L (Table 38). Of these wells, the one with the highest Cl^- concentration is a dug well in beach gravels along Lane Spit that is completed near the high tide mark. Three of these wells are in the Sandstone Aquifer (32X, 33D, 33M) and one is probably in the Greenstone Aquifer (09C). The wells completed in sandstone are located in a remote region of the study area and are hydraulically up-gradient from any homes and known anthropogenic sources of chloride. Assuming that completion depths listed in the well logs and well-head elevation measurements are accurate, two

125

hypotheses are offered to explain elevated Cl^- in bedrock wells that are completed above sea level. First, residual pockets of saline groundwater left over from Pleistocene marine inundation may occur in less permeable and infrequently used bedrock fractures (Allen, personal communication, 2005). During low water months, in aquifers that experience significant water level fluctuations, groundwater flow is concentrated in these fractures. Second, these wells could be completed near fractures that are hydraulically connected to deeper regions of the aquifer. This might induce localized active seawater intrusion if even a single fracture, serving as an extension of the drilled borehole, was connected to the freshwater/seawater mixing zone, especially if the well is completed in a steeply dipping formation or if tidal variations are great (Allen, personal communication, 2005). Water level fluctuations between sampling periods for these wells were the highest of any measured, ranging from 2.5 to 26.6 feet (Tables 19 and 20); (33M was recorded as going dry in September, 1994). Additionally, sandstone was mapped by Carroll (1980) as steeply dipping in the vicinity of these wells. One problem with the latter explanation is that all of the wells completed above sea level in bedrock having elevated Cl^- also have bottom elevations greater than 40 feet. Well pumps likely need to be placed very close to sea level to draw-up saline water from the mixing zone. Future study of the groundwater chemistry at these wells is required to determine the source of elevated Cl^- in these wells.

The two possible sources of elevated Cl^- in bedrock that are listed above do not apply to Pleistocene sediments that lie above sea level. Therefore, the Cl^- concentration at well 04Y (37 mg/L); (Pleistocene aquifer) is considered to comprise the upper bound for background Cl^- concentrations (Section 5.8.1). Elevated Cl^- concentrations at this location are due to sources other than seawater intrusion and may be anthropogenic. One dug well (04P), completed an elevation of 1.5 feet, has the highest Cl^- concentration of any well that is completed above sea level. This well is in beach gravels along the shoreline at Lane Spit and is highly susceptible to seawater intrusion.

Seasonal Variations in Chloride Concentrations
Chloride data collected during my study and from 1991-1992 (Whatcom County, 1994) show that seasonal variations in median Cl^- concentrations are small but the variability

among wells is great, especially in late summer. This indicates that some wells are at the greatest risk of seawater intrusion when water levels are low and pumping rates are high. Kelly (2005) concluded that sources of Cl^- other than seawater intrusion, on Whidbey and Camano islands, tend cause increased chloride concentrations that exhibit little seasonal variability. He cites higher Cl^- concentrations during summer months as the result of seawater intrusion caused by increased pumping. I also examined variations in Cl^- concentrations as an additional diagnostic method to assess seawater intrusion conditions. Changes in chloride concentrations between fall 2002 and spring 2003 were small for most wells. Approximately 1/3 of wells experienced greater than 15% change in Cl^- during this period (Table 39). Seven of the wells listed in Table 39 have Cl^- concentrations above the upper bound for background Cl^- (37 mg/L). Several of these (3 are completed above sea level; 04P, 32X, 33D) exhibit higher Cl^- concentrations in the spring. Water sampling in spring 2003 took place in May and June. Higher Cl^- concentrations in these wells during spring sampling may reflect the onset of early season increased water demands. For one well, 04P (dug well on Lane Spit), high winds and tides in winter may have introduced seawater from above. Four wells (15O, 16K, 04T, 09P) show large seasonal variation in Cl^- but have concentrations that are below the upper bound of background Cl^-. These wells are completed in Pleistocene aquifers and increased Cl^- could be the result of minor active seawater intrusion in late summer. It also illustrates the limitation of using Cl^- concentrations as the only diagnostic method to assess seawater intrusion.

Ion Ratios

The concentrations of major ionic constituents of seawater are listed in Table 3. In seawater, the ratio of the concentration of sodium ions to chloride ions is 0.56 (mixing ratio). Because major sources of Na^+ are seawater intrusion and Pleistocene marine Na^+ sorbed onto cation-exchange sites within the aquifer media, ratios Na:Cl that greatly exceed the mixing ratio are probably the result of sodium-enriching cation-exchange (Section 5.8.1). Freshening exchange at previously intruded wells might also account for occurrences of excess Na^+. The sodium-enriching cation-exchange process controls much of the chemistry of groundwater in north Lummi Island, especially in bedrock, as

most samples have ratios Na:Cl that are much larger than the mixing ratio. Therefore, groundwater that displays ratios Na:Cl that are close to the mixing ratio are probably intruded. Concentrations of Na^+ and Cl^- for all wells (Appendix D) were examined and the ratios Na:Cl that are closest to the mixing ratio are listed in Table 40. Figure 42 is a sodium-chloride concentration bivariate plot of data from all wells that provides a graphical representation of the ratio Na:Cl. Samples that plot near the mixing line may be from intruded wells. Some samples that plot to the right of the mixing line (Na:Cl ratios higher than the mixing ratio) may also be from intruded wells, but contain excess sodium. These are probably close to highly evolved compositions. Using a similar technique, Allen et al. (2001) concluded that samples that plot to the right of the mixing line indicate an additional source of Na^+ thought to be from sodium-enriching cation-exchange. Three wells (09C, 32X, 33D) with ratios Na:Cl close to the mixing ratio are completed above sea level in bedrock. Sources of elevated Cl^- concentrations in these wells are not fully understood. Notably, the ratio Na:Cl for 33D is equal to the mixing ratio, 0.56. Three wells having relatively low Cl^- concentrations (09P, 15O, 32H) plot near the mixing line in Figure 42. The ratios Ca:Cl for the wells in Table 40 greatly exceed the ratios of these ions in seawater, possibly indicating groundwater hardening, ahead of seawater intrusion or direct-salinization of immature groundwater at some of these wells.

With the exception of Ca^{2+}, that is over one order of magnitude greater, wells 04N and 09G had major ion ratios with chloride that are very close to seawater (Table 33). Additionally, these two wells had Cl^- concentrations exceeding 100 mg/L during the 2002-2003 sampling period and again in 2005, implying that they are experiencing seawater intrusion.

Chloride versus Specific Conductance

Chloride concentrations and specific conductance measurements taken during fall 2002 and spring 2003 were plotted to help delineate elevated Cl^- induced by seawater intrusion from elevated Cl^- associated with very hard groundwater (Figure 43). This diagnostic method works on the premise that specific conductance is largely proportional to TDS, so

128

a given concentration of Cl$^-$ would be associated with much higher specific conductance if the source of chloride is from very hard groundwater instead of seawater intrusion (Kelly, 2005). The freshwater, seawater intrusion, mixing, and hard groundwater fields in Figure 43 were developed by Van Denburgh et al. (1968) and modified by Kelly (2005) based, in part, on data from Whidbey and Camano islands that are almost completely comprised of Pleistocene deposits. Therefore, the fields shown in this figure are not directly applicable to samples from wells completed in bedrock on north Lummi Island, where the sodium-enriching cation-exchange process dominates groundwater chemistry. Samples from 6 wells completed in bedrock make up all but one of the samples (09G) that are located in the hard water field. Three of these (04F, 04J, 04Q) have very high Na$^+$ and very low Ca^{2+} concentrations (Appendix D), indicative of sodium-enriching cation-exchange, and probably not hard groundwater. Two (29C, 32K) have very high Na$^+$ concentrations and Ca^{2+} concentrations that are above the median for all wells. One (33M) has very high Ca^{2+} and moderate Na$^+$ concentrations and plots to the right of the hard groundwater field. Samples from 4 wells (04N, 04P, 08O, 09G) plot in the seawater intrusion field and samples from 2 additional wells (32K, 32X) plot in the mixing field.

Major Ion Chemistry

To provide a more definitive diagnostic method for assessing seawater intrusion through the use of Piper and Stiff diagrams, commonly used in geochemical analysis, major ion concentrations were analyzed for 5 wells (Table 33). Funding prevented me from conducting this analysis on more wells, so I chose wells having enigmatic water chemistries and that I thought might be representative of conditions at other wells. Three samples were taken from wells completed in bedrock and two from wells completed in Pleistocene aquifers.

Stiff Diagrams for these wells are shown in Figure 44. Results from well 09S display a freshening profile caused by either the reversal of modern seawater intrusion or sodium-enriching cation-exchange. The abundance of fine-grained sediments that serve as a source of Plesitocene marine Na$^+$, increases with depth. Results from wells 04F and 04J

(Sandstone Aquifer) also display freshening profiles, but with other processes superimposed. Samples from these wells have excess Na^+ resulting from cation-exchange in bedrock and 04F has excess SO_4^{2-} that is probably from sulfate reduction in highly reducing water. The redox measurement at 04F in spring 2003 was –101 mV. Reducing conditions in both wells are characteristic of water that has been in the aquifer for a long time. These wells also have elevated Cl^- that may be the result of salinization in the mixing zone. The freshening profiles exhibited by these wells are probably the result of sodium-enriching cation-exchange and not are from the reversal of modern seawater intrusion. Wells 04N (Sandstone Aquifer) and 09G (Nugent Aquifer) display a seawater intrusion profile.

Well 09S plots near the middle lower portion of the Piper diamond (Figure 45) in the region designated by Allen and Matsuo (2002) as chemically more evolved groundwater (Figure 31). In the groundwater evolution process described by these authors, water will continue to move toward the lower right region of the Piper diamond, as a result of sodium-enriching cation-exchange. Data from well 04J plot close to the lower right side of the Piper diamond in the region designated as sodium-rich highly-evolved groundwater (Figures 31 and 45). Groundwater moving toward a discharge region will continue to move up along the right side of the Piper diamond as it mixes with chloride-rich water near the freshwater/seawater interface (salinization). Data from well 04F also plots on the far right side of the diamond, slightly above 04J in the highly-evolved groundwater region reflecting a greater degree of salinization (Figures 31 and 45). Data from two wells (04N and 09G) plot near the middle of the Piper diamond above the mixing line in the seawater intrusion field (Figure 45). Groundwater in these wells may have undergone direct-salinization, by-passing sodium-enriching cation-exchange. This is indicative of active seawater intrusion.

Seawater Intrusion Summary

Several diagnostic methods were employed to minimize the possibility of incorrectly designated wells as either intruded or not intruded based on Cl^- concentrations alone. These methods prompted the following questions: Are Cl^- concentrations elevated? Is the well completed below sea level? Was there a large change in Cl^- concentrations between sampling periods? Is the ratio of Na:Cl close to the seawater mixing ratio and do samples plot near the mixing line on a sodium-chloride bivariate plot? Do the samples have intrusion profiles on Stiff Diagrams and do they plot in the mixing or intrusion fields of a Piper Diagram? From these criteria, I determined that 19 of 80 wells sampled during the study experienced some degree of seawater intrusion (Table 41). Seawater intrusion is not an absolute condition at most wells. This is because the actual freshwater/seawater interface is a diffuse boundary that influences water chemistry differently as it progresses inland, because other hydrochemical processes such as cation-exchange are occurring in the aquifers, and because sources of Na^+ and Cl^- ions that are not related to seawater intrusion, such as residual Pleistocene marine ions, atmospherically deposited sea salts, or anthropogenic sources, may be present. For these reasons, the wells in Table 41 are grouped into three qualitative confidence categories based on the number of criteria that were met: Definitely Intruded (met most), Probably Intruded (met more than one), Possibly Intruded (met at least one).

Most of the wells that were determined to have experienced some seawater intrusion are completed in bedrock. Water level elevations (total head) in these wells range from 1 to 180 feet (Table 41). The distance from the bottom of these wells to the predicted interface range from 49 feet above to 5784 feet below the bottom of the well with a median value of 1789 feet. Because the magnitude of total head and distances to the predicted interface are large at most wells, the potential for seawater intrusion is probably small. The fact that most wells experiencing intrusion are completed in bedrock underscores the importance of the physical properties of bedrock that control intrusion. The hydraulic conductivity in bedrock is controlled by fracture flow and is over one order of magnitude less than Pleistocene deposits. The overall low hydraulic conductivity in bedrock causes drawdown to extend over long distances and increases recovery times.

As a result, even wells with high total head may be subject to intrusion because they frequently draw down water levels beyond the point at which the predicted interface will reach the bottom of the well. Drawdown in a pumping well might only reflect the removal of water from a borehole. Simply pumping water from a borehole does not necessarily induce head changes in the surrounding aquifer, especially if the aquifer has low hydraulic conductivity. However, the hydraulic conductivity along some individual fractures can be very high and, in some cases, this may induce active seawater intrusion to wells along discrete fractures even where surrounding aquifer head remains relatively high (Allen, personal communication, 2005). A possible example is 04N that is classified as definitely intruded and has a total head of 85 feet. The possibility was investigated, that water chemistry at this well might be influenced by an arsenic treatment system that discharges NaCl backwash on the ground, about 50 feet from the well. I determined that discharge from this system is probably not responsible for elevated Cl^- at this well because the ratio of Na:Cl was 0.6. One well, with a completion elevation of about –100 feet that was sampled during 1991-1992 (Whatcom County, 1994) is located within 100 yards of 04N. This well does not show elevated Cl^- concentrations, suggesting that highly localized fracture flow intrusion may be occurring. In another example, previous studies identified greatly elevated chlorides at several wells along Nugent Rd, north of the Ferry Dock (Figure 38c). Two wells sampled in this study (04I, 04K) are located near these wells from previous studies and have Cl^- concentrations within background levels. The fracture flow mechanism is hypothesized to explain why some wells that are further inland may be intruded while adjacent wells and those located closer to shore may not be intruded. It is also possible that the water chemistry in these wells and in some wells completed above sea level is being influenced by residual Pleistocene marine waters that are trapped in infrequently used fractures. Complex fracture flow patterns and large tidal fluctuations likely cause the mixing zone to occur at variable depths within the Sandstone Aquifer that might be much higher than predicted by the Ghyben-Herzberg Relation. Well 08O is completed within the mixing zone that is at least 49 feet thick. Wells 04F and 04J may be drawing water from the mixing zone. These wells plot in the highly evolved composition field on a Piper Diagram (Figures 31 and 45) and are likely

undergoing salinization. Wells that have similar water chemistry, but were not sampled for major ion analysis, are also likely drawing water from the mixing zone (04D, 04Q).

Few wells experiencing some degree of seawater intrusion are completed in Pleistocene aquifers. Only one, 09G, is designated as definitely intruded. The other wells are designated as possibly intruded because Cl$^-$ concentrations are not greatly elevated, but did have much higher Cl$^-$ concentrations in fall 2002 and Na:Cl ratios that indicate intrusion. Water level elevations (total head) in these wells range from 7 to 8.4 feet (Table 41). Kelly (2005) concluded that 97% of all wells in Pleistocene deposits experiencing seawater intrusion on Whidbey and Camano islands had total head elevations less than 8.4 feet. He noted that wells in Pleistocene deposits having total head elevations greater than 20 feet have limited risk of intrusion, regardless of pumping rates. Kelly's observations are for Pleistocene aquifers only and may not apply to bedrock where pressure losses are transmitted over greater distances. Total head elevations are less than 20 feet in all Pleistocene aquifers that lie near sea level in north Lummi Island (Figures 22b and 22c). The distance from well screen elevations to the Ghyben-Herzberg predicted interface in Pleistocene wells ranges from 95 to 949 feet with a median distance of 343 feet (Table 37). Intrusion at 09G shows that the predicted interface can be pulled up over 200 feet in Pleistocene deposits.   Pleistocene aquifers in north Lummi Island that are in contact with the sea are mostly confined and relatively thin. Barring the effects of intrusion, seawater likely does not naturally exist at depth in most Pleistocene aquifers.   Intrusion to Pleistocene aquifers likely occurs when a critical rise in the predicted interface is achieved, allowing seawater to laterally advance inland. This may explain why few wells in Pleistocene aquifers are intruded and why ones that exhibit signs of intrusion do so in late summer when water levels are low and pumping rates are high. Sampling conducted during previous studies show that one well, correlated to 08G (not sampled in this study); (Table 21), had Cl$^-$ concentrations exceeding 2300 mg/L (Figure 38c). This well is in the Village Point Aquifer and lies within 100 yards of 08O.

My assessment of seawater intrusion yielded several spatial trends. Considering that more than 78% of drilled wells that were sampled are completed below sea level and only 19 wells showed some degree of intrusion (4 of these are completed above sea level), intrusion does not seem to be occurring on an aquifer-wide scale. From this study and previous studies (Figure 38c), the region having the highest density of intruded wells is along the eastern shoreline, north of the ferry dock to about Centerview Rd. This is also one of the more densely populated shoreline areas in the Sandstone Aquifer. Wells in the bedrock aquifers are more prone to seawater intrusion because the low yield of this media causes large drawdowns over greater distances than in Pleistocene deposits. Where fracture density is high or fracture aperture is large, localized intrusion can occur along discrete fractures and possibly even in wells that are completed slightly above sea level. Wells affected by intrusion are located along the shoreline, though several in bedrock are located further inland, probably as a result of fracture flow intrusion. The greater number of intruded wells located along the shoreline could be the result of a higher well density, wells that are drilled too close to the mixing zone that is shallowest near shore, lower water levels that create a diminished protection factor (especially in bedrock), allowing seawater to laterally intrude, or a combination of these. The low number of intruded wells and lower median Cl⁻ concentrations in the Pleistocene aquifers underscores their relative resistance to intrusion. This is probably because these aquifers have relatively high storage and horizontal hydraulic conductivity properties hence higher horizontal flow that acts to drive the interface seaward.

The risk of seawater intrusion is greatest in late summer when water levels are low and pumping rates are high. Median Cl⁻ concentrations for all wells during my study and in 1991-1992 (Whatcom County, 1994) show little change or even a small decrease in median Cl⁻ during fall 2002 (September-October), yet the range of Cl⁻ values among wells increases dramatically. This is the effect of active seawater intrusion due to pumping. The negligible effect on median Cl⁻ concentrations at most wells indicates that intrusion is highly localized, especially in bedrock. Seasonal water level fluctuations are greatest in the bedrock and negligible in Pleistocene aquifers, contributing to the greater risk of intrusion in the bedrock.

6.0 CONCLUSIONS

The north half of Lummi island, where I focused my study, is 3.87 square miles of gently sloping topography. Residents in the study area rely entirely on groundwater resources where half of all wells are in bedrock and nearly 80% are completed below sea level. A three-dimensional stratigraphic model created for this study reveals a highly complex hydrostratigraphic setting. A dramatically undulating bedrock surface is concealed nearly everywhere by Plesitocene deposits up to 300 feet thick. The bedrock consists of tightly-folded sandstone, shale, and conglomerate of the Chuckanut Formation (sandstone) in the north part of the study area and metamorphosed volcanics of the Fidalgo ophiolite sequence (greenstone) in the south. The sandstone and greenstone are separated by a deep southeast-northwest trending trough that is filled with unconsolidated deposits. The Pleistocene mantle is dominated by silt-clay diamicton (about 80% of the volume of unconsolidated deposits) that is likely associated with glaciomarine drift and till to about sea level and Cherry Point silt below. Coarse-grained lenses within the silt-clay diamicton are correlated to emergence beach deposits at land surface and Vashon advance outwash near sea level. Coarse-grained lenses become finer and thinner with depth below sea level and are likely sand interbeds within the Cherry Point silt.

At least 12 distinct aquifers were identified from the stratigraphic model and water-level data. The Sandstone Aquifer occupies 56% of the study area and has more wells (49 of 130) than any other aquifer. The Greenstone Aquifer, in the southeastern region of the study area, is much smaller and has fewer wells (13 of 130). Bedrock aquifers are confined in most places below elevations of about 150 feet, where they are mantled by less permeable silt-clay diamicton. Ten, thin and discontinuous Pleistocene aquifers fill depressions in the bedrock surface and many are in contact with the bedrock aquifers. Seven of these lie at or below sea level including the two largest Pleistocene aquifers, the Legoe Bay and Nugent aquifers, that comprise much of the southern half of the study area. Most Pleistocene aquifers are confined or semi-confined and several may be hydraulically connected in a leaky aquifer system.

Hydraulic properties were estimated from well log data. The Pleistocene aquifers have a geometric mean horizontal hydraulic conductivity of 9 ft/day. The Greenstone Aquifer has the lowest hydraulic properties with a geometric mean horizontal hydraulic conductivity of <0.1 ft/day. The Sandstone Aquifer has a geometric mean horizontal hydraulic conductivity of 0.3 ft/day. Groundwater flow within the Sandstone Aquifer might be controlled by closely-spaced fractures in the fine-grained facies of the Chuckanut Formation where sodium enriching cation-exchange is an important process. Or, flow might be concentrated in highly fractured sandstone facies. Further examination of well-log data and geophysical studies may be necessary to determine which flow regime is dominate in the Sandstone Aquifer.

Water level fluctuations measured over two seasons range from 0.02-26.6 feet with a median value of 0.2 feet. The greatest fluctuations occurred in the upper reaches of the bedrock aquifers. There is limited data from long-term water level monitoring in wells, but a comparison of water levels in 7 wells measured during this study and in the early 1990s (Whatcom County, 1994) indicates a difference in water levels of less than one foot. Therefore, wells that have been reported by residents as drying-up are likely completed within the range of seasonal water level fluctuations, or are in small, isolated sand lenses that will support only limited withdrawal, or may be experiencing the effects of interference drawdown from nearby wells. Potentiometric surfaces mapped for three of the major aquifers indicate hydraulic gradients are highest in bedrock (0.035-0.08) and lowest in Pleistocene aquifers (0.0028-0.0044). Estimated average linear velocities are similar for bedrock and Pleistocene aquifers (within one order of magnitude) due to variations in hydraulic gradient and horizontal hydraulic conductivity between these aquifers.

Total groundwater storage capacity was estimated from the saturated volume and assigned effective porosity of each aquifer. Due to its size, the volume of water in storage in the Sandstone Aquifer is estimated to be over ten times the sum of the volume of water in all Pleistocene aquifers. The method used greatly overestimates the quantity

of groundwater that is available for exploitation but provides a means to compare relative volumes of water in storage among aquifers.

Slope, soils, and sub-soil geology likely have little effect on recharge magnitudes that are probably controlled by evapotranspiration. The glacial drift mantle stores water from precipitation and transmits it downward at a rate that the underlying bedrock can accept. This is likely the most important recharge mechanism because bedrock aquifers comprise the majority of the study area and many Pleistocene aquifers receive recharge, in part, where they abut saturated bedrock. Another important mechanism is infiltration through glacial drift into underlying Pleistocene aquifers, especially where coarse-grained lenses breach land surface. Recharge areas that were identified from the stratigraphic model, potentiometric surfaces, sub-soil geology, and groundwater chemistry are located in the upper and inland regions and are more extensive than those mapped by Schmidt (1978). The most important recharge areas are those that provide primary recharge to the Sandstone, Legoe Bay, and Nugent aquifers. Recharge magnitudes, estimated from a site-specific water-mass balance, average 8 inches per year, or 24% of average annual precipitation. A chloride-mass balance, used as a semi-independent method to check recharge magnitude, provides a lower bound. Recharge using this method was estimated to be 4 inches, or 11% of average annual precipitation.

A survey of selected parameters from over 80 wells during two seasons indicates that groundwater chemistry varies among bedrock and Pleistocene aquifers. Sodium and calcium cation concentrations in the bedrock aquifers reflect groundwater evolution patterns observed in the neighboring Gulf Islands of British Columbia where sandstone aquifers are common and sodium enriching cation-exchange is an important process (for example Allen and Matsuo, 2002). Groundwater chemistry in the Pleistocene aquifers is similar to other Puget Sound islands such as nearby Guemes Island (Kahle and Olsen, 1995). Exceptions are small Pleistocene aquifers that have similar groundwater chemistry to bedrock aquifers and likely receive significant recharge from the bedrock.

Although most wells are completed below sea level, passive seawater intrusion on an aquifer-wide scale is not evident. Chemical analyses, including chloride concentrations, indicate 5 wells are definitely intruded. Various diagnostic methods suggest that up to 14 additional wells may be experiencing some degree of intrusion. An examination of previous studies identified 13 additional wells having chloride concentrations exceeding 100 mg/L. Nearly all wells experiencing intrusion are in the Sandstone Aquifer, near the eastern shoreline. Intrusion of wells in the bedrock is likely controlled by fractures that are in contact with saline water, causing occurrences of seawater intrusion to be localized. Fracture flow and low storage properties of the bedrock are probably responsible for the apparent intrusion of wells with high hydraulic head (greater than 50 feet). Sources of elevated chloride in some wells completed above sea level in bedrock are not fully understood and require further study. Seawater intrusion was confirmed in only one well completed in a Pleistocene aquifer.

7.0 FUTURE WORK

This study is intended to provide a general overview of the hydrostratirgaphic, hydrogeologic, and hydrochemical setting of north Lummi Island. To improve the overall understanding of the hydrogeology of Lummi Island, I suggest future researchers should:

- Refine the stratigraphic model in regions with limited well log data.

- Accompany local drillers during drilling of new water wells and collect and analyze samples from cuttings

- Perform pump tests of selected wells in discrete groundwater basins

- Update potentiometric maps

- Conduct major ion analysis of selected wells

- Conduct long-term monitoring of selected wells in discrete groundwater basins

- Survey additional hydrologic data

- Use the stratigraphic model as the basis for groundwater flow modeling

8.0 REFERENCES

Allen, D.M., personal communication regarding the hydrochemistry of Gulf Islands, British Columbia, 15 February 2005.

Allen, D.M., Matsuo, G..P., Suchy, M., and Abbey, D.G., A Multidisciplinary approach to studying the nature and occurrence of saline groundwater in the Gulf Islands, British Columbia, Canada, Proceedings of the 1st International Conference on Seawater Intrusion, Morocco, 19-25 April, 2001.

Allen, D.M. and Matsuo G.P., Results of the groundwater geochemistry study on Hornby Island, British Columbia, Department of Earth Sciences, Simon Fraser University, Burnaby, British Columbia, 2002.

Allen, D.M., Sources of ground water salinity on islands using ^{18}O, ^{2}H, and ^{34}S, National Groundwater Association publication Groundwater vol. 42 no. 1 p. 17-31, 2004.

Armstrong, J.E., Crandell, D.R., Easterbrook, D.J., and Noble, J.B., Late Pleistocene stratigraphic chronology in southwestern British Columbia and northwestern Washington [abstract], Geological Society of America Special Paper 82, 1965.

Blake, M.C., personal communication regarding bedrock geology of Lummi Island, Washington, 27 November 2002.

Blake, M.C. and Engebretson, D., personal communication regarding bedrock geology of Lummi Island, Washington, 10 June 2004.

Bauer, H.H. and Vaccaro, J.J., Documentation of a deep percolation model for estimating ground-water recharge, United States Department of the Interior Geological Survey Open-File Report 86-536, 1987.

Bauer, H.H. and Mastin, M.C., Recharge from precipitation in three small glacial-till-mantled catchments in the Puget Sound Lowland, Washington, United States Department of the Interior Geological Survey, Water- Resources Investigations Report 96-4219, 1997.

Bear, J., Hydraulics of ground water, New York, New York, McGraw-Hill, 1979.

Bidlake, W.R. and Payne, K.L., Estimating recharge to ground water from precipitation at Naval Submarine Base Bangor and vicinity, Kitsap County, Washington, United States Department of the Interior Geological Survey, Water- Resources Investigations Report 01-4110, 2001.

Brady, N.C. and Weil, R.R., Elements of the Nature and Properties of Soils, Prentice Hall, Upper Saddle River, New Jersey, 2000.

Brandon, M.T., Cowen, D.S., and Feehan, J.G., The late Cretaceous San Juan thrust system, San Juan Islands, Washington. Geological Society of America, Special Paper 221, p. 81, 1988.

Brown, E.H., Ophiolite on Fidalgo Island Washington, In: Coleman, R.G. and Irwin, W.P. (Eds.), North American ophiolites, Oregon Dept. of Geology and Mineral Industries Bulletin no. 95, p. 67-73, 1977.

Brown, E.H., Bradshaw, J.Y., and Mustoe, G.E., Plagiogranite and keratophyre in ophiolite on Fidalgo Island, Washington, Geolological Society of America, Bulletin no. 90, p. 493-507, 1979.

Burmester, R.F., Clarke, M.C., and Engebretson, D.C., Remagnetization during Cretaceous normal superchron in eastern San Juan Islands, Wa.: Implications for tectonic history. Tectonphysics Bulletin no. 326, p. 73-77, 2000 .

Calkin, P.E., The geology of Lummi and Eliza Islands, Whatcom County, Washington, M.S. Thesis, University of British Columbia, Vancouver, British Columbia, 1959.

Carroll, P.R., Petrology and structure of pre-Tertiary rocks of Lummi and Eliza Islands, Washington, M.S. Thesis, University of Washington, Seattle Washington, 1980.

Culhane, T., High chloride concentrations in ground water withdrawn from above sea level aquifers, Whidbey Island, Washington, Washington State Department of Ecology Open-File Technical Report 93-07, 1993.

Dakin, R.A., Farvolden, J.A., and Fritz, P., Origin of dissolved solids in groundwaters of Mayne Island, British Columbia, Canada, Journal of Hydrogeology vol. 63 p. 233-270, 1983.

Dethier, D. P., Pessl, F. Jr., Keuler, R.F., Balzarini, M.A., and Pevear, D.R., Late Wisconsinan glaciomarine deposition and isostatic rebound, northern Puget Lowland, Washington, Geological Society of America Bulletin, vol. 107, no.11, 1995.

Dethier, D. P., White, D. P., and Brookfield, C. M., Maps of the surficial geology and depth to bedrock of False Bay, Friday Harbor, Richardson, and Shaw Island 7.5-minute quadrangles, San Juan County, Washington, Washington Division of Geology and Earth Resources Open File Report 96-7, 1996.

Dingman, S. L., Physical Hydrology, McMillan College Publishing Company, New York, New York, 1994.

Dingman, S. L, Physical Hydrology, University of New Hampshire, Prentice Hall, Upper Saddle River, New Jersey, 2002.

Dion, N.P. and Sumioka, S.S., Seawater intrusion into coastal aquifers in Washington, 1978, Washington Department of Ecology Water-Supply Bulletin 56, p.14, 1984.

Dragovich, J. D. and Grisamer, C. L., Quaternary stratigraphy, cross sections, and general geohydrologic potential of the Bow and Alger 7.5-minute quadrangles, western Skagit County, Washington, Washington Division of Geology and Earth Resources Open File Report 98-8, 1998.

Dragovich, J. D., Norman, D. K., Grisamer, C. L., Logan, R. L., and Anderson, G., Geologic Map and interpreted geologic history of the Bow and Alger 7.5-minute quadrangles, western Skagit County, Washington, Washington Division of Geology and Earth Resources Open File Report 98-5, 1998.

Dragovich, J. D., Norman, D. K., Lapen, T. J., and Anderson, G., Geologic map of the Sedro-Wooley North and Lyman 7.5-minute quadrangles, western Skagit County, Washington, Washington Division of Geology and Earth Resources Open File Report 99-3, 1999.

Dragovich, J. D., Logan, R. L., Schasse, H. W., Walsh, T. J., Lingley, W. S. Jr., Norman, D. K., Gerstel, W. J., Lapen, T. J., Schuster, E. J., and Meyers, K. D., Geologic map of Washington- northwest quadrant, Washington Division of Geology and Earth Resources, Geologic Map GM-50, 2002.

Drever, J. I., The Geochemistry of Natural Waters, Surface and Groundwater Environments, University of Wyoming, Prentice Hall, Upper Saddle River, New Jersey, 1997.

Duxbury, A.C. and Duxbury, A.B., An Introduction To The World's Oceans, third edition, Wm.C. Brown Publishers, Dubuque, Iowa, 1989.

Easterbrook, D. J., Pleistocene geology of the northern part of the Puget Lowland, Washington, Doctor of Philosophy Thesis, University of Washington, Seattle, Washington, 1962.

Easterbrook, D. J., Late Pleistocene geology of the northern part of the Puget Lowland, Washington, Geological Society of America Bulletin, vol. 74, no. 12, 1963.

Easterbrook, D. J. and Kovanen, D.J., Radiocarbon chronology of late Pleistocene deposits in northwest Washington, Science, vol. 152, no. 3723, 1966b.

Easterbrook, D. J., Geology and geomorpology of western Whatcom County, Washington, Department of Geology, Western Washington University, Bellingham, Washington, 1971.

Easterbrook, D. J., Environmental geology of western Whatcom County, Washington, Department of Geology, Western Washington University, Bellingham, Washington, 1973.

Easterbrook, D. J., Advance and retreat of Cordilleran ice sheets in Washington, U.S.A, Geographie physique et quaternaire, vol. 46, no. 1, 1992.

Ferris, J.G., Knowles, D.B., Brown, R.H., and Stallman, R.W., Theory of aquifer tests, United States Department of the Interior Geological Survey Water Supply Paper 1536-E, 1962.

Fetter, C.W. Jr., Applied Hydrogeology, University of Wisconsin- Oshkosh, Charles E. Merrill Publishing Co., Columbus Ohio, 1980.

Garver, J., Stratigraphy, depositional setting and tectonic significance of the clastic cover of the Fidalgo ophiolite, San Juan Islands, Washington, Canadian Journal of Earth Science no. 25, p. 417-432, 1988.

Gusey, D. and Brown, E.H., The Fidalgo ophiolite, Washington, In: Geological Society of America, Centennial Field Guide-Cordilleran Section, p. 389-392, 1987.

Heath, R.C., Basic Ground-Water Hydrology, United States Geological Survey, Water Supply Paper 2220, 1983.

Johnson, S.Y., Stratigraphy, sedimentology, and tectonic setting of the Eocene Chuckanut Formation, northwest Washington, Doctor of Philosophy Thesis, University of Washington, Seattle, Washington, 1982.

Kahle, S.C. and Olsen, T.D., Hydrogeology and quality of ground water on Guemes Island, Skagit County, Washington, United States Department of the Interior Geological Survey, Water- Resources Investigations Report 94-4236, 1995.

Kahle, S.C., Hydrogeology of Naval Base Bangor and vicinity, Kitsap County, Washington, United States Department of the Interior Geological Survey, Water- Resources Investigations Report 97-4060, 1998.

Kelleher, K., personal communication regarding study of Lake Whatcom watershed using Distributive Hydrologic-Soils-Vegetation Model (DHSVM), Whatcom County, Washington, Master of Science Thesis study in progress, Department of Geology, Western Washington University, Bellingham, Washington, November, 2004.

Kelly, D.J., Seawater Intrusion Topic Paper Final Draft, Island County Health Department, Coupeville, Washington, 2005.

Kelly, D.J., personal communication regarding water chemistry data in Island County, Washington, 10 February, 2005.

Kelly, J. M., Mineralogy and petrography of the basal Chuckanut Formation in the vicinity of Lake Samish, Washington, M.S. Thesis, Western Washington University, Bellingham, Washington, 1970.

Kelly, T.A., Hydrostratigraphy and ground water resources of northern Lummi Island, Washington. Summer Field Project, Western Washington University, Bellingham, Washington, 1998.

Kovanen, D.J. and Easterbrook, D.J., Late Pleistocene, post-Vashon, alpine glaciation of the Nooksack drainage, North Cascades, Washington, Geological Society of America Bulletin, vol. 113, 2001.

Landsat 4 Thematic Mapper (TM) Sub-Scene, compiled in Arc/Info 7.4 format grid coverage by Chris Behee, Whatcom County Planning and Development Services, August, 1991.

Lapen, T. J., Geologic map of the Bellingham 1:100,000 quadrangle, Washington, Washington Division of Geology and Earth Resources Open File Report 2000-5, 2000.

Livermore, D.E. and Boulton, B., personal communication regarding well drilling on Lummi Island, Washington, July 2004.

Mace, R.E., Estimating transmissivity using specific-capacity data, draft version, Bureau of Economic Geology, University of Texas at Austin, Austin, Texas, 2000.

Marshall, A., Brown, J., Evans, C., and Simmerman, N., written communication regarding precipitation data collection northern Lummi Island, Washington, November, 2004.

McLellan, R.D., The geology of San Juan Islands, University of Washington Publications in Geology, vol. 2, 1927.

McWorter, D.B. and Sunada, D.K., Groundwater Hydrology and Hydraulics, Water Resources Publications, Fort Collins, Colorado, 1977.

Monteith, J.L., Evaporation and environment, In: Proceedings of the 19th Symposium of the Society for Experimental Biology, Cambridge University Press, 1965.

National Climatic Data Center, Record of Climatological Observations, Bellingham International Airport, October 2001-October 2004, National Oceanographic and Atmospheric Administration, National Weather Service, http://ncdc.noaa.gov/dly/DLY?stnid=20027993

Nielson, K. C. and Armfield, V.D., written communication regarding runoff measurement study, northern Lummi Island, Washington, October 2004.

Orr, L. A., Is seawater intrusion affecting groundwater on Lopez Island, Washington?, United States Department of the Interior Geological Survey Fact Sheet 057-00, 2000.

Orr, L. A., Bauer, H. H., and Wayenberg, J.A., Estimates of ground-water recharge from precipitation to glacial-deposit and bedrock aquifers on Lopez, San Juan, Orcas, and Shaw Islands, San Juan County, Washington, United States Department of the Interior Geological Survey, Water- Resources Investigations Report 02-4114, 2002.

Penman, H.L., Natural evaporation from open water, bare soil, and grass, Royal Society of London Proceedings, Series A, 193, 1948.

Pessl, F. Jr., Dethier, D. P., Booth, D.B., and Minard, J.P., Surficial geologic map of the Port Townsend 30 by 60 minute quadrangle, Puget Sound region, Washington, United States Department of the Interior Geological Survey Miscellaneous Investigations Series Map I-1198-F, scale 1:100,000. 1989.

Riley, J.P. and Skirrow, Chemical Oceanography, vol. 1 2d ed., Academic Press Inc., New York, New York, 1975.

Russell R.H., editor, Geology and water resources of the San Juan Islands, San Juan County, Washington, Washington Department of Ecology Water-Supply Bulletin 46, 1975.

Russell, R.H., editor, Geology and water resources of the San Juan Islands, San Juan County, Washington, Washington Department of Ecology Office of Technical Services, Water-Supply Bulletin, no. 46, p. 171, 1979.

Sapik, D.B., Bortleson, G.C., Drost, B.W., Jones, M.A., and Frych, E.A., Ground-water resources and simulation of flow in aquifers containing freshwater and seawater, Island County, Washington, United States Department of the Interior Geological Survey Water Investigations Report 87-4182, 1988.

Schmidt, R.G., The water resources of northern Lummi Island, Robinson and Noble, Inc., Tacoma, Washington, 1978.

Selby, M. J., Hillslope Materials and Processes, 2d ed., Oxford University Press, New York, New York, 2000.

Soil Conservation Service, Soil Survey of Whatcom County Area, Washington, United States Department of Agriculture, 1980.

Sumioka, B.B. and Bauer, H.H., Estimating ground-water recharge from precipitation on Whidbey and Camano islands, Island County, Washington, Water Years 1998 and 1999,

United States Department of the Interior Geological Survey Water- Resources Investigations Report 03-4101, 2003.

Vaccaro, J.J., Hansen, A.J. Jr., and Jones, M..A., Hydrogeologic framework of the Puget Sound Aquifer System, Washington and British Columbia, United States Department of the Interior Geological Survey Professional Paper 1424-D, 1998.

Van Denburgh, A.S., Anderson, H.W., and Easterbrook, D.J., Pleistocene Stratigraphy of Island County (Part I) and Ground-Water Resources of Island County (Part II), Washington State Department of Water Resources and United States Geological Survey, Water Resources Division, Water Supply Bulletin, no. 25, 1968.

WAC 246-290-310, Maximum Contaminant Levels (MCL) and Maximum Residual Disinfectant Levels (MRDL), Washington Administrative Code, Washington State Legislature, Olympia, Washington, 1988.

WAC 173-200-040, Water Quality Standards for Ground Waters in Washington State, Criteria, Washington Administrative Code, Washington State Legislature, Olympia, Washington, 1991.

Walters, K. L., Reconnaissance of Seawater Intrusion along Coastal Washington 1966-1968, Washington State Department of Ecology Water Supply Bulletin 12, 1971.

Warren, R. E., City of Bainbridge Island Level II Assessment, An Element of the Water Resources Study, Kato and Warren, Inc. and Robinson and Noble, Inc., 2000.

Washington State Department of Conservation, Water Resources of the Nooksack River Basin and Certain Adjacent Streams, Division of Water Resources Water Supply Bulletin No. 12, 1960.

Washington State Department of Ecology, Coastal Zone Atlas of Washington, Vol. 2, Washington State Department of Ecology, DOE 77-21-2, 1978.

Washington State Department of Ecology, Seawater Intrusion Policy, 1991.

Watson, I. and Burnett, A..D., Hydrology, An Environmental Approach, Theory and Applications of Ground Water and Surface Water for Engineers and Geologists, CRC Lewis Publishers, Boca Raton, Florida, 1995.

Whatcom County Health Department, Lummi Island Ground Water Study, Bellingham, Washington, 1994.

Whatcom County Planning Department, Lummi Island Plan, Bellingham, Washington, 1979.

Whiteman, K. J., Molenaar, D., Bortleson, C. G., and Jacoby, J. M., Occurrence, quality, and use of groundwater in Orcas, San Juan, Lopez, and Shaw Islands, San Juan County, Washington, United Stated Department of Interior Geological Survey Water-Resource Investigations Report 83-4019, scale 1:62,500, 1983.

Wildrick, L., Neumiller, C. M., Garrigues, R., and Sinclair K., Investigation of water resources, water quality, and seawater intrusion, Anderson Island, Pierce County, Washington, Washington State Department of Ecology, publication number 01-11-013, October 2001.

Willing, P., Isle Aire Beach Water Association, Lummi Island Washington, well test report, Water Resources Consulting LLC, Bellingham, Washington, 1997.

Winter, T.C., Delineation of buried glacial-drift-aquifers, U.S. Department of the Interior Geological Survey Journal of Research, vol. 3, no. 2, Mar.-Apr., p. 137-148, 1975.
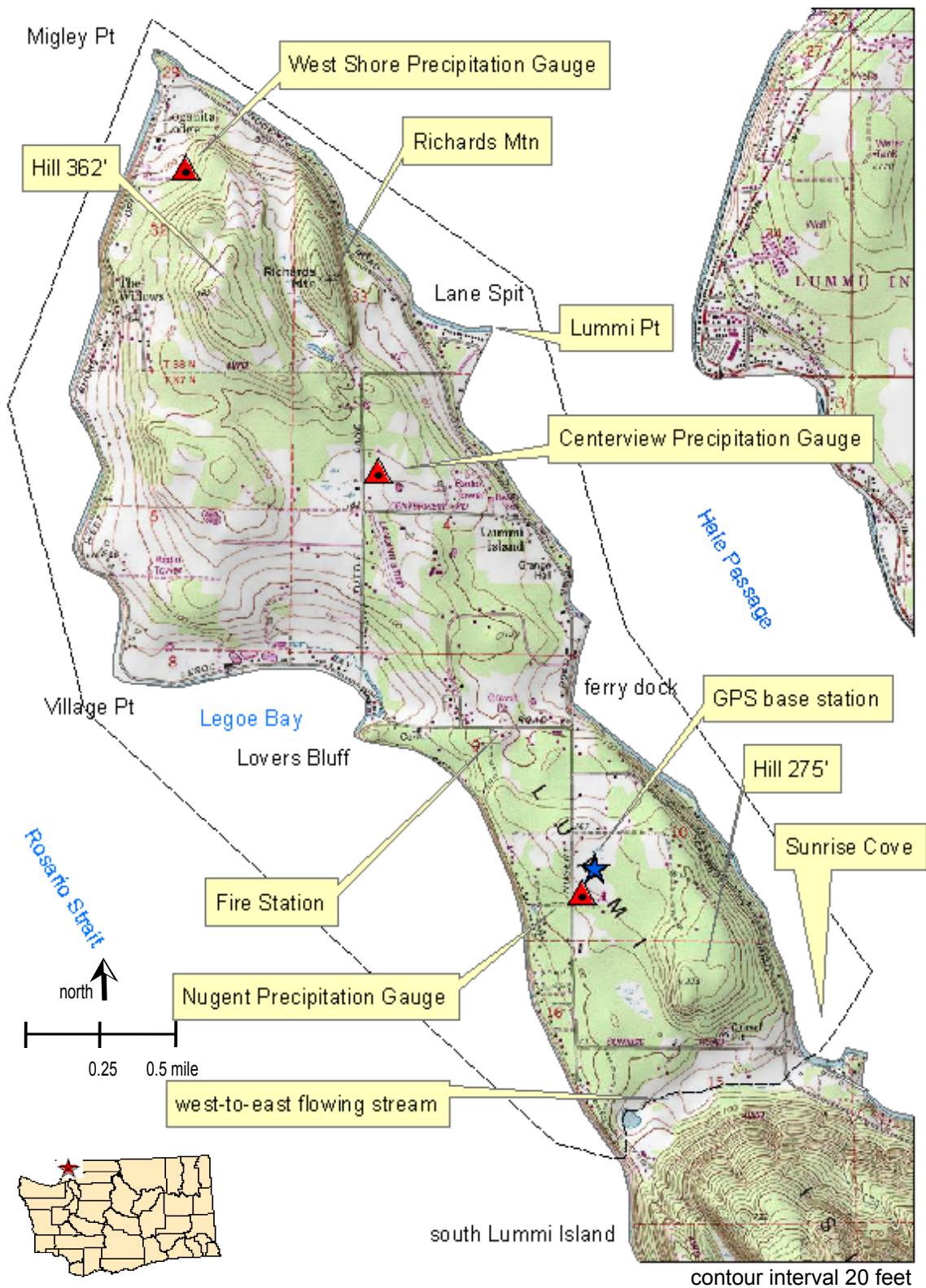
Figure 1. The north Lummi Island study area occupies 3.87 square miles in western Whatcom County, Washington. The southern boundary of the study area is designated as the west-east flowing stream.

147
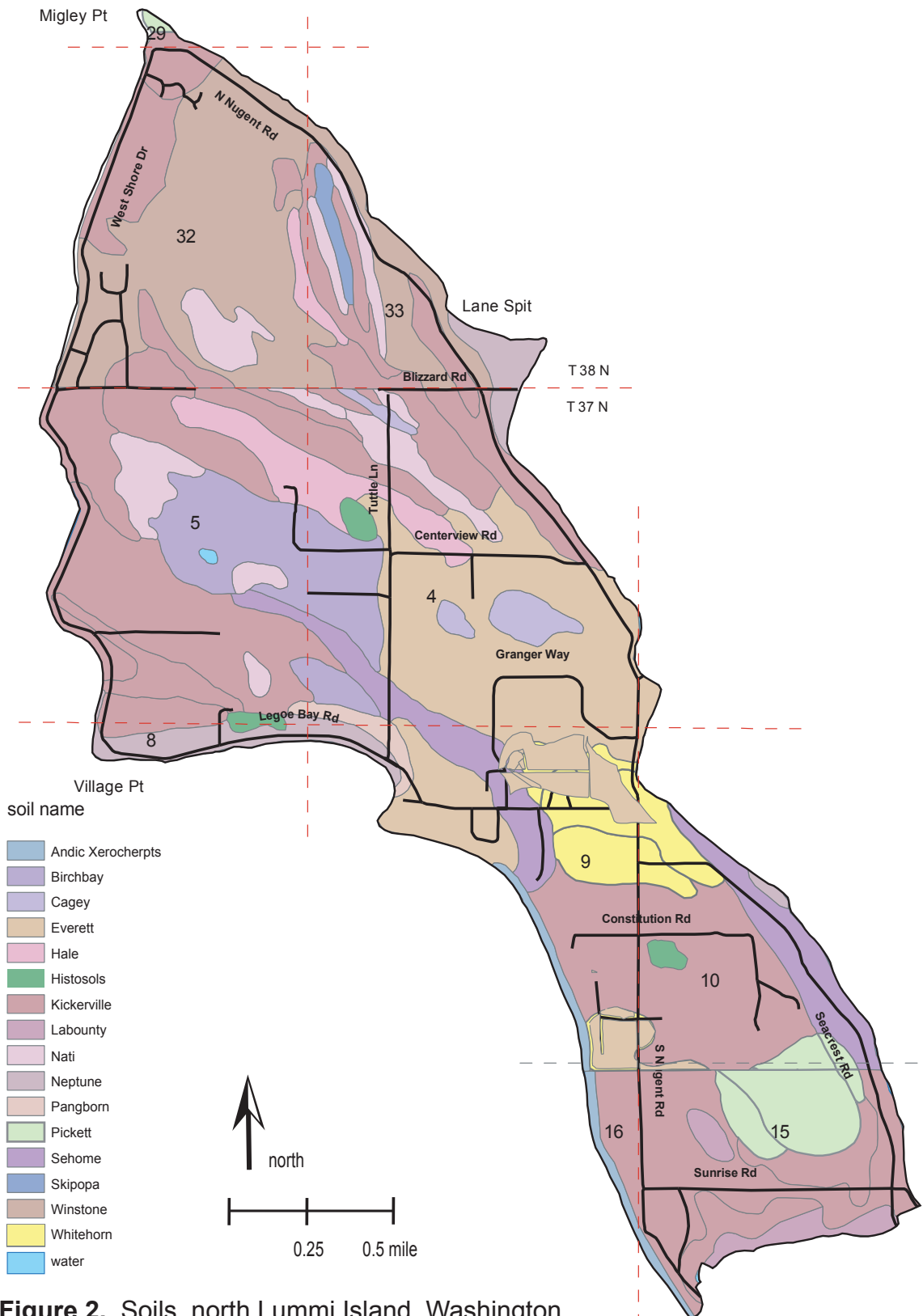
Figure 2. Soils, north Lummi Island, Washington.
Source: Soil Conservation Service (NRCS); (1980)

land cover classes

- clear water
- turbid/silted water
- coniferous forest
- mixed coniferous/deciduous forest
- deciduous forest
- scrub shrub vegetation
- long grasses
- medium grasses
- short grasses
- fallow field
- urban cover
- rock

north

0.25   0.5 mile
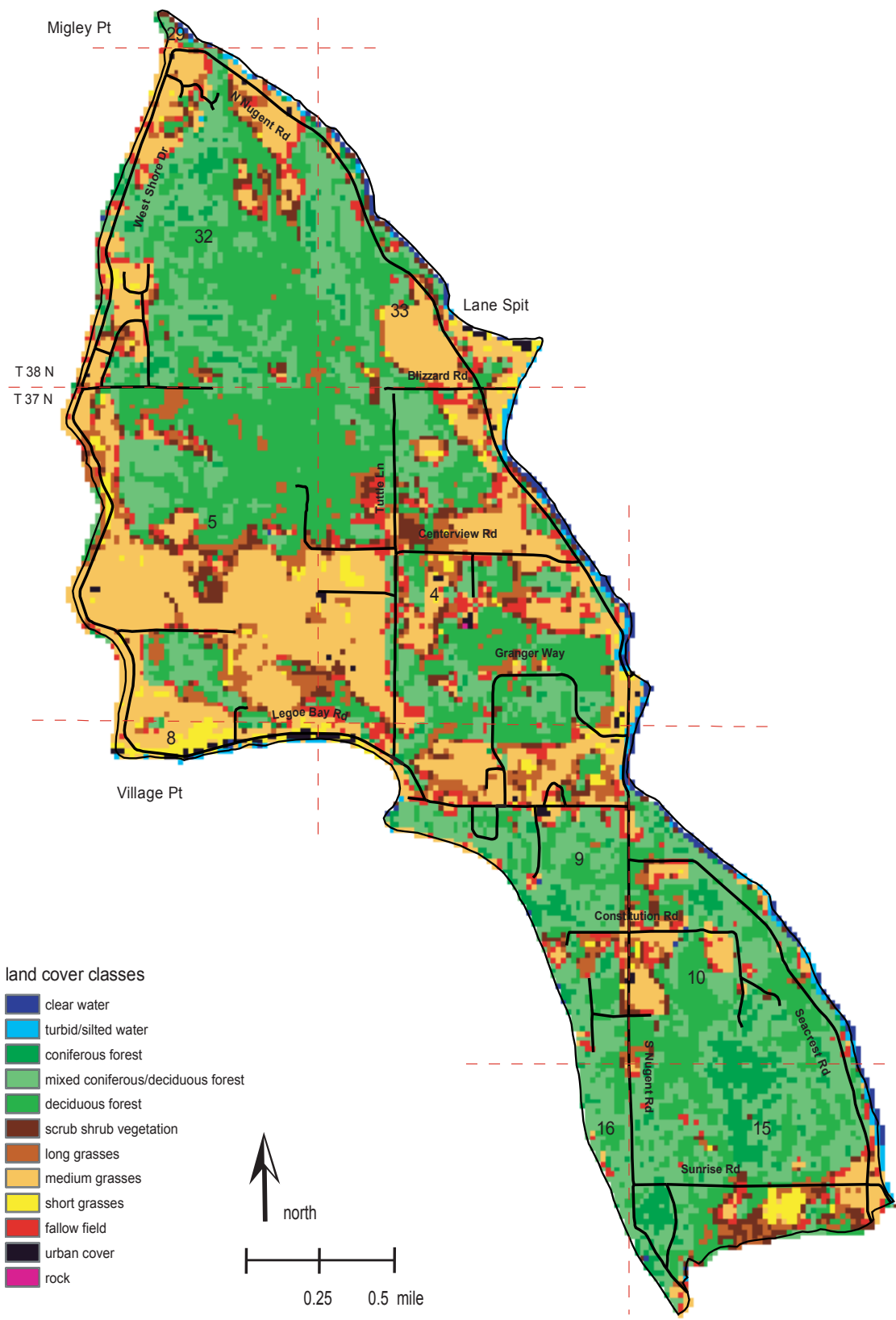
Figure 3. Land cover, north Lummi Island, Washington.
Source: 30-meter Landsat IV   149
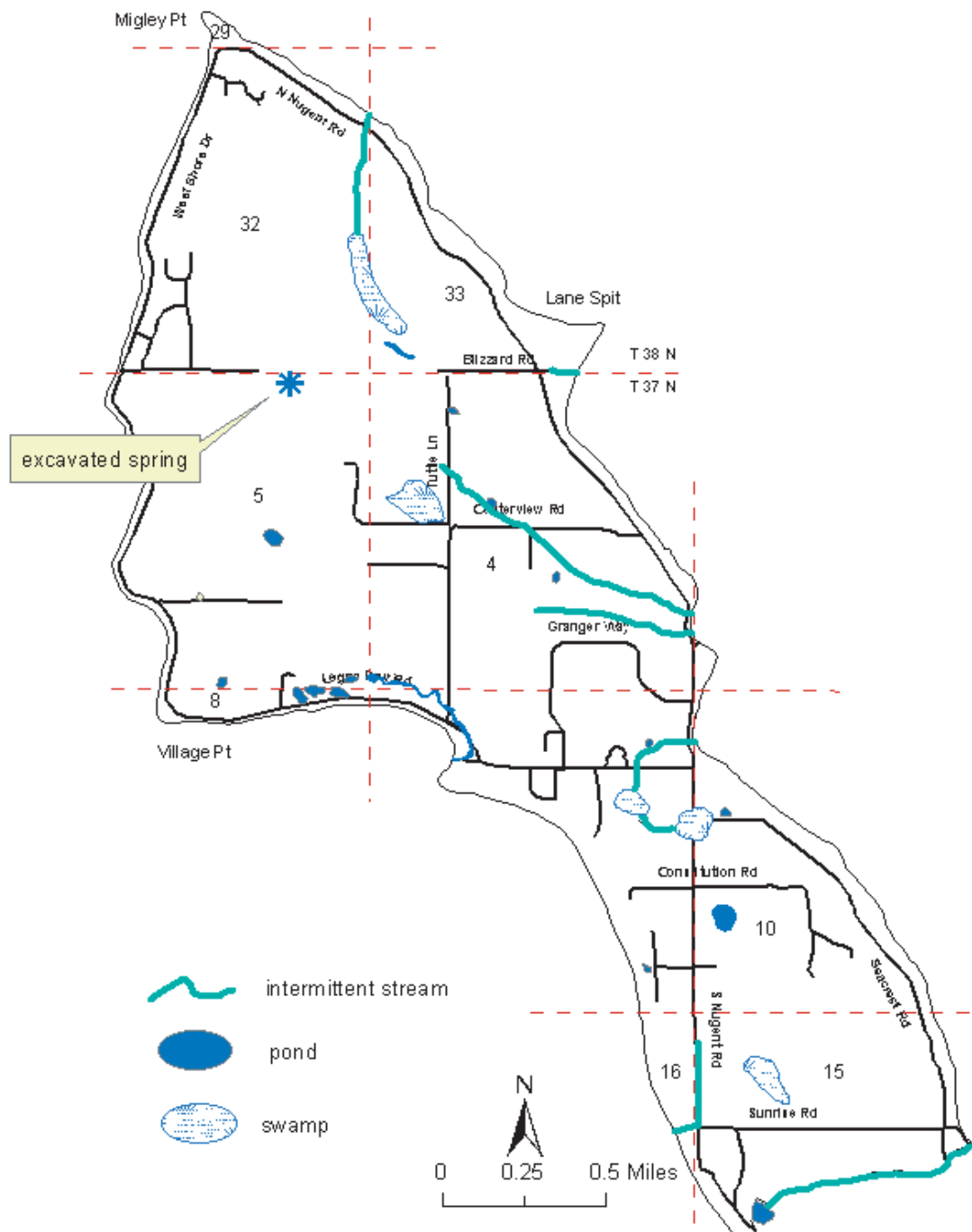
Figure 4. Major hydrologic features, north Lummi Island, Washington. The largest intermittent streams drain to the east. According to local residents, nearly all ponds are man-made. Locations and extents of features were approximated from filed observations and a USGS topographic map.
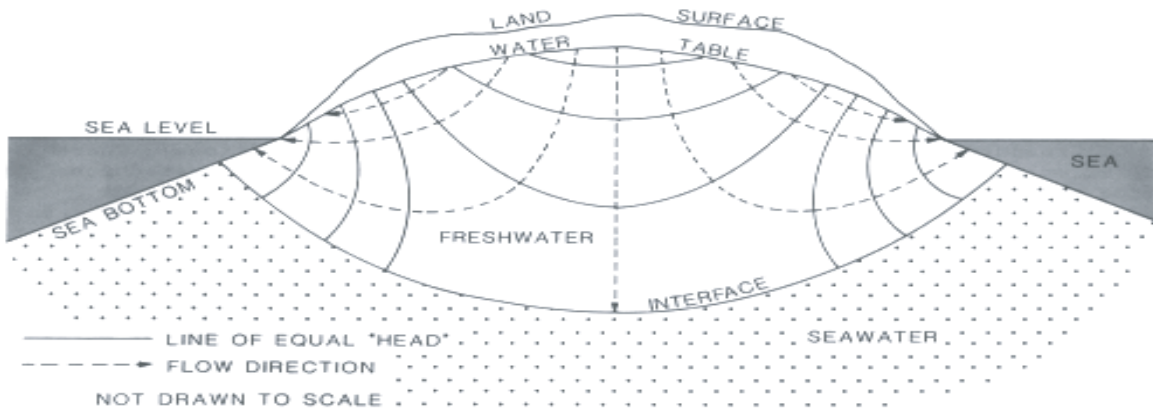
Figure 5. Conceptual model of head distribution and groundwater flow directions in a homogeneous unconfined island aquifer. Figure is from Dion et al., (1988)
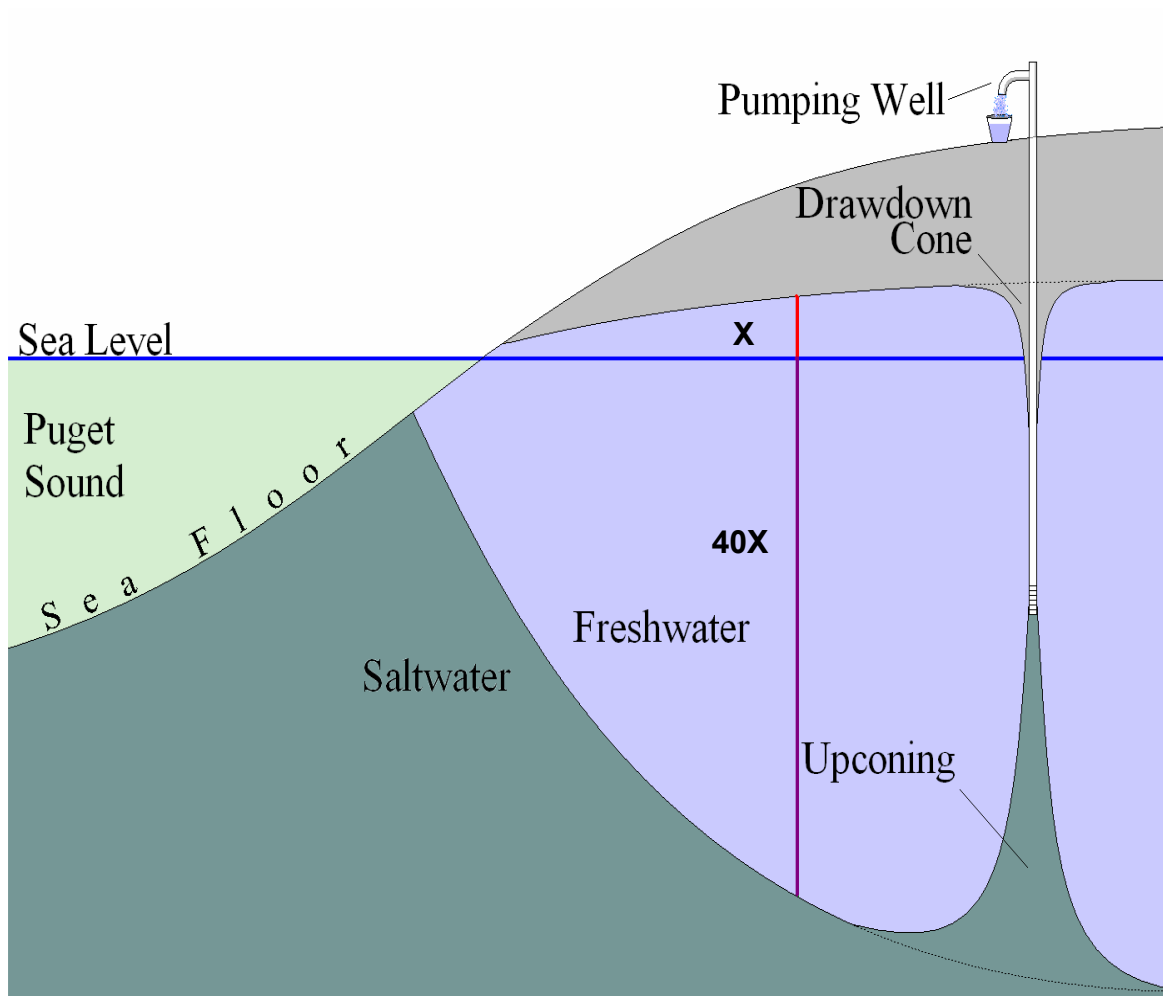
Figure 6. The Ghyben-Herzberg Relation states that under steady state conditions, the depth to the freshwater/seawater interface is 40 times the height of the water level above sea level (X). When seawater is present in the aquifer beneath a pumping well, it can be pulled up toward the well screen causing localized intrusion known as upconing. Figure modified from Kelly (2005).
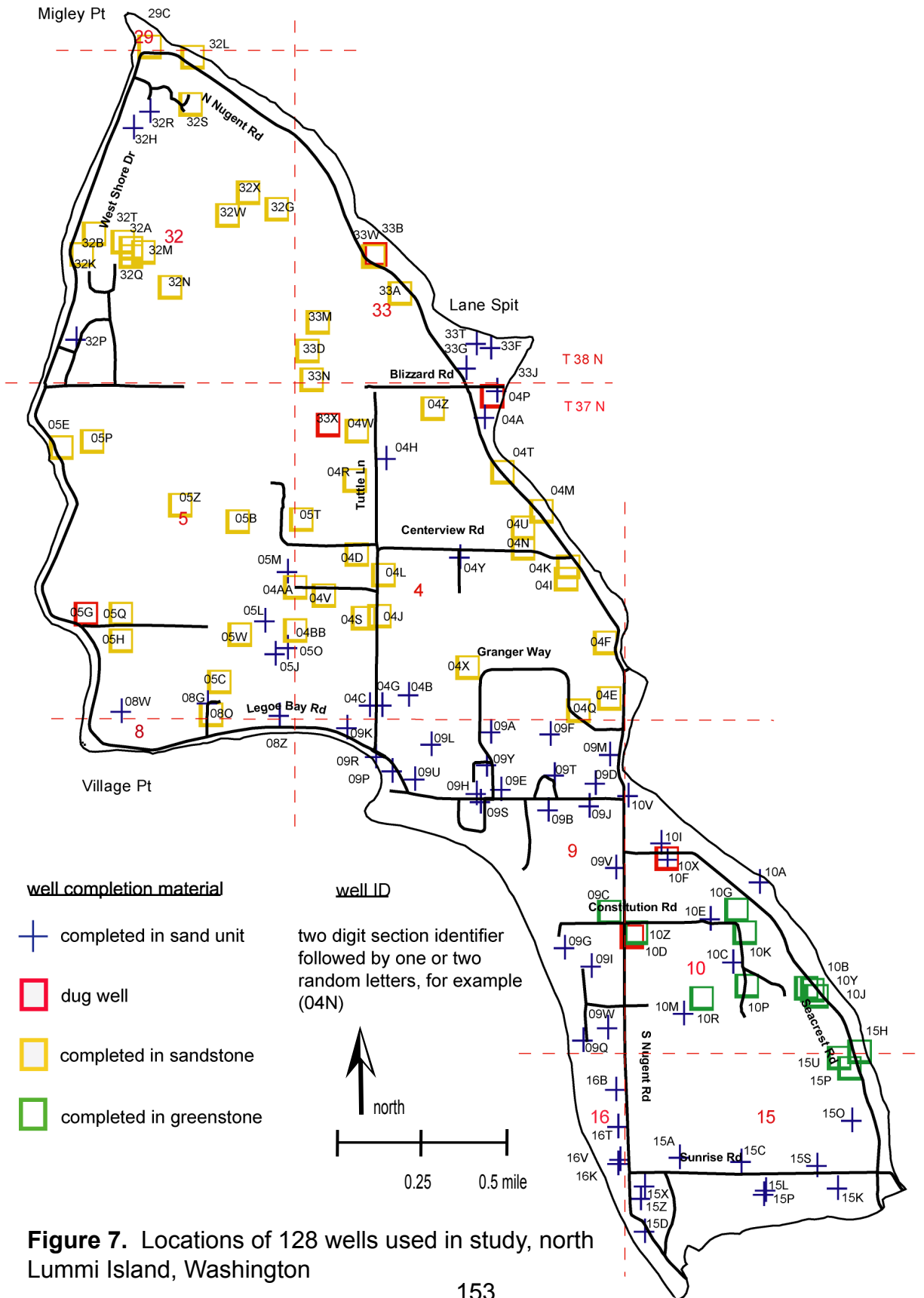
Figure 7. Locations of 128 wells used in study, north Lummi Island, Washington

153
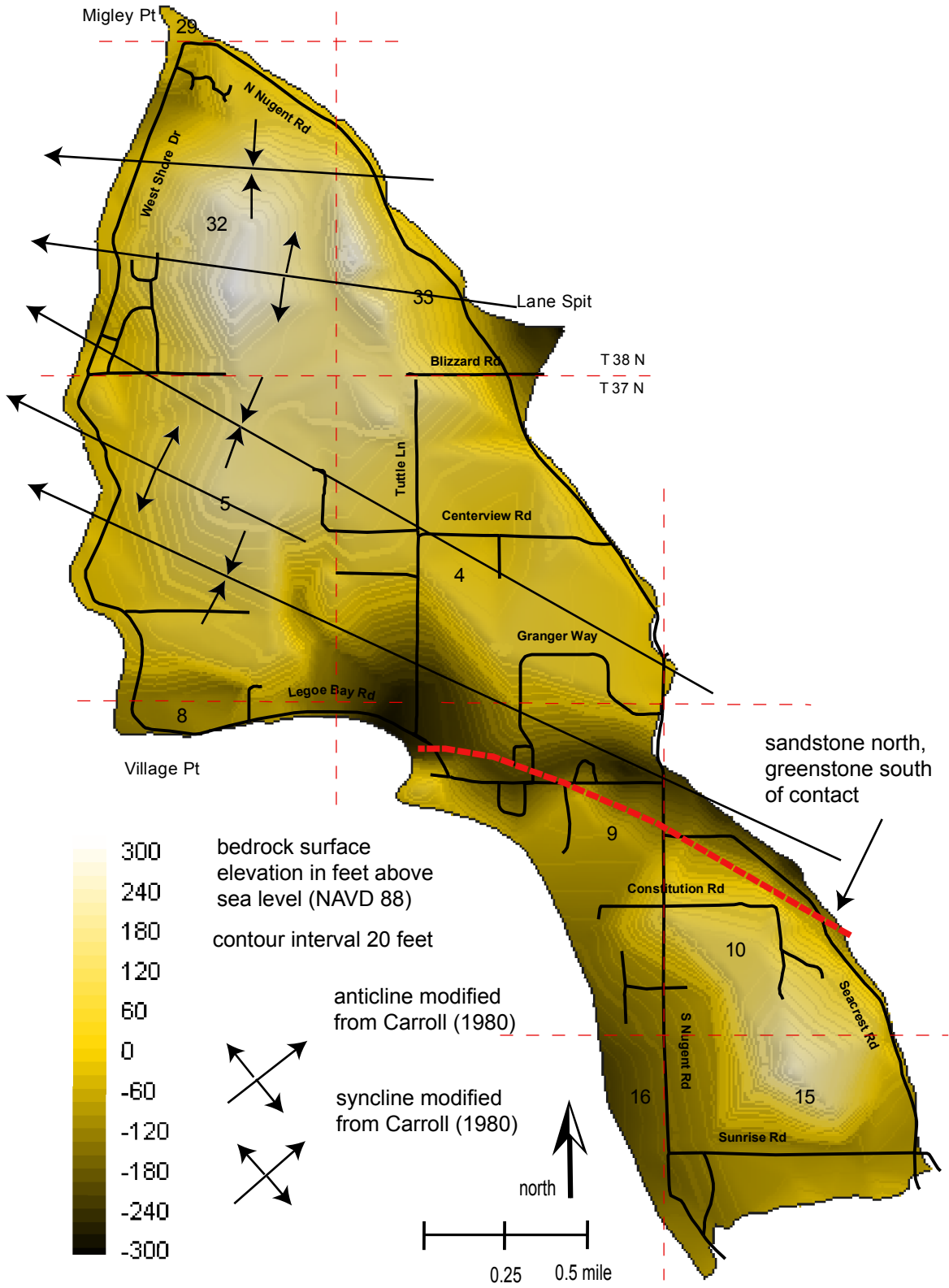
Figure 8. Bedrock surface modeled using well log and surficial geologic data, north Lummi Island, Washington

154
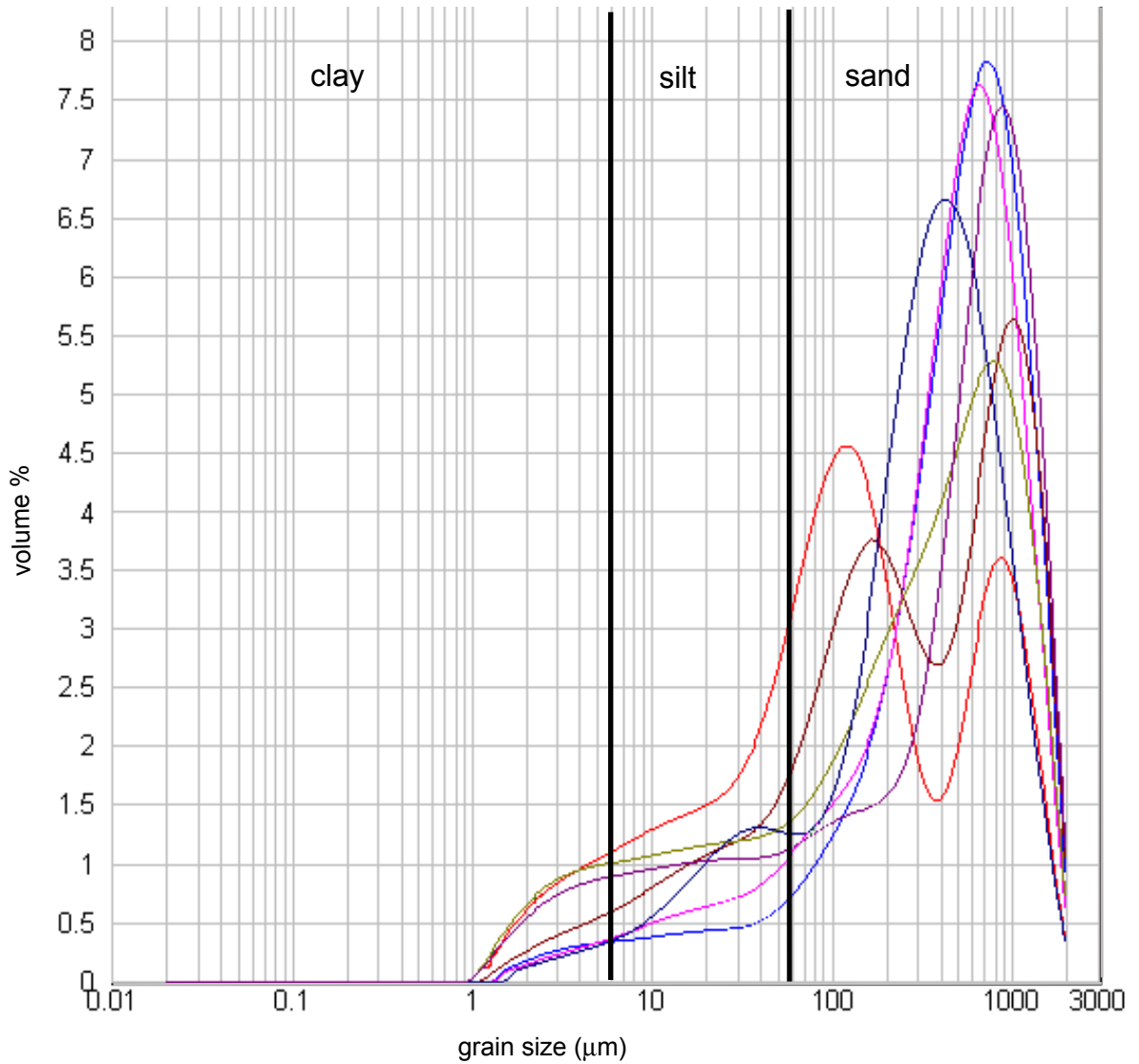
Figure 9. Grain size analysis for 7 samples collected from shorline bluffs, north Lummi Island, Washington. Silt size particles dominate the fine fraction of most samples. Size classes are Wentworth Scale. Analysis conducted using Malvern Instruments Mastersizer 2000 Particle Size Analyzer.
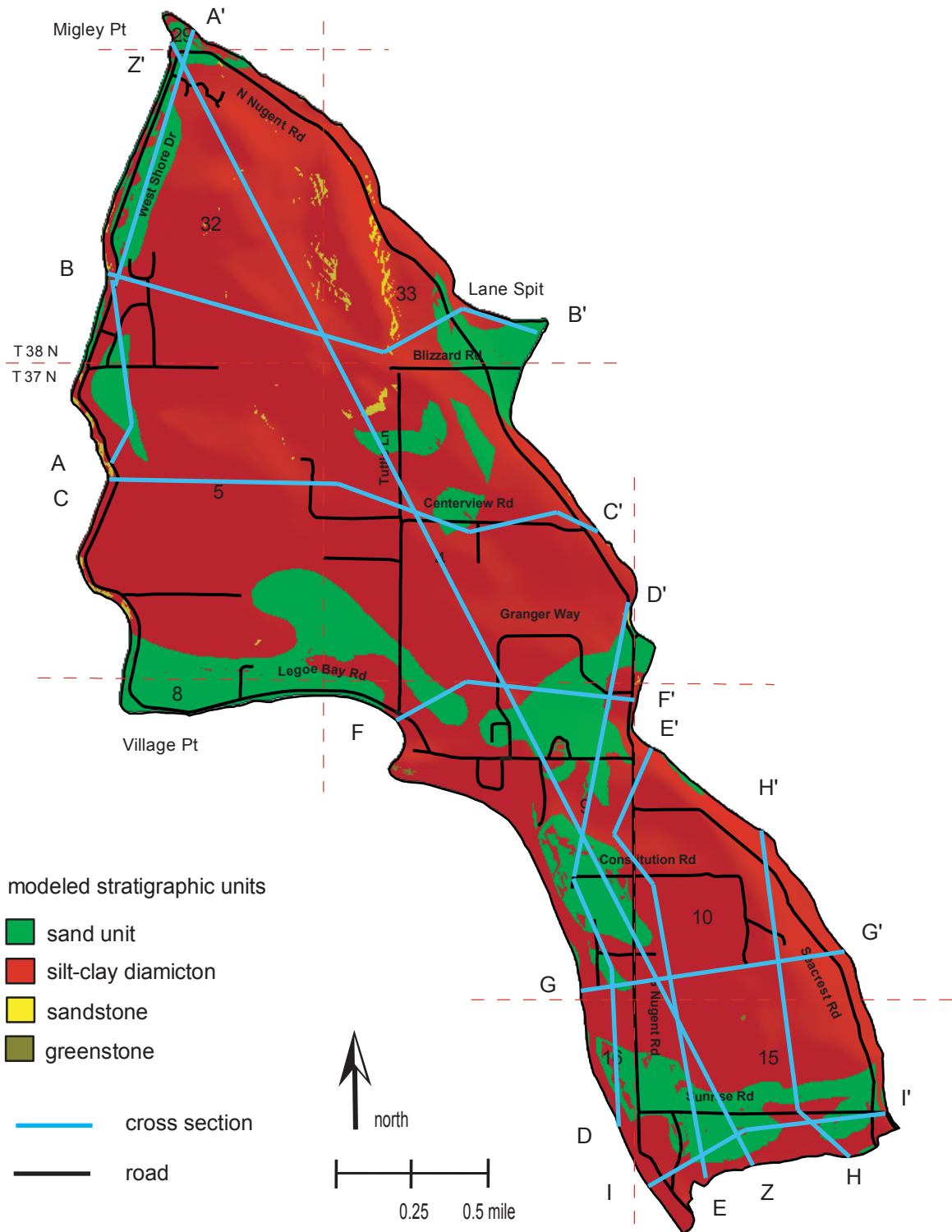
Figure 10. Geologic interpretive map created from modeled stratigraphy, north Lummi Island, Washington. In plan view, sand units correlate to emergence beach deposits, silt-clay diamicton likely correlates to glaciomarine drift, sandstone correlates to the Chuckanut Formation, and greenstone correlates to Fidalgo ophiolite rocks. Geologic unit correlations are from various sources (Section 2.1).
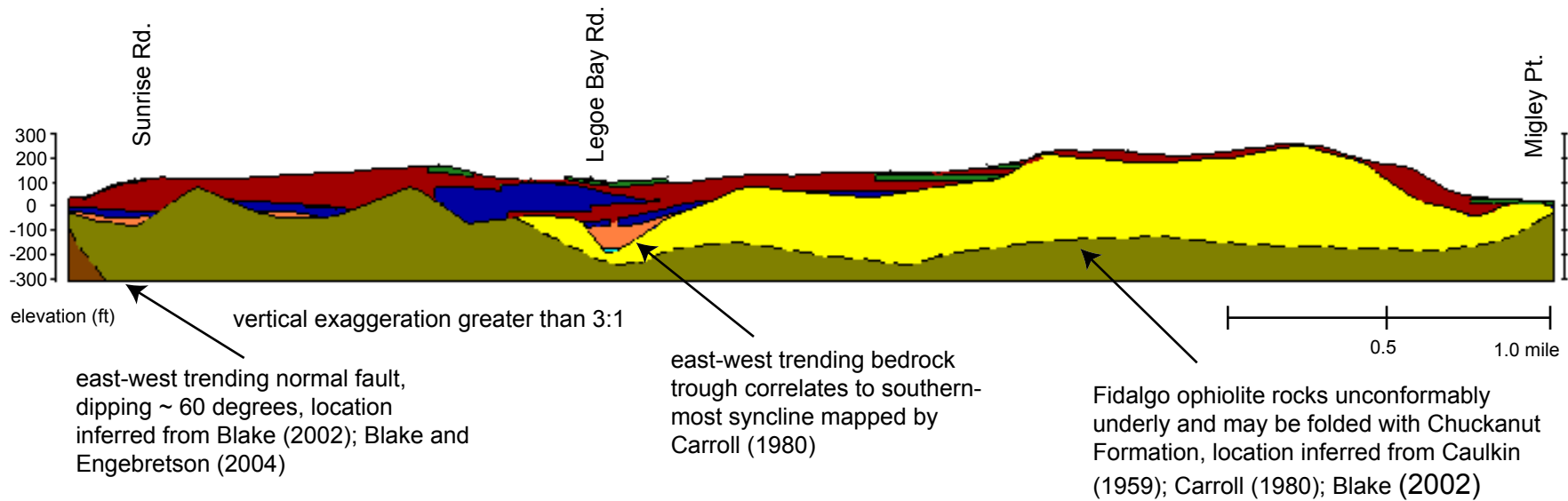
Geologic Units (various sources see Section 2.1)

⬛ (green) emergence beach deposits and coarse interbeds within glaciomarine drift, Everson Insterstade	⬛ (cyan) coarse interbeds within Cherry Point silt, Olympia non-glacial period
⬛ (crimson) undifferentiated till and glaciomarine drift, Vashon Stade and Everson Interstade	⬛ (yellow) Chuckanut Formation, Tertiary
⬛ (blue) advance outwash, pre-Vashon Stade	⬛ (olive) Fidalgo ophiolite rocks, Decatur terrane, pre-Tertiary
⬛ (orange) Cherry Point silt, Olympia non-glacial period	⬛ (brown) mid-oceanic rocks, Decatur terrane, pre-Tertiary

Figure 11. Geologic interpretive cross section Z-Z' cut through modeled stratigraphy, north Lummi Island, Washington. View is looking west. Geologic unit designations were made using information from various sources.
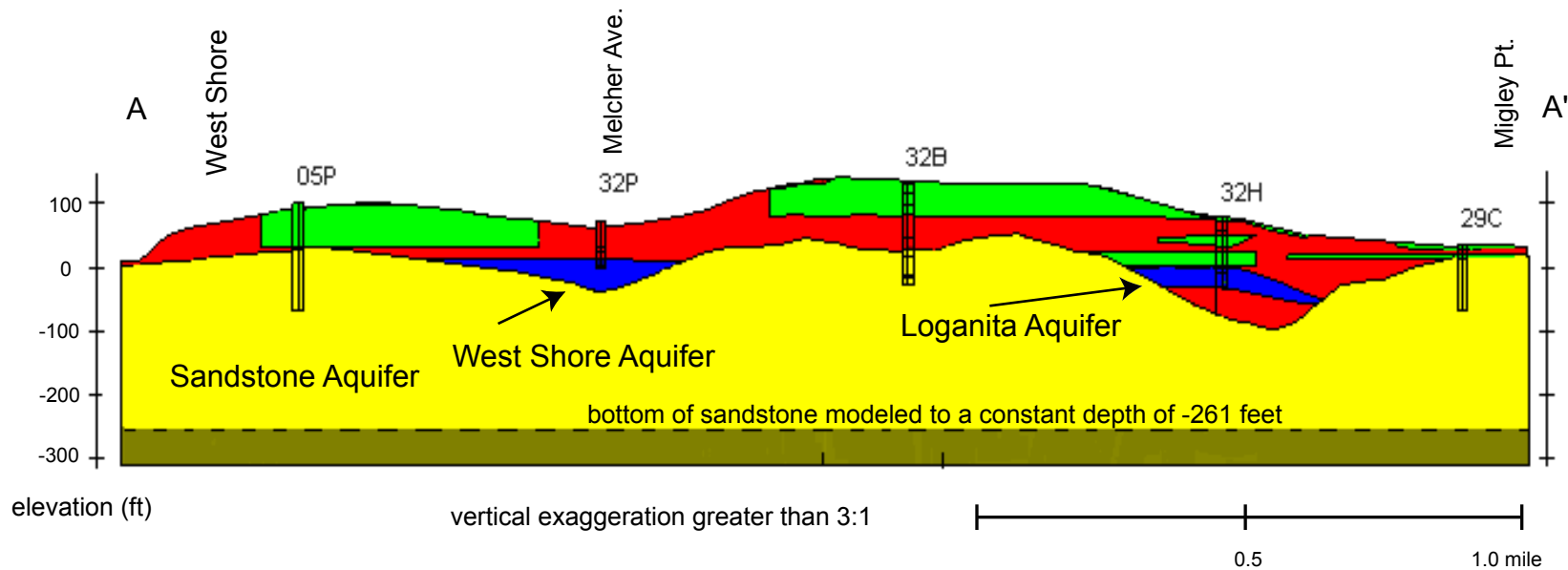
Figure 12a. Cross section A-A' cut through modeled hydrostratigraphy, north Lummi Island, Washington

158
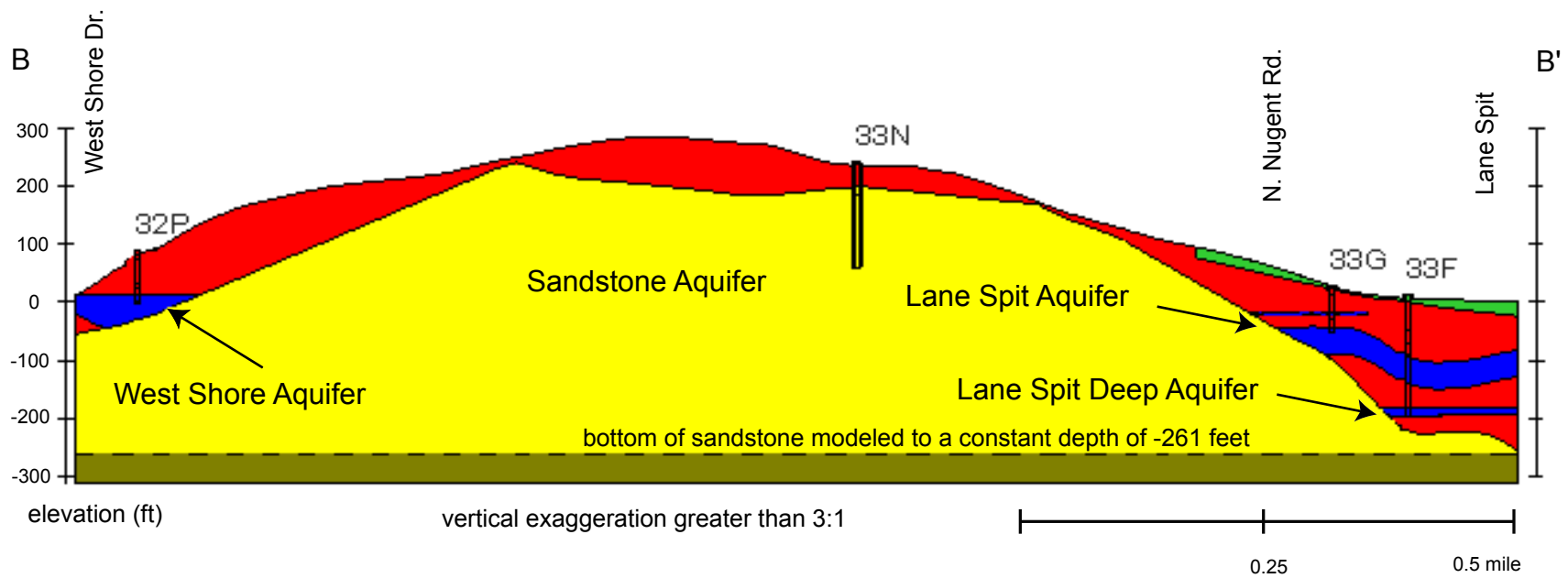
Figure 12b. Cross section B-B' cut through modeled hydrostratigraphy, north Lummi Island, Washington

159
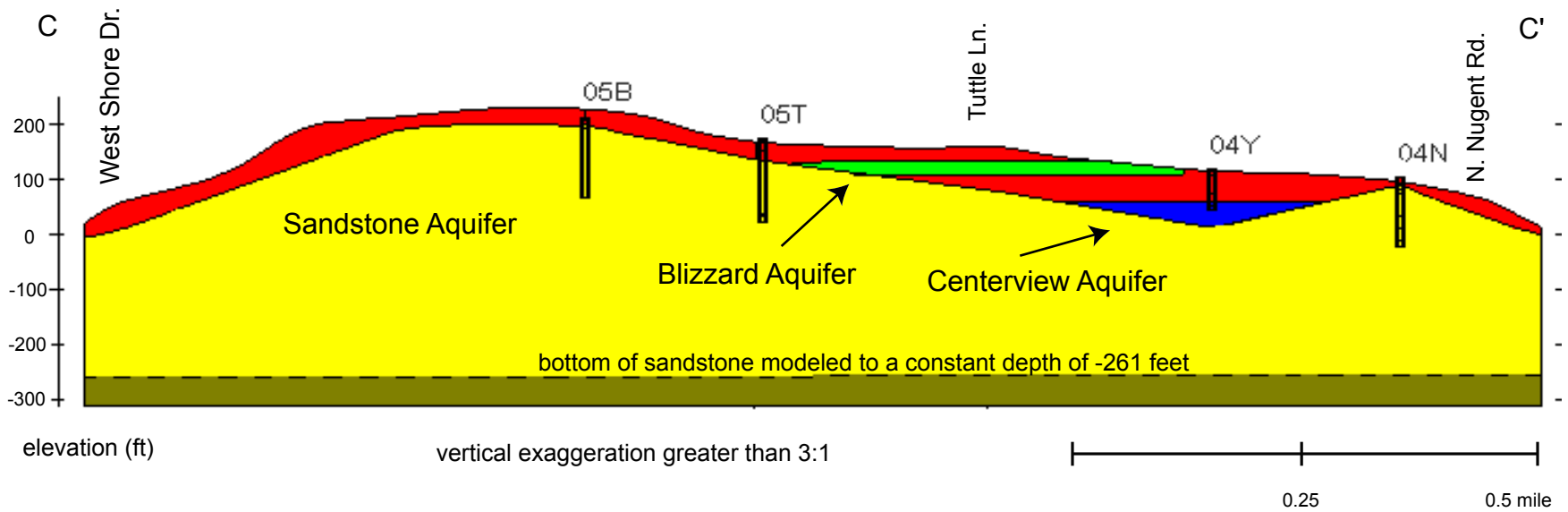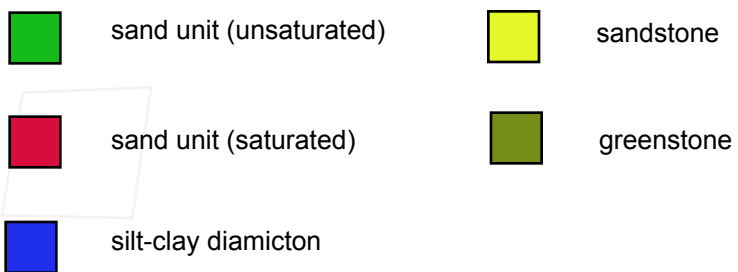
Figure 12c. Cross section C-C' cut through modeled hydrostratigraphy, north Lummi Island, Washington
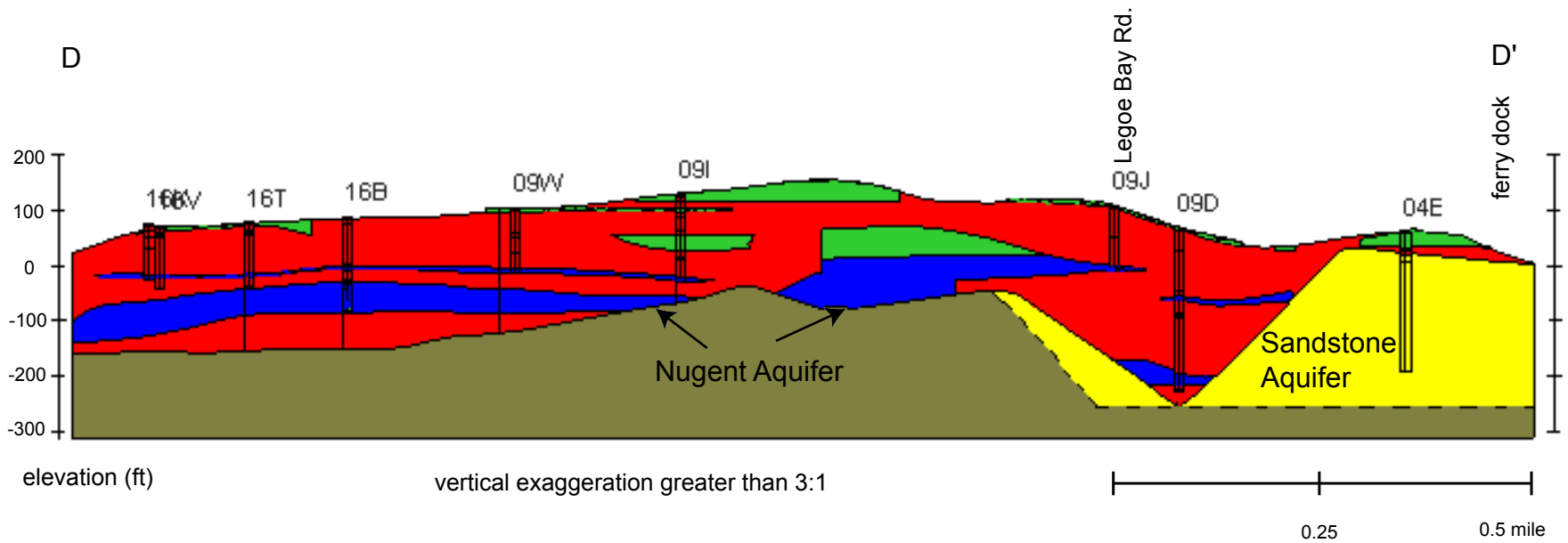
Figure 12d. Cross section D-D' cut through modeled hydrostratigraphy, north Lummi Island, Washington

161

Figure 12e. Cross section E-E' cut through modeled hydrostratigraphy, north Lummi Island, Washington

162

Figure 12f. Cross section F-F' cut through modeled hydrostratigraphy, north Lummi Island, Washington

163
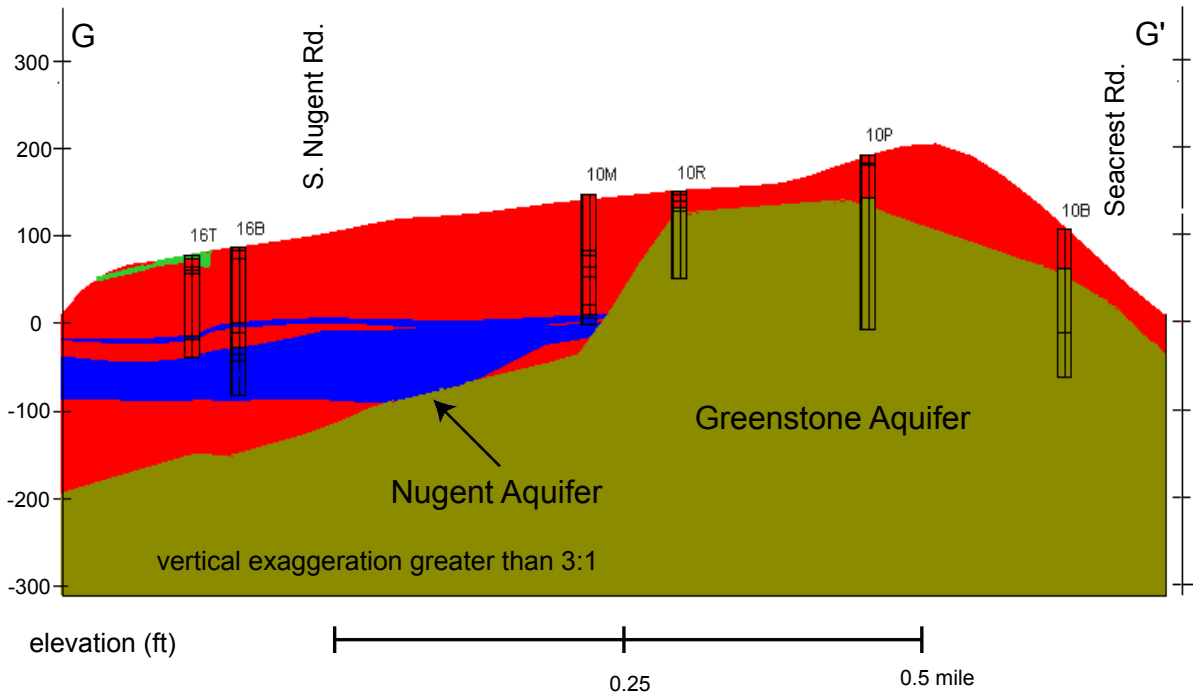
Figure 12g. Cross section G-G' cut through modeled hydrostratigraphy, north Lummi Island, Washington
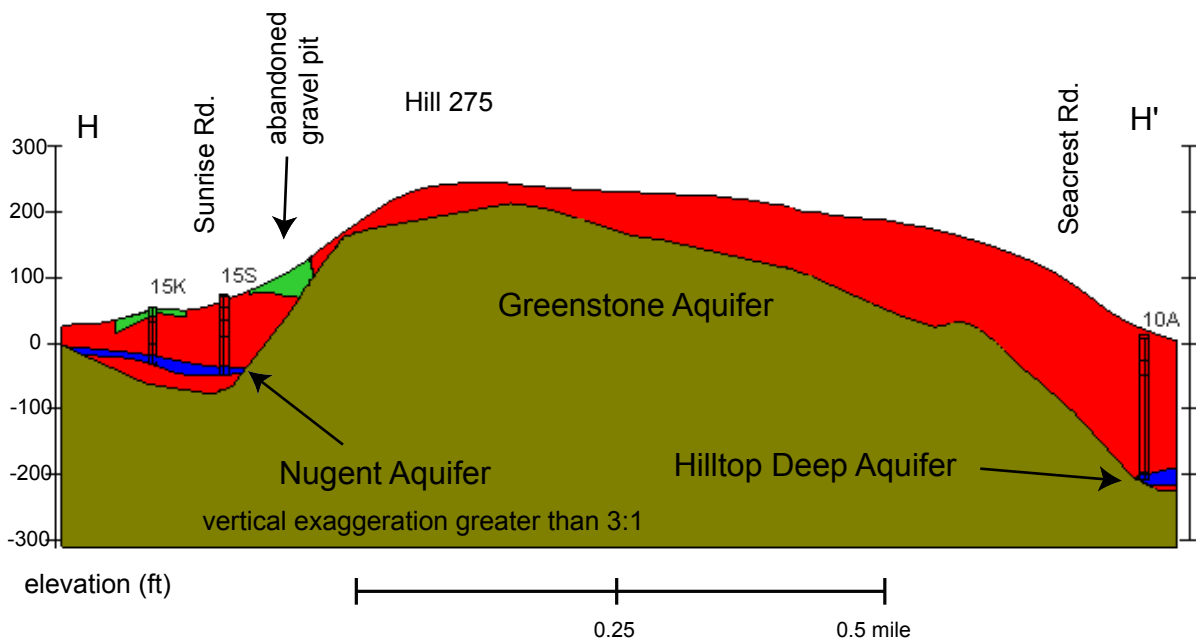
Figure 12h. Cross section H-H' cut through modeled hydrostratigraphy, north Lummi Island, Washington

164
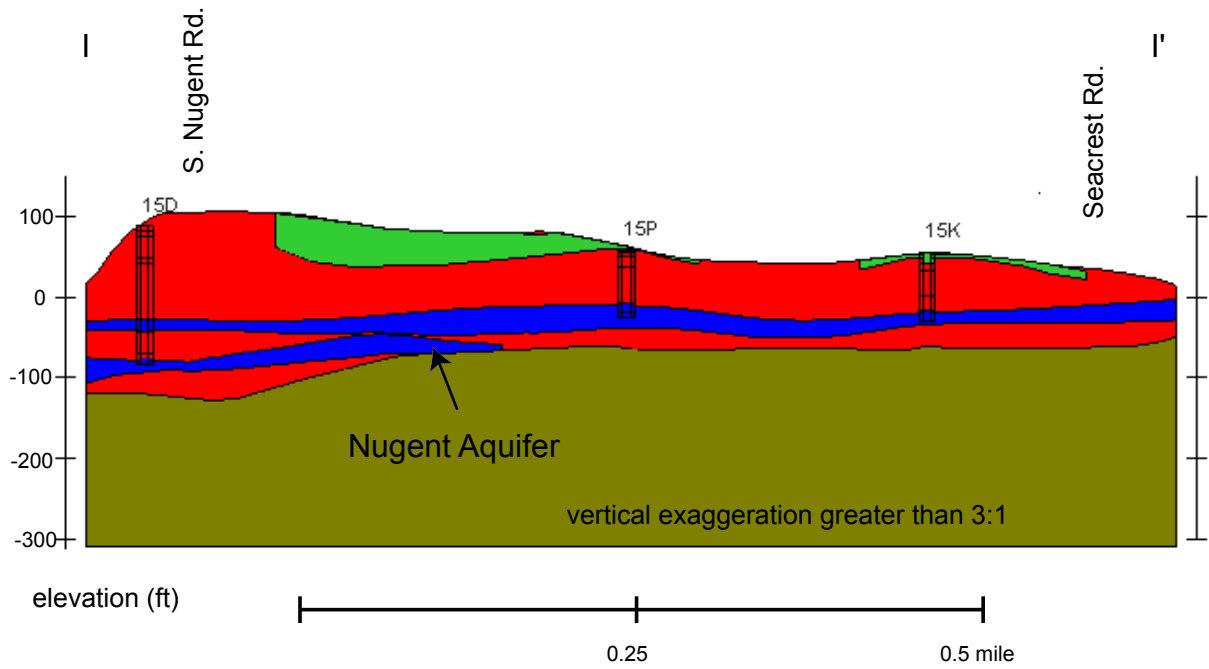
Figure 12i. Cross section I-I' cut through modeled hydrostratigraphy, north Lummi Island, Washington

165

Migley Pt.

sea level represented by
black outline of island

Village Pt.

Lane Spit
Aquifer

Legoe Bay Aquifer

Nugent Aquifer

Hill 275

**Modeled
hydrostratigraphic
units**

sand unit (unsaturated)

southern boundary
of study area

sand unit (saturated)   sandstone

silt-clay diamicton   greenstone   vertical exaggeration
greater than 3:1
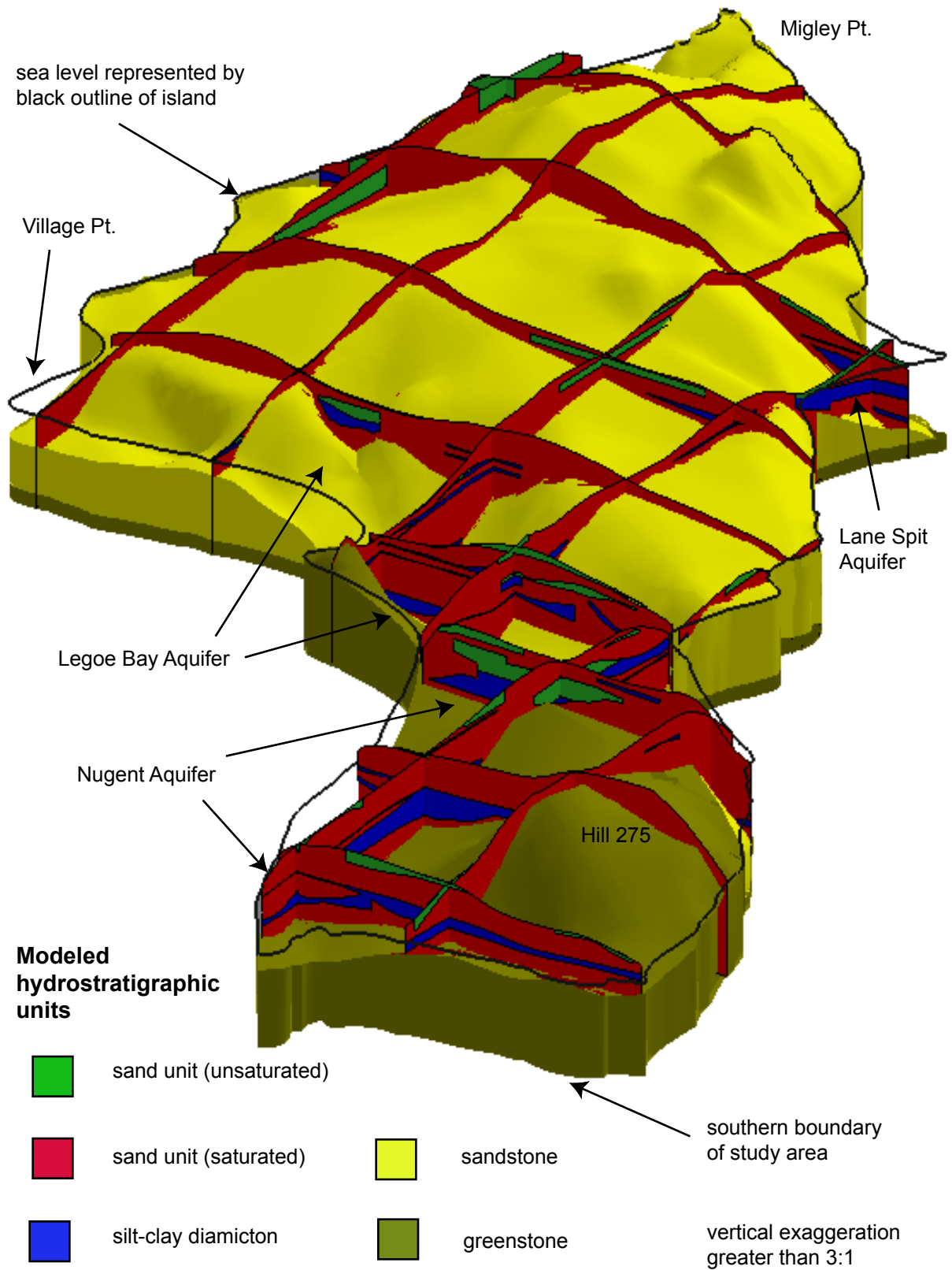
Figure 13a. Fence diagrams cut through modeled hydrostratigraphy, looking north, north Lummi Island, Washington.

Constitution Aquifer

sea level represented by
black outline of island

Hill 275

southern
boundary
of study area

**Modeled
hydrostratigraphic
units**

sand unit (unsaturated)   sandstone

sand unit (saturated)   greenstone

silt-clay diamicton

Nugent Aquifer

vertical exaggeration
greater than 3:1
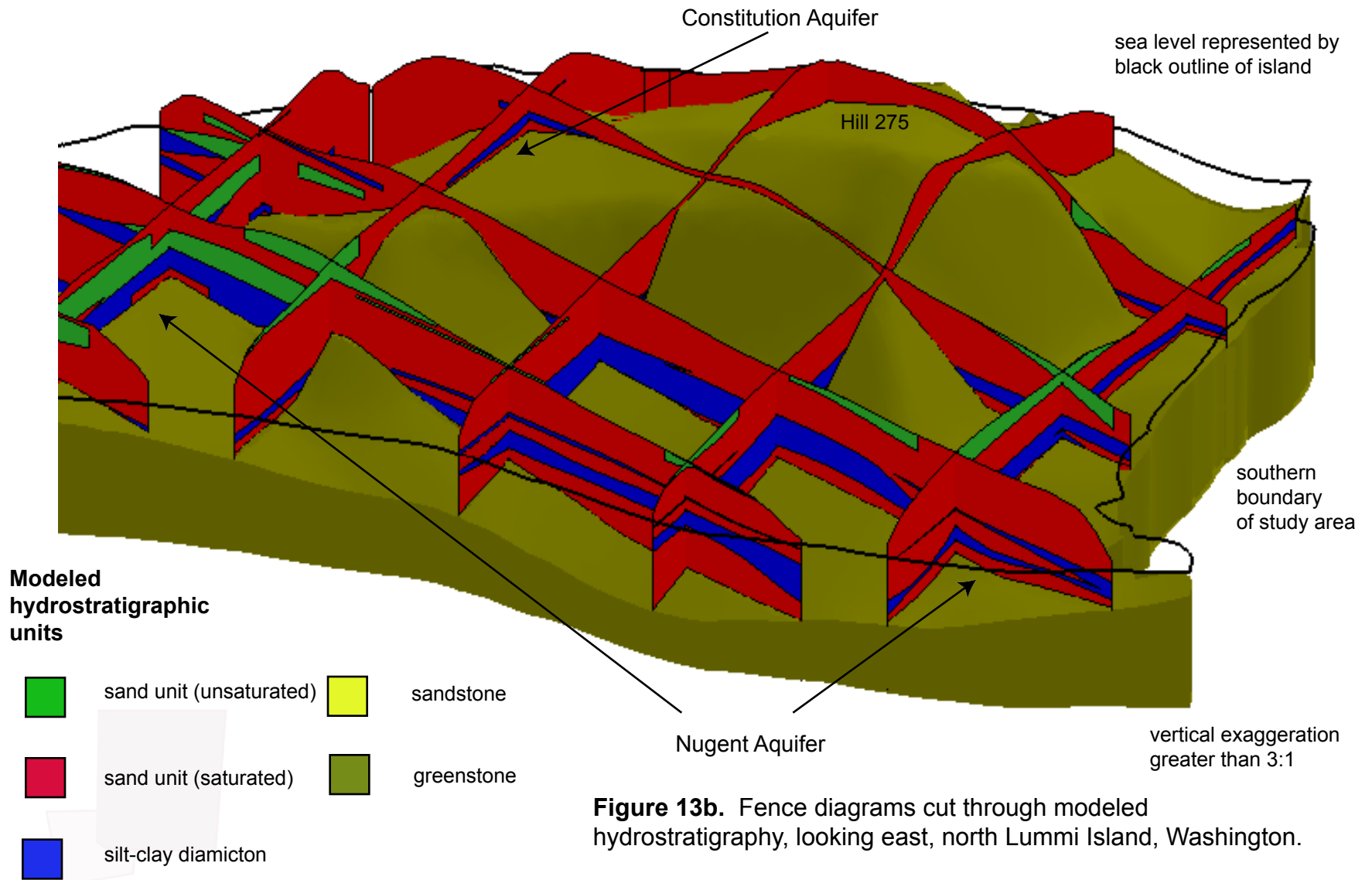
Figure 13b. Fence diagrams cut through modeled
hydrostratigraphy, looking east, north Lummi Island, Washington.

167
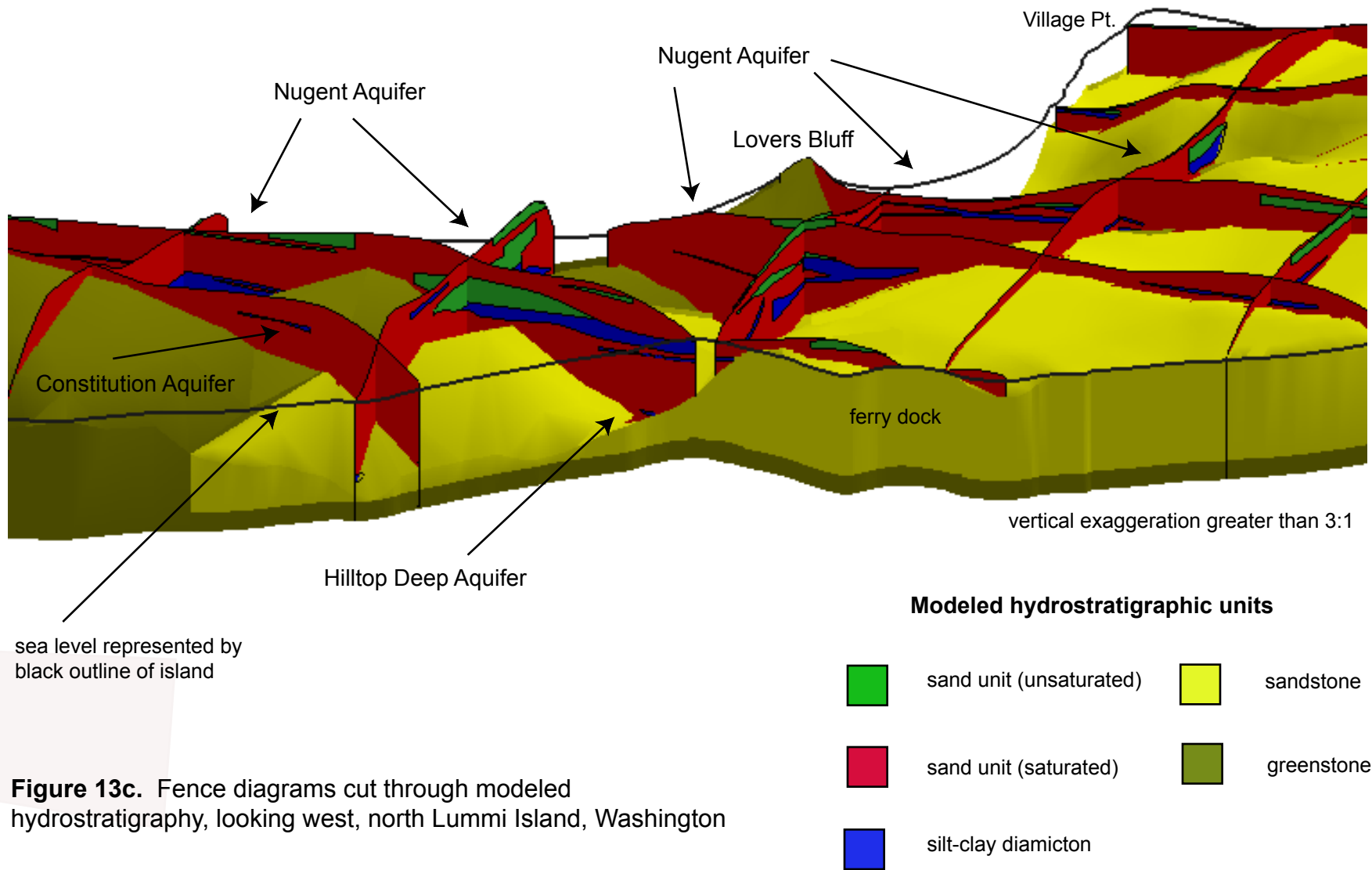
Figure 13c. Fence diagrams cut through modeled hydrostratigraphy, looking west, north Lummi Island, Washington

Nugent Aquifer

Nugent Aquifer

Village Pt.

Lovers Bluff

Constitution Aquifer

Hilltop Deep Aquifer

ferry dock

vertical exaggeration greater than 3:1

sea level represented by black outline of island

Modeled hydrostratigraphic units

- sand unit (unsaturated)
- sand unit (saturated)
- silt-clay diamicton
- sandstone
- greenstone

168

Labels on figure:

sea level represented by
black outline of island

southern boundary
of study area

Hill 275

Nugent Aquifer

Lovers Bluff

Legoe Bay Aquifer

Village Pt.

Modeled hydrostratigraphic units

- sand unit (unsaturated)
- sand unit (saturated)
- silt-clay diamicton
- sandstone
- greenstone

vertical exaggeration
greater than 3:1

Figure 13d. Fence diagrams cut through modeled hydrostratigraphy, looking southeast, north Lummi Island, Washington.

Village Pt.

sea level represented by
black outline of island

Legoe Bay Aquifer

Lovers Bluff

Centerview Aquifer

Blizzard Aquifer

Lane Spit Aquifer

Lane Spit Deep Aquifer

vertical exaggeration
greater than 3:1

Modeled hydrostratigraphic units

sand unit (unsaturated)

sand unit (saturated)

sandstone

silt-clay diamicton

greenstone
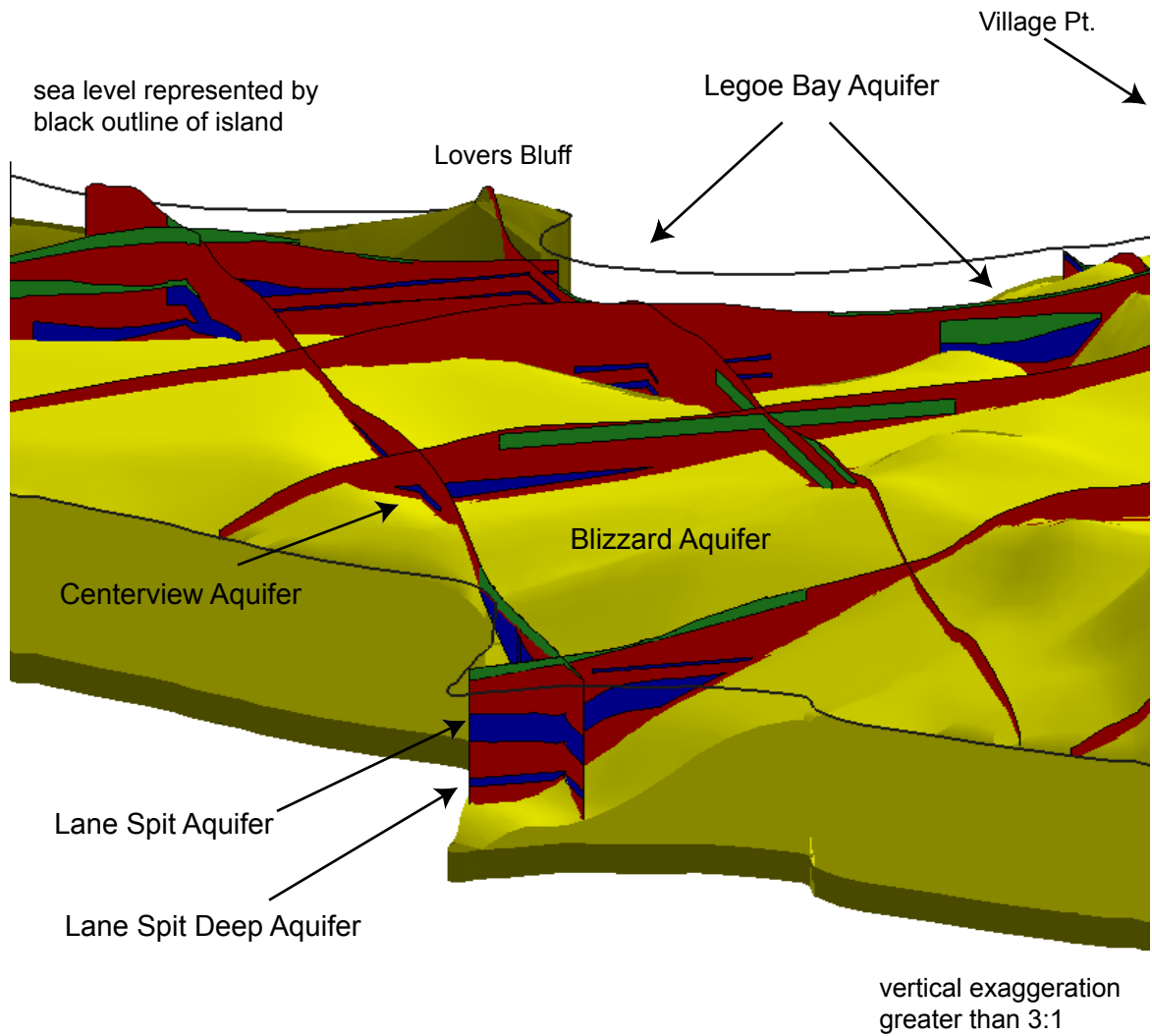
Figure 13e. Fence diagrams cut through modeled hydrostratigraphy, looking southwest, north Lummi Island, Washington.

Figure 14. Groundwater flow along glaciomarine drift-sandstone contact, northeastern shoreline, north Lummi Island, Washington

Modeled aquifer material

- sand aquifer (saturated region)
- sand aquifer (Nugent Aquifer) (saturated region)
- sand aquifer (Hilltop Deep Aquifer) (saturated region)
- sand aquifer (unsaturated region)
- sandstone
- greenstone

not shown:

*Lane Spit Deep Aquifer (lies beneath and may be part of Lane Spit Aquifer)

* Village Pt. Aquifer may occupy a small region at Village Pt.

north

0.25   0.5 mile

Figure 15. Distribution of modeled aquifers, north Lummi Island, Washington

172

Figure 16. Orthographic view of modeled aquifers with the overlying silt-clay diamicton solid removed. View is from the southwest, looking to the northeast. The black outline of the island represents sea level.
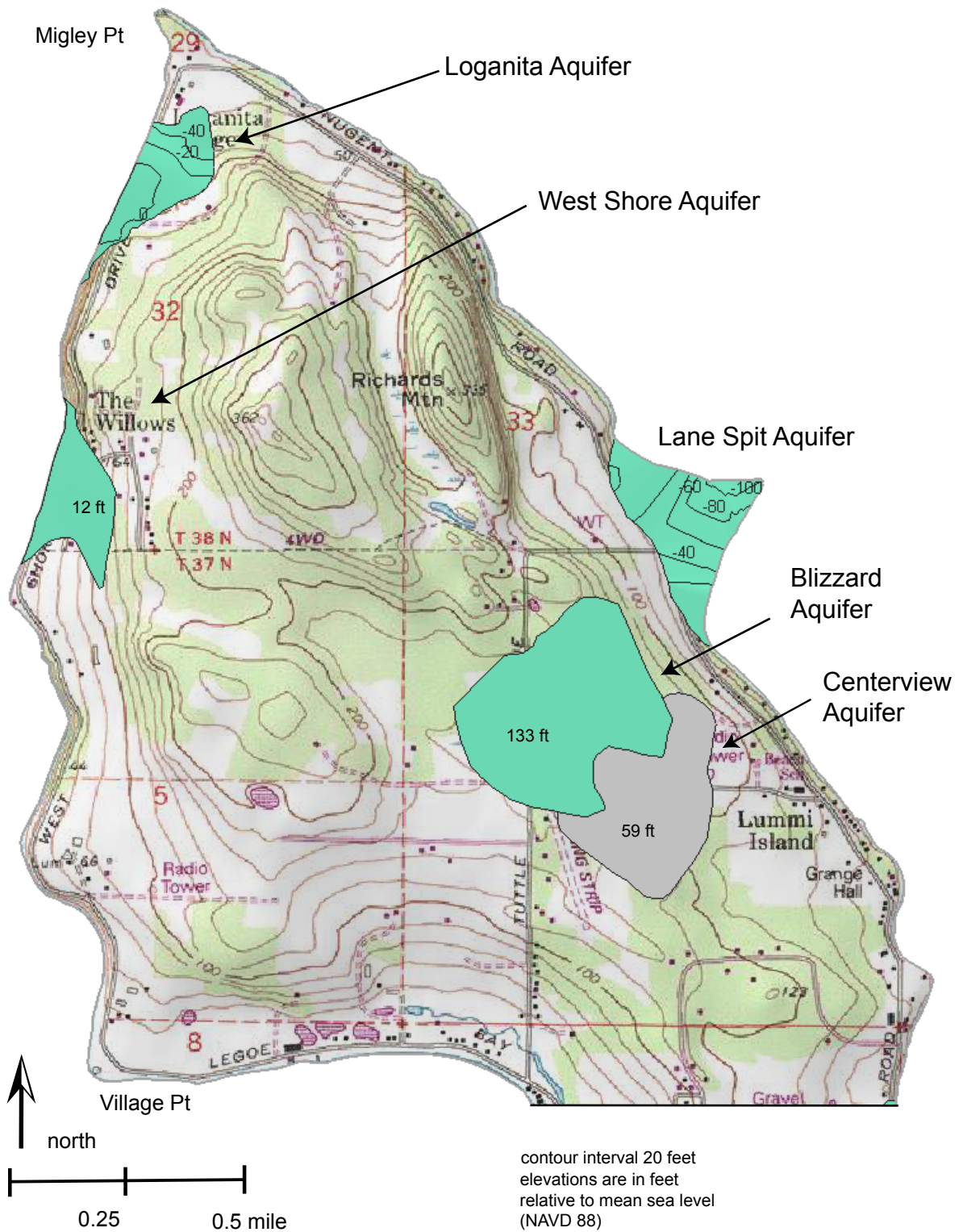
Figure 17a. Top of aquifer elevations for selected Pleistocene aquifers, north half of study area, north Lummi Island, Washington. Lane Spit Deep Aquifer is not shown. Due to limited well log data, the Blizzard, Centerview, and West Shore aquifers were modeled to the constant elevations shown.

174
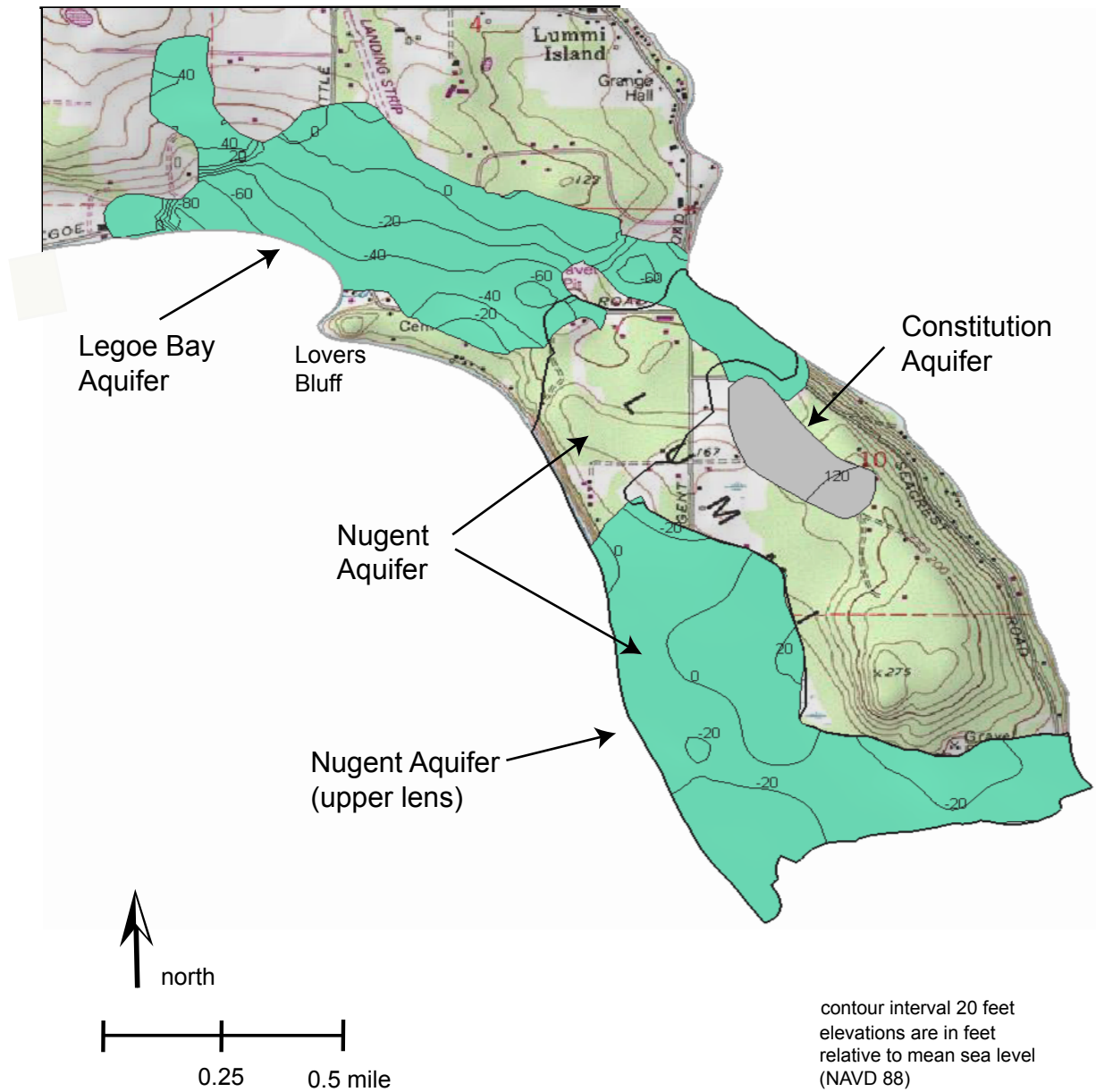
Figure 17b. Top of aquifer elevations for Pleistocene aquifers, south half of study area, north Lummi Island, Washington. Hilltop Deep Aquifer is not shown. Only the upper lens of the Nugent Aquifer is shown.
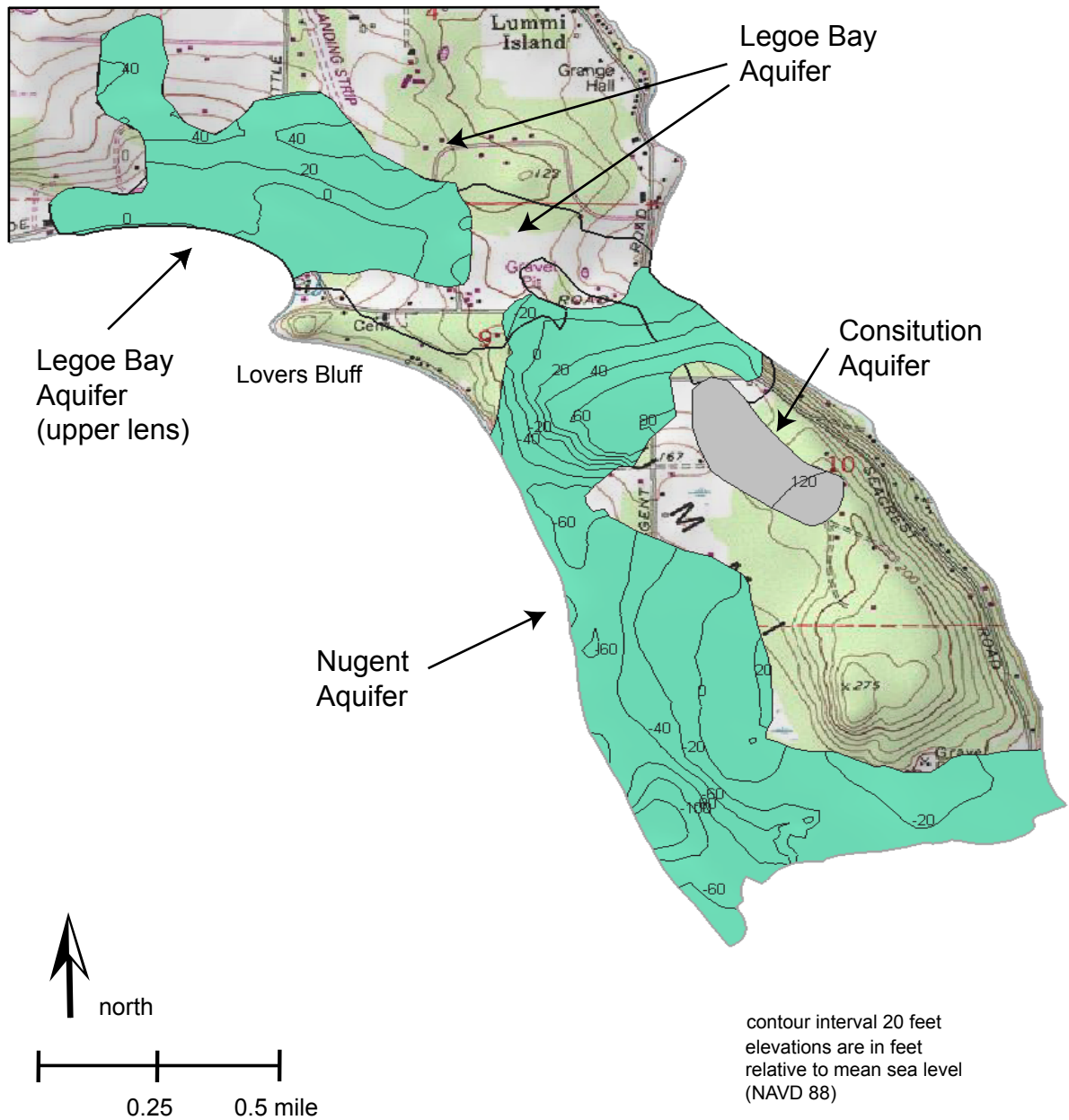
Figure 17c. Top of aquifer elevations for selected Plesitocene aquifers, south half of study area, north Lummi Island, Washington. Hilltop Deep Aquifer is not shown. Only the upper lens of the Legoe Bay Aquifer is shown.
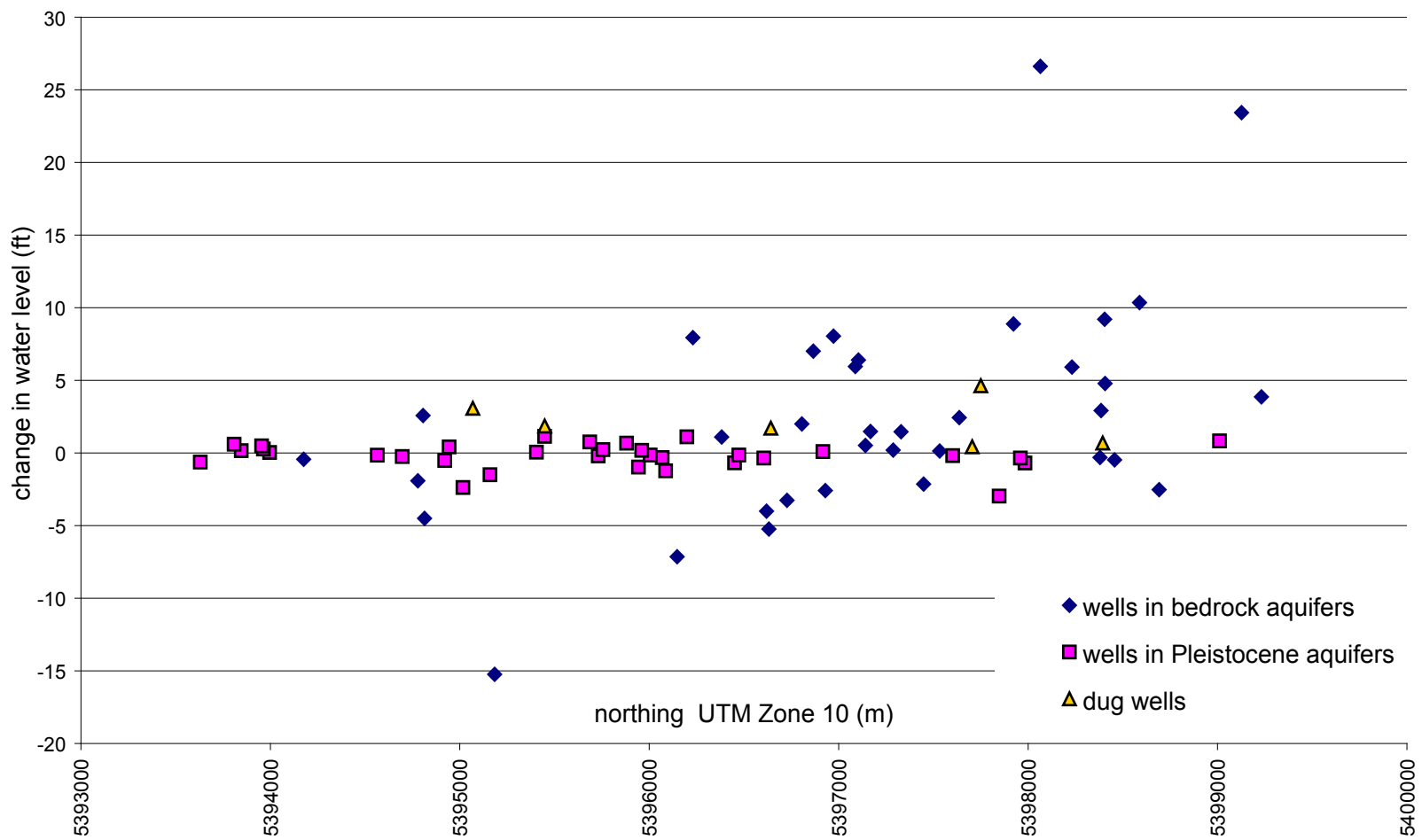
Figure 18. Water level changes by aquifer material, fall 2002 to spring 2003, north Lummi Island, Washington

177
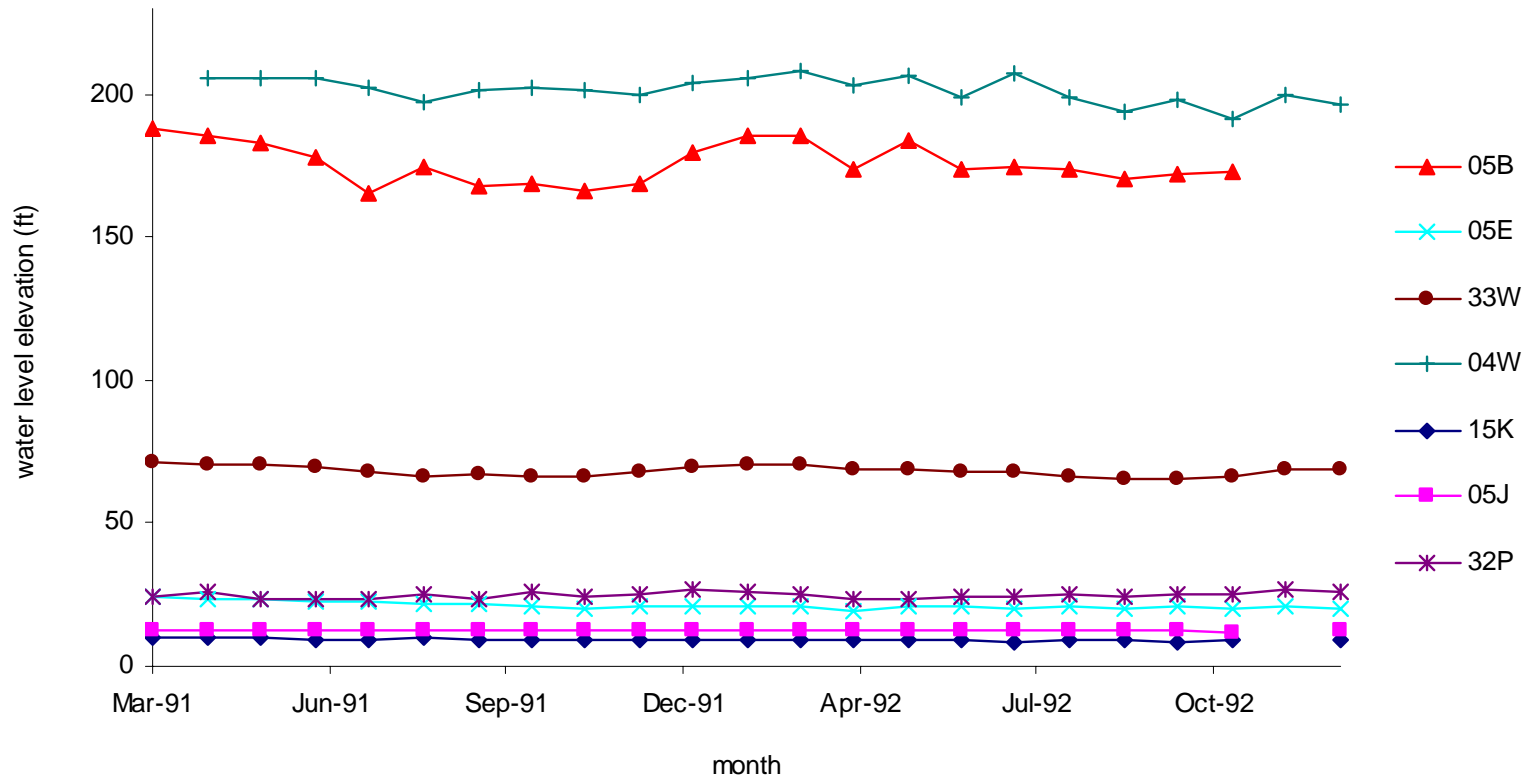
Figure 19. Well Hydrographs for 7 wells monitored from March, 1991-January, 1993 and during this study. Water level elevations are from water level measurements in Whatcom County (1994) and well-head elevations measured during this study.

178
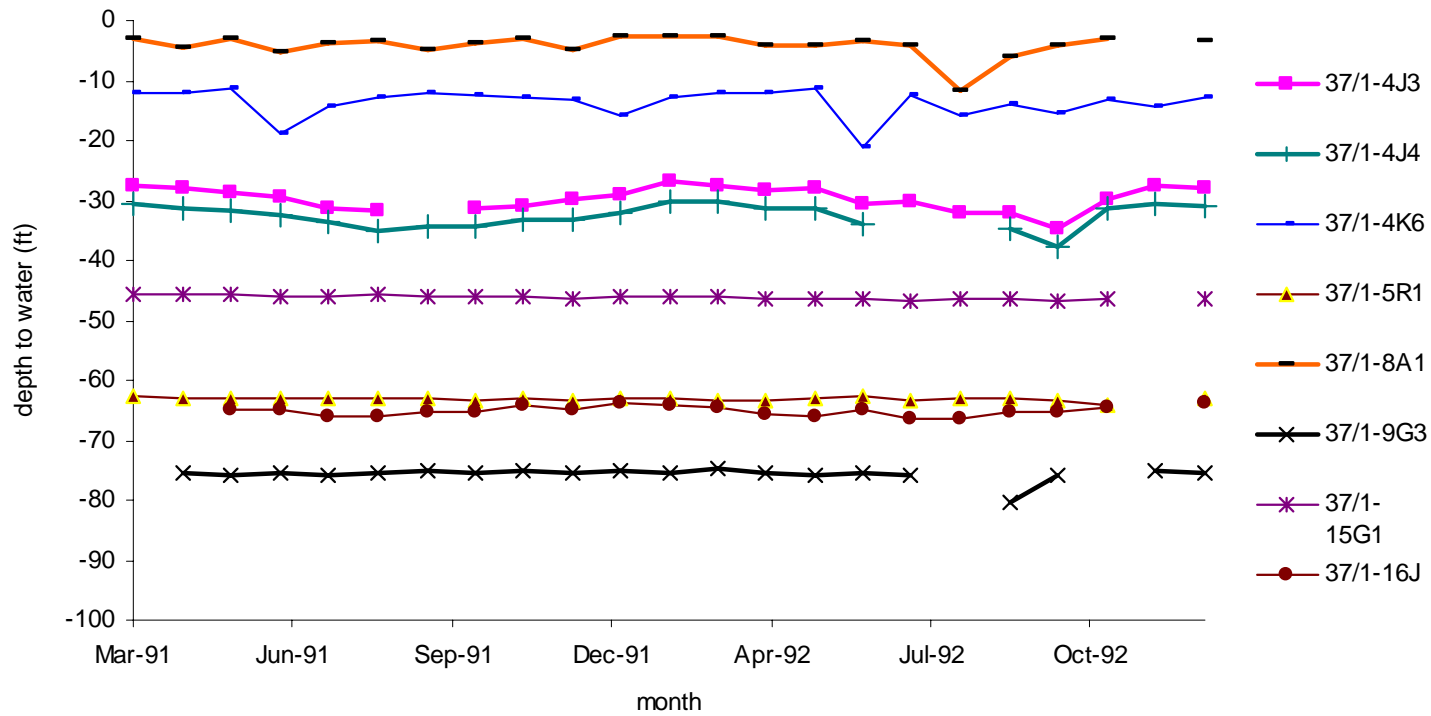
Figure 20. Well hydrographs for 8 wells not correlated to wells used in the current study, monitored from March, 1991-January, 1993 (Whatcom County, 1994)
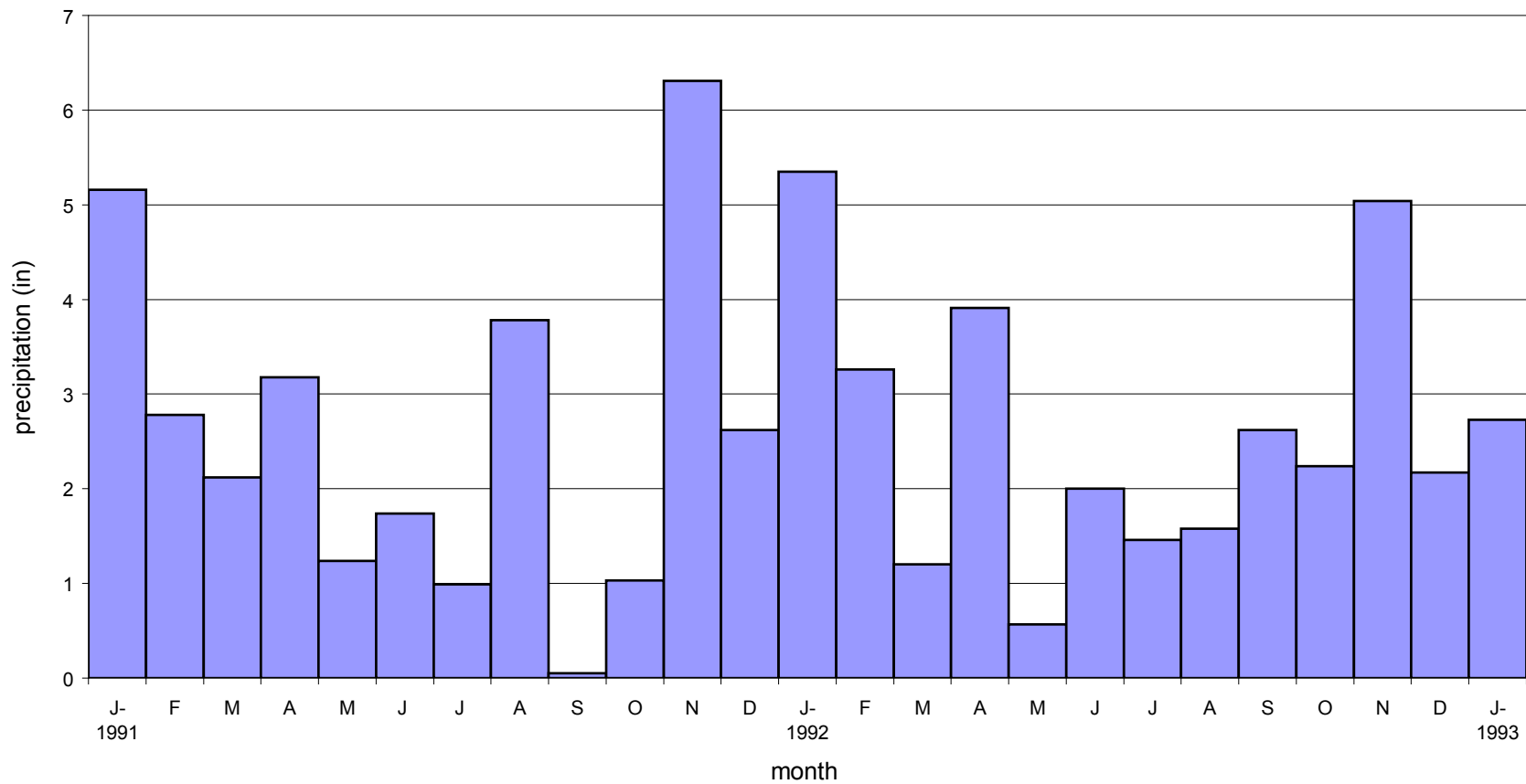
Figure 21. Precipitation (West Shore Gauge), north Lummi Island, Washington, January 1991- January 1993. Source: Whatcom County (1994)
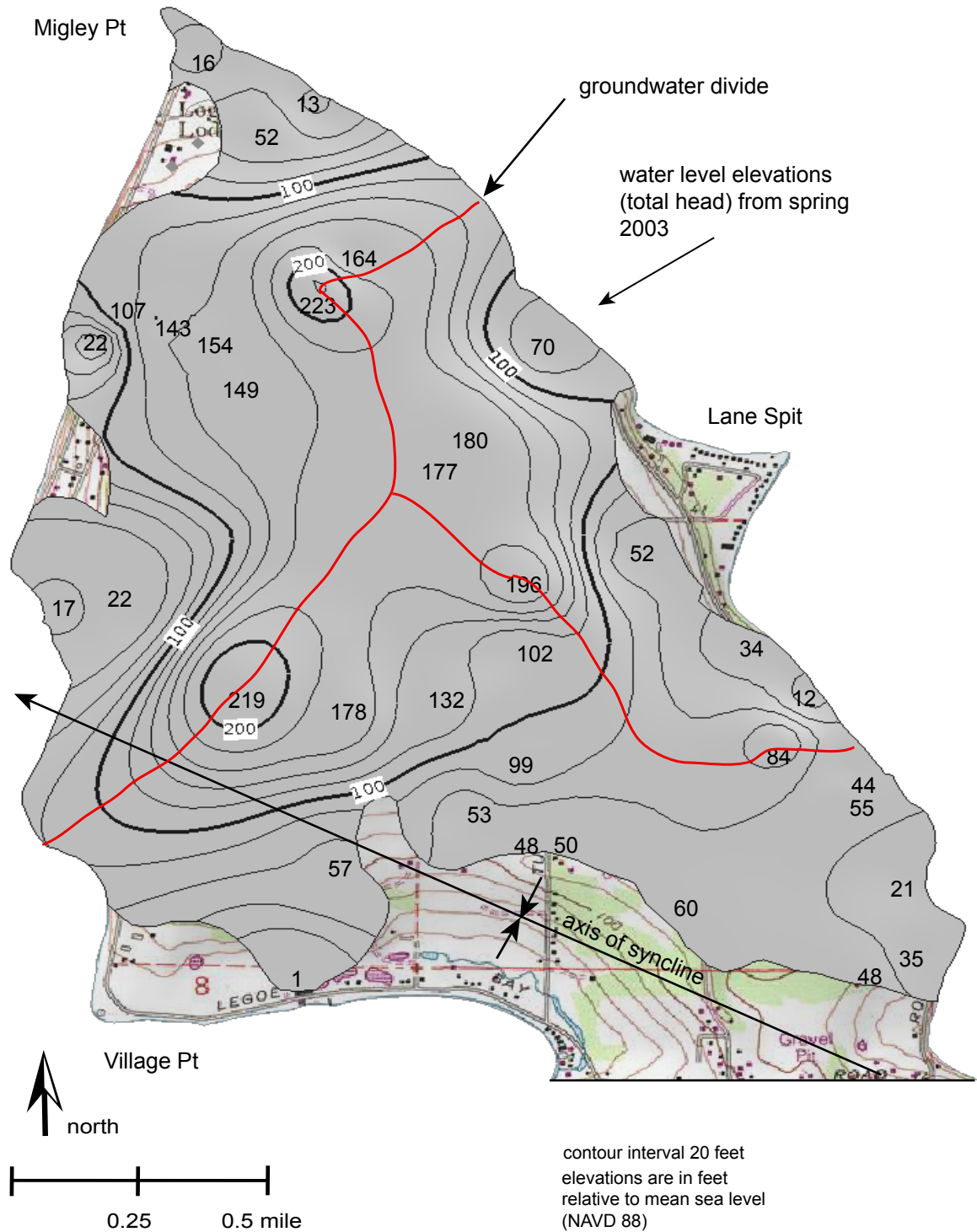
Figure 22a. Potentiometric map, Sandstone Aquifer, north Lummi Island, Washington, spring 2003. The axis of the southern-most syncline mapped by Carroll (1980) may divert flow to the east and west, isolating sandstone in the vicinity of Village Point.

181
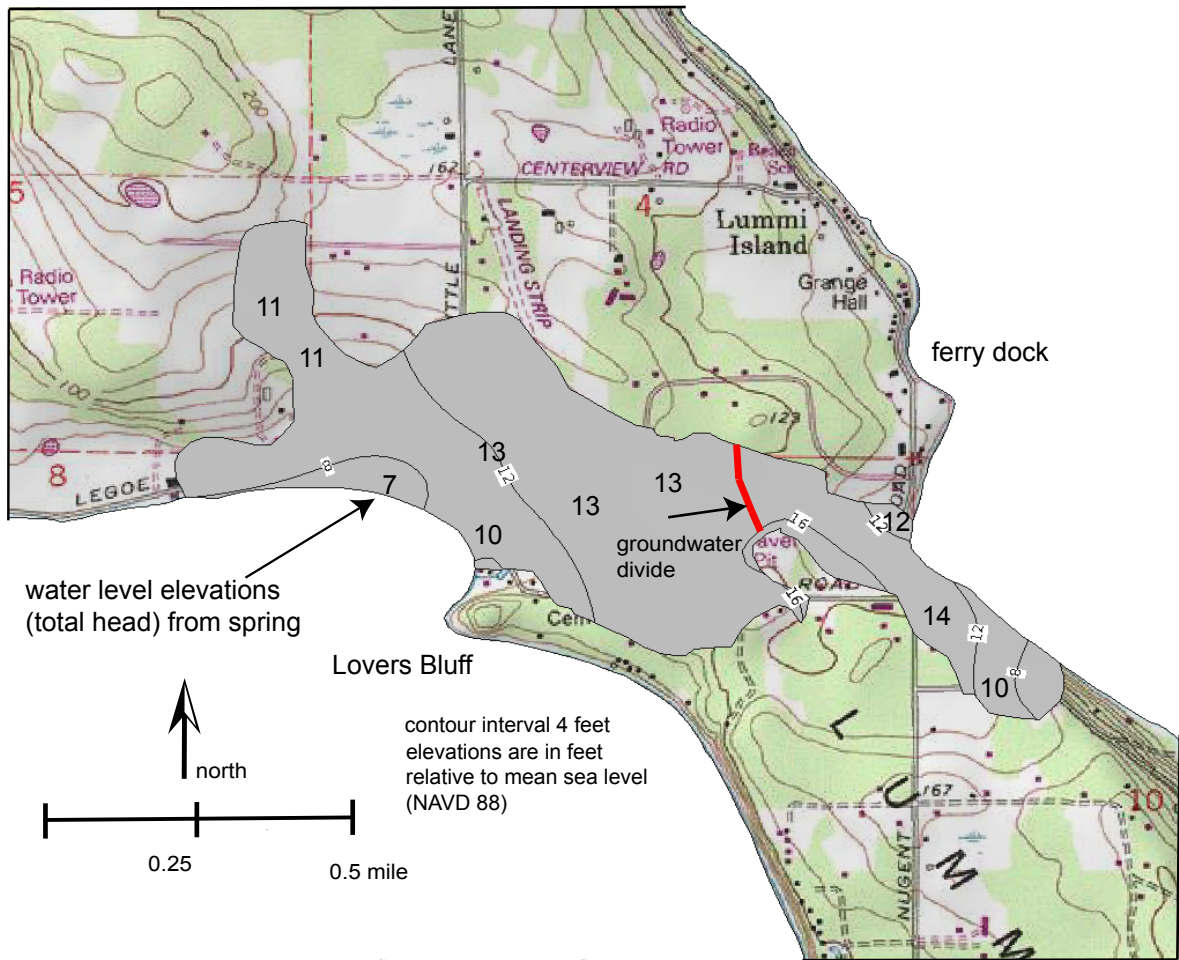
Figure 22b. Potentiometric map, Legoe Bay Aquifer, north Lummi Island, Washington, spring 2003. The 16 foot contour is due to the influence of 09J which is actually in the Nugent Aquifer. This contour illustrates head distribution in the Legoe Bay Aquifer, assuming there is appreciable continuity between these two aquifers that likely share a common recharge area.

182
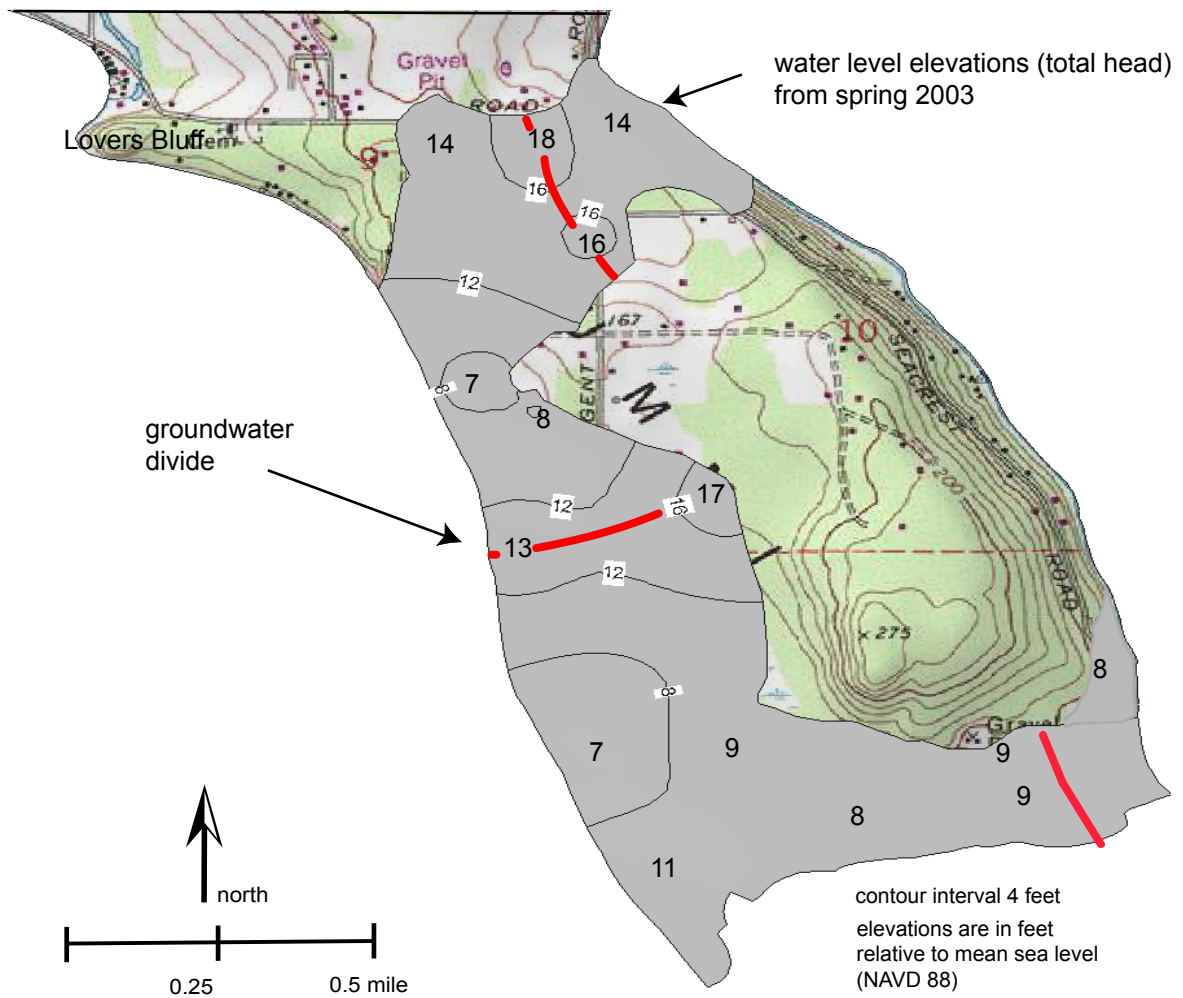
Figure 22c. Potentiometric map, Nugent Aquifer, north Lummi Island, Washington, spring 2003
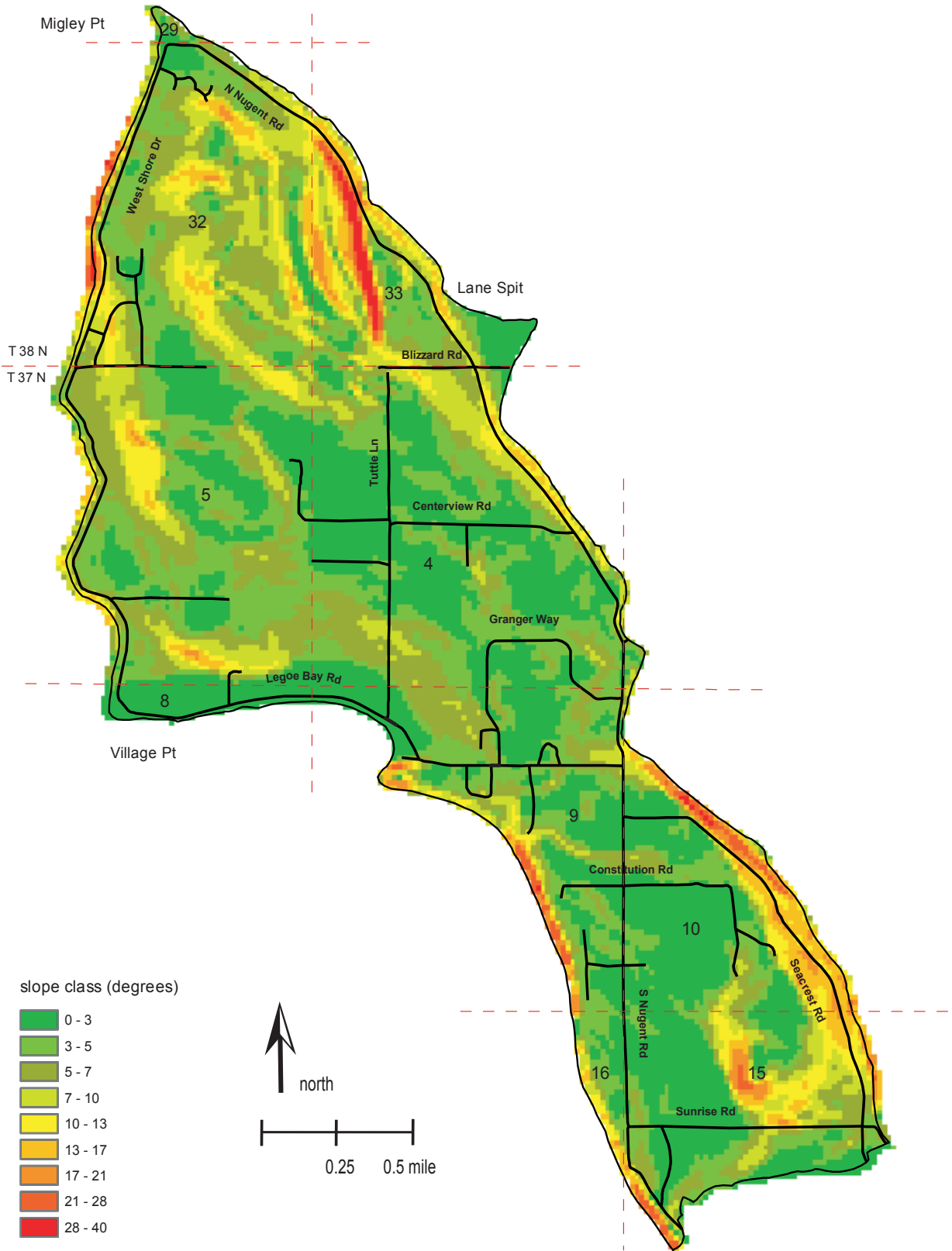
Figure 23. Slope, north Lummi Island, Washington.
Source: USGS 10-meter Digital Elevation Model

184
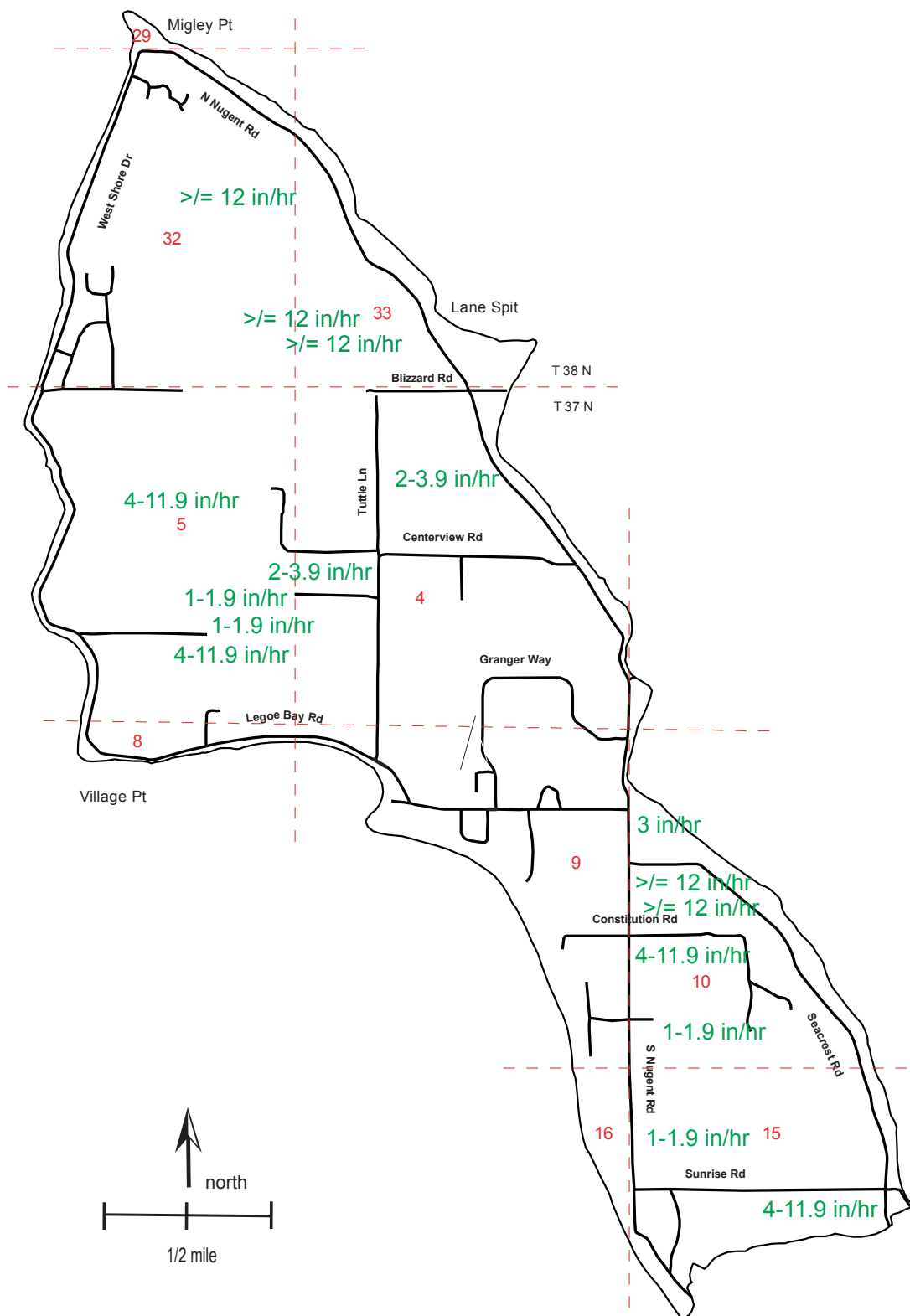
Figure 24. Percolation rate classes (inches per hour) from 16 on-site sewage (OSS) applications, north Lummi Island, Washington. Percolation rates were estimated at 4-5 feet below land surface, in subsoil.
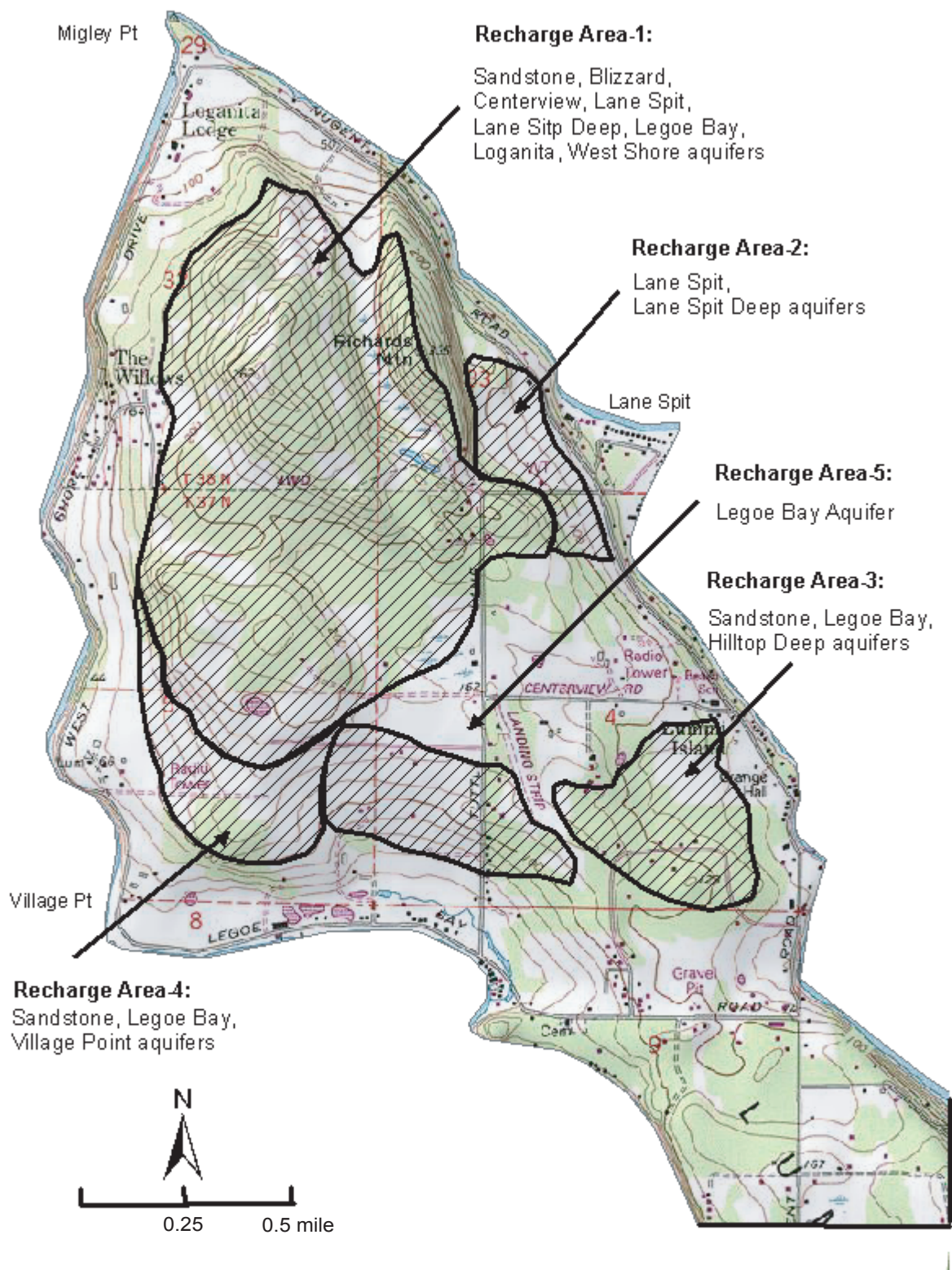
Figure 25a. Major recharge areas, north half of the study area, north Lummi Island, Washington
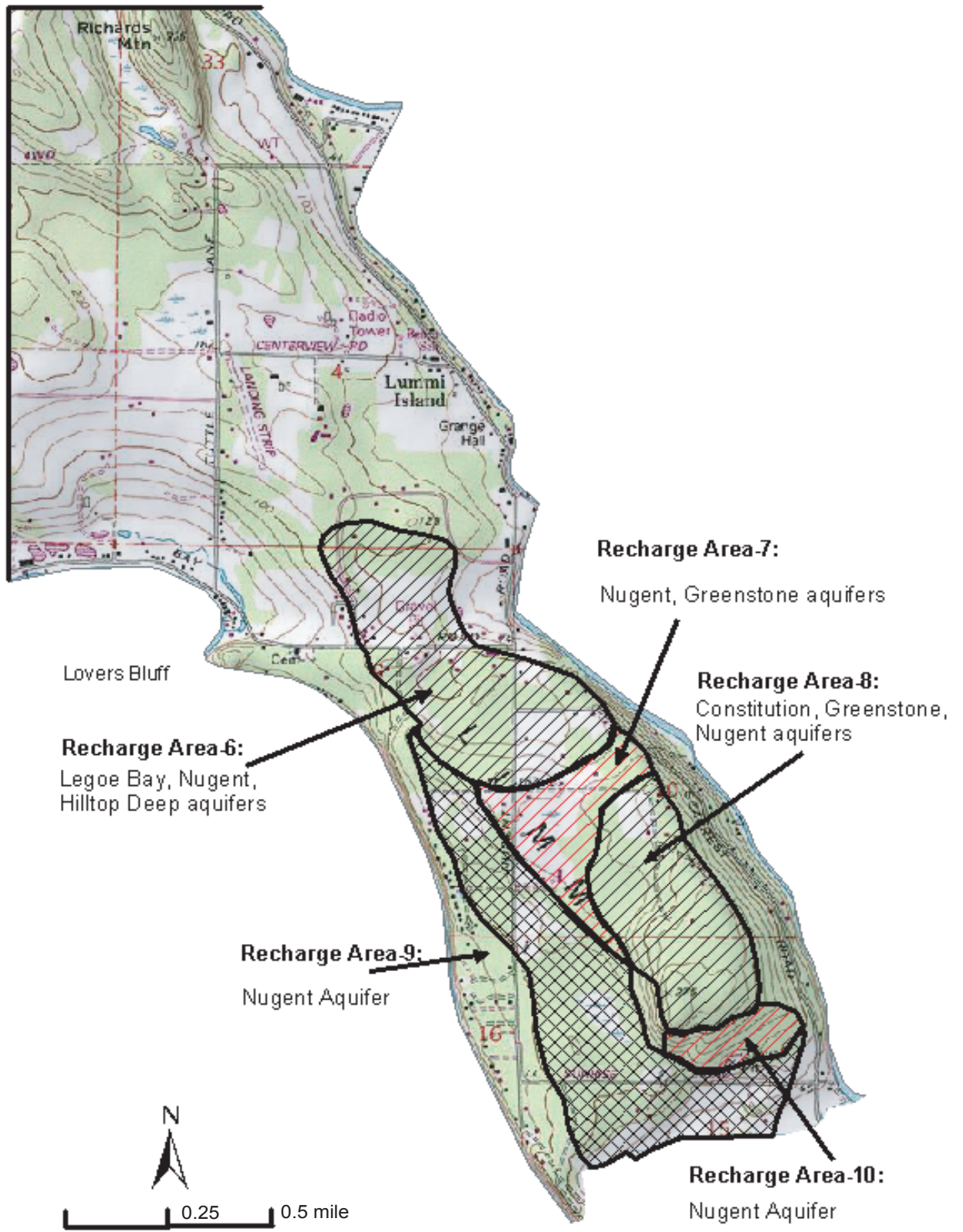
Figure 25b. Major recharge areas, south half of the study area, north Lummi Island, Washington
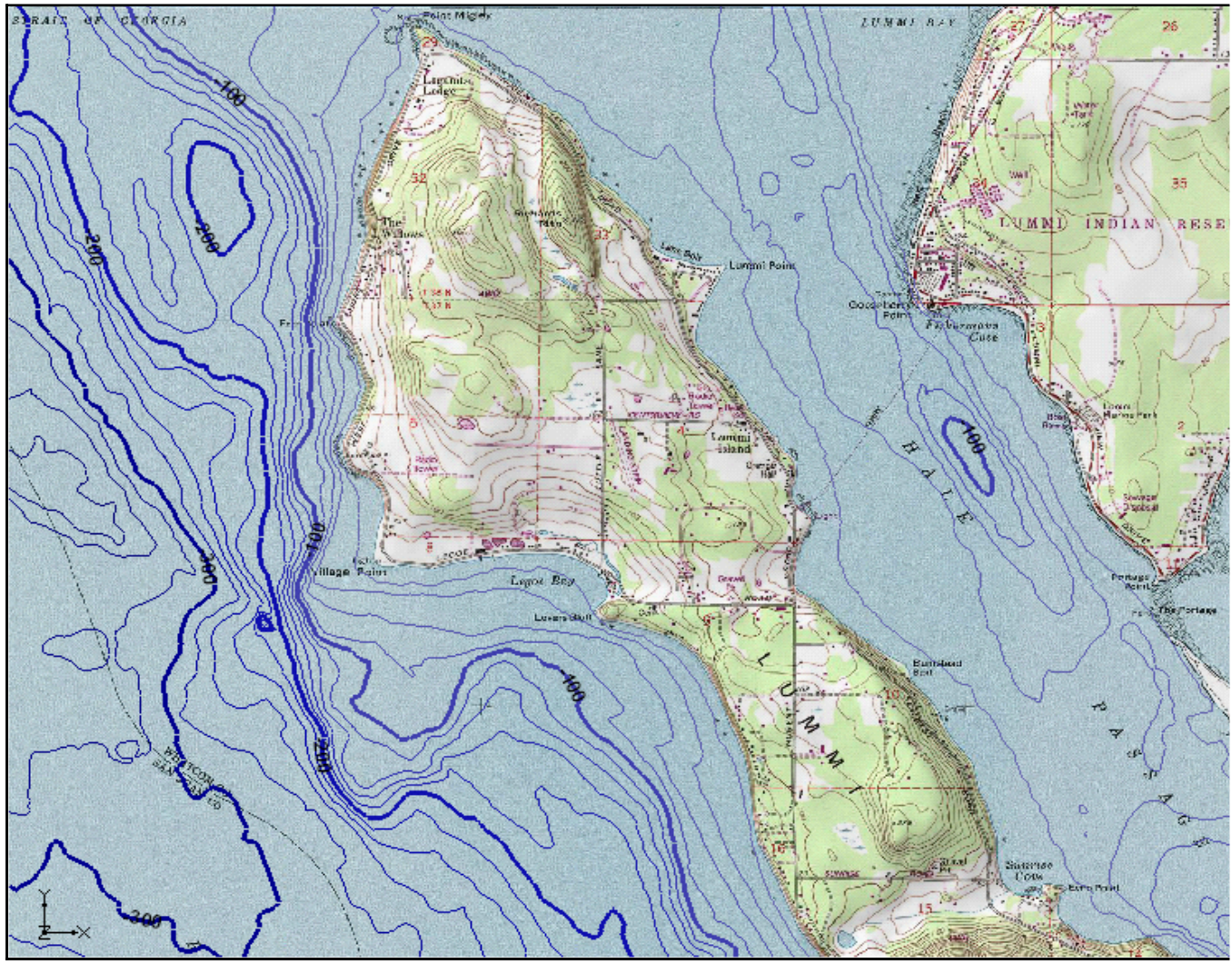
Figure 26. Bathymetry in the vicinity of north Lummi Island, Washington. Elevations are feet below mean sea level. Contour interval is 20 feet
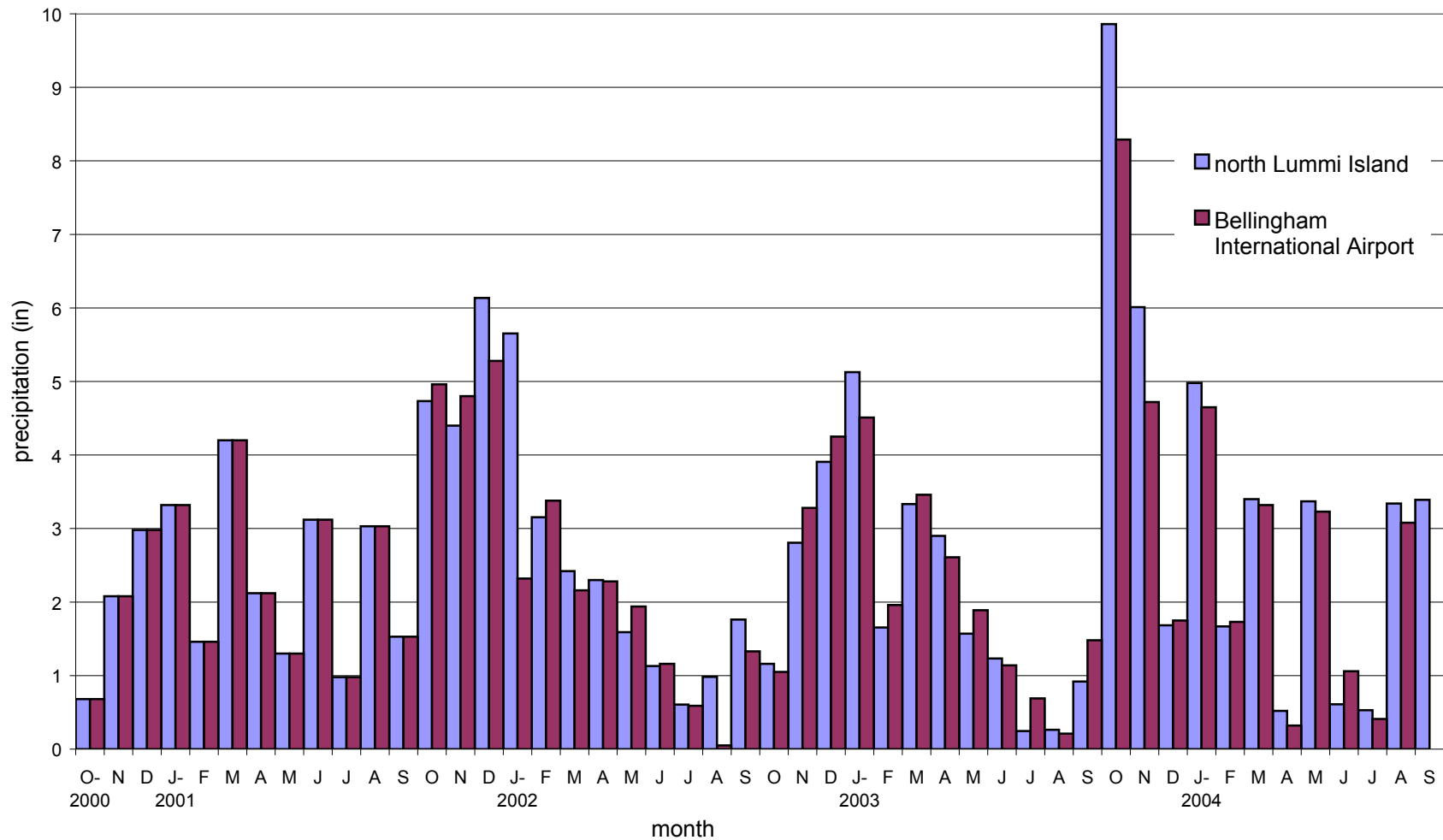
Figure 27. Monthly precipitation, north Lummi Island (average of three local gauges) and Bellingham International Airport, Washington, Water Years 2001-2004

189
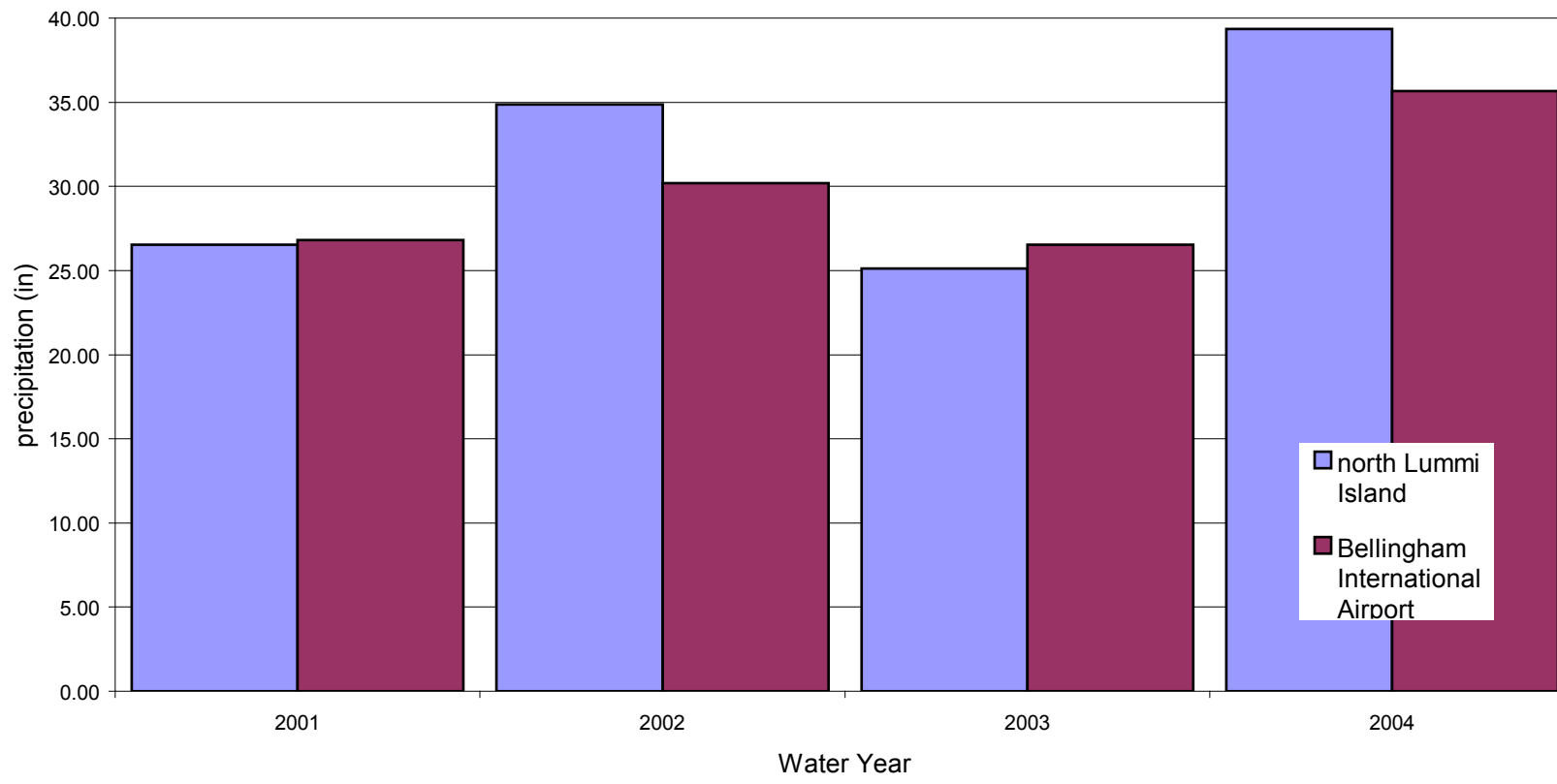
Figure 28. Annual precipitation for north Lummi Island (average of three local gauges) and Bellingham International Airport, Water Years 2001-2004
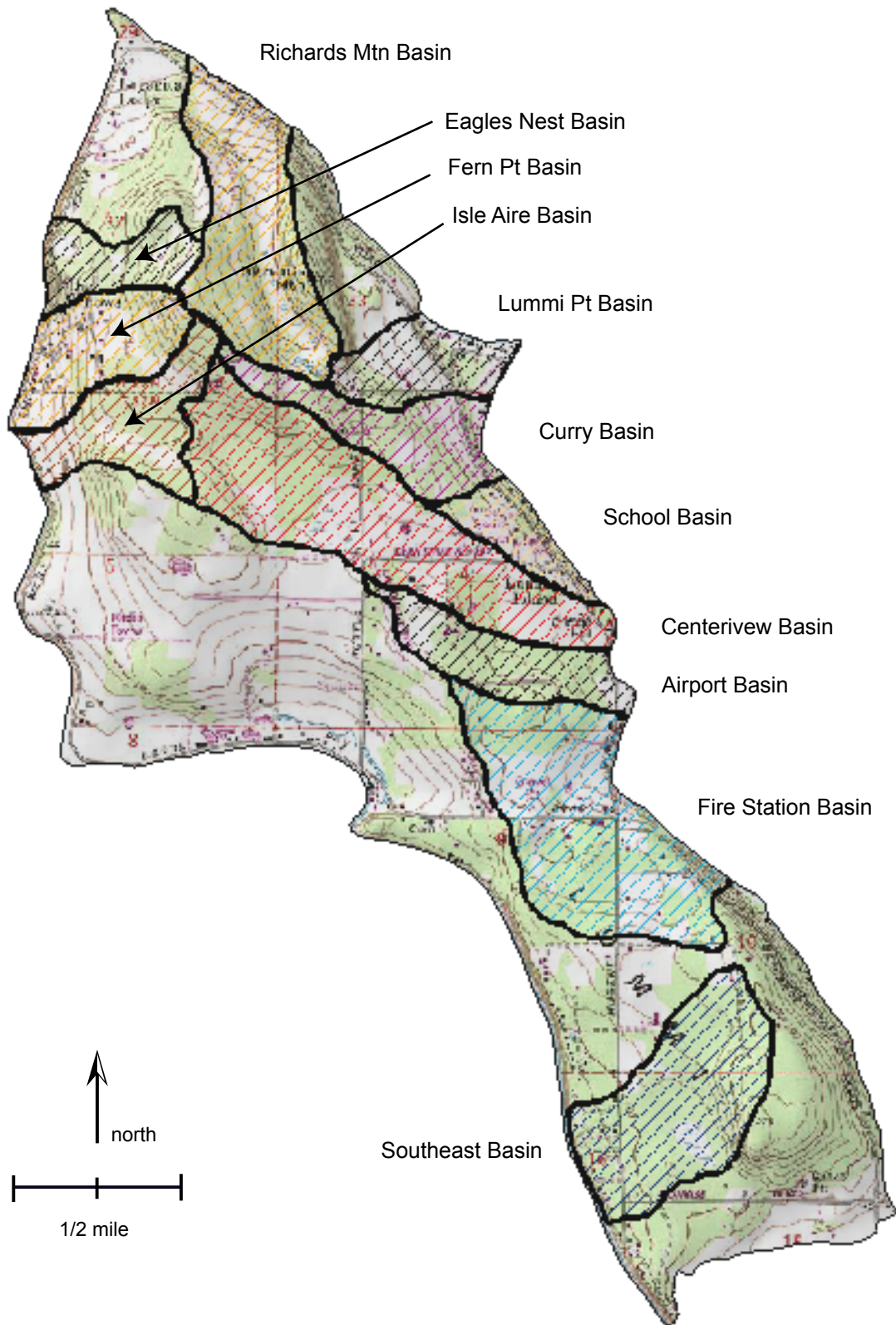
Figure 29. Drainage basins monitored for direct discharge by Nielson and Armfield, north Lummi Island Washington, Water Year 2004. Figure modified from Neilson and Armfield, unpublished
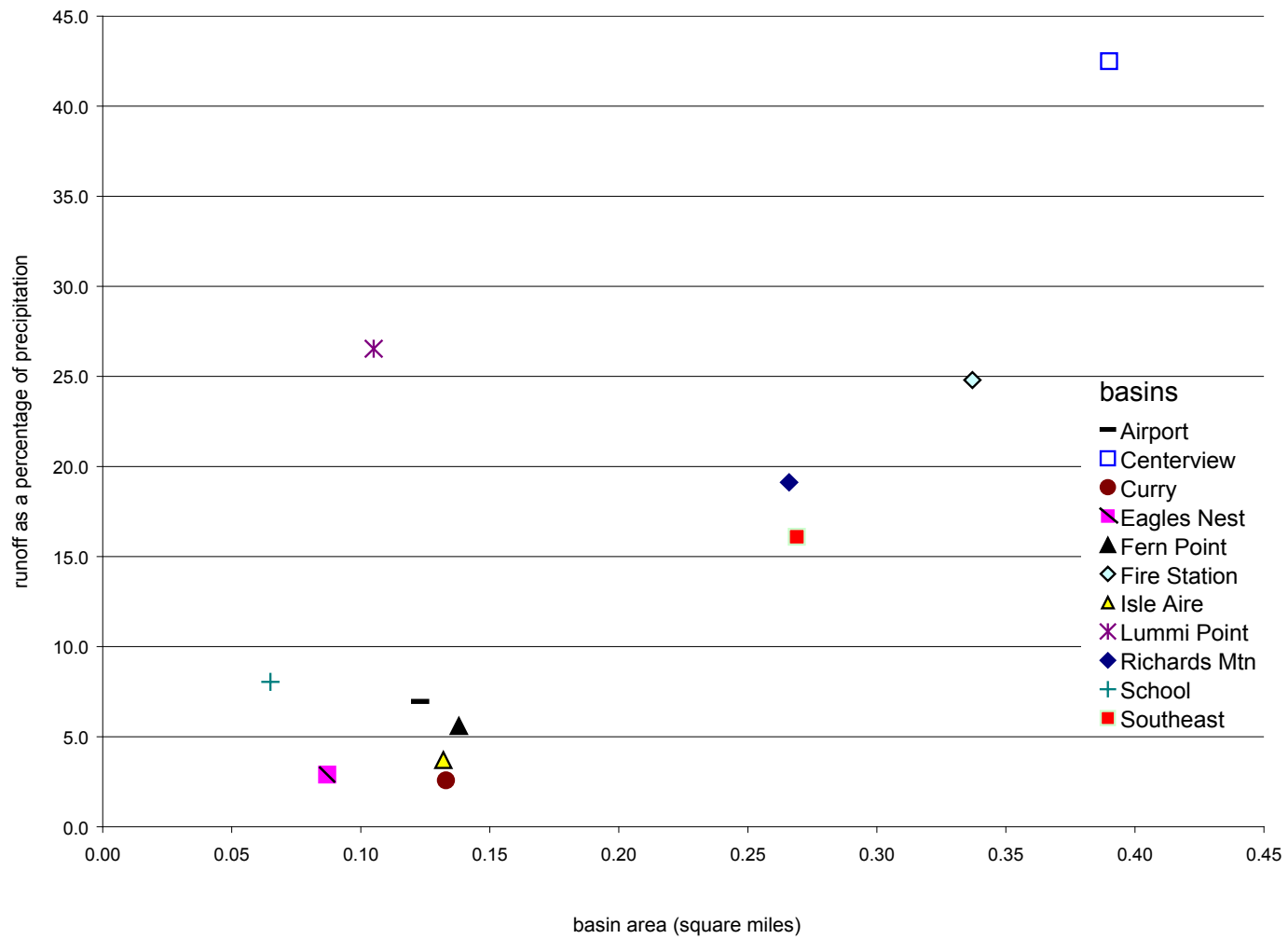
Figure 30. Basin area and runoff for 11 basins monitored during Water Year 2004, north Lummi Island, Washington. Figure modified from Nielson and Armfield (written communication)

192
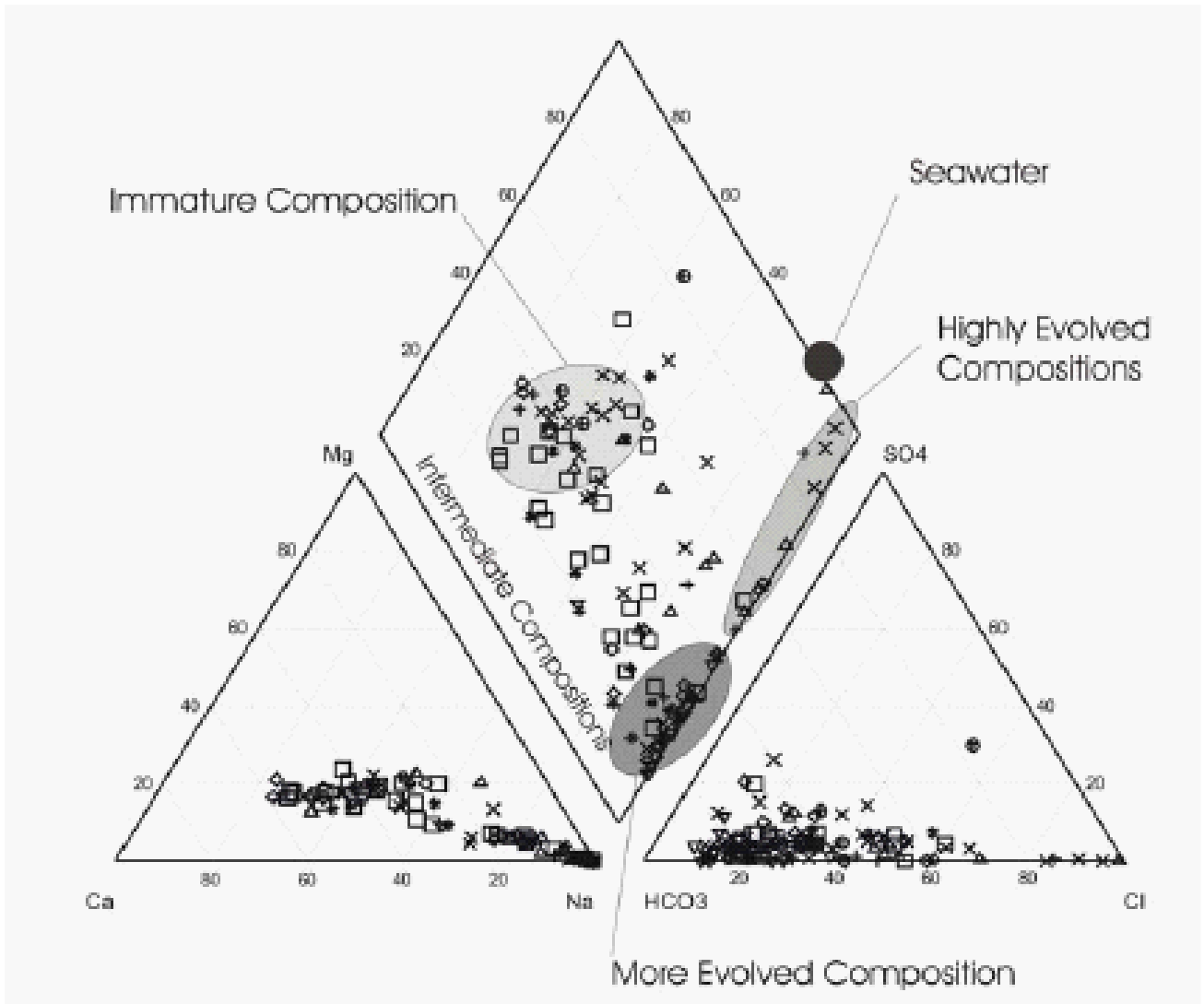
Figure 31. Piper Diagram with groundwater evolution composition fields and sample plots observed on Hornby Island, British Columbia, from Allen and Matsuo (2002)

193
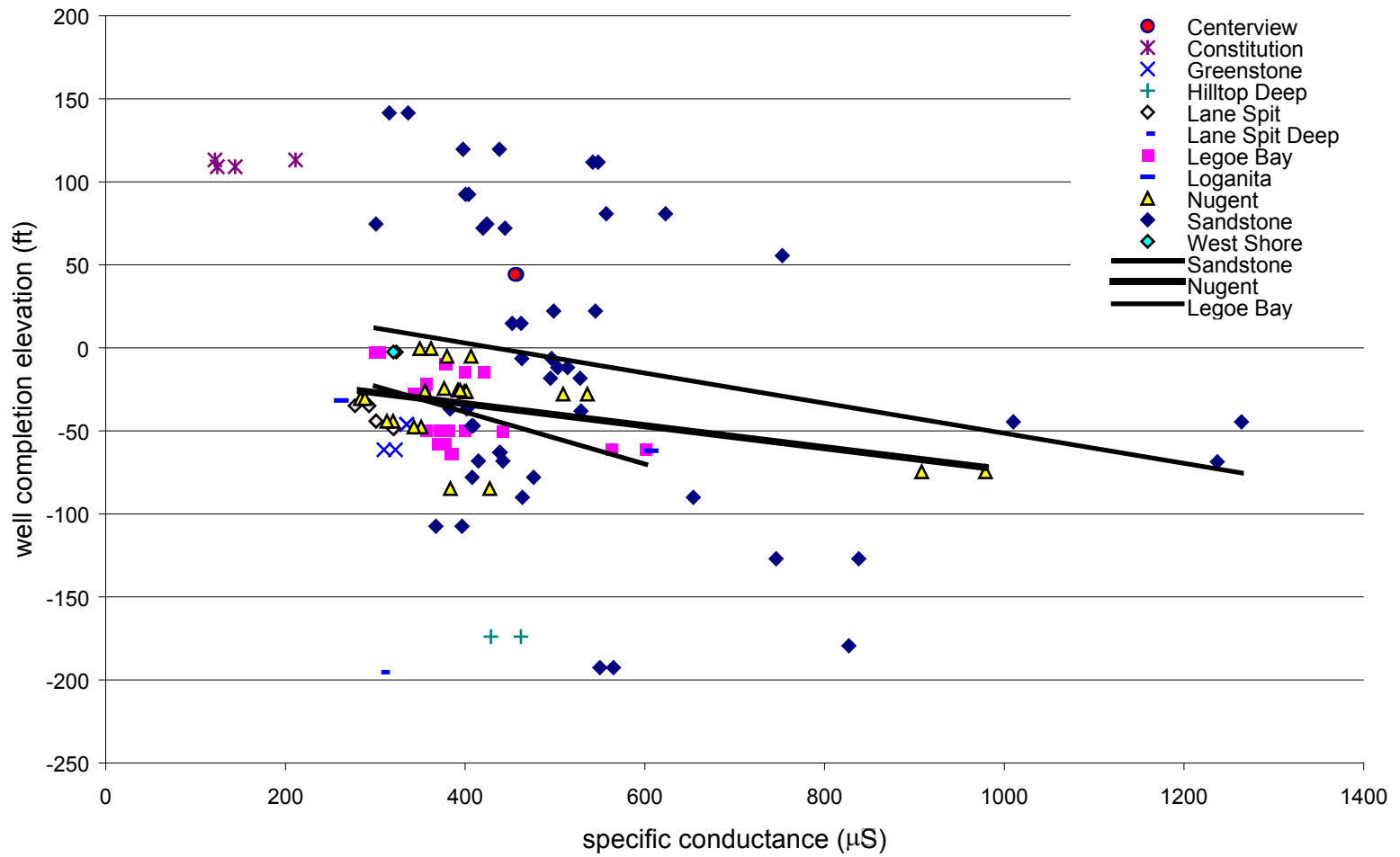
Figure 32. Specific conductance and well completion elevation, north Lummi Island, Washington, fall 2002-spring 2003 (excluding highest values located at 08O)
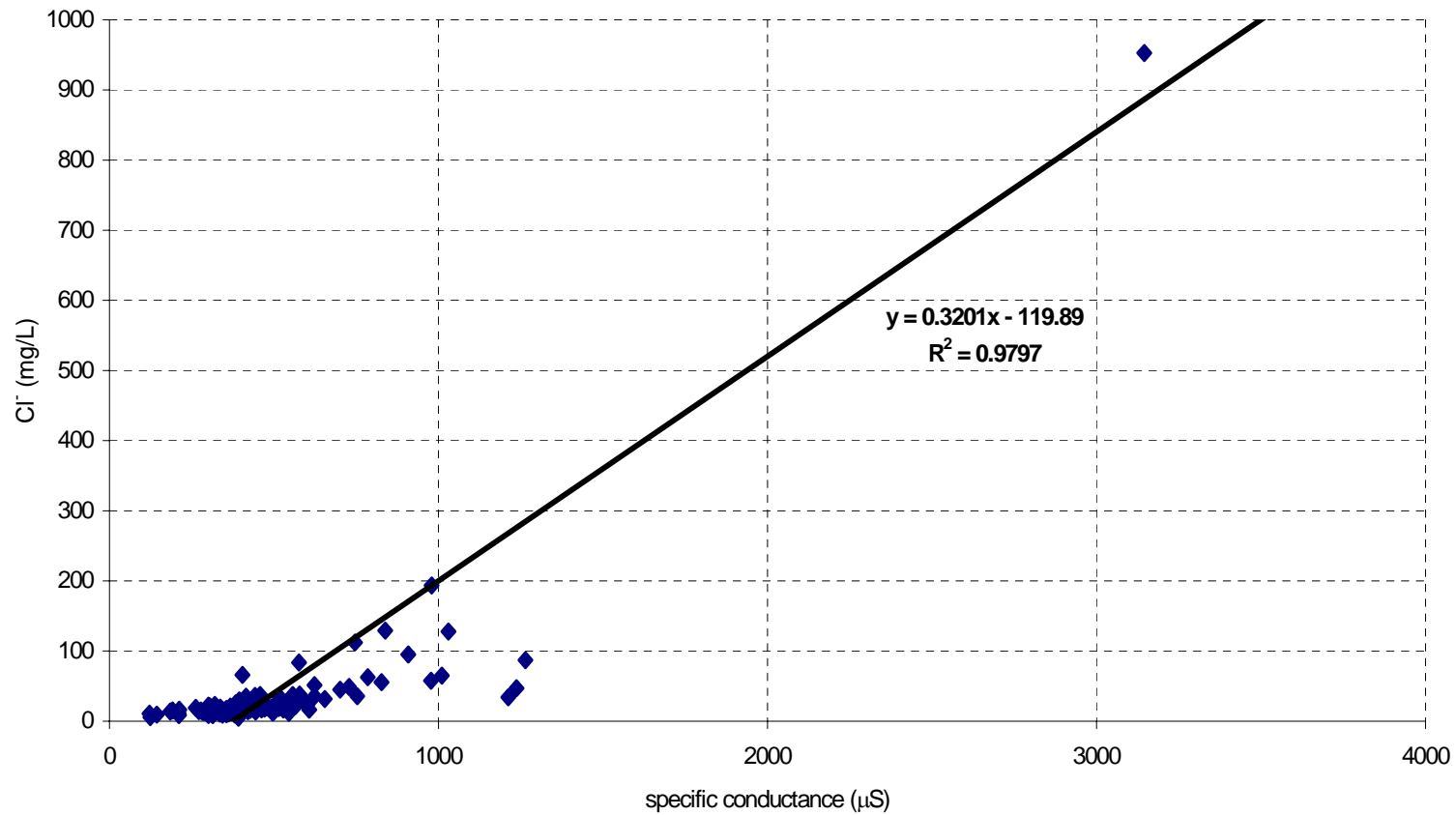
Figure 33a. Relationship between specific conductance and chloride concentrations, north Lummi Island, Washington, fall 2002-spring 2003. R^2 represents "very high" data correlation.
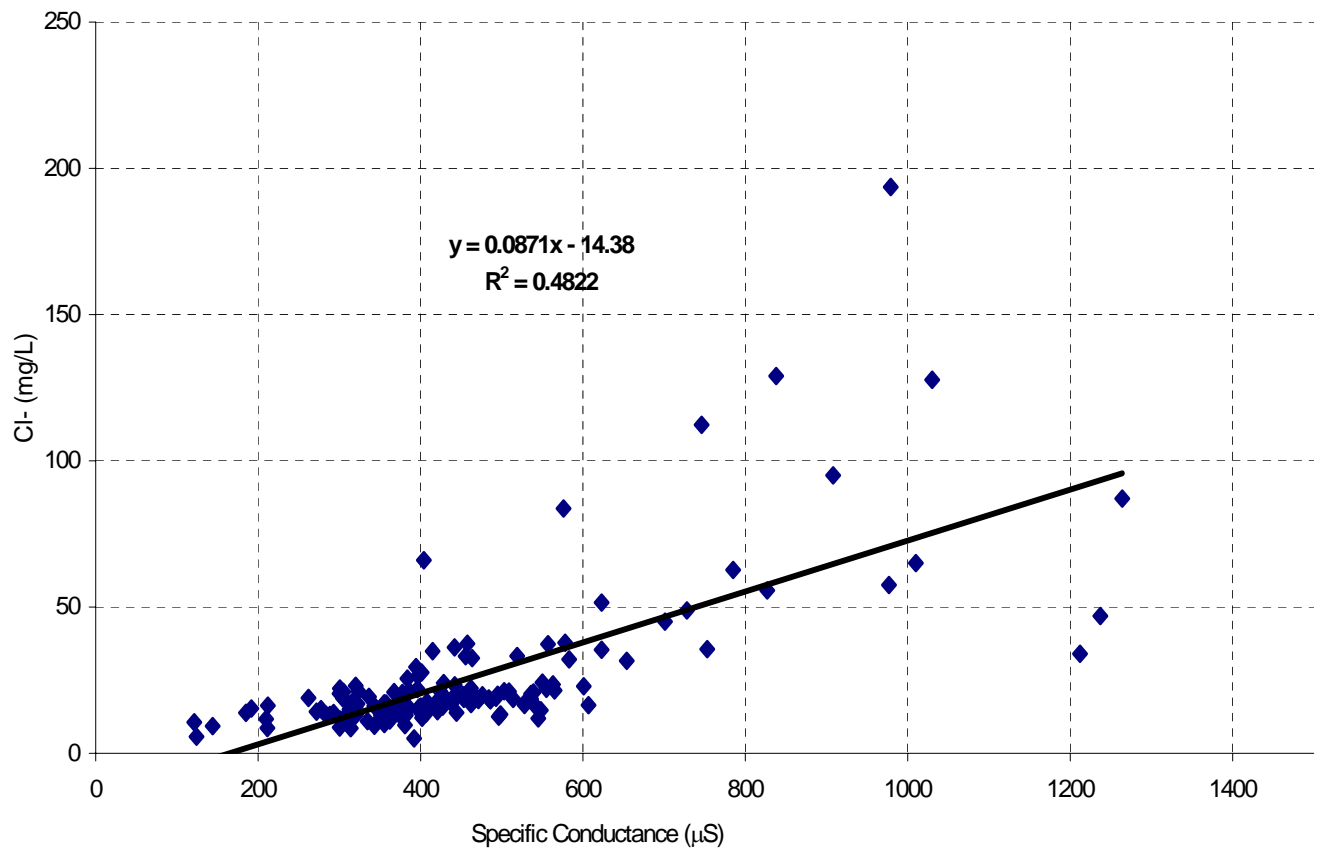
Figure 33b. Relationship between specific conductance and chloride concentrations, north Lummi Island, Washington, fall 2002-spring 2003. The three highest specific conductance-chloride data pair values are excluded. R^2 represents "poor" data correlation.
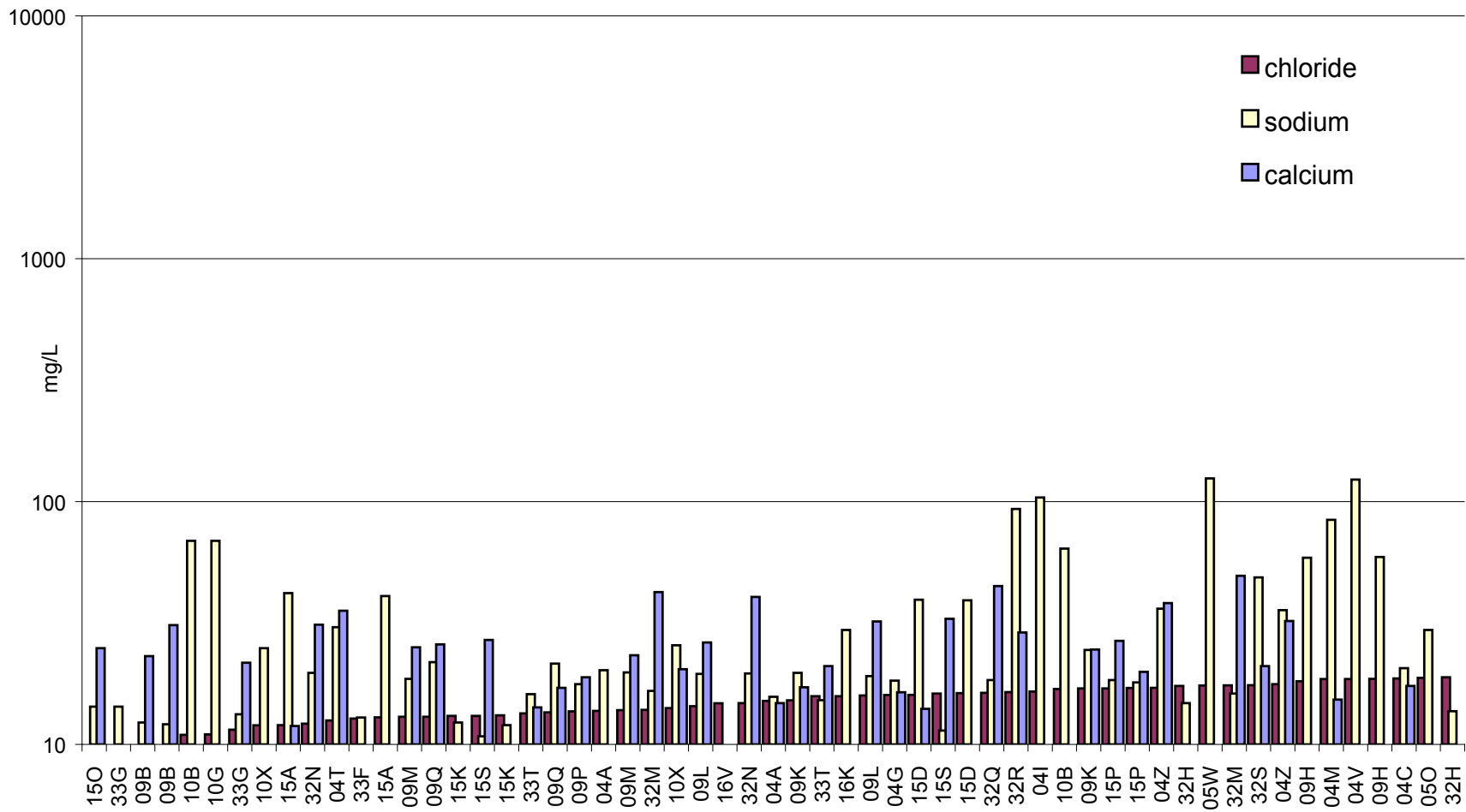
Figure 34a. Concentrations of sodium, calcium, and chloride (less than 19 mg/L) in samples from wells completed below sea level, north Lummi Island, Washington, fall 2002- spring 2003
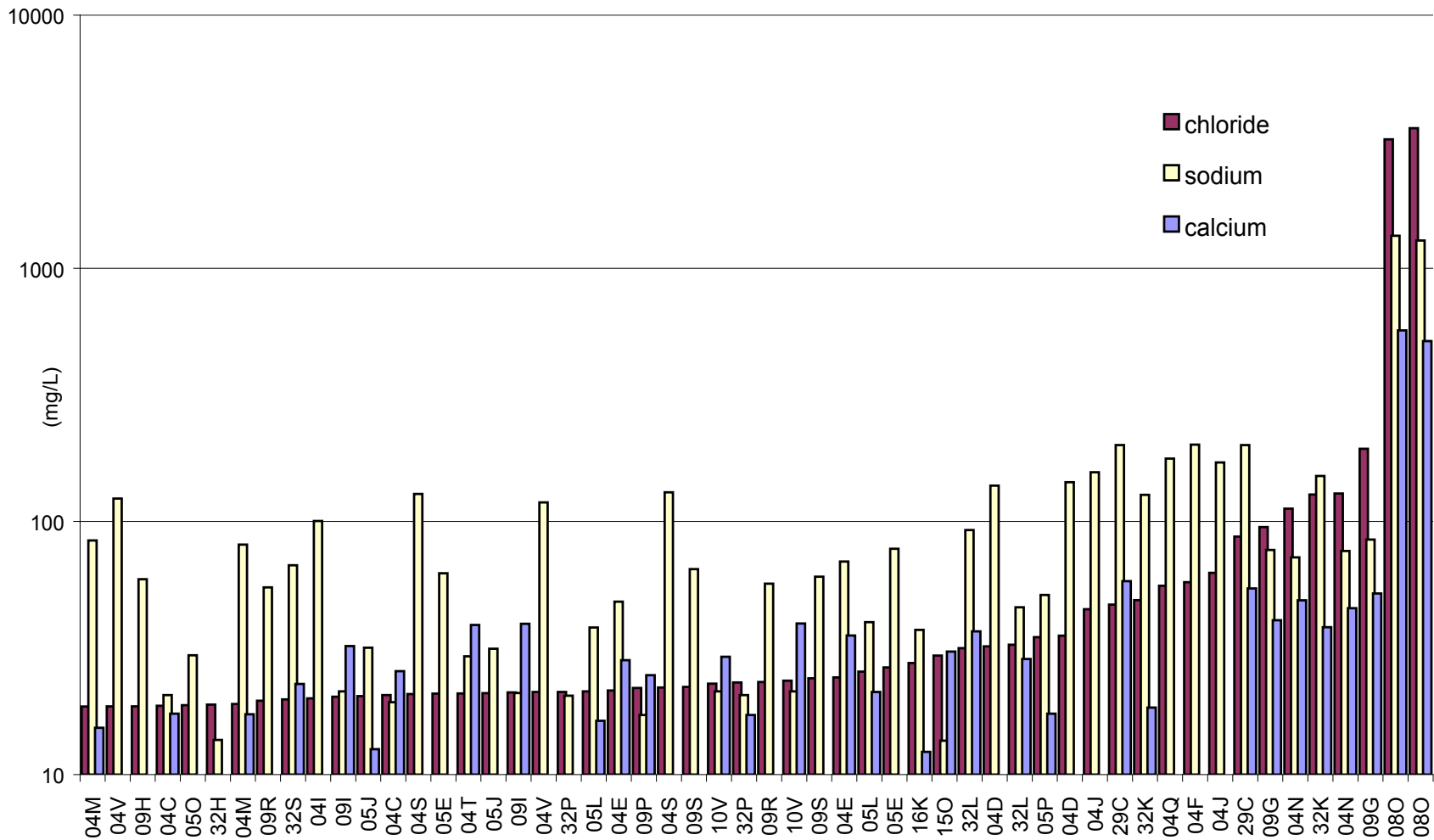
Figure 34b. Concentrations of sodium, calcium, and chloride (greater than 19 mg/L) in samples from wells completed below sea level, north Lummi Island, Washington, fall 2002- spring 2003

198
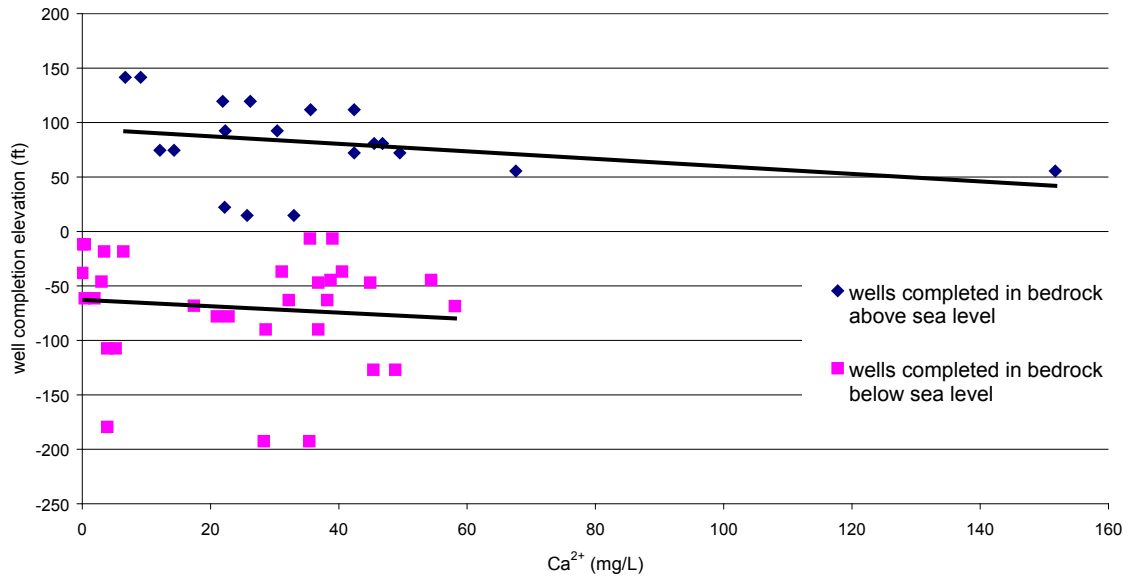
Figure 35a. Calcium concentrations and completion elevations for wells in bedrock, north Lummi Island, Washington, fall 2002- spring 2003
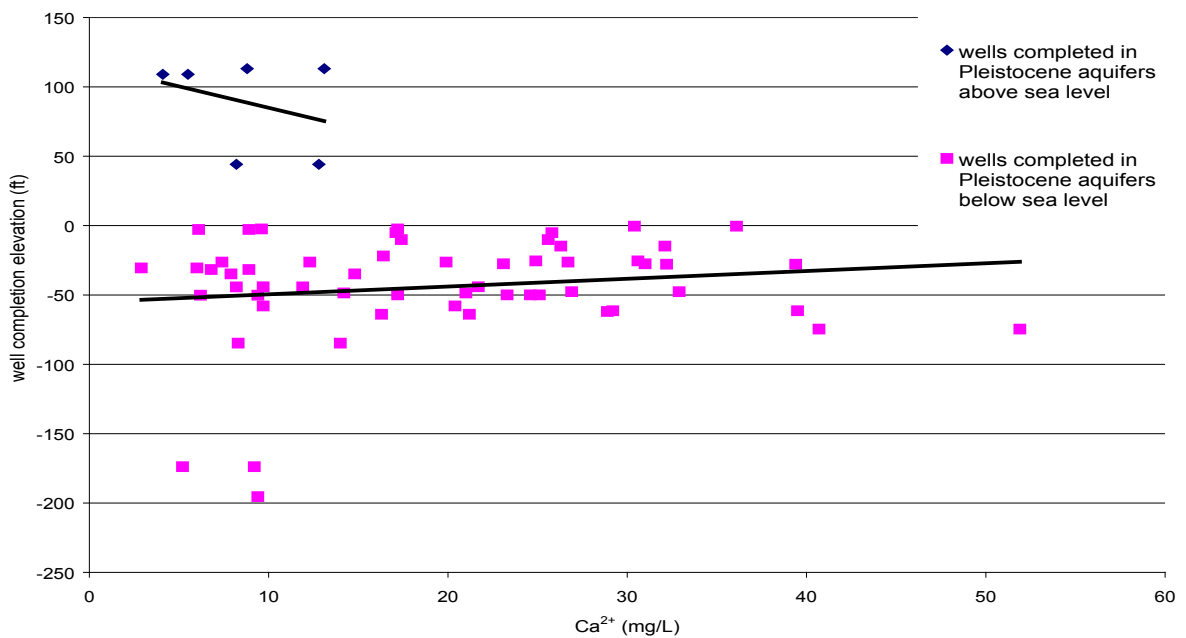
Figure 35b. Calcium concentrations and completion elevations for wells in Pleistocene aquifers, north Lummi Island, Washington, fall 2002- spring 2003
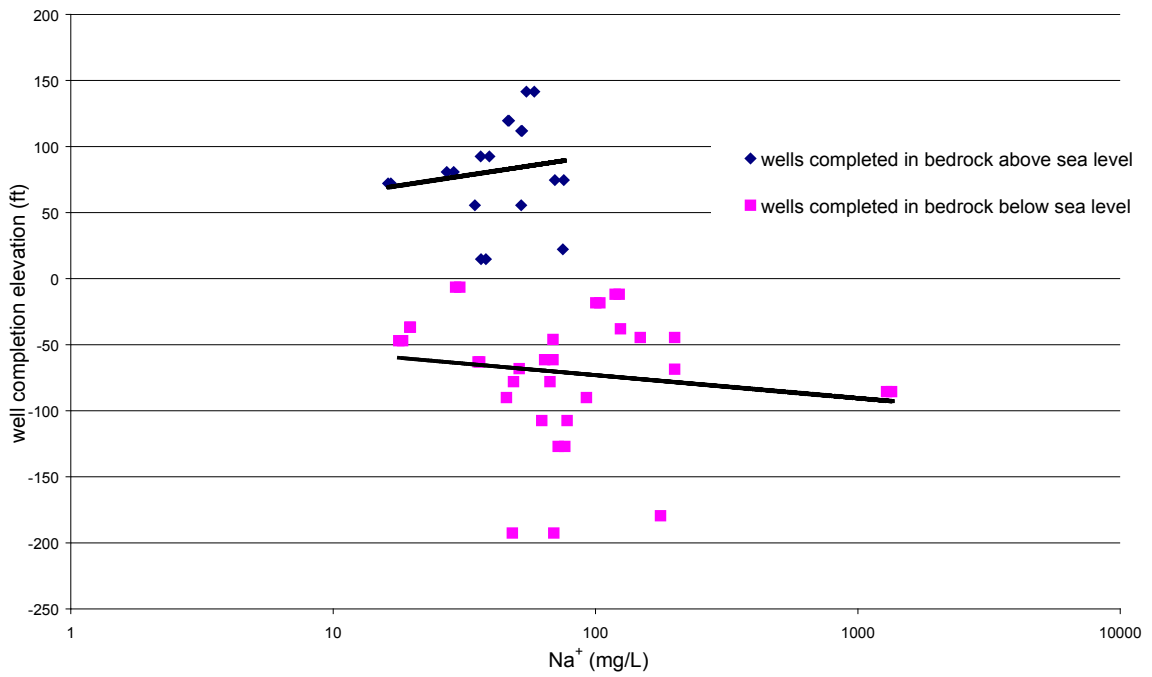
Figure 36a. Sodium concentrations and completion elevations for wells in bedrock, north Lummi Island, Washington, fall 2002- spring 2003
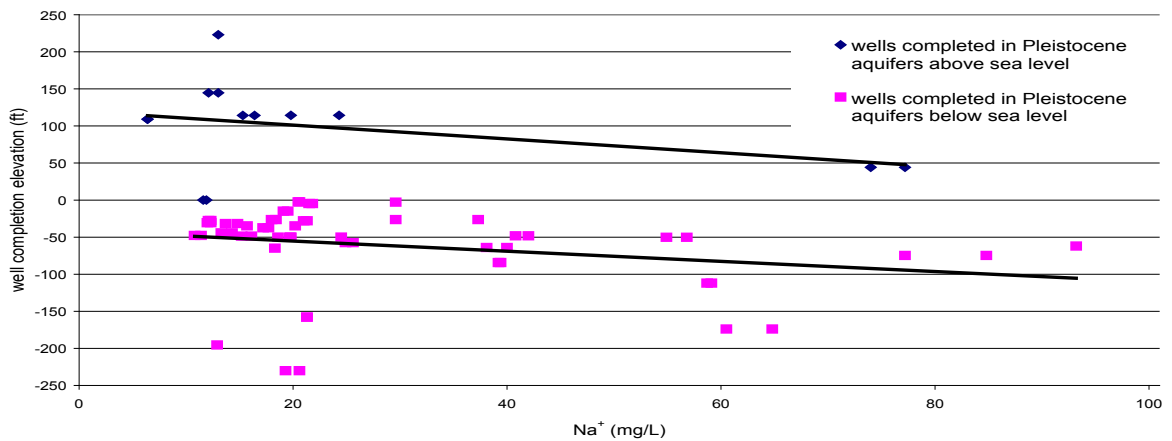
Figure 36b. Sodium concentrations and completion elevations for wells in Pleistocene aquifers, north Lummi Island, Washington, fall 2002- spring 2003

200
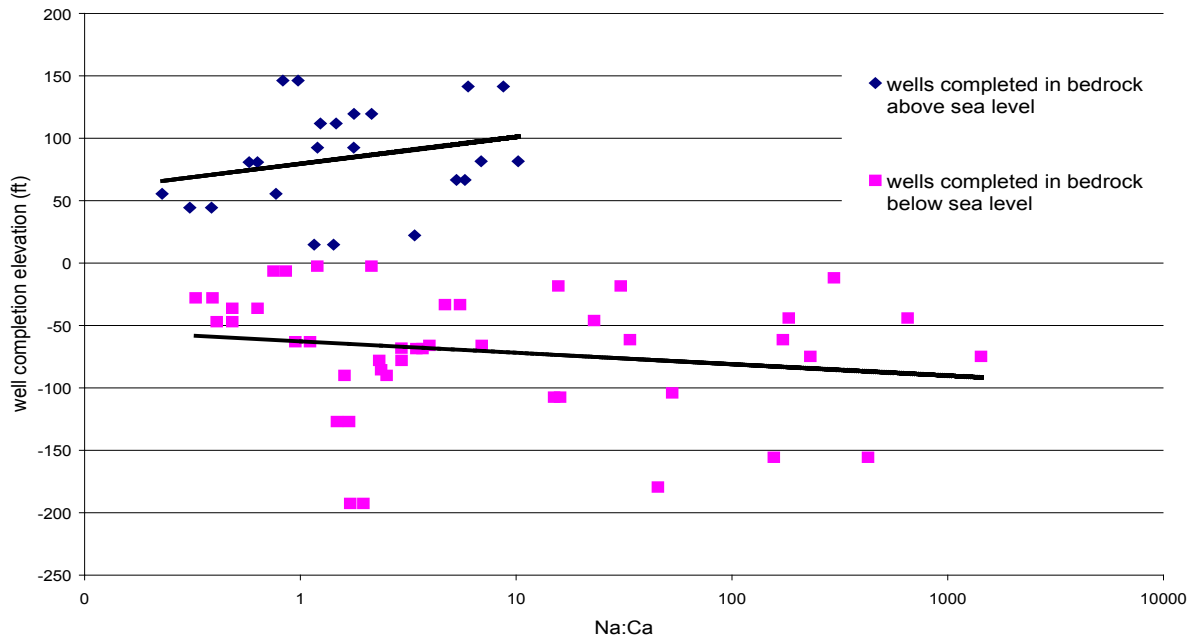
Figure 37a. Sodium to calcium ratios and completion elevations for wells in bedrock, north Lummi Island, Washington, fall 2002- spring 2003
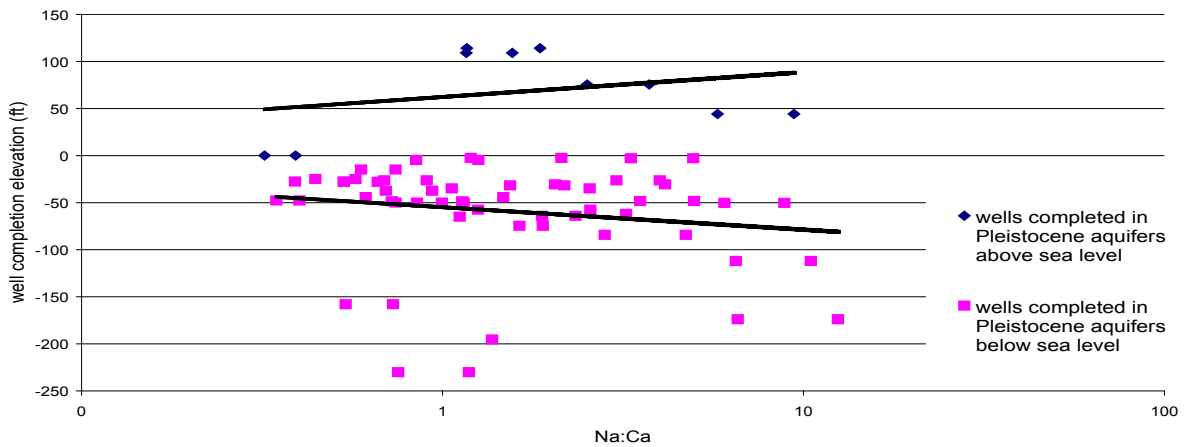
Figure 37b. Sodium to calcium ratios and completion elevations for wells in Pleistocene aquifers, north Lummi Island, Washington, fall 2002- spring 2003

201
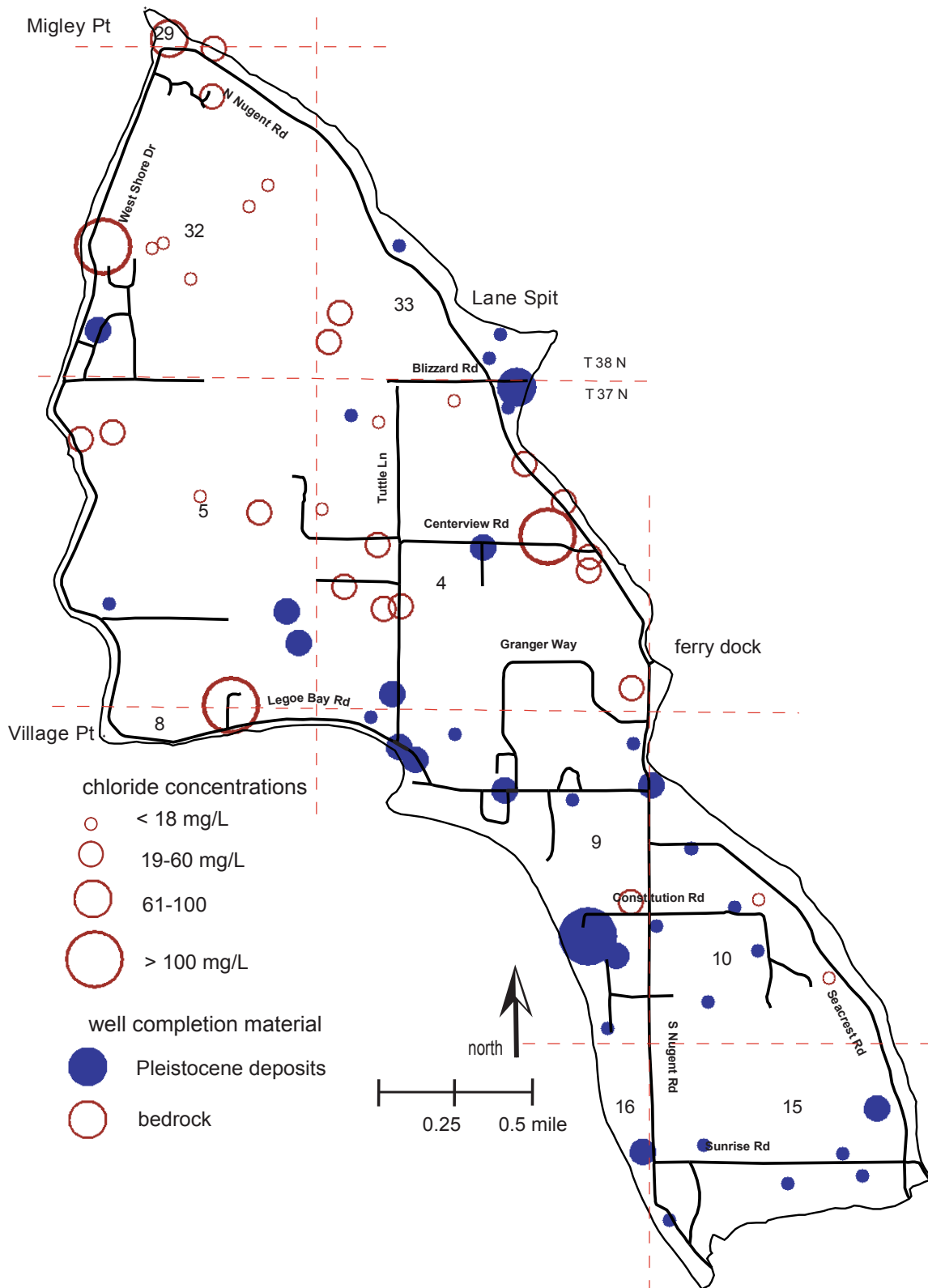
Figure 38a. Chloride concentrations, north Lummi Island, Washington, fall 2002
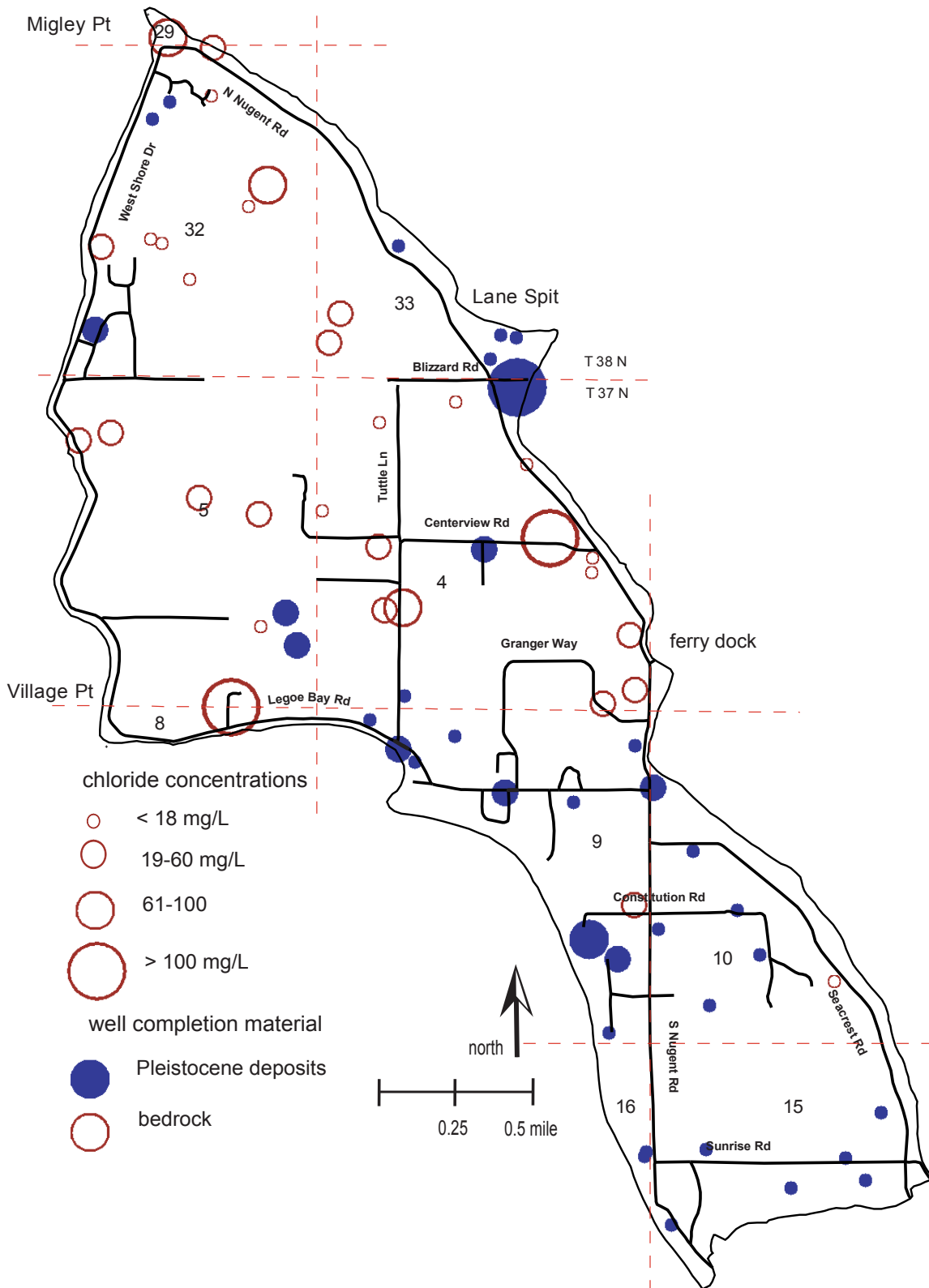
Figure 38b. Chloride concentrations, north Lummi
Island, Washington, spring 2003
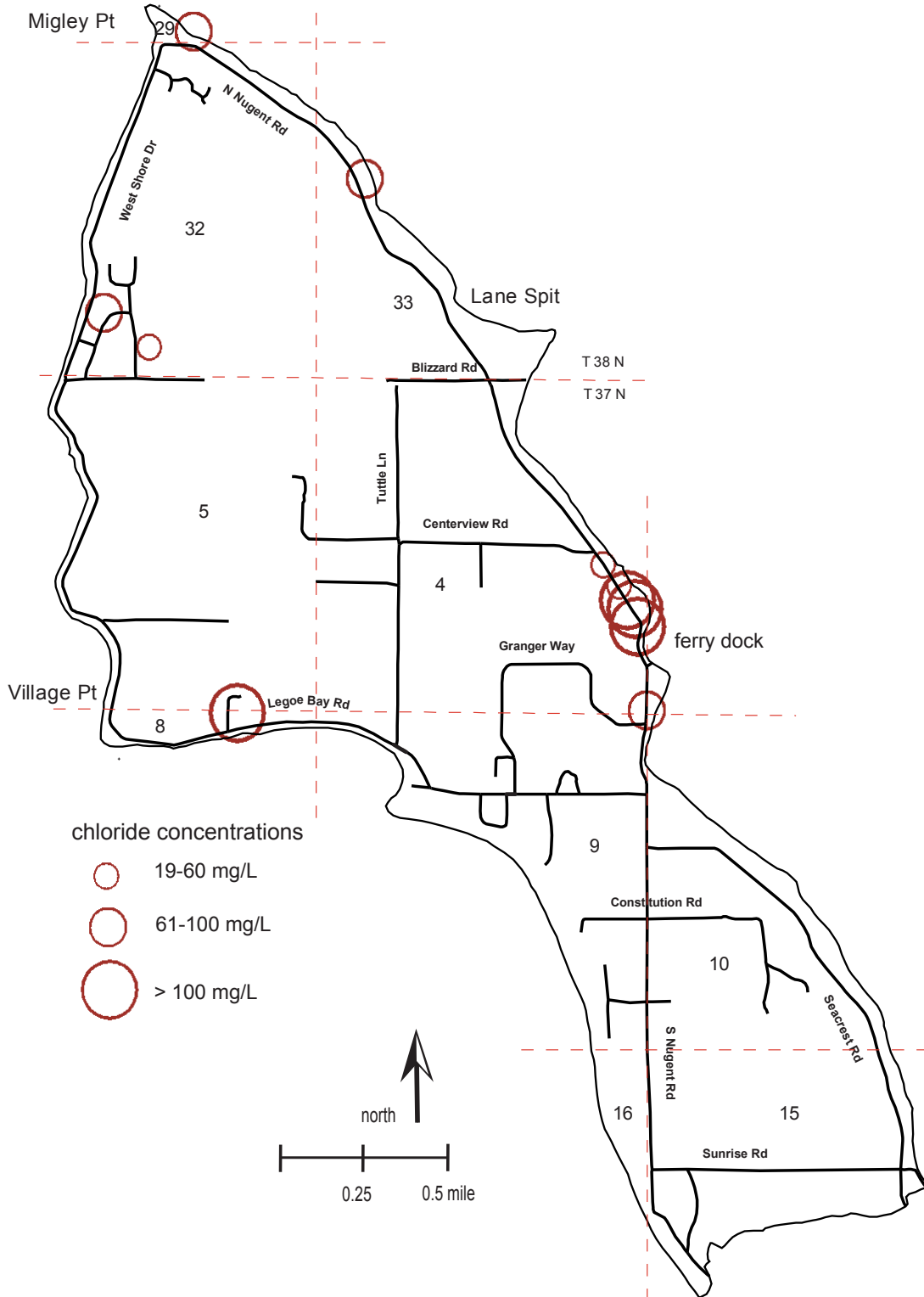
Figure 38c. Elevated chloride concentrations in 11 wells sampled during previous studies, north Lummi Island, Washington. Most of these wells are likely completed in bedrock (Sandstone Aquifer). Source: Schmidt (1978), Dion and Sumioka (1984), and Whatcom County (1994).
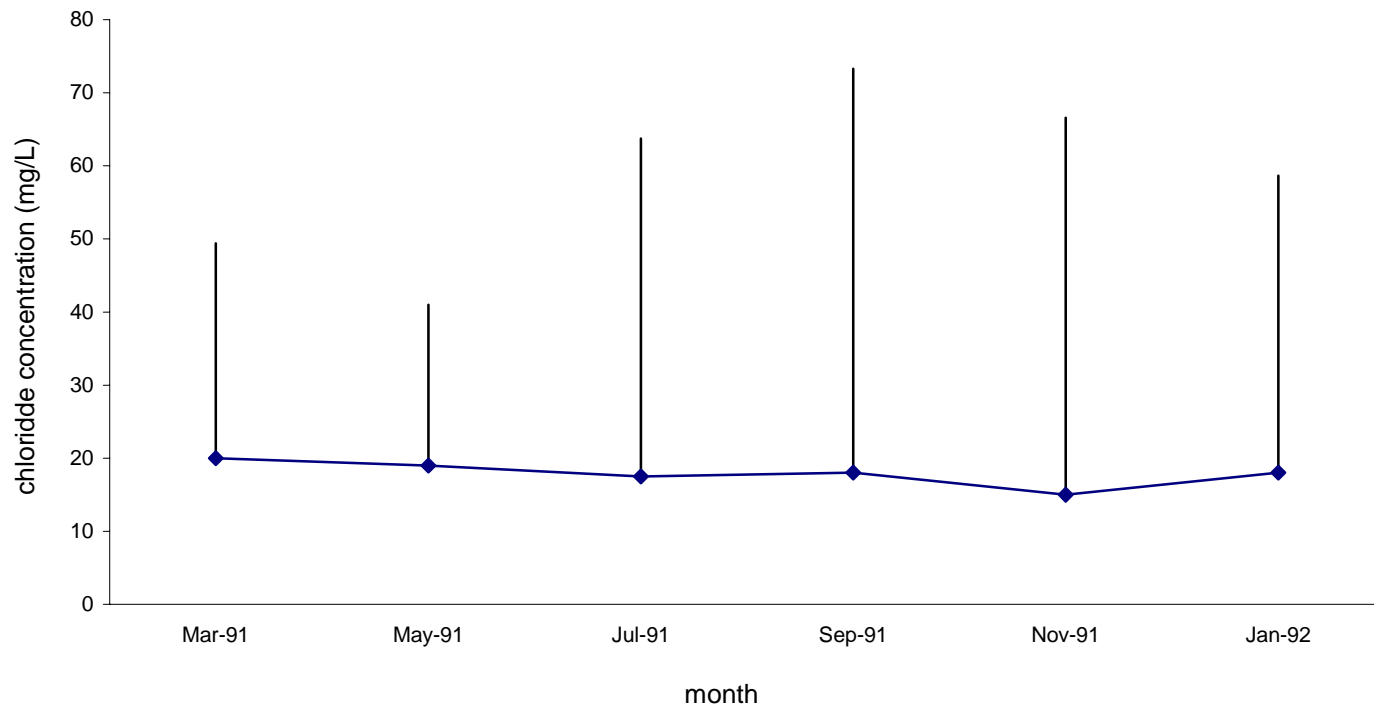
Figure 39. Bi-monthly median chloride and positive standard deviation for 15 wells sampled March, 1991-January, 1992, north Lummi Island, Washington. Source: Whatcom County (1994)
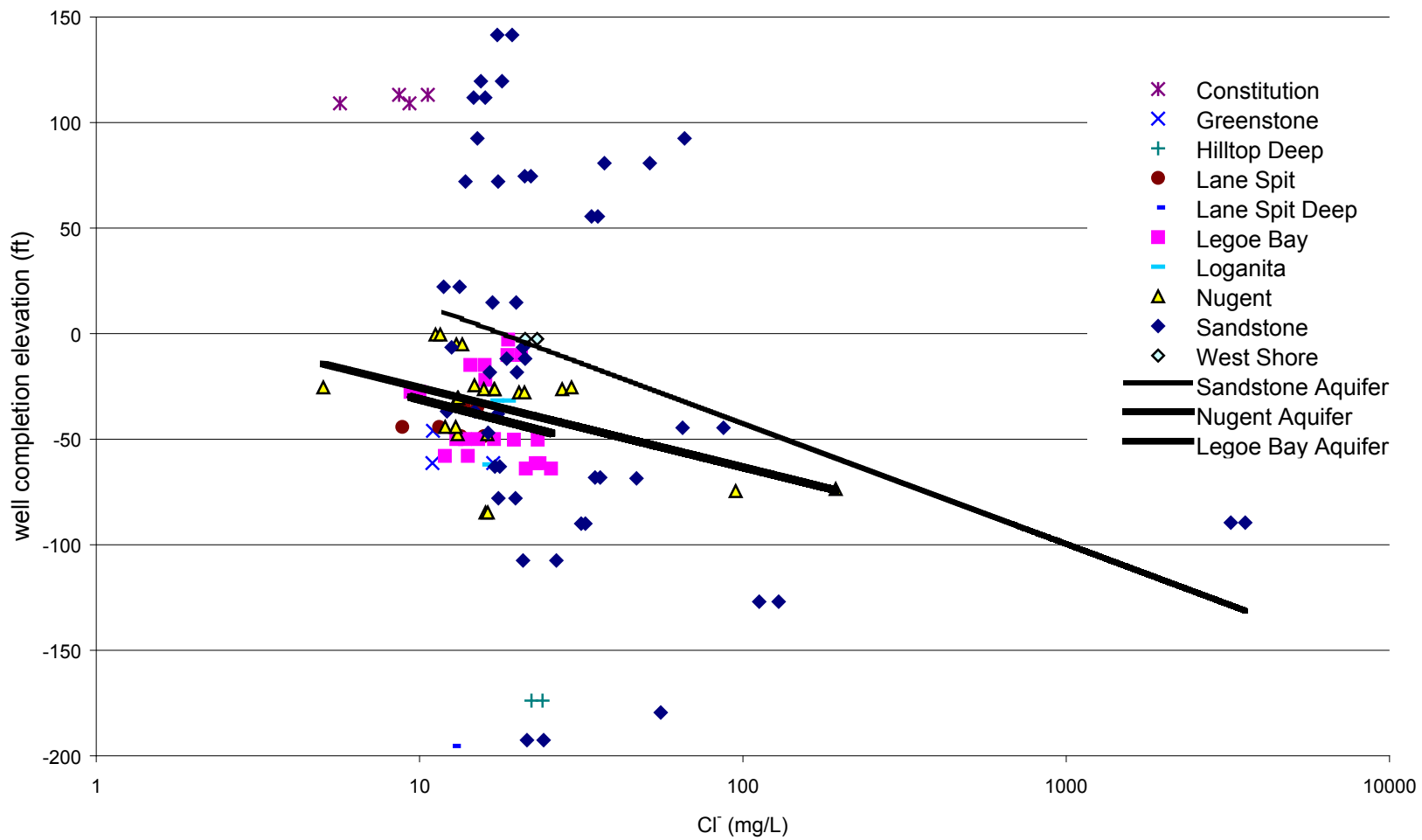
Figure 40. Chloride concentrations and completion elevations for drilled wells, north Lummi Island, Washington, fall 2002- spring 2003
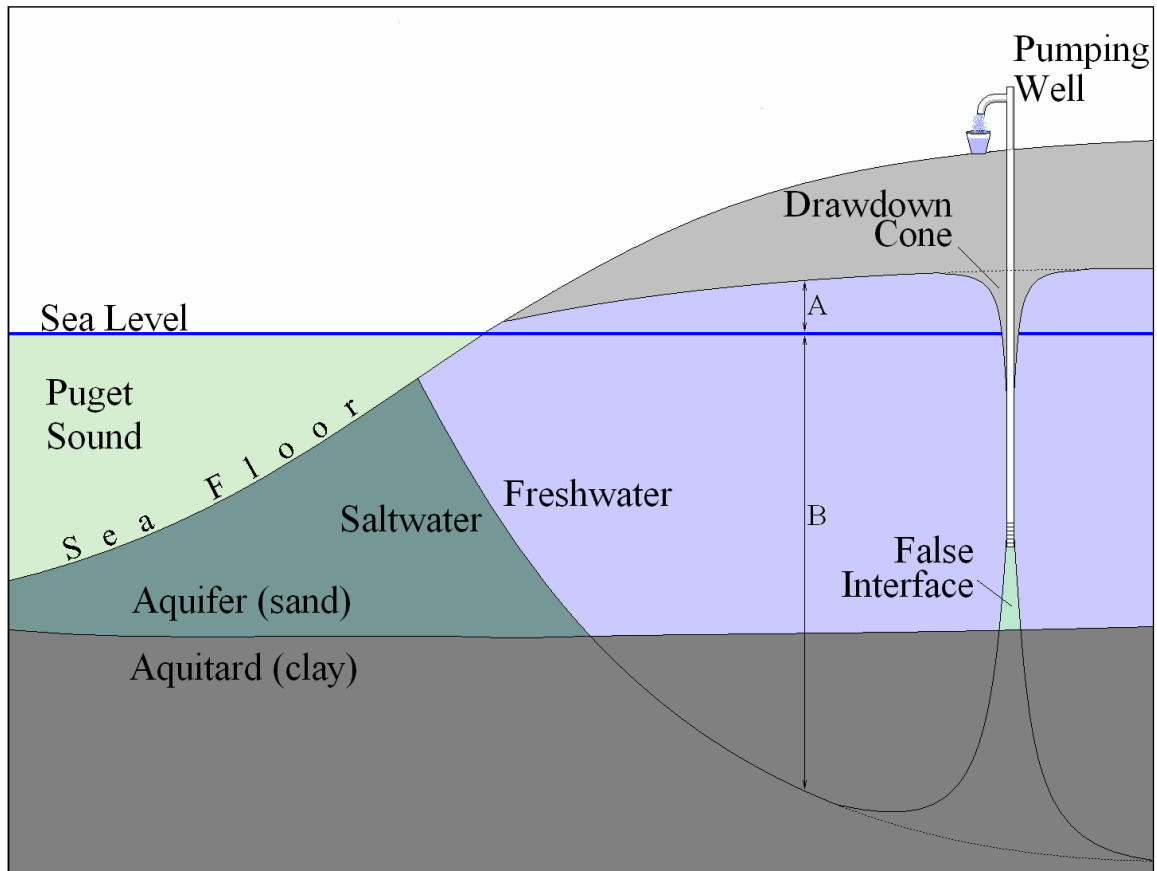
Figure 41. Pumping well drawdown causing the Gyben-Herzberg theoretical interface to reach the well screen. This is known as a false interface because the pumping well is not experiencing intrusion. Aquifer head between the well and the shoreline (A) depresses the interface (B) enough to prevent seawater from advancing inland. A decline in the magnitude of (A), that determines the protection factor this well has against intrusion, will allow the interface to rise to the bottom of the aquifer. Upon reaching this critical rise in interface depth, intrusion can occur over a short time interval. Figure and discussion are modified from Kelly (2005).
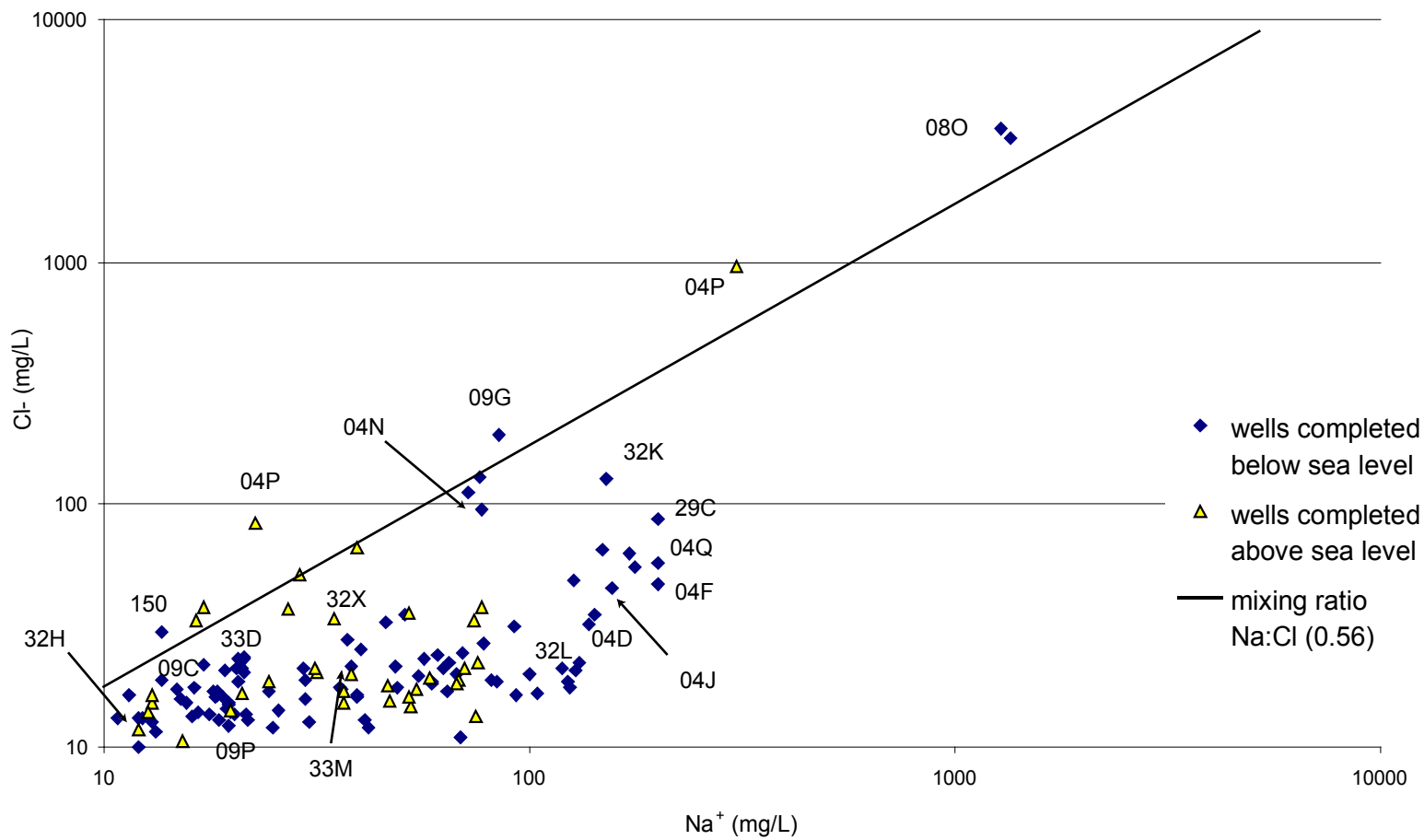
Figure 42. Sodium-chloride bivariate plot, north Lummi Island, Washington, fall 2002- spring 2003
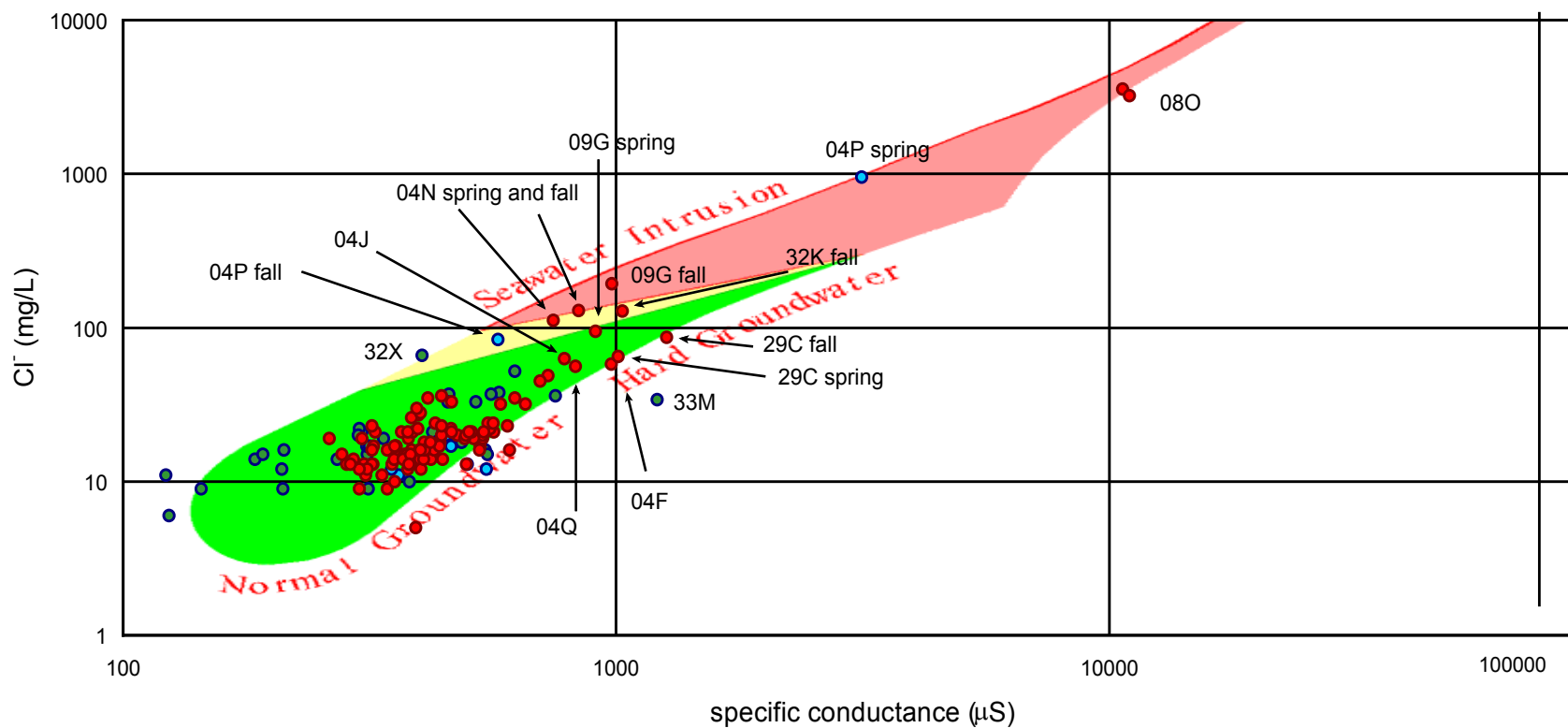
Figure 43. Chloride and specific conductance plot with freshwater, hard water, mixing, and intrusion fileds, north Lummi Island, Washington, fall 2002-spring 2003. Samples for selected wells are labeled. Red dots are wells completed below sea level, blue are near sea level, and green are above sea level. Figure modified from Van Denburgh et al. (1968)
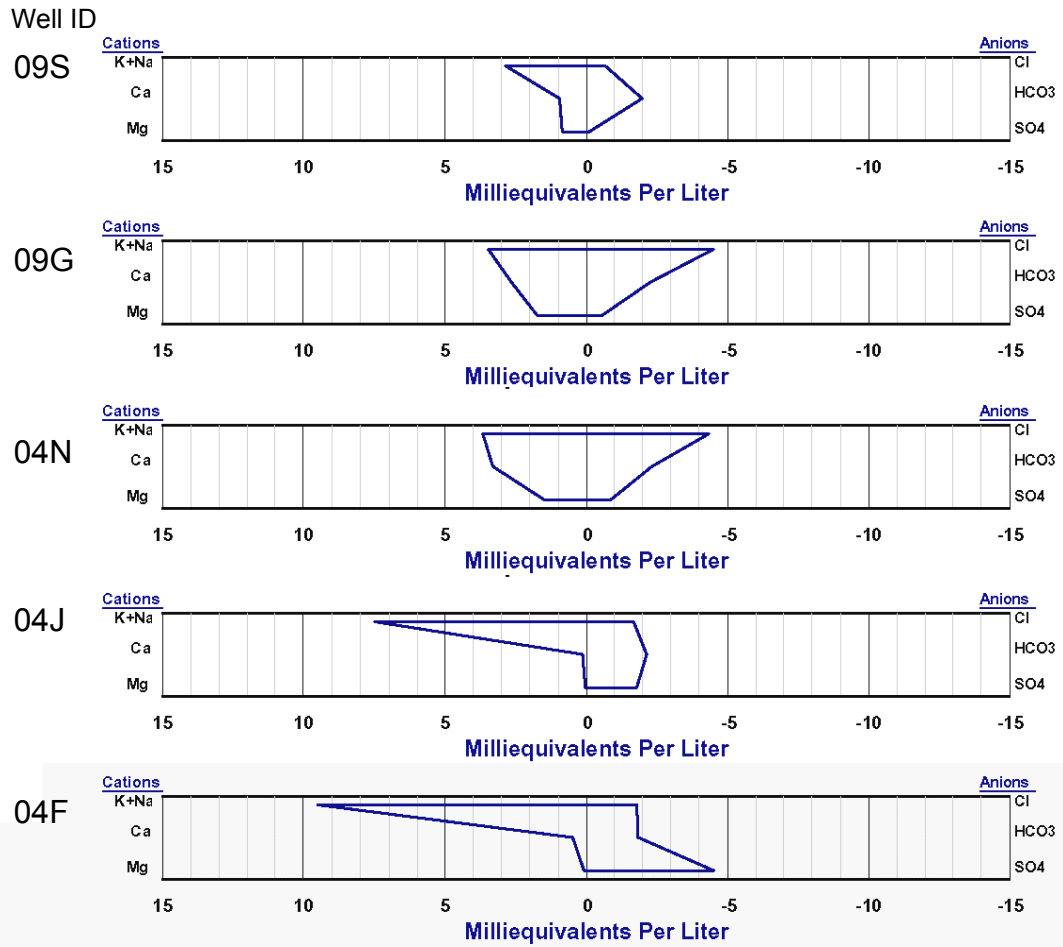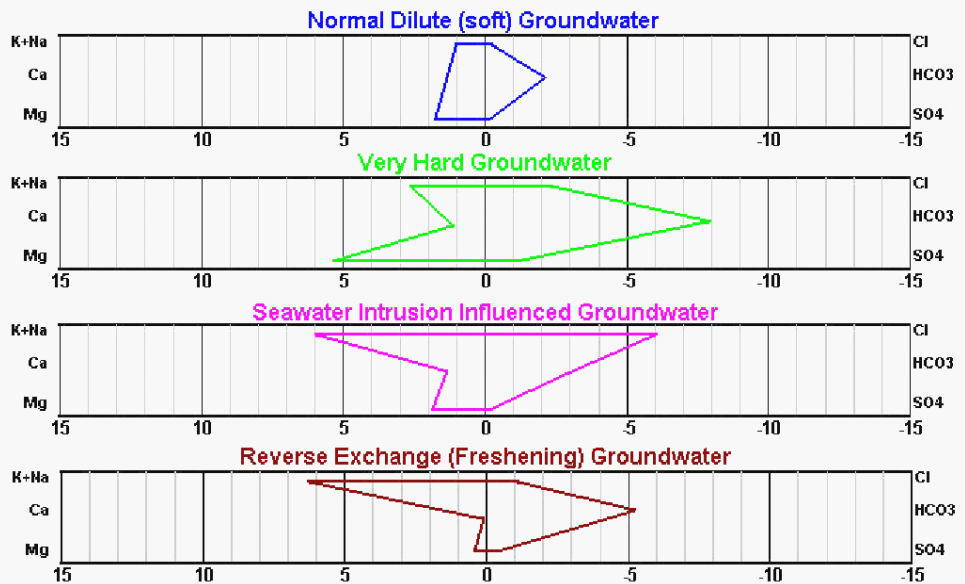
Figure 44. Stiff Diagrams for 5 wells, north Lummi Island, Washington, winter 2005

210
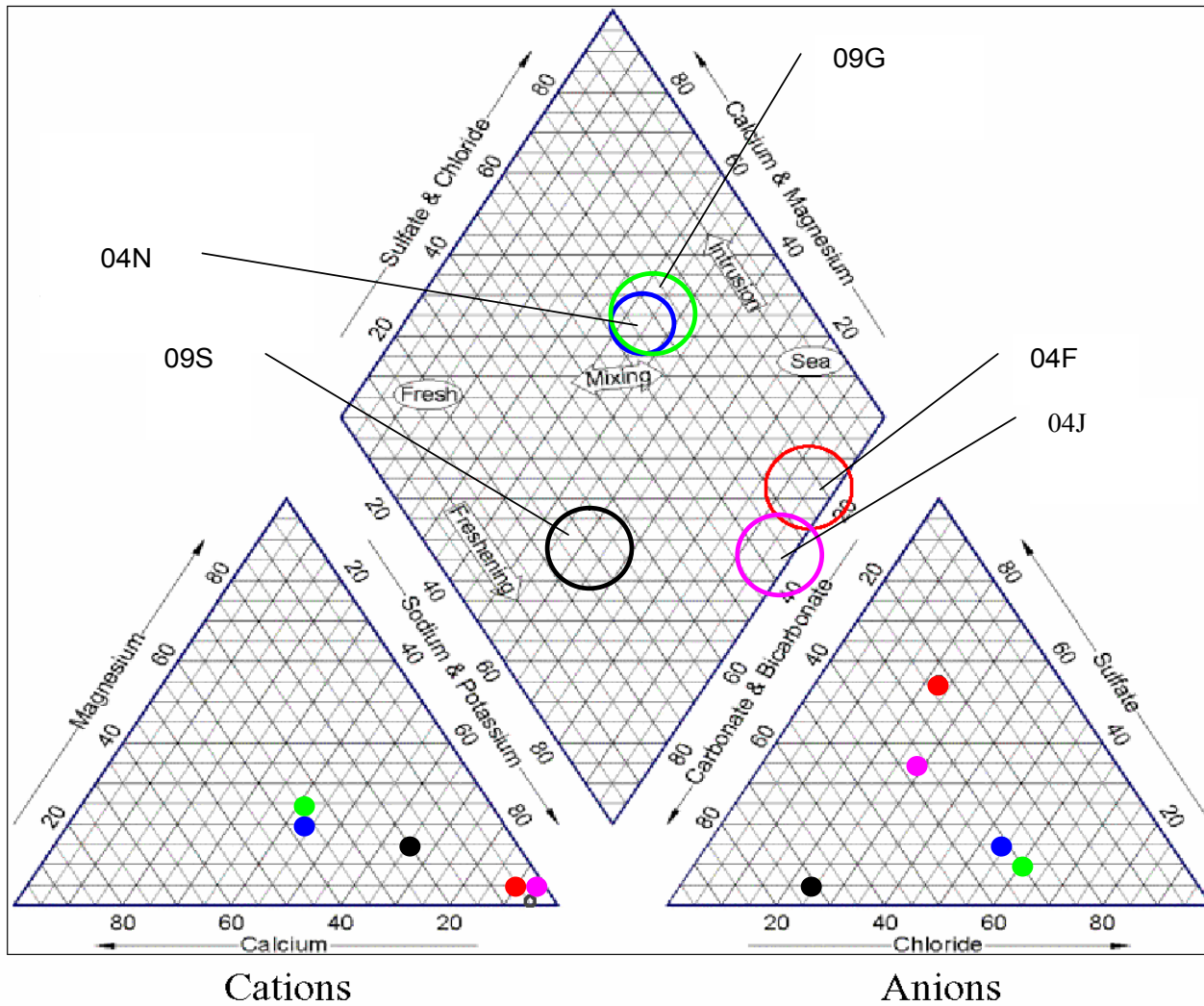
Figure 45. Piper Diagram for 5 wells, north Lummi Island, Washington, winter 2005

Table 1. Soil cover determined from Soil Conservation Service (Natural Resource Conservation Service);(1980) using GIS, north Lummi Island, Washington

soil name	Unified Soil Classification (USC) designation	average permeability in upper horizon (in/hr)	area (square miles)	percent of study area
Kickerville	ML	1.3	1.52	39.3
Winston	ML, MH	1.3	0.51	13.1
Everett	GM	1.0	0.50	13.0
Birch Bay	ML	1.3	0.22	5.7
Sehome	ML, SM	1.3	0.20	5.1
Nati	ML	1.3	0.18	4.7
Pickett	GM	1.3	0.13	3.3
Hale	ML	1.3	0.11	3.0
Neptune	GM	1.1	0.11	2.8
Labounty	ML	1.3	0.04	1.2
Cagey	-	-	0.04	1.1
Andic Xerochrepts	ML	1.0	0.04	1.0
Histosols	PT	1.3	0.03	0.7
Pangborn	PT	1.3	0.02	0.6
Skipopa	ML, MH	1.3	0.02	0.4
Whitehorn	-	-	0.19	4.9
water	-	-	0.01	0.2
total			**3.87**	**100.0**

Table 2. Land cover determined from Landsat 4, 1991-1993 using GIS, north Lummi Island, Washington

land cover class	area (square miles)	percent of study area
clear water	0.05	1.2
turbid/silted water	0.04	0.9
coniferous forest	0.17	4.5
mixed coniferous/deciduous forest	0.99	25.6
deciduous forest	1.02	26.4
scrub shrub vegetation	0.20	5.1
long grasses	0.26	6.6
medium grasses	0.84	21.6
short grasses	0.09	2.2
fallow fields/exposed soil	0.20	5.3
urban	0.02	0.5
rock	<0.01	<0.1
total	**3.87**	**100.0**

Table 3. Major constituents of seawater, north Lummi Island, Washington.

constituent		concentration (mg/L)	ratio of concentration to Cl^-
chloride	Cl^-	19,350	1.00
sodium	Na^+	10,760	0.56
sulfate	SO_4^{2-}	2,710	0.14
magnesium	Mg^{2+}	1,290	0.07
calcium	Ca^{2+}	410	0.02
potassium	K^+	390	0.02
bicarbonate	HCO_3^-	140	0.01

Source: Riley and Skirrow (1975)

Table 4. Washington State groundwater and drinking water standards for selected parameters

parameter	maximum contaminant level (MCL)	type contaminant
pH	6.5-8.5	secondary
specific conductance	700 μS*	physical characteristic
total dissolved solids (TDS)	500 mg/L	physical characteristic
sodium (Na+) *	unspecified	primary
chloride (Cl-)	250 mg/L	secondary
sulfate (SO_4^{2-})	250 mg/L	secondary

Primary contaminants can impose a public health hazard if MCL is exceeded. No MCL is specified for sodium, however US EPA has recommended 20 mg/L for people restricted to a low-sodium diet.

Secondary contaminants can degrade the aesthetic quality of water and create a nuissance if MCL is exceeded.

Sources: (WAC 173-200-040, 1991)
       *(WAC 246-290-310, 1988)

Table 5. Numbers and purpose of study wells, north Lummi Island, Washington

purpose of well	number of wells
total used in study	130
used in constructing the stratigraphic model	111
total monitored during field work	89
water level measured at least once	87
water level measured fall 2002 and spring 2003	77
water sample taken at least once	80
water sample taken fall 2002 and spring 2003	71
located using survey-grade GPS	86
located with DEM overaly and topographic map using GIS	42

214

Table 6. Characteristics of sand units and total volumes of Pleistocene deposits identified in the stratigraphic model, north Lummi Island, Washington

sand unit ID	area (square miles)	volume (yds^3)	minimum thickness (ft)	maximum thickness (ft)	average thickness (ft)	average top elevation (ft)	wells completed in sand unit?	well logs used to define
SU-1	0.13	3.07E+05	2	35	4	-187	Y	04B, 04C, 09D, 09S, 09T, 10A
SU-2	0.09	1.21E+06	4	39	14	-40	Y	09D, 09F, 09M, 10I, 10V, 10X
SU-3	0.30	4.15E+06	3	65	13	-28	Y	04B, 04C, 04G, 08Z, 09A, 09B, 09E, 09F, 09K, 09L, 09R, 09U, 09S
SU-4	0.15	8.14E+06	6	92	52	35	Y	09B, 09J, 09V, 10I, 10V
SU-5	0.25	5.19E+06	2	107	20	18	Y	04B, 05L, 05M, 05O, 08Z, 09A, 09K, 09L, 09R, 09Y
SU-6	0.38	1.46E+07	5	90	38	-39	Y	09G, 10M, 15A, 15D, 15X, 15Z, 16B
SU-7	0.42	5.58E+06	2	25	13	-11	Y	09I, 09Q, 09W, 10M, 15A, 15C, 15D, 15K, 15L, 15P, 15S, 16B, 16K, 16T, 16V
SU-8	0.15	6.07E+06	10	65	40	60	N	04Q, 09B, 09F, 09T, 09Y
SU-9	0.05	6.34E+05	2	7	5	120	Y	10C, 10E, 10K, 10X
SU-10	0.15	2.41E+06	2	27	15	88	N	04E, 04Q, 09B, 09D, 09F, 09J, 09T, 09Y, 10I
SU-11	0.08	2.04E+06	3	50	24	136	N	09I, 09G
SU-12	0.04	2.71E+05	2	11	6	104	N	09I, 09W
SU-13	0.16	3.53E+06	2	42	22	88	N	15A, 15C, 15K, 15L, 15P, 16K, 16T, 16V
SU-14	0.22	1.14E+06	2	8	5	25	N	04BB, 04G, 05L, 08Z, 09L, 15O, 15W
SU-15	0.05	2.24E+06	5	50	40	115	N	32B, 32H
SU-16	0.07	3.05E+06	10	67	41	99	N	05P
SU-17	0.03	1.19E+05	2	5	4	31	N	29C
SU-18	0.04	2.18E+05	2	7	6	19	N	29C
SU-19	0.04	3.91E+05	2	14	10	170	N	04H
SU-20	0.04	1.63E+05	2	3	4	112	N	04N, 04Y
SU-21	0.14	3.27E+06	2	25	22	133	Y	04H
SU-22	0.09	1.60E+06	2	45	17	59	Y	04Y
SU-23	0.01	1.80E+05	2	14	13	-181	Y	33F
SU-25	0.06	1.01E+06	4	20	17	35	N	33F, 33G, 33J
SU-24	0.05	6.25E+05	5	18	12	-61	Y	33F, 33G, 33J, 33T
SU-26	0.01	5.99E+05	15	75	39	20	Y	04A
SU-27	0.03	7.17E+05	2	76	21	12	Y	32P
SU-28	0.03	7.13E+05	3	32	21	-21	Y	32H, 32R
SU-29	0.02	5.01E+05	2	22	20	25	N	32H

Total Volume of Pleistocene Deposits

material	volume (yds^3)
all sand units	6.94E+07
all silt-clay diamicton	2.96E+08
all Pleistocene deposits	3.65E+08

Table 7a. Published values for porosity and effective porosity of geologic material, north Lummi Island, Washington

material	porosity I*	porosity II*	effective porosity I	effective porosity II	average of effective porosity I and II
clay	0.50	0.42	0.20	0.06	0.13
silt	-	0.45	-	0.20	0.20
fine sand	-	0.43	-	0.33	0.33
medium sand	0.25	-	0.22	0.32	0.27
coarse sand	-	0.39	-	0.30	0.30
medium gravel	0.20	-	0.19	0.24	0.22
sandstone (medium)	0.11	0.34	0.06	0.27	0.17
siltstone	-	0.35	-	0.12	0.12
basalt	0.11	0.17	-	-	-

*Porosities for bedrock are combined primary/secondary porosity

Source: I = Heath (1983)
         II = McWorter and Sunada (1977)

Table 7b. Effective porosities assigned to geologic material using average of published values in Table 7a, north Lummi Island, Washington

geologic material	assigned effective porosity
fine sand	0.33
medium sand	0.27
coarse sand	0.30
sand + gravel	0.26
medium gravel	0.22
sandstone	0.17
greenstone	0.17
silt-clay diamicton*	0.50

* Porosities of silt range from 0.35-0.50 (Freeze and Cherry, 1979). Upper limit used to account for clay occurring in silt-clay diamicton

Table 7c. Textures and effective porosities assigned to modeled sand units using values from Tables 7a and 7b, north Lummi Island, Washington. Textures are intepreted from well log data.

sand unit ID	primary texture	secondary texture	assigned effective porosity
SU-1	clean fine sand	sand + gravel	0.33
SU-2	med sand, gravel	sand + gravel, clay	0.27
SU-3	sand + gravel	med sand, gravel, fine sand	0.26
SU-4	coarse sand	sand +gravel, gravel	0.30
SU-5	sand + gravel	gravel	0.26
SU-6	fine-coarse sand + gravel	fine sand, gravel, coarse sand	0.26
SU-7	sand + gravel	fine sand, coarse sand, gravel	0.26
SU-8	sand + gravel	-	0.26
SU-9	gravel	sand, fine sand, clay	0.22
SU-10	sand + gravel	gravel	0.26
SU-11	sand + gravel	clay	0.26
SU-12	sand + gravel	clay	0.26
SU-13	sand + gravel	clay	0.26
SU-14	sand + gravel	sand	0.26
SU-15	sand + gravel	-	0.26
SU-16	sand	-	0.27
SU-17	sand + gravel	-	0.26
SU-18	sand + gravel	-	0.26
SU-19	sand	silt	0.27
SU-20	sand + gravel	-	0.26
SU-21	sand + gravel	-	0.26
SU-22	coarse sand	sand + gravel	0.30
SU-23	sand + gravel	clay	0.26
SU-24	fine sand	sand + gravel, clay	0.33
SU-25	gravel	sand	0.22
SU-26	sand	-	0.27
SU-27	fine sand	coarse sand	0.30
SU-28	sand + gravel	gravel	0.26
SU-29	sand + gravel	-	0.26

Table 8. Possible correlations of modeled sand units to units in published geologic studies, north Lummi Island, Washington

sand unit ID	geologic unit match (Interpretation A)	other possible geologic unit match	underlain by	overlain by
SU-1	Cherry Pt silt interbed	other pre-vashon deposits	Cherry Pt silt	Cherry Pt silt
SU-2	Vashon advance outwash	Cherry Pt silt interbed	Cherry Pt.silt	glaciomarine drift and till
SU-3	Vashon advance outwash		Cherry Pt silt	glaciomarine drift and till
SU-4	Vashon advance outwash	Cherry Pt silt interbed	Cherry Pt silt	glaciomarine drift and till
SU-5	Vashon advance outwash	emergence and newer deposits	Cherry Pt silt	glaciomarine drift and till
SU-6	Vashon advance outwash	Cherry Pt silt interbed	Cherry Pt silt	glaciomarine drift and till
SU-7	Vashon advance outwash	Cherry Pt silt interbed	Cherry Pt silt	glaciomarine drift and till
SU-8	Vashon advance outwash		Cherry Pt silt	glaciomarine drift and till
SU-9	glaciomarine drift interbed	Vashon advance outwash	glaciomarine drift and till	glaciomarine drift and till
SU-10	emergence beach deposits	glaciomarine drift interbed	glaciomarine drift and till	none
SU-11	emergence beach deposits		glaciomarine drift and till	none
SU-12	emergence beach deposits	glaciomarine drift interbed	glaciomarine drift and till	none
SU-13	emergence beach deposits		glaciomarine drift and till	none
SU-14	emergence beach deposits	newer beach deposits	glaciomarine drift and till	none
SU-16	Vashon advance outwash		Cherry Pt silt	glaciomarine drift and till
SU-15	emergence beach deposits	glaciomarine drift interbed	glaciomarine drift and till	none
SU-17	emergence beach deposits		glaciomarine drift and till	none
SU-18	glaciomarine drift interbed		sandstone	glaciomarine drift and till
SU-19	emergence beach deposits		glaciomarine drift and till	none
SU-20	emergence beach deposits		glaciomarine drift and till	none
SU-21	glaciomarine drift interbed		glaciomarine drift and till	glaciomarine drift and till
SU-22	Vashon advance outwash	other pre-vashon deposits	sandstone	glaciomarine drift and till
SU-23	Vashon advance outwash	Cherry Pt silt interbed	older fines	Cherry Pt silt
SU-24	Vashon advance outwash		Cherry Pt silt	glaciomarine drift and till
SU-25	emergence beach deposits		glaciomarine drift and till	none
SU-26	Vashon advance outwash	emergence and newer deposits	sandstone and Cherry Pt silt	none
SU-27	Vashon advance outwash	Cherry Pt silt interbed	sandstone	glaciomarine drift and till
SU-28	Vashon advance outwash	Cherry Pt silt interbed	Cherry Pt silt or older fine	glaciomarine drift and till
SU-29	Vashon advance outwash	Cherry Pt silt interbed	Cherry Pt silt or older fine	glaciomarine drift and till

218

Table 9. Well completion elevations, north Lummi Island, Washington. Completion elevations represent the bottom of the screened/open interval. The screened interval lies above the bottom of some wells. Dug wells are not included.

aquifer	minimum (ft)	maximum (ft)	median (ft)	average (ft)	number of wells
all wells	-289	146	-37	-41	121
all wells below sea level	-289	-2	-50	-72	94
all in Pleistocene deposits	-228	113	-43	-47	61
all in bedrock	-289	146	-31	-35	60
Blizzard	-	-	-	108	1
Centerview	-	-	-	44	1
Constitution	109	113	-	111	2
Greenstone	-89	52	-18	-24	10
Hilltop Deep	-228	-171	-174	-188	5
Lane Spit	-66	-35	-46	-48	4
Lane Spit Deep	-	-	-	-196	1
Legoe Bay	-102	42	-50	-38	19
Loganita	-32	-62	-	-47	2
Nugent	-118	0	-28	-41	21
Sandstone	-289	141	-21	-27	38
Village Pt	-	-	-	-84	1
West Shore	-	-	-	-2	1

Table 10. Well length (total depth), north Lummi Island, Washington

aquifer	minimum (ft)	maximum (ft)	median (ft)	average (ft)	number of wells
all wells	7	360	122	143	127
all in Pleistocene deposits	7	295	111	120	67
all in bedrock	45	360	156	170	60
dug wells	7	14	11	11	6
Blizzard	-	-	-	77	1
Centerview	-	-	-	75	1
Constitution	54	62	-	48	2
Greenstone	95	300	170	180	13
Hilltop Deep	205	295	251	250	5
Lane Spit	48	82	67	66	4
Lane Spit Deep	-	-	-	209	1
Legoe Bay	63	250	108	118	20
Loganita	109	130	-	120	2
Nugent	85	207	126	136	20
Sandstone	45	360	150	168	46
Village Pt	84	121	-	101	3
West Shore	-	-	-	92	1

Table 11. Length of screened/open interval in wells, north Lummi Island, Washington.
Values of zero represent casings that are open at the bottom of the well. Dug wells and
wells with no screened/open interval data are not included

aquifer	minimum (ft)	maximum (ft)	median (ft)	average (ft)	number of wells
all wells	0	250	6	49	106
all in Pleistocene deposits	0	20	5	5	57
all in bedrock	0	350	92	102	49
Sandstone	5	350	95	107	38
Greenstone	0	210	80	88	11

Table 12. Characteristics of modeled aquifers, north Lummi Island, Washington

Aquifer name	Sandstone
area (miles^2)	2.16
total volume (yds^3)	8.10E+08
est. avg. thickness (ft)	363
confined	Y most places below 150-200 ft elevation where overlain by silt-clay diamicton
est. avg. saturated thickness (ft)	312
est. avg. unsaturated thickness (ft)	50-80 ft thickest on Hill 362
saturated volume (yds^3)	7.75E+08
unsaturated volume (yds^3)	3.50E+07
saturated volume below sea level	83%
primary recharge	upland region in the center of the aquifer, at elevations above about 150 ft
secondary recharge	upland regions in the southwest and southeast, at elevations above 50-100 ft
primary discharge	offshore to Rosario Strait and Hale Passage
secondary discharge	to sand units in contact with bedrock at depth, especially along the southern boundary of the aquifer
wells screened in aquifer	04E, 04I, 04K, 04L, 04N, 04Q, 04U, 04V, 04W, 04X, 04Z, 04AA, 04BB, 05B, 05C, 05E, 05H, 05P, 05Q, 05T, 05W, 08O, 29C, 32A, 32B, 32G, 32L, 32M, 32N, 32Q, 32S, 32T, 32X, 33A, 33D, 33M 33N
geologic unit correlation	Chuckanut Formation may include Fidalgo ophiolite rocks folded into sandstone at depth
notes	areal extent encloses all wells known to be completed in sandstone; modeled to elevation of -261 ft, the deepest well in sandstone that penetrates into greenstone

Aquifer name	Greenstone
area (miles^2)	0.41
total volume (yds^3)	1.63E+08
est. avg. thickness (ft)	300 ft
confined	Y below approximately 200 ft elevation where overlain by Pleistocene deposits
est. avg. saturated thickness (ft)	250 ft
est.avg. unsaturated thickness (ft)	50 ft
saturated volume (yds^3)	1.56E+08
unsaturated volume (yds^3)	7.11E+06
saturated volume below sea level	79%

primary recharge	above 150 ft contour on Hill 275
secondary recharge	
primary discharge	offshore to Hale Passage to east; glacial drift to north, west, and south including bedrock troughs in middle and southern portion of study area
secondary discharge	to sand units of Nugent Aquifer to north, east, and south; to sand unit of overlying Constitution Aquifer
wells screened in aquifer	10B, 10C, 10G, 10K, 10J, 10P, 10R, 10Y, 10Z, 15H, 15R, 15U, 15O
geologic unit correlation	Fidalgo ophiolite
notes	15O penetrates a few feet into bedrock, screened above bedrock in Pleistocene deposits likely Nugent Aquifer

Aquifer name	Legoe Bay
composite of sand units	SU-2, SU-3, SU-5
area (miles^2)	0.40
total volume (yds^3)	1.05E+07
est. avg. thickness (ft)	15
confined	Y except upper regions of SU-5 in vicinity of 04B, 05L, 05M, 05O, 09Y, 09B
est. avg. saturated thickness (ft)	11
est.avg. unsaturated thickness (ft)	14 range 2-65 ft thickest at 05O
saturated volume (yds^3)	4.47E+06
unsaturated volume (yds^3)	6.11E+06
saturated volume below sea level	53%
primary recharge	through coarse lenses of glacial drift that extend to the surface in the upper and inland regions of the aquifer and where the aquifer abuts the Sandstone Aquifer near wells 04AA, 04Q, and 09F
secondary recharge	through silt-clay diamicton of overlying glaciomarine drift at nearly all places
primary discharge	offshore at Legoe Bay
secondary discharge	to sea at Hale Passage in middle of study area; upper lens (SU-5) intersects land surface and likely discharges to wetlands west of Tuttle Ln, in vicinity of Legoe Bay Lagoon
wells screened in aquifer	04C, 04G, 04O, 04BB, 05L, 05M, 08Z, 09A, 09B, 09E, 09F, 09K, 09L, 09M, 09R, 09U, 10I, 10V, 10X
geologic unit correlation (Interp A)	Vashon advance outwash; upper portion likely emergence beach deposits west of Tuttle Ln
geologic unit correlation (Interp B)	marine outwash
notes	SU-2 and SU-3 converge upslope in vicinity of 09F; SU-3 and SU-5 converge upslope in vicinity of 09A, 09I, 09Y; possibly connected to Nugent Aquifer along southeastern edge

222

Aquifer name	Nugent
composite of sand units	SU-4, SU-6, SU-7
area (miles^2)	0.6
total volume (yds^3)	2.84E+07
est. avg. thickness (ft)	34
confined	Y except upper regions of SU-4 in vicinity of 09V and SU-6, SU-7 in vicinity of 15A
est. avg. saturated thickness (ft)	39
est.avg. unsaturated thickness (ft)	6 range 2-55 ft thickest at 09V
saturated volume (yds^3)	2.44E+07
unsaturated volume (yds^3)	3.98E+06
saturated volume below sea level	91%
primary recharge	from overlying emergence deposits (SU-4, SU-10) that are in contact with unsaturated regions of the aquifer between wells 09B and 09V, from emergence deposits along southern and eastern slopes of Hill 275 (SU-, and where the aquifer abuts the Greenstone Aquifer along its eastern margin
secondary recharge	through overlying silt-clay diamicton in most areas, especially where topography is flat east of S Nugent Rd
primary discharge	offshore to Rosario Strait in vicinity of 16V in the south, and in vicinity of 09G in the north
secondary discharge	offshore to Hale Passage in vicinity of 10I in the north
wells screened in aquifer	09C, 09G, 09I, 09J, 09Q, 09V, 09W, 10M, 15A, 15C, 15D, 15K, 15L, 15P, 15S, 15X, 15Z, 16B, 16K, 16T, 16V
geologic unit correlation (Interp A)	Vashon advance outwash
geologic unit correlation (Interp B)	marine outwash
notes	sand units SU-6/SU-7 and SU-6/SU-4 converge upslope; possibly connected to Legoe Bay Aquifer in vicinity of 09B, 09J, 10I, 10V in the north; may also include well 15O

Aquifer name	Blizzard
composite of sand units	SU-21
area (miles^2)	0.14
total volume (yds^3)	3.27E+06
est. avg. thickness (ft)	22
confined	N
est. avg. saturated thickness (ft)	17
est.avg. unsaturated thickness (ft)	5

saturated volume (yds^3)	2.50E+06
unsaturated volume (yds^3)	7.68E+05
saturated volume below sea level	0%
primary recharge	from overlying glaciomarine drift
secondary recharge	from sandstone to north and west of 04H
primary discharge	unclear; possibly to unidentified coarse unit at depth; some discharge likely to wetland and drainage to south and southwest of 04H
wells screened in aquifer	04H
geologic unit correlation (Interp A)	coarse interbed within glaciomarine drift
geologic unit correlation (Interp B)	marine outwash
notes	lateral extent of aquifer estimated based on contact with bedrock to north and west, topography, and absence of aquifer in adjacent well logs

Aquifer name	Centerview
composite of sand units	SU-22
area (miles^2)	0.09
total volume (yds^3)	1.60E+06
est. avg. thickness (ft)	17
confined	Y
est. avg. saturated thickness (ft)	17
est.avg. unsaturated thickness (ft)	0
saturated volume (yds^3)	1.60E+06
unsaturated volume (yds^3)	0
saturated volume below sea level	0%
primary recharge	sandstone to the north and west
secondary recharge	from overlying glaical drift
primary discharge	sandstone on eastern side and bottom
secondary discharge	
wells screened in aquifer	04Y
geologic unit correlation (Interp A)	Vashon advance outwash
geologic unit correlation (Interp B)	Vashon advance outwash or marine outwash
notes	groundwater gradient not defined due to limited water level data; possible that groundwater passes through aquifer as part of larger Sandstone Aquifer

224

Aquifer name	Consitution
composite of sand units	SU-9
area (miles^2)	0.05
total volume (yds^3)	6.34E+06
est. avg. thickness (ft)	5
confined	Y
est. avg. saturated thickness (ft)	5
est.avg. unsaturated thickness (ft)	0
saturated volume (yds3)	6.34E+06
unsaturated volume (yds3)	0
saturated volume below sea level	0
primary recharge	from greenstone and or interface of greenstone and overlying sediments along the western boundary of the aquifer
secondary recharge	
primary discharge	unclear possibly wetland area along northern boudary, north of Seacrest Dr. or subterranean to SU-2 or SU-4
secondary discharge	possibly on slope to the east
wells screened in aquifer	10C, 10E
geologic unit correlation (Interp A)	coarse interbed within glaciomarine drift
geologic unit correlation (Interp B)	coarse interbed within glaciomarine drift
notes	aquifer appears to be comprised of 2-3 water bearing sand lenses with limited hydraulic connectivity; significant head difference between 10C and 10E (24 ft) suggest each well could be screened in separate water bearing sand lenses; may extend farther to the east than modeled

Aquifer name	Hilltop Deep
composite of sand units	SU-1
area (miles^2)	0.13
total volume (yds^3)	3.07E+05
est. avg. thickness (ft)	4
confined	Y
est. avg. saturated thickness (ft)	4
est.avg. unsaturated thickness (ft)	0
saturated volume (yds^3)	3.07E+05

225

unsaturated volume (yds^3)	0	
saturated volume below sea level	100%	
primary recharge	from bounding sandstone to north and south and possibly from below	
secondary recharge	from overlying glaciomarine drift	
primary discharge	offshore, likely extends some distance beneath Hale Passage	
wells screened in aquifer	04B, 09D, 09S, 09T, 10A	
geologic unit correlation (Interp A)	sand interbeds within pre-Vashon Cherry Pt silt	
geologic unit correlation (Interp B)	Vashon advance outwash	
notes	laterally discontinuous; may be two or more separate sand units; likely banded sand, silt, clay	

Aquifer name	Lane Spit
composite of sand units	SU-24, SU-26
area (miles^2)	0.06
total volume (yds^3)	1.22E+06
est. avg. thickness (ft)	26
confined	Y except in vicinity of 04A in the south
est. avg. saturated thickness (ft)	17
est.avg. unsaturated thickness (ft)	3
saturated volume (yds^3)	1.02E+06
unsaturated volume (yds^3)	2.00E+05
saturated volume below sea level	84%
primary recharge	from emergence deposits uphill from Lane Spit, west and northwest of N. Nugent Rd
secondary recharge	from sandstone where aquifer abuts bedrock
primary discharge	extends some distance offshore beneath Hale Passage
secondary discharge	
wells screened in aquifer	04A, 33F, 33G, 33J, 33T
geologic unit correlation (Interp A)	Vashon advance outwash
geologic unit correlation (Interp B)	marine outwash
notes	SU-24 and SU-26 separated by thin silt-clay diamicton layer at most places

Aquifer name	Lane Spit Deep
composite of sand units	SU-23
area (miles^2)	0.01

226

total volume (yds^3)	1.80E+05
est. avg. thickness (ft)	13
confined	Y
est. avg. saturated thickness (ft)	13
est.avg. unsaturated thickness (ft)	0
saturated volume (yds^3)	1.80E+05
unsaturated volume (yds^3)	0
saturated volume below sea level	100%
primary recharge	from sandstone along western boundary
secondary recharge	
primary discharge	extends some distance offshore beneath Hale Passage
secondary discharge	
wells screened in aquifer	33F
geologic unit correlation (Interp A)	Vashon advance outwash
geologic unit correlation (Interp B)	marine outwash
notes	

Aquifer name	Loganita
composite of sand units	SU-28, SU-29
area (miles^2)	0.03
total volume (yds^3)	1.21E+06
est. avg. thickness (ft)	40
confined	Y except possibly in southern portion
est. avg. saturated thickness (ft)	21
est.avg. unsaturated thickness (ft)	20
saturated volume (yds^3)	7.13E+05
unsaturated volume (yds^3)	5.01E+05
saturated volume below sea level	100%
primary recharge	from sandstone along eastern and southeastern boundary
secondary recharge	
primary discharge	offshore to Rosario Strait
secondary discharge	
wells screened in aquifer	32H, 32R

geologic unit correlation (Interp A)	Vashon advance outwash
geologic unit correlation (Interp B)	marine outwash
notes	sand units SU-28/29 converge southwest of 32H, where aquifer is unconfined

Aquifer name	West Shore
composite of sand units	SU-27
area (miles^2)	0.03
total volume (yds^3)	7.17E+05
est. avg. thickness (ft)	21
confined	Y
est. avg. saturated thickness (ft)	21
est.avg. unsaturated thickness (ft)	0
saturated volume (yds^3)	7.17E+05
unsaturated volume (yds^3)	0
saturated volume below sea level	55%
primary recharge	from sandstone along eastern boundary
secondary recharge	through overlying glaciomarine drift
primary discharge	offshore to Rosario Strait
secondary discharge	
wells screened in aquifer	32P
geologic unit correlation (Interp A)	Vashon advance outwash
geologic unit correlation (Interp B)	marine outwash
notes	extent of aquifer defined from well 32P, adjacent wells completed in bedrock and nearby bedrock outcrops

Aquifer name	Village Point
area (miles^2)	<.1
total volume (yds^3)	unknown
est. avg. thickness (ft)	unknown
confined	Y
est. avg. saturated thickness (ft)	unknown
est.avg. unsaturated thickness (ft)	-
saturated volume (yds^3)	unknown

unsaturated volume (yds^3)	-
saturated volume below sea level	100%
primary recharge	from sandstone north of aquifer
secondary recharge	-
primary discharge	offshore to Legoe Bay
secondary discharge	
wells screened in aquifer	05AA, 08W, 08G
geologic unit correlation (Interp A)	Vashon advance outwash or coarse lens within Cherry Point Silt
notes	not modeled due to limited data (05AA not located); probably a discontinuous extension of the lower sand unit of Leoge Bay Aquifer (SU-3); may be overlain by thicker coarse unit correlating to Vashon advance outwash

Table 13a. Hydraulic properties of wells completed in bedrock, north Lummi Island, Washington. Well logs with performance test and open interval data were used to calculate specific capacity, transmissivity, and horizontal hydraulic conductivity

well ID	aquifer	yield or pumping rate (gpm)	yield or pumping rate (ft³/day)	drawdown (ft)	pumping duration (hrs)	pumping duration (days)	screened interval length (ft)	specific capacity (gpm/ft)	transmissivity (ft²/day)	horizontal hydraulic conductivity
10B	Greenstone	8.0	1540	140	1.0	0.042	80	0.1	10.4	0.1
10J	Greenstone	1.0	192	80	3.0	0.125	98	<0.1	2.2	<0.1
10K	Greenstone	0.66	127	132	0.5	0.021	105	<0.1	0.7	<0.1
10P	Greenstone	2	385	176	2.0	0.083	151	<0.1	2.0	<0.1
10R	Greenstone	10	1925	94	2.0	0.083	76	0.1	21.8	0.3
04AA	Sandstone	6	1155	55	2.0	0.083	55	0.1	22.4	0.4
04E	Sandstone	12.0	2310	17	4.0	0.167	67	0.7	174.8	2.6
04I	Sandstone	10.0	1925	85	1.0	0.042	67	0.1	23.0	0.3
04K	Sandstone	10.0	1925	85	1.0	0.042	29	0.1	23.0	0.8
04L	Sandstone	1.5	289	205	6.0	0.250	256	<0.1	1.3	<0.1
04N	Sandstone	7.0	1347	115	2.0	0.083	99	0.1	11.9	0.1
04Q	Sandstone	7.0	1347	200	4.0	0.167	227	0.0	6.9	0.0
04T	Sandstone	20.0	3850	15	1.0	0.042	41	1.3	313.8	7.7
04U	Sandstone	10	1925	40	2.0	0.083	86	0.3	54.8	0.6
04V	Sandstone	9.0	1732	12	0.5	0.021	63	0.8	160.9	2.6
04W	Sandstone	1.5	289	93	0.5	0.021	84	<0.1	2.4	<0.1
04Z	Sandstone	20.0	3850	10	1.0	0.042	70	2.0	484.0	6.9
05H	Sandstone	7	1347	20	0.5	0.021	161	0.4	70.6	0.4
05T	Sandstone	2.0	385	90	3.0	0.125	103	<0.1	4.1	<0.1
05W	Sandstone	0.5	96	194	8.0	0.334	5	<0.1	0.5	0.1
05Z	Sandstone	7.0	1347	85	0.5	0.021	66	0.1	14.7	0.2
08O	Sandstone	15.0	2887	96	1.0	0.042	45	0.2	31.3	0.7
29C	Sandstone	5.0	962	85	4.0	0.167	61	0.1	12.2	0.2
32A	Sandstone	15.0	2887	50	1.5	0.063	20	0.3	65.3	3.3
32B	Sandstone	2.5	481	60	2.0	0.083	55	<0.1	7.9	0.1
32G	Sandstone	12	2310	30	4.0	0.167	92	0.4	95.4	1.0
32M	Sandstone	22.0	4235	72	4.0	0.167	82	0.3	71.2	0.9
32Q	Sandstone	60.0	11550	64	15.0	0.626	166	0.9	256.7	1.5
32T	Sandstone	2.0	385	188	2.0	0.083	156	<0.1	1.8	<0.1
32X	Sandstone	8.0	1540	90	2.0	0.083	72	0.1	17.9	0.2
33D	Sandstone	2.5	481	57	0.5	0.021	41	<0.1	7.3	0.2
33M	Sandstone	15.0	2887	90	0.5	0.021	125	0.2	31.6	0.3
33N	Sandstone	15	2887	110	1.0	0.042	162	0.1	27.0	0.2

Table 13b. Hydraulic properties of wells completed in Pleistocene aquifers, north Lummi Island, Washington. Well logs with performance test and screened interval data were used to calculate specific capacity, transmissivity, and horizontal hydraulic conductivity

well ID	aquifer	yield or pumping rate (gpm)	yield or pumping rate (ft3/day)	drawdown (ft)	pumping duration (hrs)	pumping duration (days)	screened interval length (ft)	specific capacity (gpm/ft)	transmissivity (ft2/day)	horizontal hydraulic conductivity (ft/day)
04H	Blizzard	6.0	1155	77	2.0	0.083	5	0.1	15.6	3.1
04Y	Centerview	12.0	2310	42	4.0	0.167	5	1.4	66.5	13.3
10C	Constitution	1.5	289	28	0.5	0.021	20	0.1	9.1	0.5
10E	Constitution	10.0	1925	7	0.5	0.021	open	1.4	321.8	6.4
04B	Hilltop Deep	20.0	3850	150	1.0	0.042	5	0.1	26.3	5.3
09D	Hilltop Deep	9.0	1732	99	4.0	0.167	5	0.1	19.5	3.9
09T	Hilltop Deep	15.0	2887	9	4.0	0.167	5	1.6	423.6	84.7
33G	Lane Spit	3.0	577	49	5.0	0.209	5	0.1	13.1	2.6
33J	Lane Spit	15.0	2887	20	1.0	0.042	5	0.8	169.5	33.9
33T	Lane Spit	5.5	1059	61	1.0	0.042	6	0.1	17.2	2.9
33F	Lane Spit Deep	10.0	1925	165	5.0	0.209	15	0.1	12.8	0.9
04G	Legoe Bay	3.5	674	20	4.0	0.167	5	0.2	38.7	7.7
05L	Legoe Bay	20.0	3850	10	2.0	0.083	5	2.0	506.5	101.3
08Z	Legoe Bay	4.0	770	101	2.0	0.083	5	0.0	7.5	1.5
09A	Legoe Bay	8.0	1540	26	2.0	0.083	5	0.3	68.5	13.7
09E	Legoe Bay	4.5	866	51	4.0	0.167	5	0.1	18.8	3.8
09K	Legoe Bay	5.0	962	57	4.0	0.167	5	0.1	18.7	3.7
09L	Legoe Bay	7.0	1347	12	1.5	0.063	10	0.6	133.3	13.3
09M	Legoe Bay	20.0	3850	33	3.0	0.125	5	0.6	145.7	29.1
09R	Legoe Bay	10.0	1925	6	0.5	0.021	open	1.7	379.6	6.4
09U	Legoe Bay	5.5	1059	17	4.0	0.167	5	0.3	74.8	15.0
10V	Legoe Bay	1.0	192	33	0.5	0.021	open	0.0	4.9	0.6
10X	Legoe Bay	8.0	1540	52	2.0	0.083	open	0.2	32.5	1.3
09Y	Legoe Bay	6.0	1155	85	2.0	0.083	5	0.1	14.0	2.8
32H	Loganita	12.5	2406	9	4.0	0.167	5	1.5	381.8	76.4
09G	Nugent	19.0	3657	119	4.0	0.167	5	0.2	35.7	7.1
09J	Nugent	5.0	962	15	1.0	0.042	10	0.3	70.9	7.1

09V	Nugent	30.0	5775	4	1.0	0.042	10	7.5	1978.0	197.8
09W	Nugent	5.0	962	5	4.0	0.167	open	1.0	253.4	0.4
10M	Nugent	11.0	2117	20	2.0	0.083	open	0.6	127.7	1.8
15A	Nugent	5.0	962	40	3.0	0.125	10	0.1	26.6	2.7
15C	Nugent	10.0	1925	14	4.0	0.167	9.5	0.7	184.0	19.4
15D	Nugent	11.0	2117	40	2.0	0.083	open	0.3	60.7	1.8
15K	Nugent	15.0	2887	17	4.0	0.167	5	0.9	227.8	45.6
15L	Nugent	15.0	2887	2	4.0	0.167	5	7.5	2146.0	429.2
15P	Nugent	15.0	2887	14	4.0	0.167	5	1.1	283.4	56.7
15S	Nugent	15.0	2887	8	4.0	0.167	5	1.9	494.2	98.8
15X	Nugent	15.0	2887	18	4.0	0.167	5	0.8	208.6	41.7
15Z	Nugent	10.0	1925	35	0.5	0.021	open	0.3	56.8	6.4
16K	Nugent	10.0	1925	7	3.0	0.125	5	1.5	393.3	78.7
16T	Nugent	2.0	385	48	5.5	0.229	5	<.1	8.6	1.7
16V	Nugent	2.0	385	48	5.5	0.229	5	<.1	8.6	1.7
08G	Village Pt	15.0	2887	18	4.0	0.167	4	0.5	205.6	51.4
32P	West Shore	20.0	3850	12	0.5	0.021	4	1.7	379.6	94.9

Table 14. Well yield, north Lummi Island, Washington. Well yield values are from well log well performance test data on well logs. Dug wells and well logs with no well yield data are not included

aquifer	minimum (gpm)	maximum (gpm)	median (gpm)	average (gpm)	number of wells
all aquifers	0.5	60.0	10.0	10.8	101
all Pleistocene aquifers	1.0	30.0	10.0	10.6	55
all in bedrock	0.5	60.0	8.0	11.0	46
Blizzard	-	-	-	6.0	1
Centerview	-	-	-	12.0	1
Constitution	1.5	10.0	-	5.8	2
Greenstone	0.5	35.0	2.0	7.2	11
Hilltop Deep	9.0	20.0	15.0	14.8	5
Lane Spit	3.0	20.0	10.3	10.9	4
Lane Spit Deep	-	-	-	10.0	1
Legoe Bay	1.0	20.0	6.5	8.2	17
Loganita	12.5	20.0	-	16.3	2
Nugent	2.0	30.0	12.0	12.3	20
Sandstone	0.5	60.0	9.5	11.8	36
Village Pt	8.0	15.0	-	11.5	2
West Shore	-	-	-	20.0	1

Summary of Well Yield

yield range (gpm)	number of wells	percent of wells
0-5	28	28
6-10	31	31
11-20	36	36
>20	6	6
total	**101**	**101**

Table 15. Specific capacity, north Lummi Island, Washington. Dug wells and logs with incomplete well performance test data are not included

aquifer	minimum (gpm/ft)	maximum (gpm/ft)	median (gpm/ft)	average (gpm/ft)	number of wells
all aquifers	<0.1	7.5	0.2	0.8	83
all Pleistocene aquifers	<0.1	7.5	0.3	0.9	46
all in bedrock	<0.1	2.0	0.1	0.6	37
Blizzard	-	-	-	0.1	1
Centerview	-	-	-	0.3	1
Constitution	0.1	1.4	-	0.7	2
Greenstone	<0.1	0.4	0.1	0.1	7
Hilltop Deep	0.1	1.6	-	0.6	3
Lane Spit	0.1	0.8	-	0.3	3
Lane Spit Deep	-	-	-	0.1	1
Legoe Bay	<0.1	1.7	0.3	0.7	14
Loganita	-	-	-	1.5	1
Nugent	<0.1	7.5	0.6	1.5	17
Sandstone	<0.1	2.0	0.1	0.3	30
Village Pt	0.5	0.8	-	0.7	2
West Shore	-	-	-	1.7	1

Table 16. Wells with zero drawdown on well performance test data contained in well logs, north Lummi Island, Washington. Zero drawdown during well performance tests indicates the pumping rate was insufficient to stress the aquifer

well ID	aquifer	pumping rate (gpm)	pumping duration (hours)
04C	Legoe Bay	5	2
05E	Sandstone	6	0.5
09I	Nugent	13	2
09Q	Nugent	20	0.5
09S	Hilltop Deep	15	0.5
10A	Hilltop Deep	15	2
16B	Nugent	18	2
32R	Loganita	20	1
32S	Sandstone	25	1

Summary of Well Specific Capacity

specific capacity range (gpm/ft)	number of wells	percent of wells
0-0.5	14	17
0.6-1	55	66
>1	14	17
total	**83**	**100**

Table 17. Transmissivity, north Lummi Island, Washington

aquifer	minimum (ft^2/day)	maximum (ft^2/day)	median (ft^2/day)	geometric mean (ft^2/day)	number of well logs
all aquifers	0.5	2146.0	32.5	40.2	77
all Pleistocene aquifers	5.0	2146.0	70.0	76.0	44
all bedrock aquifers	0.5	484.0	21.8	17.3	33
Blizzard	-	-	-	15.6	1
Centerview	-	-	-	67.0	1
Constitution	9.0	322.0	-	54.0	2
Greenstone	0.7	21.8	2.2	3.7	5
Hilltop Deep	19.5	423.6	26.3	60.0	3
Lane Spit	13.0	169.5	17.0	34.0	3
Lane Spit Deep	-	-	-	13.0	1
Legoe Bay	5.0	507.0	39.0	46.0	13
Loganita	-	-	-	382.0	1
Nugent	9.0	2146.0	184.0	132.0	17
Sandstone	0.5	484.0	23.0	22.8	28
Village Pt	-	-	-	205.6	1
West Shore	-	-	-	380.0	1

Table 18. Horizontal hydraulic conductivity, north Lummi Island, Washington

aquifer	minimum (ft/day)	maximum (ft/day)	median (ft/day)	geometric mean (ft/day)	number of well logs
all aquifers	<.01	429.2	2.55	1.87	77
all Pleistocene aquifers	0.4	429.2	7.0	9.0	44
all bedrock aquifers	<.01	7.7	0.3	0.2	33
Blizzard	-	-	-	3.1	1
Centerview	-	-	-	13.3	1
Constitution	-	-	-	2.0	2
Greenstone	<.01	0.3	<0.1	<0.1	5
Hilltop Deep	19.5	423.6	5.0	12.0	3
Lane Spit	3.0	34.0	3.0	6.0	3
Lane Spit Deep	-	-	-	0.9	1
Legoe Bay	1.0	101.0	6.0	6.0	13
Loganita	-	-	-	76.4	1
Nugent	0.4	429.2	7.0	12.0	17
Sandstone	<0.1	7.7	0.3	0.3	28
Village Pt	-	-	-	51.4	1
West Shore	-	-	-	94.9	1

Table 19. Water level elevations and water level changes in wells, north Lummi Island, Washington, fall 2002-spring 2003. Positive values represent higher water levels in spring

well ID	aquifer	water level elev. (ft) fall 2002[1]	water level elev. (ft) spring 2003[1]	change in water level (ft)[2]
04Y	Centerview	99	99	0.1
10C	Constitution	156	157	0.4
10E	Constitution	134	133	-1.5
04P	dug well	6	6	0.4
05G	dug well	62	64	1.7
10D	dug well	146	149	3.1
10F	dug well	114	116	1.9
33B	dug well	75	76	0.7
33X	dug well	228	233	4.6
09C	Greenstone	132	117	-15.2
10B	Greenstone	69	65	-4.5
10J	Greenstone	57	55	-1.9
10Y	Greenstone	68	70	2.6
09S	Hilltop Deep	12	12	-0.2
04A	Lane Spit	15	15	-0.2
33G	Lane Spit	5	2	-3.0
33T	Lane Spit	12	12	-0.4
33F	Lane Spit Deep	-	8	-
04C	Legoe Bay	13	14	1.1
04G	Legoe Bay	-	12	-
05J	Legoe Bay	12	11	-0.7
05L	Legoe Bay	11	11	-0.4
05O	Legoe Bay	11	11	-0.1
09A	Legoe Bay	13	13	-0.3
09B	Legoe Bay	13	14	0.8
09J	Legoe Bay	-	18	-
09K	Legoe Bay	8	7	-1.2
09L	Legoe Bay	13	13	-0.1
09M	Legoe Bay	11	12	0.2
09P	Legoe Bay	8	8	0.7
09R	Legoe Bay	11	10	-1.0
09V	Legoe Bay	16	16	0.1
10V	Legoe Bay	14	14	0.2
10X	Legoe Bay	9	10	1.1
32H	Loganita	6	7	0.8
32R	Loganita	-	9	-
09G	Nugent	10	7	-2.4
09I	Nugent	8	8	-0.5
09Q	Nugent	13	13	-0.2
10M	Nugent	17	17	-0.3
15A	Nugent	9	9	0.0
15D	Nugent	12	11	-0.6

15K	Nugent	9	9	0.2
15O	Nugent	9	8	-0.4
15P	Nugent	8	8	0.6
15S	Nugent	9	9	0.5
16K	Nugent	7	7	0.3
16V	Nugent	-	4	-
04D	Sandstone	101	99	-2.6
04E	Sandstone	27	35	7.9
04F	Sandstone	-	21	-
04I	Sandstone	53	55	2.0
04J	Sandstone	55	50	-5.2
04K	Sandstone	37	44	7.0
04M	Sandstone	12	12	0.5
04N	Sandstone	77	85	8.0
04Q	Sandstone	-	48	-
04R	Sandstone	102	102	0.2
04S	Sandstone	52	48	-4.0
04T	Sandstone	33	34	1.5
04V	Sandstone	56	53	-3.3
04W	Sandstone	196	196	0.1
04X	Sandstone	58	60	1.1
04Z	Sandstone	50	52	2.4
05B	Sandstone	172	178	6.0
05E	Sandstone	19	17	-2.1
05P	Sandstone	22	-	-
05T	Sandstone	126	132	6.4
05W	Sandstone	-	57	-
05Z	Sandstone	217	219	1.5
08O	Sandstone	8	1	-7.1
29C	Sandstone	-	16	-
32A	Sandstone	190	192	-1.4
32B	Sandstone	36	35	1.6
32K	Sandstone	22	22	-0.3
32L	Sandstone	8	12	3.9
32M	Sandstone	149	154	4.8
32N	Sandstone	143	149	5.9
32Q	Sandstone	138	147	9.2
32S	Sandstone	29	52	23.4
32T	Sandstone	143	143	-0.5
32W	Sandstone	213	223	10.4
32X	Sandstone	167	164	-2.5
33D	Sandstone	168	177	8.9
33M	Sandstone	154	180	26.6
33W	Sandstone	67	70	2.9
32P	West Shore	25	24	-0.7

1. Precision of water level elevations is detmined to be < 1 foot for wells surveyed using survey-grade GPS; up to 15 feet for those estimated with DEM
2. The magnitude of water level changes are based on measurments precise to two significant digits, displayed here to one significant digit

Table 20. Water level changes in aquifers, north Lummi Island, Washington, fall 2002-spring 2003. Positive values represent higher water levels in spring.

aquifer	minimum change (ft)	maximum change (ft)	median change (ft)	average change (ft)	standard deviation	number wells
all wells	< 0.1	26.6	0.2	1.2	5.3	78
all bedrock wells	< 0.1	26.6	1.4	2.3	7.3	40
all drilled Pleistocene wells	0.1	-2.4	-0.2	-0.2	1.0	39
Centerview	-	-	-	0.1	-	1
Constitution	0.4	-1.5	-	-0.5	-	2
Dug Wells	0.4	4.6	1.9	2.1	1.6	6
Greenstone	-0.4	-15.2	-1.9	-3.9	6.8	5
Hilltop Deep	-	-	-	-0.2	-	1
Lane Spit	-0.2	-3.0	-0.4	-1.2	-	3
Legoe Bay	-0.1	-1.2	-0.1	0.0	0.8	13
Loganita	-	-	-	0.8	-	1
Nugent	0.1	-2.4	0.0	-0.2	0.8	11
Sandstone	< 0.1	26.6	1.5	3.2	7.0	34
West Shore	-	-	-	-0.7	-	1

Table 21. Wells correlated to ones used in previous studies, north Lummi Island, Washington

well ID	well ID in previous studies
04W	37/1-5H2
05B	37/1-5H1 or A1
05E	37/1-5C1
05J	37/1-5R1
05P	37/1-5F
08G	37/1-8C
09C	37/1-9J1
09Q	37/1-16H
10G	37/1-10L2
15K	37/1-15G1
15Z	37/1-15E
32K	38/1-32L
32P	38/1-32P1
33D	38/1-33N
33W	38/1-33L

Previous studies include Schmidt (1978), Dion and Sumioka (1984), and Whatcom County (1994)

Table 22. Total groundwater storage capacity, north Lummi Island, Washington. Values for effective porosity are from Table 7c

aquifer	comprised of sand units	average effective porosity	saturated volume (yds^3)	total groundwater volume (acre-feet)
all aquifers	-	-	9.73E+08	1.05E+05
all bedrock aquifers	-	0.17	9.30E+08	9.80E+04
all Pleistocene aquifers	-	0.28	4.22E+07	7.33E+03
all silt-clay diamicton	-	0.5*	2.96E+07	9.20E+04
Blizzard	SU-21	0.26	2.50E+06	4.03E+02
Centerview	SU-22	0.30	1.60E+06	2.97E+02
Constitution	SU-9	0.22	6.34E+06	8.65E+02
Greenstone	-	0.17	1.56E+08	1.64E+04
Hilltop Deep	SU-1	0.33	3.07E+05	6.29E+01
Lane Spit	SU-24, SU-26	0.30	1.02E+06	1.90E+02
Lane Spit Deep	SU-23	0.26	1.80E+05	2.91E+01
Legoe Bay	SU-2, SU-3, SU-5	0.26	4.47E+06	7.21E+02
Loganita	SU-28, SU-29	0.26	7.13E+05	1.15E+02
Nugent	SU-4, SU-6, SU-7	0.27	2.44E+07	4.08E+03
Sandstone	-	0.17	7.75E+08	8.17E+04
Village Pt	-	-	-	-
West Shore	SU-27	0.30	7.17E+05	1.33E+02

*Value is for porosity, not effective porosity

Table 23. Slope determined from a USGS 10-meter DEM using GIS, north Lummi Island, Washington

slope class (degrees)	area (square miles)	percent of study area
0-5	2.65	68.5
6-10	0.79	20.4
11-15	0.27	7.0
16-20	0.08	2.1
20-36	0.08	2.1
total	**3.87**	**100.0**

Table 24. Subsoil textures and percolation rate classes from 16 on-site sewage (OSS) applications, north Lummi Island, Washington

OSS ID (Figure 24)	same lot as well with ID	soil texture (at depth 4-5 ft)	perc rate class (in/hr)
1	32W	sand gravel and rocks light brown	>/= 12
2	-	loamy sand w/gravel very light brown	>/= 12
3	-	sand and gravel brown	>/= 12
4	04H	sandy loam grey brown	2-3.9
5	10M	clay loam mottled	1-1.9
6	04AA	sand and gravel brown	1-1.9
7	04D	sandy loam w/gravel brown	2-3.9
8	05Z	sand gravel and rocks light brown	4-11.9
9	05W	sand, gravel and rocks grey brown	4-11.9
10	05L	sand and gravel brown	1-1.9
11	10V	mottled clay w/sand	3
12	10D	sand and gravel brown	4-11.9
13	10X	sand and gravel	>/= 12
14	-	coarse sand and gravel	>/= 12
15	15A	sandy clay loam	1-1.9
16	15K	sand light yellow brown	4-11.9

Source: Whatcom County Health Department

Table 25. Major recharge areas, north Lummi Island, Washington. Recharge areas are shown in Figures 25a and 25b

recharge area (RCA)	primary recharge to aquifer	secondary recharge to aquifer	mechanism of recharge
RCA-1	Sandstone, Centerview, Lane Spit Deep, Loganita, West Shore	Blizzard, Lane Spit, Legoe Bay	-through silt-clay diamicton of glaiciomarine drift, into fractured bedrock -from fractured bedrock where Pleistocene aquifers abut bedrock
RCA-2	Lane Spit	Lane Spit Deep	-through emergence beach deposits at the surface
RCA-3	Hilltop Deep	Sandstone, Leoge Bay	-through silt-clay diamicton of glaiciomarine drift, into fractured bedrock -from fractured bedrock where Pleistocene aquifers abut bedrock
RCA-4	Village Point	Sandstone, Leoge Bay	-through silt-clay diamicton of glaiciomarine drift, into fractured bedrock -from fractured bedrock where Pleistocene aquifers abut bedrock
RCA-5	Legoe Bay	-	-through emergence beach deposits at the surface -through silt-clay diamicton of overlying glaiciomarine drift
RCA-6	Legoe Bay, Nugent	Hilltop Deep	-through emergence beach deposits at the surface -through silt-clay diamicton of overlying glaiciomarine drift
RCA-7	-	Nugent, Greenstone	-through silt-clay diamicton of glaiciomarine drift, into fractured bedrock -from fractured bedrock where Pleistocene aquifers abut bedrock
RCA-8	Consitution, Greenstone, Nugent	-	-through silt-clay diamicton of glaiciomarine drift, into fractured bedrock -from fractured bedrock where Pleistocene aquifers abut bedrock
RCA-9	Nugent	-	-through emergence beach deposits at the surface
RCA-10	-	Nugent	-through silt-clay diamicton of overlying glaiciomarine drift

Table 26. Precipitation, north Lummi Island and Bellingham International Airport, Water Years 2001-2004

	month	West Shore (in)	Nugent (in)	Tuttle (in)	average of Lummi Island gauges (in)	Bellingham Intl. Airport (in)
WY 2001	O	2.71	2.25	2.42	2.46	0.68
	N	2.74	2.61	2.70	2.68	2.08
	D	3.75	4.04	3.83	3.87	2.98
	J	3.31	3.29	3.17	3.26	3.32
	F	1.21	1.38	1.30	1.30	1.46
	M	2.78	3.81	3.11	3.23	4.20
	A	1.95	2.18	2.23	2.12	2.12
	M	1.23	1.07	1.20	1.17	1.30
	J	2.19	2.08	2.72	2.33	3.12
	J	0.84	1.09	0.92	0.95	0.98
	A	2.17	2.42	2.23	2.27	3.03
	S	0.91	0.60	1.12	0.88	1.53
	total	**25.79**	**26.82**	**26.95**	**26.52**	**26.80**
WY 2002	O	5.23	3.91	5.06	4.73	4.96
	N	4.41	4.37	4.42	4.40	4.80
	D	5.56	6.26	6.59	6.14	5.28
	J	5.57	5.93	5.46	5.65	2.32
	F	3.21	3.00	3.25	3.15	3.38
	M	2.29	2.60	2.37	2.42	2.16
	A	2.44	2.26	2.20	2.30	2.28
	M	1.73	1.31	1.73	1.59	1.94
	J	0.80	1.30	1.29	1.13	1.16
	J	0.61	0.48	0.73	0.61	0.59
	A	2.04	0.47	0.44	0.98	0.01
	S	2.04	1.40	1.85	1.76	1.33
	total	**35.93**	**33.29**	**35.39**	**34.87**	**30.21**
WY 2003	O	1.26	1.04	1.18	1.16	1.05
	N	3.34	2.60	2.48	2.81	3.28
	D	3.49	4.33	3.90	3.91	4.25
	J	5.00	5.33	5.05	5.13	4.51
	F	1.80	1.60	1.56	1.65	1.96
	M	3.30	3.39	3.31	3.33	3.46
	A	2.94	3.00	2.76	2.90	2.61
	M	1.64	1.69	1.38	1.57	1.89
	J	1.07	1.40	1.23	1.23	1.14
	J	0.26	0.25	0.23	0.25	0.69
	A	0.22	0.28	0.29	0.26	0.21
	S	0.87	1.07	0.82	0.92	1.48
	total	**25.19**	**25.98**	**24.19**	**25.12**	**26.53**
WY 2004	O	9.74	9.82	10.02	9.86	8.29
	N	6.07	5.88	6.08	6.01	4.72
	D	1.53	2.03	1.49	1.68	1.75
	J	4.98	-	-	4.98	4.65
	F	1.67	-	-	1.67	1.73
	M	3.40	-	-	3.40	3.32
	A	0.52	-	-	0.52	0.32
	M	3.37	-	-	3.37	3.23
	J	0.61	-	-	0.61	1.06
	J	0.53	-	-	0.53	0.41
	A	3.34	-	-	3.34	3.08
	S	3.39	-	-	3.39	3.12
	total	**39.15**	**-**	**-**	**39.36**	**35.68**

242

Table 27a. Climate, solar radiation, and other data as input parameters for the Penman-Monteith Equation used to estimate Potential Evapotranspiration from north Lummi Island, Washington, Water Year 2001

month	T_a	v_a	T_d	C	K_{ET}	e_a	e_{sat}	W_p	τ	γ_s	K_{cs}	K_{in}	K	ε_{sat}	L	γ	K_E	s	γ_v	C_{at}	C_{+leaf}	L_t	$\Delta\theta$	$G(\Delta\theta)$	$G(T_a)$	$\Delta\rho_v$	$G(\Delta\rho_v)$	$G(K_{in})$	C_{leaf}	C_{can}	$PET_{cm/day}$	$PET_{in/day}$	days	$PET_{in/month}$
O	10.1	208.57	7.00	0.62	237.97	10.03	12.39	1.72	0.46	0.41	164.99	101.21	82.99	0.92	-58.42	0.66	1.45E-04	0.08	591.60	1.55E+06	0.56	4.70	0.00	1.00	0.81	1.81	0.88	0.35	0.14	5.68E+04	0.097	0.04	31	1.18
N	4.8	216.30	1.44	0.55	368.49	6.78	8.63	1.22	0.50	0.38	262.96	173.81	142.53	0.85	-97.47	0.66	1.45E-04	0.06	594.57	1.61E+06	0.56	4.70	0.00	1.00	0.47	1.44	0.90	0.49	0.12	4.73E+04	0.063	0.02	28	0.70
D	2.7	239.47	-0.44	0.56	561.09	5.91	7.41	1.09	0.51	0.38	403.62	264.05	216.52	0.84	-101.50	0.66	1.45E-04	0.05	595.80	1.78E+06	0.56	4.70	0.00	1.00	0.28	1.17	0.92	0.61	0.09	3.52E+04	0.039	0.02	31	0.47
J	4.5	220.16	1.67	0.53	765.54	6.89	8.43	1.24	0.50	0.39	545.75	368.16	301.89	0.85	-99.61	0.66	1.45E-04	0.06	594.76	1.64E+06	0.56	4.70	0.00	1.00	0.44	1.20	0.92	0.70	0.16	6.40E+04	0.071	0.03	30	0.84
F	3.4	266.51	-0.83	0.53	922.20	5.75	7.80	1.06	0.51	0.38	664.42	448.22	367.54	0.83	-109.70	0.66	1.45E-04	0.06	595.39	1.99E+06	0.56	4.70	0.00	1.00	0.34	1.61	0.89	0.75	0.13	5.19E+04	0.078	0.03	31	0.95
M	6.7	293.54	2.61	0.47	993.39	7.38	9.84	1.31	0.49	0.39	705.09	504.42	413.62	0.84	-109.55	0.66	1.45E-04	0.07	593.51	2.19E+06	0.56	4.70	0.00	1.00	0.61	1.91	0.87	0.77	0.23	9.33E+04	0.166	0.07	30	1.96
A	8.5	308.99	3.39	0.43	959.54	7.80	11.11	1.38	0.49	0.39	678.50	503.85	413.16	0.83	-116.21	0.66	1.45E-04	0.08	592.51	2.30E+06	0.56	4.70	0.00	1.00	0.72	2.56	0.83	0.77	0.26	1.05E+05	0.251	0.10	31	3.06
M	11.5	247.20	6.06	0.42	830.23	9.40	13.59	1.62	0.47	0.41	578.80	433.75	355.68	0.85	-108.16	0.66	1.45E-04	0.09	590.81	1.84E+06	0.56	4.70	0.00	1.00	0.87	3.20	0.79	0.74	0.28	1.14E+05	0.340	0.13	31	4.15
J	13.3	278.09	8.61	0.55	643.14	11.20	15.28	1.90	0.45	0.42	441.47	291.81	239.29	0.91	-65.86	0.66	1.45E-04	0.10	589.81	2.07E+06	0.56	4.70	0.00	1.00	0.93	3.09	0.79	0.64	0.26	1.06E+05	0.310	0.12	30	3.66
J	15.8	324.44	10.28	0.67	440.85	12.53	18.03	2.11	0.44	0.43	299.24	173.38	142.17	0.96	-28.07	0.66	1.45E-04	0.12	588.37	2.42E+06	0.56	4.70	0.00	1.00	0.98	4.13	0.72	0.49	0.20	7.96E+04	0.319	0.13	31	3.89
A	16.6	262.64	13.00	0.59	277.89	15.01	18.88	2.49	0.41	0.45	184.84	117.15	96.06	0.97	-26.39	0.66	1.45E-04	0.12	587.96	1.96E+06	0.56	4.70	0.00	1.00	0.99	2.90	0.81	0.39	0.17	7.06E+04	0.199	0.08	30	2.35
S	13.5	200.85	10.67	0.80	203.40	12.86	15.50	2.16	0.43	0.44	137.68	67.60	55.43	1.01	5.47	0.66	1.45E-04	0.10	589.69	1.50E+06	0.56	4.70	0.00	1.00	0.93	2.00	0.87	0.26	0.12	4.85E+04	0.093	0.04	31	1.14
																																Total (in)		**24.36**

Table 27b. Climate, solar radiation, and other data as input parameters for the Penman-Monteith Equation used to estimate Potential Evapotranspiration from north Lummi Island, Washington, Water Year 2002

month	T_a	v_a	T_d	C	K_{ET}	e_a	e_{sat}	W_p	τ	γ_s	K_{cs}	K_{in}	K	ε_{sat}	L	γ	K_E	s	γ_v	C_{at}	C_{+leaf}	L_t	$\Delta\theta$	$G(\Delta\theta)$	$G(T_a)$	$\Delta\rho_v$	$G(\Delta\rho_v)$	$G(K_{in})$	C_{leaf}	C_{can}	$PET_{cm/day}$	$PET_{in/day}$	days	$PET_{in/month}$
0	9.00	274.23	6.17	0.62	237.97	9.47	11.50	1.64	0.47	0.41	165.80	101.70	83.39	0.91	-62.64	0.66	1.45E-04	0.08	592.22	2.04E+06	0.56	4.70	0.00	1.00	0.75	1.56	0.90	0.35	0.13	5.40E+04	0.080	0.03	31	0.97
N	7.78	297.41	4.58	0.55	368.49	8.48	10.58	1.48	0.48	0.40	258.98	171.19	140.37	0.88	-84.82	0.66	1.45E-04	0.07	592.91	2.22E+06	0.56	4.70	0.00	1.00	0.68	1.62	0.89	0.49	0.17	6.71E+04	0.102	0.04	31	1.13
D	3.78	355.34	0.50	0.56	561.09	6.34	8.01	1.15	0.50	0.38	402.05	263.02	215.68	0.85	-98.72	0.66	1.45E-04	0.06	595.17	2.65E+06	0.56	4.70	0.00	1.00	0.38	1.31	0.91	0.61	0.12	4.75E+04	0.059	0.02	31	0.71
J	3.94	308.99	2.06	0.53	765.54	7.09	8.11	1.27	0.49	0.39	544.78	367.51	301.36	0.85	-96.91	0.66	1.45E-04	0.06	595.08	2.30E+06	0.56	4.70	0.00	1.00	0.39	0.80	0.95	0.70	0.14	5.87E+04	0.044	0.02	30	0.52
F	4.39	305.13	0.39	0.53	922.20	6.29	8.37	1.15	0.50	0.38	661.11	445.99	365.71	0.84	-105.61	0.66	1.45E-04	0.06	594.82	2.27E+06	0.56	4.70	0.00	1.00	0.43	1.63	0.89	0.74	0.16	6.49E+04	0.099	0.04	31	1.20
M	3.50	390.10	-0.67	0.47	993.39	5.82	7.86	1.08	0.51	0.38	715.23	511.68	419.58	0.82	-119.85	0.66	1.45E-04	0.06	595.33	2.91E+06	0.56	4.70	0.00	1.00	0.35	1.60	0.89	0.78	0.14	5.57E+04	0.084	0.03	30	0.99
A	8.28	293.54	4.06	0.43	959.54	8.17	10.95	1.44	0.48	0.40	676.22	502.16	411.77	0.84	-112.31	0.66	1.45E-04	0.07	592.63	2.19E+06	0.56	4.70	0.00	1.00	0.71	2.14	0.86	0.77	0.26	1.07E+05	0.213	0.08	31	2.59
M	10.72	262.64	5.89	0.42	830.23	9.29	12.91	1.61	0.47	0.41	579.35	434.16	356.01	0.85	-107.96	0.66	1.45E-04	0.09	591.25	1.96E+06	0.56	4.70	0.00	1.00	0.83	2.77	0.82	0.74	0.28	1.14E+05	0.294	0.12	31	3.58
J	15.17	293.54	10.33	0.55	643.14	12.58	17.27	2.11	0.44	0.43	436.38	288.45	236.53	0.93	-55.43	0.66	1.45E-04	0.11	588.75	2.19E+06	0.56	4.70	0.00	1.00	0.97	3.54	0.76	0.63	0.26	1.07E+05	0.360	0.14	30	4.25
J	16.44	281.96	12.17	0.67	440.85	14.21	18.75	2.36	0.42	0.45	295.13	171.00	140.22	0.98	-13.53	0.66	1.45E-04	0.12	588.03	2.10E+06	0.56	4.70	0.00	1.00	0.99	3.40	0.77	0.49	0.21	8.49E+04	0.279	0.11	31	3.41
A	16.50	235.61	11.83	0.59	277.89	13.90	18.81	2.32	0.42	0.45	186.51	118.21	96.93	0.95	-35.54	0.66	1.45E-04	0.12	587.99	1.76E+06	0.56	4.70	0.00	1.00	0.99	3.68	0.75	0.39	0.16	6.64E+04	0.237	0.09	30	2.79
S	13.56	196.98	10.28	0.80	203.40	12.53	15.56	2.11	0.44	0.43	138.06	67.79	55.59	1.00	2.49	0.66	1.45E-04	0.10	589.65	1.47E+06	0.56	4.70	0.00	1.00	0.94	2.29	0.85	0.26	0.12	4.76E+04	0.105	0.04	31	1.28
																																Total (in)		**23.44**

Table 27c. Climate, solar radiation, and other data as input parameters for the Penman-Monteith Equation used to estimate Potential Evapotranspiration from north Lummi Island, Washington, Water Year 2003

month	T_a	v_a	T_d	C	K_{ET}	e_a	e_{sat}	W_p	τ	γ_s	K_{cs}	K_{in}	K	ε_{sat}	L	γ	K_E	s	γ_v	C_{at}	C_{+leaf}	L_t	$\Delta\theta$	$G(\Delta\theta)$	$G(T_a)$	$\Delta\rho_v$	$G(\Delta\rho_v)$	$G(K_{in})$	C_{leaf}	C_{can}	$PET_{cm/day}$	$PET_{in/day}$	days	$PET_{in/month}$
O	8.78	139.05	6.28	0.62	237.97	9.54	11.33	1.65	0.47	0.41	165.69	101.64	83.34	0.91	-61.77	0.66	1.45E-04	0.08	592.35	1.04E+06	0.56	4.70	0.00	1.00	0.74	1.37	0.91	0.35	0.13	5.38E+04	0.068	0.03	31	0.83
N	7.61	274.23	4.39	0.55	368.49	8.37	10.46	1.47	0.48	0.40	259.24	171.36	140.51	0.88	-85.67	0.66	1.45E-04	0.07	593.01	2.04E+06	0.56	4.70	0.00	1.00	0.67	1.62	0.89	0.49	0.16	6.61E+04	0.100	0.04	28	1.11
D	5.39	336.03	2.44	0.56	561.09	7.29	8.97	1.30	0.49	0.39	398.56	260.74	213.81	0.86	-91.32	0.66	1.45E-04	0.06	594.26	2.50E+06	0.56	4.70	0.00	1.00	0.51	1.31	0.91	0.60	0.16	6.40E+04	0.079	0.03	31	0.96
J	6.28	293.54	3.28	0.53	765.54	7.73	9.54	1.37	0.48	0.39	541.61	365.37	299.61	0.86	-93.89	0.66	1.45E-04	0.07	593.76	2.19E+06	0.56	4.70	0.00	1.00	0.58	1.40	0.91	0.69	0.20	8.25E+04	0.108	0.04	30	1.28
F	4.28	189.26	1.22	0.53	922.20	6.68	8.30	1.21	0.50	0.38	658.74	444.38	364.40	0.85	-101.45	0.66	1.45E-04	0.06	594.89	1.41E+06	0.56	4.70	0.00	1.00	0.42	1.27	0.92	0.74	0.16	6.51E+04	0.077	0.03	31	0.94
M	7.33	374.66	3.61	0.47	993.39	7.92	10.26	1.40	0.48	0.39	701.65	501.96	411.61	0.85	-105.29	0.66	1.45E-04	0.07	593.16	2.79E+06	0.56	4.70	0.00	1.00	0.65	1.81	0.88	0.77	0.25	1.00E+05	0.171	0.07	30	2.02
A	9.33	316.72	5.39	0.43	959.54	8.97	11.76	1.56	0.47	0.40	671.45	498.62	408.87	0.85	-106.63	0.66	1.45E-04	0.08	592.04	2.36E+06	0.56	4.70	0.00	1.00	0.77	2.14	0.86	0.77	0.28	1.15E+05	0.231	0.09	31	2.82
M	11.67	251.06	7.67	0.42	830.23	10.50	13.74	1.79	0.46	0.42	573.30	429.63	352.30	0.87	-98.71	0.66	1.45E-04	0.09	590.72	1.87E+06	0.56	4.70	0.00	1.00	0.87	2.47	0.84	0.74	0.30	1.22E+05	0.280	0.11	31	3.42
J	15.44	270.37	11.00	0.55	643.14	13.15	17.59	2.20	0.43	0.44	434.31	287.08	235.40	0.93	-50.77	0.66	1.45E-04	0.11	588.59	2.01E+06	0.56	4.70	0.00	1.00	0.98	3.34	0.78	0.63	0.27	1.09E+05	0.345	0.14	30	4.07
J	17.72	262.64	12.50	0.67	440.85	14.52	20.33	2.41	0.42	0.45	294.38	170.56	139.86	0.99	-11.05	0.66	1.45E-04	0.13	587.30	1.96E+06	0.56	4.70	0.00	1.00	1.00	4.33	0.71	0.49	0.19	7.87E+04	0.331	0.13	31	4.04
A	17.11	235.61	12.39	0.59	277.89	14.42	19.56	2.40	0.42	0.45	185.72	117.71	96.52	0.96	-31.47	0.66	1.45E-04	0.12	587.65	1.76E+06	0.56	4.70	0.00	1.00	1.00	3.85	0.74	0.39	0.16	6.56E+04	0.245	0.10	30	2.89
S	14.67	204.71	11.22	0.80	203.40	13.34	16.73	2.23	0.43	0.44	137.13	67.33	55.21	1.01	9.94	0.66	1.45E-04	0.11	589.03	1.52E+06	0.56	4.70	0.00	1.00	0.96	2.55	0.83	0.26	0.12	4.77E+04	0.118	0.05	31	1.44
																																Total (in)		**25.81**

243

Table 27d. Climate, solar radiation, and other data as input parameters for the Penman-Monteith Equation used to estimate Potential Evapotranspiriation from north Lummi Island, Washington, Water Year 2004

month	T_a	v_a	T_d	C	K_{ET}	e_a	e_{sat}	W_p	τ	γ_s	K_{cs}	K_{in}	K	ε_{at}	L	γ	K_E	s	γ_v	C_{at}	C^*_{leaf}	L_t	$\Delta\theta$	$G(\Delta\theta)$	$G(T_a)$	$\Delta\rho_v$	$G(\Delta\rho_v)$	$G(K_{in})$	C_{leaf}	C_{can}	$PET_{cm/day}$	$PET_{in/day}$	days	$PET_{in/month}$
O	11.33	347.62	8.22	0.62	237.97	10.91	13.44	1.86	0.45	0.42	163.76	100.45	82.37	0.93	-51.45	0.66	1.45E-04	0.09	590.91	2.59E+06	0.56	4.70	0.00	1.00	0.86	1.94	0.87	0.35	0.15	5.97E+04	0.111	0.04	31	1.36
N	4.44	308.99	-0.28	0.55	368.49	5.99	8.40	1.10	0.51	0.38	264.90	175.10	143.58	0.84	-105.18	0.66	1.45E-04	0.06	594.79	2.30E+06	0.56	4.70	0.00	1.00	0.43	1.88	0.87	0.49	0.11	4.28E+04	0.075	0.03	28	0.83
D	4.67	351.48	1.44	0.56	561.09	6.78	8.53	1.22	0.50	0.38	400.40	261.94	214.79	0.86	-95.38	0.66	1.45E-04	0.06	594.67	2.62E+06	0.56	4.70	0.00	1.00	0.45	1.36	0.91	0.61	0.14	5.67E+04	0.073	0.03	31	0.89
J	3.67	332.17	0.78	0.53	765.54	6.47	7.95	1.17	0.50	0.38	547.89	369.61	303.08	0.84	-102.68	0.66	1.45E-04	0.06	595.23	2.47E+06	0.56	4.70	0.00	1.00	0.37	1.16	0.92	0.70	0.13	5.38E+04	0.059	0.02	30	0.69
F	5.50	239.47	2.06	0.53	922.20	7.09	9.04	1.27	0.49	0.39	656.26	442.72	363.03	0.85	-99.10	0.66	1.45E-04	0.06	594.20	1.78E+06	0.56	4.70	0.00	1.00	0.52	1.52	0.90	0.74	0.19	7.87E+04	0.111	0.04	31	1.36
M	7.83	320.58	3.61	0.47	993.39	7.92	10.62	1.40	0.48	0.39	701.65	501.96	411.61	0.85	-106.05	0.66	1.45E-04	0.07	592.88	2.39E+06	0.56	4.70	0.00	1.00	0.68	2.09	0.86	0.77	0.25	1.03E+05	0.201	0.08	30	2.37
A	10.83	212.43	4.83	0.43	959.54	8.63	13.00	1.51	0.48	0.40	673.47	500.12	410.10	0.84	-112.08	0.66	1.45E-04	0.09	591.19	1.58E+06	0.56	4.70	0.00	1.00	0.84	3.34	0.78	0.77	0.28	1.14E+05	0.351	0.14	31	4.29
M	12.67	270.37	8.61	0.42	830.23	11.20	14.68	1.90	0.45	0.42	569.89	427.08	350.20	0.87	-94.13	0.66	1.45E-04	0.10	590.16	2.01E+06	0.56	4.70	0.00	1.00	0.91	2.64	0.82	0.73	0.31	1.25E+05	0.309	0.12	31	3.77
J	15.67	266.51	10.44	0.55	643.14	12.67	17.84	2.13	0.43	0.44	436.04	288.22	236.34	0.93	-55.01	0.66	1.45E-04	0.11	588.46	1.99E+06	0.56	4.70	0.00	1.00	0.98	3.88	0.74	0.63	0.26	1.04E+05	0.385	0.15	30	4.55
J	18.28	289.68	13.28	0.67	440.85	15.28	21.06	2.53	0.41	0.46	292.58	169.52	139.01	0.99	-4.63	0.66	1.45E-04	0.13	586.99	2.16E+06	0.56	4.70	0.00	1.00	1.00	4.30	0.71	0.49	0.19	7.88E+04	0.331	0.13	31	4.04
A	18.22	293.54	13.83	0.59	277.89	15.85	20.98	2.62	0.40	0.46	183.60	116.36	95.42	0.97	-20.12	0.66	1.45E-04	0.13	587.02	2.19E+06	0.56	4.70	0.00	1.00	1.00	3.83	0.75	0.39	0.16	6.55E+04	0.246	0.10	30	2.91
S	14.44	231.75	11.11	0.80	203.40	13.25	16.49	2.22	0.43	0.44	137.24	67.39	55.26	1.01	9.03	0.66	1.45E-04	0.11	589.15	1.73E+06	0.56	4.70	0.00	1.00	0.96	2.44	0.84	0.26	0.12	4.79E+04	0.114	0.04	31	1.39

Total (in) 28.44

All values are monthly averages

T_a	temperature ($^{\circ}$C)	$z_{veg}=$	1471 cm
v_a	wind speed (km/day)		
T_d	dew point temp ($^{\circ}$C)		
C	cloudiness factor	$G(\Delta\theta)$	leaf conuctance as a function of soil moisture deficit
K_{ET}	extraterrestial solar radiation flux (cal cm^{-2} day^{-1})	$G(T_a)$	leaf conductance as a function of air temperature
e_a	vapor pressure (mb)	$\Delta\rho_v$	difference between actual and saturated air humidity (g m^3)
e_{sat}	saturation vapor pressure (mb)	$G(\Delta\rho_v)$	leaf conductance as a function of air humidity deficit
W_p	precipitable-water content	$G(K_{in})$	leaf conductance as a function of incident solar radiation
τ	atmospheric transmissivity	C_{leaf}	leaf conductance (cm s^{-1})
γ_s	radiation scattering coefficient	C_{can}	canopy conductance
K_{cs}	clear-sky solar r (cal cm^{-2} day^{-1})	PET_{cm}/day	potential evapotranspiration rate (cm/day)
K_{in}	incoming solar r (cal cm^{-2} day^{-1})	PET_{in}/day	potential evapotranspiration rate (in/day)
K	net short-wave solar radiation (cal cm^{-2} day^{-1})	days	number of days that month
ε_{at}	effective emissivity	$PETi_n$/month	monthly potential evapotransiration rate (in/month)
L	net long-wave solar radiation (cal cm^{-2} day^{-1})		
γ	psychrometric constant (mb$^{\circ}$C^{-1})		
K_E	turbelent mass transfer coefficient (cm km^{-1} mb^{-1})		
s	slope of saturation vapor pressure expression (mb$^{\circ}$C^{-1})		
γ_v	latent heat of vaporization (cal g^{-1})		
C_{at}	atmospheric conductance for water vapor (cm/day^{-1})		
C^*_{leaf}	maximum leaf conductance (cm s̀1)		
L_t	transpiriational leaf-area index		
$\Delta\theta$	soil moisture deficit (0-8.4 cm)		

Table 28. Characteristics and runoff for 11 basins, north Lummi Island, Water Year 2004

study basins[1]	dominant geology[2]	precipitation (acre-ft)	runoff (acre-ft)	area (square miles)	area as percentage of all study basins[3]	area as percentage of entire study area[4]	runoff (in)	runoff as a precentage of precipitation
Airport	gmd	258	18	0.12	6.0	3.2	2.7	7.0
Centerview	gmd, ss upper reaches	819	348	0.39	19.1	10.1	16.7	42.5
Curry	ebd	279	7	0.13	6.5	3.4	1.0	2.6
Eagles Nest	gmd, ebd lower, ss upper reaches	183	5	0.09	4.3	2.2	1.1	2.9
Fern Point	gmd	290	16	0.14	6.7	3.6	2.2	5.6
Fire Station	gmd, lesser ebd	707	175	0.34	16.5	8.7	9.8	24.8
Isle Aire	gmd	277	10	0.13	6.5	3.4	1.5	3.7
Lummi Point	ebd	220	58	0.11	5.1	2.7	10.4	26.5
Richards Mtn	ss, lesser gmd	558	107	0.27	13.0	6.9	7.5	19.1
School	gmd	136	11	0.07	3.2	1.7	3.2	8.0
Southeast	gmd	565	91	0.27	13.2	6.9	6.3	16.1

1. Study basins are shown in Figure 29

2. Dominant geology is listed first: glaciomarine drift (gmd), emergence beach deposits (ebd), sandstone (ss). Geology of basins is based on Figure 10 and possible correlations to units in published Interpretation A (Section 5.1)

3. Total area of 11 basins is 2.05 square miles

4. Total area of north Lummi Island study area is 3.87 square miles

Sources:

Study basin names, areas, and runoff volumes are from Nielson and Armfiled, written communication

Precipitation is based on West Shore Gauge (39.36 inches), from Marshall et al., written communication

Table 29. Recharge estimates and variables of water-mass balance equation, north Lummi Island, Water Years 2001-2004. The water-mass balance equation is discussed in Section 5.7.

water year	precipitation (in)	actual evapotranspiration (in)	potential evapotranspiration (in)	runoff (in)	runoff (in)	recharge[1] (in)	recharge[2] (in)	recharge (in)	recharge
		lower bound	upper bound	lower bound	upper bound	lower bound	upper bound	average	as a percentage of precipitation
2001	26.5	16.0	24.4	2.0	3.8	0.0	8.5	4.2	16.0
2002	34.9	16.0	23.4	2.7	5.1	6.4	16.2	11.3	32.3
2003	25.1	16.0	25.8	1.9	3.6	0.0	7.2	3.6	14.3
2004	39.4	16.0	28.4	3.0	5.7	5.2	20.3	12.8	32.4
							average	**8.0**	**23.8**

1. Lower bounds for recharge were calculated using the upper bounds for evapotranspiration and runoff. The lower bounds for recharge during WY 2001 and WY 2003 were set to zero to avoid using a negative value

2. Upper bounds for recharge were calculated using the lower bounds for evapotranspiration and runoff

Table 30. Recharge estimates and input variables for the chloride-mass balance equation, north Lummi Island, Washington, Water Year 2004. The chloride-mass balance equation is discussed in Section 5.7.

water year	precipitation (in)	FWD[1] (mg/m^2)	$C_g{}^2$ (mg/l)	runoff (in)	runoff (in)	recharge (in)	recharge (in)	recharge (in)	recharge
				lower bound	upper bound	lower bound	upper bound	average	as a percentage of precipitation
2004	39.4	2359	19	3.0	5.7	4.2	4.5	4.3	10.9

1. FWD = total of wet and dry atmospherically-deposited chloride (mg/m^2). The average of two years (1997-1998) measured on Lopez Island (Orr et al., 2002) was used as FWD input

2. C_g = concentration of chloride in groundwater (mg/L). Median chloride in groundwater used as input is from wells completed above sea level sampled fall 2002 and spring 2003

Table 31a. Median values of selected water chemistry parameters for all aquifers, north Lummi Island Washington, fall 2002

parameter	minimum	maximum	median	standard deviation	number of samples
pH	6.8	9.8	8	0.67	66
specific conductance[1] (μS)	122	11000	401	1249.9	74
total dissolved solids (mg/L)	50	>10000	160	1155	72
oxidation-reduction potential (mV)	-283	168	94	75.7	69
salinity (g/L)	0.1	6.3	0.2	0.7	73
chloride (mg/L)	9.3	3231	18.8	376.1	73
calcium (mg/)	0.4	568.3	22.2	65.7	73
sodium (mg/L)	6.4	1345.2	31.7	157	73

1. Specific conductance is temperature corrected by YSI-30 meter using reference temp of 25°C

Table 31b. Median values of selected water chemistry parameters for all aquifers, north Lummi Island, Washington, spring 2003

parameter	minimum	maximum	median	standard deviation	number of samples
pH	6.7	9.6	8.1	0.6	44
specific conductance[1] (μS)	124	10650	408	1121	77
total dissolved solids (mg/L)	10	>10000	140	1134	75
oxidation-reduction potential (mV)	-189	185	84	75.4	76
salinity (g/L)	0.1	6.1	0.2	0.7	76
chloride (mg/L)	5.0	3578.4	17.5	423.3	75
calcium (mg/)	<.1	>516	16.4	63.2	75
sodium (mg/L)	2.0	1288.0	31.0	152.4	75

1. Specific conductance is temperature corrected by YSI-30 meter using reference temp of 25°C

Table 32. Median values for selected water chemistry parameters by aquifer, north Lummi Island, Washington, fall 2002-spring 2003

parameter	dug wells	Centerview	Constitution	Greenstone	Hilltop Deep	Lane Spit	Lane Spit Deep	Legoe Bay	Loganita	Nugent	Sandstone	West Shore
sample size	11	2	4	5	2	6	1	25	3	22	63	2
pH[1]	7	8	7.8	8.5	7.8	8	-	8.3	7.3	8.1	7.9	7.3
specific conductance (μS)[2]	292.2	456.6	134.2	335	445.4	300.8	308	377.7	434.6	379.8	456.6	321.9
total dissolved solids (mg/L)	110	165	65	135	150	120	90	140	165	140	180	110
redox potential[3] (mV)	136	98	115	99	111	-20	0	100	72	97	74	90
salinity[4] (g/L)	0.1	0.2	0.1	0.2	0.2	0.1	0.1	0.2	0.2	0.2	0.2	0.2
chloride (mg/L)	15.8	35.3	9.0	16.9	23.1	13.6	12.8	17.9	17.4	15.8	20.9	22.2
calcium (mg/L)	9.1	10.5	7.0	3.0	7.2	14.5	9.4	20.4	8.9	25.4	10.5	13.4
sodium (mg/L)	13.0	75.6	10.9	64.0	62.7	15.5	13.0	21.3	14.8	21.2	67.3	20.6

1. Sample size is 7 for dug wells, 1 for Hilltop Deep, 4 for Lane Spit, 18 for Legoe Bay, 1 for Loganita, 16 for Nugent, 47 for Sandstone, and 1 for West Shore aquifers

2. Sample size is 10 for dug wells, 6 for Greenstone, 23 for Nugent, and 66 for Sandstone aquifers

3. Sample size is 8 for dug wells, 6 for Greenstone, 2 for Loganita, and 61 for Sandstone aquifers

4. Sample size 64 for Sandstone Aquifer

No data available for Blizzard or Village Point aquifers

Table 33. Major ion concentrations for 5 wells and their ratios to chloride in seawater, north Lummi Island, Washington, winter 2005. Concentrations of major ions in seawater are listed in Table 3.

well ID	Cl⁻ (mg/L)	Na⁺ (mg/L)	SO₄²⁻ (mg/L)	Mg2+ (mg/L)	Ca²⁺ (mg/L)	K⁺ (mg/L)	HCO₃⁻ (mg/L)
04J	59	172	86	ND	3	ND	131
04N	154	82	42	18	66	3	143
09G	160	76	27	21	53	6	139
09S	24	62	5	10	19	6	123
04F	64	217	216	1	10	3	113
				ratio to Cl⁻			
04J	1	2.92	1.46	0.00	0.05	0.00	2.22
04N	1	0.53	0.27	0.12	0.43	0.02	0.93
09G	1	0.47	0.17	0.13	0.33	0.04	0.87
09S	1	2.57	0.20	0.41	0.80	0.23	5.13
04F	1	3.39	3.38	0.02	0.16	0.05	1.77
seawater	**1**	**0.56**	**0.14**	**0.07**	**0.02**	**0.02**	**0.01**

ND = not detected

Table 34a. Calcium concentrations related to sea level, north Lummi Island, Washington, fall 2002-spring 2003

	minimum (mg/L)	maximum (mg/L)	median (mg/L)	standard deviation	number samples
bedrock wells completed above sea level	152	7	30	32	19
bedrock wells completed below sea level	568	0	29	19	31
Pleistocene drilled wells completed above sea level	13	4	9	4	6
Pleistocene wells completed below sea level	52	3	17	11	57

Table 34b. Sodium concentrations related to sea level, north Lummi Island, Washington, fall 2002-spring 2003

	minimum (mg/L)	maximum (mg/L)	median (mg/L)	standard deviation	number samples
bedrock wells completed above sea level	76	16	46	17	19
bedrock wells completed below sea level	1345	18	69	304	33
Pleistocene drilled wells completed above sea level	77	6	16	34	6
Pleistocene wells completed below sea level	93	11	21	19	57

Table 34c. Chloride concentrations related to sea level, north Lummi Island, Washington, fall 2002-spring 2003

	minimum (mg/L)	maximum (mg/L)	median (mg/L)	standard deviation	number samples
bedrock wells completed above sea level	66	12	17.75	14	20
bedrock wells completed below sea level	11	3578	20.9	819	33
Pleistocene drilled wells completed above sea level	6	37	9.95	14	6
Pleistocene wells completed below sea level	194	5	15.9	26	57

Table 35a. Ratio of sodium to calcium (Na:Ca) related to sea level, north Lummi Island, Washington, fall 2002-spring 2003

	minimum (mg/L)	maximum (mg/L)	median (mg/L)	standard deviation	number samples
bedrock wells completed above sea level	0.2	10.2	1.4	2.9	23
bedrock wells completed below sea level	0.3	1428.0	3.2	243.5	44
Pleistocene drilled wells completed above sea level	0.3	23.0	1.6	5.9	21
Pleistocene wells completed below sea level	0.3	12.5	1.3	2.5	59
dug wells	0.5	23.0	1.5	7.8	11

Table 35b. Ratio of sodium to chloride (Na:Cl) related to sea level, north Lummi Island, Washington, fall 2002-spring 2003

	minimum (mg/L)	maximum (mg/L)	median (mg/L)	standard deviation	number samples
bedrock wells completed above sea level	0.5	5.6	2.4	1.4	23
bedrock wells completed below sea level	0.4	7.1	2.9	2.0	43
Pleistocene drilled wells completed above sea level	0.5	2.2	0.9	0.6	10
Pleistocene wells completed below sea level	0.0	5.7	1.2	0.9	59
dug wells	0.3	6.5	1.0	1.8	12

Table 36. Ranges of chloride concentrations by aquifer, fall 2002-spring 2003, north Lummi Island, Washington.

aquifer	minimum (mg/L)	maximum (mg/L)	median (mg/L)	number of samples
dug wells	12	953	15.8	11
Blizzard	-	-	-	0
Centerview	33	38	35.3	2
Constitution	6	11	9.0	4
Greenstone	11	38	16.9	5
Hilltop Deep	22	24	23.1	2
Lane Spit	9	16	13.6	6
Lane Spit Deep	13	13	12.8	1
Legoe Bay	9	26	17.9	25
Loganita	16	19	17.4	3
Nugent	5	194	15.8	22
Sandstone	9	3578	20.9	63
Village Pt	-	-	-	0
West Shore	21	23	22.2	2

Table 37. Distance from bottom of well to Ghyben-Herzberg predicted freshwater/seawater interface for wells completed below sea level, north Lummi Island, Washington

well ID	aquifer	water level elev. (ft)	completion elev (ft)	distance bottom of well to theoretical interface (ft)	water level elev. when theoretical interface reaches bottom of well	Cl⁻ fall (mg/L)	Cl⁻ spring (mg/L)
33F	Lane Spit Deep	8	-195	114	5	-	13
04E	Sandstone	35	-193	1168	5	24	21
04Q	Sandstone	48	-179	1690	4	-	56
09S	Hilltop Deep	12	-174	294	4	24	22
04J	Sandstone	50	-156	1778	4	45	63
04N	Sandstone	85	-32	3356	1	112	129
05E	Sandstone	17	-107	566	3	27	21
04F	Sandstone	21	-104	728	3	-	58
32L	Sandstone	12	-90	392	2	32	33
08O	Sandstone	1	-85	-49	2	3231	3578
15D	Nugent	11	-85	342	2	16	16
32S	Sandstone	48	-78	1789	2	20	18
09G	Nugent	7	-75	217	2	194	95
05P	Sandstone	22	-68	790	2	35	36
05L	Legoe Bay	11	-64	370	2	26	21
04Z	Sandstone	52	-63	1966	2	17	18
32R	Loganita	9	-62	307	2	-	16
10V	Legoe Bay	14	-61	477	2	24	23
10B	Greenstone	65	-61	2470	2	17	11
10X	Legoe Bay	10	-58	343	1	14	12
10J	Greenstone	55	-51	2092	1	-	-
09R	Legoe Bay	10	-50	333	1	23	20
09M	Legoe Bay	12	-50	399	1	13	14
09K	Legoe Bay	7	-50	230	1	17	15
33T	Lane Spit	12	-49	422	1	16	13
15S	Nugent	9	-48	322	1	16	13
32Q	Sandstone	138	-47	5341	1	16	-
29C	Sandstone	16	-45	597	1	87	65
15A	Nugent	9	-44	322	1	12	13
33G	Lane Spit	12	-44	410	1	12	9
05W	Sandstone	57	-38	2170	1	-	17
32N	Sandstone	149	-37	5784	1	15	12
04A	Lane Spit	3	-35	95	1	15	14
32H	Loganita	7	-32	247	1	19	17
15K	Nugent	9	-31	318	1	13	13
32B	Sandstone	35	-29	1332	1	-	-
09I	Nugent	8	-28	283	1	21	20
09B	Legoe Bay	13	-28	460	1	10	9
16K	Nugent	7	-26	246	1	28	16
15P	Nugent	8	-26	294	1	17	17
15O	Nugent	8	-25	293	1	30	5

16V	Nugent	4	-24	150	1	-	15
32T	Sandstone	143	-24	5538	1	-	-
09V	Nugent	16	-22	611	1	-	-
04G	Legoe Bay	12	-22	432	1	-	16
04I	Sandstone	55	-18	2112	0	20	16
09L	Legoe Bay	13	-15	473	0	16	14
04V	Sandstone	53	-12	2041	0	21	19
09A	Legoe Bay	13	-11	485	0	-	-
04C	Legoe Bay	14	-10	555	0	21	19
09J	Nugent	18	-7	694	0	-	-
04T	Sandstone	34	-6	1332	0	21	13
09Q	Nugent	13	-5	501	0	13	14
10Y	Greenstone	70	-4	2733	0	-	-
05O	Legoe Bay	11	-3	434	0	19	-
32P	West Shore	24	-2	949	0	23	21
10M	Nugent	17	0	650	0	11	12

Table 38. Wells completed above sea level with chloride concentrations greater than 19 mg/L (median Cl⁻ concentration for all wells), north Lummi Island, Washington, fall 2002-spring 2003

well ID	aquifer	completion elev. (ft)	Cl⁻ (mg/L) highest
04P	dug well	2	953
04Y	Centerview	44	37
09C	Greenstone	44	38
32X	Sandstone	93	66
33D	Sandstone	81	52
33M	Sandstone	56	36

Table 39. Changes in ion concentrations for wells experiencing greater than 15% change in chloride, north Lummi Island, Washington, fall-2002-spring 2003. Positive values indicate higher concentrations in fall.

well ID	aquifer	water level elev. (ft)	completion elev. (ft)	Cl^- fall (mg/L)	Cl^- spring (mg/L)	percent change	Na^+ fall (mg/L)	Na^+ spring (mg/L)	percent change	Ca^{2+} fall (mg/L)	Ca^{2+} spring (mg/L)	percent change
15O	Greenstone	8	-25	30	5	83	14	14	-5	31	25	19
32K	Greenstone	9	-66	128	49	62	151	127	16	38	18	52
09G	Nugent	7	-75	194	95	51	85	77	9	52	41	22
16K	Nugent	7	-26	28	16	43	37	30	21	12	7	40
04T	Sandstone	34	-6	21	13	40	29	30	-4	39	36	9
10E	Constitution	133	109	9	6	39	6	6	0	6	4	25
09P	Legoe Bay	8	-37	22	14	38	17	18	-3	25	19	23
10B	Greenstone	65	-61	17	11	35	64	69	-8	2	0	79
10D	dug well	149	145	16	12	28	13	12	7	8	8	5
29C	Sandstone	16	-69	87	65	25	200	148	26	54	-	-
33G	Lane Spit	12	-44	12	9	23	13	14	-8	22	10	55
05E	Sandstone	17	-107	27	21	21	78	62	20	5	4	25
32M	Sandstone	154	-28	18	14	21	16	17	-2	50	42	14
15S	Nugent	9	-48	16	13	19	11	11	5	33	27	18
10C	Constitution	157	114	11	9	18	15	16	-7	13	9	33
32N	Sandstone	149	-36	15	12	18	20	20	-1	41	31	23
04I	Sandstone	55	-18	20	16	18	100	104	-4	6	3	47
05L	Legoe Bay	11	-64	26	21	16	40	38	5	21	16	23
09R	Legoe Bay	10	-50	23	20	16	57	55	3	9	6	34
04K	Sandstone	48	15	20	17	16	38	37	4	33	26	22
10F	dug well	116	114	14	18	-30	20	24	-23	19	29	-57
33D	Sandstone	177	81	37	52	-38	27	29	-6	47	46	3
04J	Sandstone	50	-156	45	63	-39	157	171	-9	1	0	60
32X	Sandstone	164	92	15	66	-337	37	39	-8	30	22	27
04P	dug well	6	1	84	953	-1038	23	307	-1252	48	172	-260

Table 40. Wells with ratios of sodium to chloride (Na:Cl) close to seawater (mixing ratio), north Lummi Island, Washington, fall 2002-spring 2003

well ID	aquifer	completion elev. (ft)	Na:Cl	Ca:Cl
08O (spring)	Sandstone	-85	0.36	0.10
08O (fall)	Sandstone	-85	0.42	0.17
09G (fall)	Nugent	-75	0.44	0.27
09C (fall)	Greenstone	44	0.46	1.50
15O (fall)	Nugent	-25	0.46	1.00
09C (spring)	Greenstone	44	0.50	1.20
33D (spring)	Sandstone	81	0.56	0.89
04N (spring)	Sandstone	-32	0.59	0.35
32X (spring)	Sandstone	92	0.60	0.33
04N (fall)	Sandstone	-127	0.64	0.44
15S (fall)	Nugent	-48	0.70	2.03
32H (fall)	Loganita	-32	0.72	0.47
33D (fall)	Sandstone	81	0.73	1.27

mixing ratio Na:Cl = 0.56
mixing ratio Ca:Cl = 0.02

Table 41. Wells experiencing some degree of seawater intrusion, north Lummi Island, Washington, fall 2002-spring 2003

	well ID	aquifer	water level elev. (ft)
Definitely Intruded	04N	Sandstone	85
	04P	dug well	6
	08O	Sandstone	1
	09G	Nugent	8
	32K	Sandstone	9
Probably Intruded	04F	Sandstone	21
	04J	Sandstone	50
	04Q	Sandstone	48
	15O	Nugent	8
	29C	Sandstone	16.5
Possibly Intruded	04D	Sandstone	99
	04T	Sandstone	34
	09C	Greenstone	112
	09P	Legoe Bay	8
	16K	Nugent	7
	32L	Sandstone	12
	32X	Sandstone	165
	33D	Sandstone	177
	33M	Sandstone	180

APPENDIX A: Detailed Methods, Assumptions and Sources of Error

Additional details of methods, assumptions, and sources of error for tasks accomplished in support of the objectives of this study are listed below. Section, figure and table numbers correspond to numbers in the body of the study text. Two new tables (A-1 and A-2) are introduced in this Appendix.

DETAILED METHODS

Domestic Well Data Base (Section 4.1)

- Twelve drilled wells could not be matched to well logs. Ten of these wells were assigned to aquifers by creating dummy logs. After comparing surveyed well-head elevations and measured completion depths to the stratigraphic model, I determined that 8 of these wells (04D, 04F, 04M, 04R, 04S, 05J, 09C, 32K, 32W, 33W) were completed in the Sandstone Aquifer and one (09P) is completed in the Nugent Aquifer. It is unclear whether well 09C is completed in Pleistocene deposits or greenstone. Well 09H is completed in Pleistocene deposits at a depth greater than the modeled depth of the Legoe Bay Aquifer and less than the depth of the Hilltop Deep Aquifer. As a result, data from these two wells were generally not used.

- Dummy well logs were constructed for 2 wells with no well log available (04I, 04K) based on measured total depth and an adjacent well log that lies within 200 feet of these wells. These wells were determined to be completed in the Sandstone Aquifer.

- The 12 wells listed above were not used in developing the stratigraphic model. Water level and water chemistry data from these wells were used.

Bedrock Surface Elevation Model (Section 4.2)

Detailed procedures used in developing the bedrock surface elevation model are listed below.

- Well driller's descriptions of bedrock strata were interpreted on a broad and specific basis (Appendix B). The broad interpretation, used in modeling bedrock, classifies all bedrock as either sandstone or greenstone. The specific interpretation, used to identify specific facies, classifies bedrock as sandstone, shale, or conglomerate (of the Chuckanut Formation) and greenstone. Limited data prevented me from using the specific interpretation in modeling the bedrock.

- Bedrock outcrops mapped in previous geologic studies were incorporated into Groundwater Modeling Software (GMS) as dummy well logs consisting entirely of sandstone or greenstone. Over 60 dummy well logs created to represent the shape of mapped bedrock-unconsolidated contacts and to capture the elevations of bedrock outcrops.

- A preliminary bedrock surface triangle irregular network (TIN) was created in GMS through linear interpolation of 3-D vertices from dummy boreholes and from 49 well logs for wells that penetrate to bedrock.

- An additional 48 well logs from located wells completed in unconsolidated deposits were incorporated into GMS. Locations where these boreholes penetrated the preliminary bedrock surface TIN were identified. The bedrock surface elevation at these locations was nominally determined to lie 30 feet below the bottom of these wells. Using these new vertices, a second preliminary bedrock surface TIN was created.

- A DEM was imported into GMS to represent the land surface elevation. A land surface TIN was created from DEM vertices by interpolating between the vertices and extrapolating them to polygon in the shape of the study area using inverse distance-weighted (gradient plane) methods. The second preliminary bedrock surface TIN was compared to the land surface TIN and field observations.

Regions of the bedrock surface TIN that violated the land surface TIN were adjusted. At most places, it was determined that the bedrock TIN lies slightly under the DEM TIN unless a true bedrock outcrop was known to be present. Using these new vertices, a third preliminary bedrock surface TIN was created and extrapolated to a polygon in the shape of the study area using linear methods.

- The third preliminary bedrock surface TIN was validated by examining previous depth-to-bedrock (Schmidt, 1979; Kelly, 1998) and additional geologic (Carroll, 1980; Blake, in progress) mapping efforts and by incorporating additional well logs. Minor adjustments were made to lower the third preliminary bedrock surface TIN along Legoe Bay Rd, half way between Village Point and the intersection with Tuttle Ln. and near Richards Mtn. and Hill 362. These new vertices were used to create a final bedrock surface TIN representing the elevation of the bedrock surface at all locations in the study area.

- The region below the final bedrock surface TIN was filled to an elevation of -300 feet to create a bedrock solid model. This depth was chosen because it is near the bottom of the deepest well used in the study (05C, -289 feet). The sandstone is modeled to an elevation –261 feet because this is the deepest known occurrence of sandstone at what appears to be a contact between sandstone and greenstone (well 05C). Greenstone was modeled below sandstone from –261 to –300 feet.

- The location of the contact between sandstone and greenstone, in map view, was delineated based on well logs to the north that are completed in sandstone and well logs to the south that are completed in greenstone. The greenstone outcrop at Lover's Bluff was also considered in determining the location of this contact.

Pleistocene Stratigraphic Model (Section 4.2)

Detailed procedures used in developing this model are listed below.

- Well driller's descriptions of Pleistocene strata were interpreted on a broad and specific basis (Appendix B). The broad interpretation, used in modeling

262

Pleistocene stratigraphy, classifies texture as either fine-grained or coarse-grained based on assumed differences in relative hydraulic conductivities. The specific interpretation, used to make detailed examinations of variations in texture, classifies texture as either soil, hardpan, sand, fine sand, gravel/sand, clay, sand-clay, gravel-clay, or sand/gravel-clay. Limited time and data prevented me from using the specific interpretation in modeling Plestocene stratigraphy because of the highly heterogeneous stratigraphic setting.

- The broad interpretation of driller's descriptions of strata into either fine-grained (potential aquiclude) or coarse-grained (potential aquifer) material was primarily based on the presence of clay in driller's notes. In the well logs examined, driller's descriptions of fine-grained materials are dominated by mixtures of clay, silt, sand, gravel, and cobbles that were broadly designated as silt-clay diamicton. The coarse-grained materials are dominated by sands of various textures and broadly designated as sand. The broadly interpreted well log data were imported into GMS.

- Approximately 140 preliminary cross sections were manually constructed between wells in GMS using the following fundamental geologic concepts for sediments deposited in a fluvial envornment:

  a. Sedimentary units are generally deposited horizontally. Therefore, they will correspond to units in adjacent wells at roughly the same elevation, maintaining a more-or-less horizontal orientation.

  b. Lenses of coarse or fine-grained material will generally have a flat top surface but may have irregular bottoms.

  c. Lenses of coarse or fine-grained material will tend to pinch-out toward the edge of their lateral extent. Pinch-outs are common when a lens of sand or fine-grained material is discontinuous between adjacent wells. The pinch-out may be abrupt for particularly thick coarse-grained lenses.

d. Thick lenses are generally more laterally extensive than thin ones.

e. Lenses of fine-grained material are generally more laterally extensive than coarse-grained lenses.

- Using the 3-D capability of GMS, preliminary cross sections were examined from all angles to ascertain relationships between coarse-grained lenses.

- For each coarse-grained lens, a polygon was drawn in map view to represent its lateral extent.

- Each polygon was populated with vertices representing the top of each coarse-grained lens at every well where it was present and in between wells using the preliminary cross sections. These vertices were interpolated, using inverse distance-weighted (gradient plane) methods, to the polygon to create a top elevation TIN for the coarse-grained lens.

- The thickness of coarse-grained strata in 97 well logs range from 2 to 87 feet with a median thickness of 5 feet. The median value was assigned as a default coarse-grained lens thickness when no other data were available.

- The bottom of each coarse-grained lens was determined at every well were it was present and between wells using the preliminary cross sections or the median coarse-grained lens thickness of 5 feet where data were insufficient. A bottom elevation TIN was created for each coarse-grained lens using the same technique as above.

- Solid models for each coarse-grained lens were created by filling the region between top and bottom TIN's. These solids were clipped where they intersected the bedrock surface elevation model and where they intersected the land surface TIN (created from a DEM). Different shapes among top and bottom elevation TIN's and clipping solids to the modeled bedrock and land surface resulted in sand unit solids that often pinch-out along the edges.

- Overlapping coarse-grained solids were combined so that a total of 29 separate units are present in the final model. Several of these were later combined into aquifers where it was evident that the coarse-grained solids are connected and hydraulic head distributions are similar.

- All bedrock, coarse-grained, and fine-grained units were illuminated and viewed in the map plane to create a revised geologic map. Cross sections were cut through the solids of the stratigraphic model.

- Area, volume, and mean top elevation for coarse-grained solids were calculated using GMS. Minimum and maximum thicknesses of the coarse-grained solids were estimated by examining top and bottom elevation TIN's. Because the coarse-grained solids are modeled with irregular top and bottom surfaces, average thicknesses were estimated by dividing the volume of a solid by its area.

- Sixteen on-site sewage disposal applications obtained through Whatcom County Health Department were examined to define subsoil textures at depths of 4-5 feet below land surface.

Hydrostratigraphy and Aquifer Identification (Section 4.3)

Detailed procedures used to delineate hydrostratigraphy and identify aquifers are listed below.

- Well logs were examined for evidence of water to identify water bearing units. A sand unit was determined to be water bearing if the driller noted the presence of water or if wells were screened in the sand unit.

- Water bearing sand units with wells screened in them were designated as aquifers. Where two or more water bearing sand units are connected, the composite was designated as a single aquifer. Because some are composed of several sand units, all aquifers were given noun names. For example, SU-4, SU-6, and SU-7

265

comprise the Nugent Aquifer.   The aerial extents of the bedrock aquifers were
defined as the regions that enclose all wells known to be completed in either
sandstone or greenstone.

- The stratigraphic model and water level data were compared to identify saturated
  and unsaturated regions within the aquifers. For the two most areally extensive
  Plesitocene aquifers, potentiometric surfaces, derived from recently collected
  water level data, were used to create solids representing the saturated volume of
  each aquifer. Methods for developing potentiometric surfaces are described in
  Section 4.5. For less extensive aquifers with fewer water level data, available
  data were used estimate the top of the saturated portion of these aquifers. A
  potentiometric surface was also used to create a solid representing the saturated
  and unsaturated regions of the Sandstone Aquifer that has a bottom elevation of –
  261 feet, the modeled maximum depth of sandstone.

- Confining conditions within aquifers were determined to exist where the
  measured water level elevation or mapped potentiometric surface lies above the
  overlying confining layer by a nominal height of 4 feet or more. For sand units,
  the confining material is silt-clay diamicton. Available well log data were
  insufficient to determine the effect of less fractured or less permeable facies on
  confining conditions within the bedrock. Instead, confining conditions within
  bedrock were determined to exist where water level elevations are greater than the
  overlying silt-clay diamicton or land surface elevation where the silt-clay
  diamicton is absent.

Hydraulic Properties (Section 4.4)

Detailed procedures used to determine the hydraulic properties of each aquifer are listed
below.

Well Yield and Specific Capacity. Well performance tests are conducted by the driller
during drilling and are found on most well logs. Well performance test data includes a

pumping rate, semi-static drawdown water level, and pumping time to achieve the semi-static drawdown water level. Each well with this data was assigned to an aquifer by examining well log, water level data, and the stratigraphic model.

- Pumping rate data from 101 study wells were used to determine median and average well yields for each aquifer.

- Well performance test data required for calculating specific capacity were taken from well logs and, for one well (32Q), an existing pump test conducted by a consultant (Tables 13a and 13b). These data were used to solve the specific capacity equation (Fetter, 1980) for 77 study wells:

    $S_c = Q/h_0\text{-}h$

    Where S_c = specific capacity, expressed in gallons per
    minute per foot of drawdown (gpm/ft)
    Q = discharge or pumping rate (gpm)
    h_0 = static water level before test (ft)
    h = "semi-static" water level reached after pumping duration (ft)

- Results were used to determine median and average specific capacities for each aquifer

- Well performance test data showing zero drawdown in 9 wells were excluded (Table 16).

Effective Porosity.   The effective porosity of the geologic material comprising an aquifer is required to make a steady-state groundwater quantity estimate.

- Each sand unit was assigned a primary texture based on well log data and textures were assigned a value for effective porosity based published data for similar geologic materials (Appendix C and Tables 7a-7c). Each aquifer was then

267

assigned an average effective porosity from the values of its composite sand units (Table 22).

Transmissivity. Transmissivity is a property of an aquifer that can be used to determine hydraulic conductivity. It is defined as the product of hydraulic conductivity and saturated thickness. Since hydraulic conductivity was also unknown, transmissivity was calculated from well performance data in well logs. This was accomplished by iteratively solving the modified Theis equation (Ferris et al., 1962) for 77 wells with complete well performance test data and known screened interval or saturated open intervals (for wells completed in bedrock) using Math CAD. This method has been applied in other studies of local hydrogeology for example, Kahle and Olsen, 1995; Kahle, 1998:

$$s = Q/4\pi T \times \ln(2.25Tt/r^2S)$$

Where
s = semi-static water level drawdown (ft)
Q = pumping rate (ft^3/day)
T = transmissivty (ft^2/day)
t = pumping duration to achieve semi-static water level drawdown (days)
r = well diameter (ft^2)
S = storage coefficient = .0001 for confined aquifer

- For each aquifer, transmissivity was calculated using the geometric mean of values for all wells completed in the aquifer.

Hydraulic Conductivity. Well performance test data were used to quantify horizontal flow to 77 wells. Horizontal hydraulic conductivity was calculated at each well by dividing transmissivity by the length of the screened or, for wells completed in bedrock, the saturated open interval. For wells with open-ended casings (either open or gravel packed), the following equation was used (Bear, 1979):

268

Kh = Q/4πsr

Where
Kh = hydraulic conductivity (ft/day)
Q = pumping rate (ft3/day)
s = semi-static water level drawdown (ft)
r = well diameter

- For each aquifer, a value for horizontal hydraulic conductivity was calculated using the geometric mean of values for all wells completed in the aquifer.

Water Level Trends (Section 4.5)

- Static water levels were measured using a Waterline Envirotech well probe. Water levels were measured in over 80 wells during fall 2002, prior to the onset of seasonal rainfall, with the intention of capturing the lowest seasonal water levels. Most of the same wells were measured again in spring 2003 with the intent of capturing higher water levels. A difference of less than .02 feet in 5 minutes was determined represent static conditions. Water levels that did not meet this measurement criteria were not recorded.

- Each well was assigned to an aquifer by examining well log and water level data and the stratigraphic model created during this study.

- Potentiometric maps were produced for three aquifers containing sufficient numbers of wells with water level data. Potentiometric surfaces were interpolated to modeled aquifer boundaries using inverse distance weighted (Sheppard's Constant) methods for the Legoe Bay, Nugent, and Sandstone aquifers. Potentiometric surface maps for other aquifers such as the Greenstone Aquifer were not created due to insufficient water level data.

- Water level data from 9 wells with no well log available were used. These wells were assigned to aquifers upon comparing surveyed well-head elevations and

measured completion depths to the stratigraphic model. Of these, 8 wells were included in development of the potentiometric map for the Sandstone Aquifer. One well was included in development of the potentiometric map for the Legoe Bay Aquifer.

- Water levels from a previous Lummi island groundwater study, Whatcom County (1994), were used to make well hydrographs for the period March 1991 through January 1993. Of 38 wells monitored during this period, only 17 were determined to have complete water level data sets.   Seven of these wells were correlated to wells used in this study (Table 21).   Water level trends from this earlier study were evaluated to identify seasonal trends and compared to water levels that I measured to examine long-term trends.

- Precipitation data contained in the Whatcom County report were used to create a hyetograph spanning the 1991-1993 monitoring period. Well hydrographs were compared to the hyetograph to examine water level response to changes in precipitation patterns.

Recharge Estimate Using a Water-Mass Balance (Section 4.8)

A simple mass-balance equation was used to estimate aquifer recharge during Water Years 2001-2004:

RCH = PPT – ET – RNF (Freeze and Cherry, 1979)

Where
RCH = aquifer recharge
PPT = precipitation
ET = evapotranspiration
RNF = runoff

The input and output variables for this equation were quantified from various sources. Detailed procedures are listed below.

Precipitation. Volunteers have continuously recorded precipitation at three unofficial stations in the study area (Section 2.4); (Marshall, et al., written communication, 2004). Data from these gauges were averaged for WY 2001-2004 to obtain the precipitation input variable for the water-mass balance equation.

 Evapotranspiration. The Penman-Montheith equation is a mass-balance and energy budget approach modified to quantify potential evapotranspiration from vegetative surfaces (Penman, 1948; Montheith, 1965). This equation was used to develop a site-specific model to estimate potential evapotranspiration (Tables 27a-d).   Methods used to derive local climatic and vegetative data are described below.

- Local monthly climatic data for this analysis were obtained from observations recorded at the nearest National Weather Service weather station, Bellingham International Airport (National Climatic Data Center). Most climatic factors are established monthly averages that were held constant for each year between WY 2001-2004. Monthly climatic factors that display significant variation from year to year were changed for each year between WY 2001-2004. These factors are temperature, wind speed, and dew point (Table A-1).

- Local vegetative data used as input to the Penman-Montheith model were obtained from several sources. Land cover data from Landsat 4 data were evaluated using GIS (Figure 3). Land cover classes and the percentage of the study area occupied by each class are listed in Table 2. Several land cover classes were combined for input into the Penman-Monteith model (Table A-2).

- The land cover class, mixed deciduous and coniferous forest was interpreted as having equal numbers of deciduous and coniferous trees. Using this assumption, I added ½ of the area occupied by mixed forest to the area occupied by deciduous forest. And, I added ½ of the area occupied by mixed forest to the area occupied by coniferous forest (Table A-2).

271

- The percentage of the study area occupied by land cover classes short grass, medium grass, long grass, and fallow were combined (Table A-2). No fileds in fallow were observed during fieldwork. The evapotranspirative properties assigned to this combined land cover class are from the properties for grasslands found in Dingman (1994); (Table A-2).

- Based on field observations, the dominant deciduous species is red alder and the dominant coniferous species is douglas fir. These species were chosen to represent the deciduous and coniferous forest classes from Landsat 4 data. Evapotranspirative properties, maximum leaf conductance, leaf area index, and vegetation height, of red alder and douglas fir were obtained from Dingman (1994); (Table A-2).

- The following steps were taken to assign area-weighted vegetative values for input to the Penman-Monteith model:

Step 1. Calculate vegetative characteristics for each land cover class (forest/non-forest):

Forest: Fraction of total study area occupied by forest = 56.47%

C_{*Leaf} = (value from Table A-2) x (% total occupied by species)/ % total occupied by forest
     coniferous (Douglas Fir) = (.83) x (.1725)/ .5647 =   .25
     deciduous (Red Alder)   = (.29) x (.3922)/ .5647 = $\underline{+\ .20}$
                                      = .45 cm s^{-1}

LAI = 6
Z_{veg} =2500 cm

Non-forest: Fraction of total study area occupied by non-forest = 43.53%

C_{*Leaf} = (value from Table A-2) x (% total occupied by species)/ % total occupied by non-forest
     scrub shrub vegetation   = (.53) x (.051)/ .4353 =   .062
     grasses (short, medium, long, fallow) = (.8) x (.3572)/ .4353 =   .656
     rock, water, urban   = (0) x (.022)/ .4353   = $\underline{+\ \ \ 0}$
                                        = .72 cm s^{-1}

LAI = 3 (shrub, grasses) , = 0 (rock, water, urban)

Z_{veg} = (value from Table A-2) x (% total occupied by vegetation type)/ % total occupied by non-forest

shrub	= (800) x (.051)/ .4353 =	94
grasses	= (50) x (.3572)/.4353 =	41
rock, water, urban	= (0) x (.022)/ .4353 =	+ 0
		= 135 cm

Step 2. Combine vegetative characteristics for both land cover classes (forest/non-forest) for input to site-specific Penman-Montheith model:

C_{*Leaf} = (value from step 1) x (% total occupied by category)/ % total study area

Forest: (.45) x (.5647)/ 1.0 = .25

Non-forest: (.72) x (.4353)/ 1.0 = + .31

$= .56 \text{ cm s}^{-1}$

LAI= (value from step 1) x (% total occupied by category)/ % total study area

Forest: (6) x (.5647)/ 1.0 = 3.4

Non-forest: (3) x (.4353)/ 1.0 = + 1.3

= 4.7

Z_{veg}= (value from step 1) x (% total occupied by category)/ % total study area

Forest: (2500) x (.5647)/ 1.0 = 1412

Non-forest: (135) x (.4353)/ 1.0 = + 59

= 1471 cm

- Potential evapotranspiration estimates for WY 2001-2004 were derived from the Penman-Montheith model to serve as the upper bound for evapotranspiration in the water-mass balance equation. Estimated actual evapotranspiration from a study of the nearby Lake Whatcom watershed (Kelleher, personal communication, 2004) was used as a lower bound for evapotranspiration in the water-mass balance equation.

Runoff. Runoff was estimated from direct discharge measurements of 11 intermittent streams that drain small basins in the study area.

- Discharge was measured by volunteers during WY 2004 using a constant volume container (stop watch and bucket) and flow velocity meter for larger streams (Neilson and Armfield, 2004 written communication). Discharge was measured at the outlet of culverts passing under the roads that follow the shoreline of the island.

- Measurements were made for every basin roughly twice a week during the wet season and during and following precipitation events in the dry season, after streams stopped flowing in the spring. Nielson and Armfield extrapolated between discharge measurements to estimate monthly discharge for each basin.

- The areas of the 11 basins were estimated from GIS by Nielson and Armfield.

- Using discharge results of Nielson and Armfield's study, I derived a single area-weighted average to represent total runoff from the 11 basins that they measured.

- The combined area of these 11 basins represents only about one half of the total area of north Lummi Island, but almost all of the known surface water outlets. For this reason, I chose to use the area-weighted average discharge from these basins as an upper bound for runoff across the study area.

- The lower bound for runoff was established by extrapolating the area-weighted average discharge across the study area.

- The upper and lower bounds for runoff in WY 2004 were expressed as a fraction of annual precipitation. These values were used to estimate upper and lower bounds for runoff during years that do not have complete sets of discharge data, WY 2001-2003. Results were applied to the water-mass balance equation.

Recharge Estimate Using a Chloride-Mass Balance (Section 4.9)

An equation for estimating recharge through a chloride mass balance was developed by Maurer et al., 1996 and Prych, 1998 and modified by Orr et al., 2002 to account for dry deposition:

RCH = .0394 x FWD(1-RO/P)/Cg

Where

RCH = aquifer recharge (inches)

FWD = total of wet and dry atmospherically deposited chloride (mg/m^2)

RO = runoff (inches)

P = precipitation (inches)

Cg = concentration of chloride in groundwater (mg/L)

The variable FWD was not measured in this study. A value of 2359 mg/m^2 for the variable FWD was obtained by averaging total wet and dry chloride deposition measured over a two-year period (1997-1998) on neighboring Lopez Island (Orr et al., 2002). The variable RO was obtained from the lower and upper bounds for runoff during WY 2004 (Section 4.7). The variable P was obtained from data collected on north Lummi Island (Section 4.7). For the variable Cg, the median chloride concentration in groundwater for wells completed above sea level was used.

Survey Groundwater Chemistry and Assess Seawater Intrusion (Section 4.10)

Chemical Approach.

- For wells that were thought to be completed below sea level, sampling was conducted during a tide stage of +4 feet or higher in an effort to capture worst-

case conditions for seawater intrusion. This regime was only applied to sampling in fall 2002.

- After a static depth-to-water measurement was taken, sample lines were flushed for 5 minutes prior to sample collection starting from the time that the well pump was energized i.e. after the pressure tank had tripped the pump to on. This effort helped ensure samples were collected from water drawn into the well from the aquifer and not from plumbing fixtures or the well casing.

- Samples were collected prior to any known treatment, except one well (04C) was sampled after a sediment filter. In some cases, this required special arrangements by the well owner to bypass plumbing or required me to draw a sample directly from a storage tank. Water treatment systems observed during fieldwork range from sediment filters to reverse-osmosis systems to arsenic-removal systems.

- Most samples were collected prior to storage tanks that are common in study area wells.

- Samples were analyzed in the field for the following parameters immediately following collection:

pH: A Hannah Instruments pHep Microprocessor pH Tester was used. Samples were stirred until a steady pH reading could be obtained. Daily calibration was conducted in the field using pH 7 and pH 4 solutions.

Specific Conductance: A YSI-30 conductivity/salinity meter was used. This instrument measures conductivity and compensates for water temperature by using a reference temperature set at 25 $^{\circ}$ C to display readings of specific conductance.

Total Dissolved Solids: A Hannah Instruments DiST Waterproof Series Tester (conductivity dip stick) was used.

Oxidation-Reduction Potential: A Hannah Instruments ORP Series REDOX Potential Tester was used.

- Samples were analyzed for ionic constituents in one of two laboratories:

  Calcium and Sodium: These cations were analyzed at Scientific and Technical Services Laboratory, Western Washington University, using a SprectraAA Atomic Absorption Spectrophotometer with Auto Sampling. Samples were analyzed within recommended holding time for metals of 180 days, except about 1/3 of samples from spring 2003 were held up to 210 days. Field blanks from all sampling days indicated zero concentration of calcium and sodium.

  Chloride: This anion was analyzed at Scientific and Technical Services Laboratory, Western Washington University, using a Dionex 2010 Ion Chromatograph. Samples were analyzed within recommended holding time for chloride of 28 days. Field blanks from all sampling days indicated zero concentration of chloride.

  Major Ions: Analyses of 5 samples for major ions (listed above) were conducted by Edge Analytical Laboratories, Burlington, Washington. Samples were analyzed within recommended holding time for chloride of 28 days.

- Results of groundwater chemistry analyses were examined to identify trends in each aquifer identified through the stratigrahic modeling process of this study.

<u>ASSUMPTIONS</u>

Bedrock Surface Elevation Model (Section 4.2)

- Logs from numerous wells completed in the Chuckanut Formation contain descriptions of shale, conglomerate, coal, and sandstone. These facies were lumped together as sandstone in the bedrock model due to insufficient data to capture the complex structure and stratigraphy of the Chuckanut Formation on north Lummi Island.

- Modeling the sandstone to an elevation of –261 feet, based on an apparent contact with greenstone at 05C, is assumed to be a reasonable assumption. This elevation representing the base of the sandstone is close to the thickness of Chuckanut sandstone as shown in the cross section of Carroll (1980).

- For the deepest wells completed in Pleistocene deposits, the actual elevation of the bedrock surface is unknown (for example 10A, 09T, 15C) and the bedrock surface was determined to lie 30 feet below the completion depth of these wells. This serves as a minimum depth-to-bedrock at these locations. Actual bedrock surface may lie at a higher or lower elevation.

- All bedrock south of the sandstone-greenstone contact is assumed to be greenstone despite some well logs south of this contact that describe sandstone. Well logs along Seacrest Drive contain descriptions of greenstone and sandstone but almost always describe the latter as hard and green; modifiers often observed in well logs where greenstone exists. Descriptions of sandstone along Seacrest Drive open the possibility that the Chuckanut Formation extends south of the modeled contact, in a narrow band roughly paralleling Seacrest Drive. In addition, some well logs that lie south of this contact indicate the presence of a thin layer of sandstone on top of greenstone. Insufficient data exist to determine whether these sandstone occurrences are Chuckanut sandstone lying unconformably upon greenstone or a clastic member of the Fidalgo ophiolite known as Deception Pass sandstone. If they are Chuckanut sandstone, the effect

on hydrologic properties of the overall bedrock in this area is assumed to be negligible due to the small thickness of the clastic unit.

- Well 09B is assumed to be completed in bedrock as described in its well log. The presence of bedrock at this location is somewhat anomalous because surrounding wells of equal or greater depth are completed in Pleistocene deposits. Schmidt (1978) also questioned the presence of bedrock at this location but made the same assumption. This bedrock is assumed to be greenstone because it lies outside of the southern most occurrence of sandstone. Additionally, the description of rock in well log 09E is not bedrock (Livermore, 2004).

- Bedrock mapped as sandstone by Easterbrook (1971) is not present along shoreline west of Loganita Lodge. The same applies to sandstone that is also mapped along shoreline east of intersection of Legoe Bay and Nugent roads.

- At nearly all locations, bedrock is mantled by at least a thin veneer of glacial drift and soil. Bedrock outcrops are more rare than some geologic maps suggest. At most locations mapped as bedrock outcrop (Easterbrook, 1971, Lapen, 2000), bedrock is not present at land surface but lies under unconsolidated material. Caulkin, (1959) notes of the glacial drift units "Often these deposits are tightly packed and at some distance might easily be confused with the Chuckanut Formation". The geologic map of Carroll, 1980, incorporated extensive field work and more accurately shows bedrock contacts in map view as dashed lines, indicating that the outcrop is obscured and the contact is inferred.

Pleistocene Stratigraphic Model (Section 4.2)

- Although the vast majority of well logs contain the term "clay", fine-grained material in the study area is assumed to be dominated by silt-size particles. Fine-grained material was broadly classified as silt-clay diamicton for the following reasons:

a. From field observations, Easterbrook, (1971) and Lapen (2000),
    I determined that most occurrences of clayey material are poorly sorted
    diamictic mixtures of clay, silt, sand, gravel, and cobbles.

b. Unlike other parts of western Whatcom County, where clayey Bellingham
    glaciomarine drift is frequently encountered during well drilling, occurrences
    of clean clay on Lummi Island are rare (Livermore, personal communication).

- Well driller's descriptions of strata containing both fine and coarse-grained
  material are assumed to be poorly sorted mixtures of these textures with hydraulic
  properties that are dominated by the fine fraction. This assumption is based on
  data from published geologic reports, field observations, and conversations with
  well drillers experienced in drilling on Lummi Island. Therefore, except where
  the presence of water is specifically noted, poorly sorted mixtures of sand, gravel,
  and silt (described by drillers as clay) were designated as silt-clay diamicton.
  This assumption is based on the following:

  a. Local drillers typically describe mixtures of sand, gravel, and clay in random
      order with no preference for which texture is dominant (Livermore, personal
      communication). For example, a well driller's description of "sand, gravel,
      and some clay" was interpreted as silt-clay diamicton.

  b. Due to size limitations of the Lummi Island ferry, almost all well drilling on
      the island has been done by cable rig operations, which are slower than other
      methods. This method enables well drillers to describe the presence clay (or
      silt) in the strata primarily based on whether the borehole sluffs-in before the
      casing is advanced.

- Strata comprised of sand, gravel, or mixtures of both were assumed to be poorly
  sorted with hydraulic properties that are dominated by sand. These starta were
  designated as sand. Analysis of 111 well logs and descriptions of coarse-grained
  materials from Lapen (2000) indicate that occurrences of clean gravel are rare.

- Where topsoil is noted, the texture of the material immediately underlying the soils was assigned. This assumes that the topsoil is derived from and has nearly the same hydraulic properties as the underlying parent material.

- Where boulders are the only texture noted by a well driller, the texture of the material above and below the boulder was assigned.

- Where hardpan is noted, a silt-clay diamicton texture was assigned.

- The driller is alert to the presence of water, even in small quantities. The slow nature of cable rig operations give drillers a good idea of when water is encountered though, the presence of water within a lens of coarse material is not always noted on the well log. Most lenses of coarse material are water bearing and all located at or below sea level are water bearing (Livermore, personal communication).

- Despite what some well logs suggest, none are screened in clay.

- Geotechnical borehole logs are not available for the study area except for where the ferry dock is located.

- The well log for 05M is unspecific describing "gravel, sand, clay" at all depths. This well log was of limited value in defining hydrostratigraphy. However, the completion depth of this well is assumed to lie in a coarse-grained unit that defines the northern extent of Sand Unit Five (SU-5).

- The use of 111 well-distributed well logs (about 29 well logs per square mile) is sufficient to identify all major lenses of coarse material.

- Only one well log was used to determine presence of sand units SU-21, SU-22, and SU-23. Adjacent wells are completed in bedrock. Extrapolating these sand units over a short distance is a reasonable approach considering that adjacent wells are completed in bedrock.

Hydrostratigraphy and Aquifer Identification (Section 4.3)

- In calculating aquifer volumes in GMS, I assumed that all saturated regions of the aquifer are hydraulically connected and suitable for domestic water use.

- In delineating confining conditions, I made no attempt to identify strata that may cause semi-confined conditions. A semi-confined, or leaky, aquifer is bounded by strata with lower relative hydraulic conductivities that are sufficiently high to allow the vertical migration of water into or out of the aquifer.

- The sandstone aquifer is modeled to a constant depth of 261 feet below sea level.

- The Sandstone Aquifer was determined to be saturated at all places below the potentiometric surface. Determining the actual water table elevation was not possible because wells completed in bedrock collect water over a long open interval, making the demarcation between water bearing and confining strata within the sandstone difficult to identify.   This aquifer, and the Greenstone Aquifer are considered to be mostly unconfined except where in the lower reaches, where water level elevations lie above overlying silt-clay diamicton.

Hydraulic Properties (Section 4.4)

- Well performance data on well logs is assumed to be reasonably accurate. The static water level (drawdown) achieved during the course of pumping is especially important. The duration of pumping for each well was examined to ensure it was reasonably sufficient to achieve a static level.

- The number of well performance tests used to calculate hydraulic properties (77 total) is sufficient to filter the effects of poorly conducted tests.

- The pumping rate listed on well logs is close to the maximum rate that can be supported by a well. This assumes that drillers will pump a well at the highest sustainable rate during well performance testing in order stress the aquifer and satisfy client expectations. This may not always be the case for wells tested with using a drill rig bailer to withdraw water if the aquifer is capable of recharging between bailing intervals. Logs with zero drawdown were not used because the pumping rate used in the performance test did not stress the aquifer (Fetter, 1980).

- A storage coefficient commonly used for confined aquifers (.0001) was used to calculate transmissivity. The use of this value is based on the assumption that aquifers are confined in most places. This assumption will also affect calculations for horizontal hydraulic conductivity that are dependent upon transmissivty.

- During deposition, preferential orientation of bedding and platy minerals, such as clays, can cause differences among horizontal and vertical hydraulic conductivities. Vertical hydraulic conductivity was not estimated but is assumed to be lower than horizontal hydraulic conductivity in most places. An exception might be in bedrock aquifers where flow is dictated by fractures and discontinuities resulting from post-lithification deformation.

Water Level Trends (section 4.5)

- Water level data used to create the three potentiometric maps are from wells that were determined to be completed in each of these aquifers.

- The potentiometric maps represent total hydraulic head at every location and water level distributions across the aquifers assuming that aquifer material is homogeneous.

- Eight wells from the Whatcom County study correlate to wells monitored through this study. This was determined through information from people involved in the earlier study, well locations, well owner names, and water levels.

Groundwater Flow Patterns (Section4.5).

- Groundwater contours on potentiometric surface maps can be used to determine horizontal groundwater flow directions. This assumption ignores the vertical flow component that is probably greatest in the middle portion of the island.

- These contours represent hydraulic gradient and can be used with the estimated values of horizontal hydraulic conductivity for aquifer materials to determine groundwater flow magnitudes.

- Seasonal and long term changes in water levels do not significantly affect groundwater flow patterns.

- For aquifers with limited water level data where potentiometric surface maps were not developed, available water level data gives an approximation the direction of groundwater flow.

- Homogeneity of aquifer material is assumed where potentiometric surfaces were used to characterize groundwater flow patterns. The degree of heterogeneity in the sandstone is likely very high, considering the varying facies of the Chuckanut Formation and patterns of regional fractures and folded bedding. Quantifying the fracture patterns within sandstone is a complex task that is beyond the scope of this study. Fracture patterns in greenstone are unknown, but likely less heterogeneous than the sandstone due to a lack of structure observed by previous geologic mapping (Easterbrook, 1971; Carroll, 1980).

- Heterogeneity of the glacial drift aquifers was not considered but for horizontal groundwater flow is assumed to be negligible.

Total Groundwater Storage Capacity Estimate (Section 4.6)

- This estimate assumes steady state conditions. Without long-term water level monitoring of the same wells and subsequent groundwater modeling, transient state groundwater conditions are difficult to quantify. Transient conditions were not quantified in this study but seasonal change in water levels on an island-wide basis is probably small. Changes in water level elevations (total head) in study wells monitored between fall 2002 and spring 2003 were not significant for most aquifers.

- This estimate assumes the saturated volume of each aquifer has been accurately identified. Total volume and saturated volume for aquifers were taken from solids models in GMS that are based on well log, surface geology, and water level measurement data that produce a best estimate for saturated aquifer volumes.

- This estimate requires assignment of an average effective porosity for each aquifer and assumes limited heterogeneity within each aquifer. Though published values for effective porosity among geologic materials can vary by greater than 50%, most differences are small. An average value was chosen to represent textures that are common in study area, mitigating the effects of heterogeneity of effective porosities for a given aquifer.

Identify Recharge and Discharge Areas (Section 4.7)

The following assumptions were made in identifying recharge areas:

- All recharge to the study area is from precipitation.

- Recharge areas generally lie in topographic highs where unconfined aquifer conditions are present.

- Bedrock is sufficiently fractured to allow recharge along preferential flow paths. In addition to fractures, bedding planes in the sandstone serve as a significant

preferential flow path. Bedding dip data of Carroll (1980) show steeply dipping beds in the sandstone commonly 40 to 60 degrees and in excess of 80 degrees in places.

- Based on the large area covered by the bedrock aquifers, recharge to these aquifers is the major source of recharge for all aquifers. Recharge to sand aquifers through overlying sediments is assumed to be less significant due to smaller areal extent of these aquifers.

- The silt-clay diamicton mantle has moderate vertical hydraulic conductivity. Bedrock receives significant recharge through overlying fine-grained sediments where the silt-clay diamicton mantle is thin. There are very few locations where bedrock is not mantled by at least a thin veneer of glacial drift or soil.

- Where the silt-clay diamction is especially thick, significant recharge does not take place

- Recharge to bedrock through coarse-grained units within the Pleistocene mantle is significant in places.

- Aquifers identified as unconfined receive significant recharge from overlying strata while confined aquifers receive most recharge from an up gradient source.

- Sand units identified in the stratigraphic model abut against bedrock in places, and receive recharge from bedrock at these locations. Potentiometric maps indicate significant decreases in hydraulic head where sand units abut bedrock.

The following assumptions were made in identifying discharge areas:

- If an overlying confining layer is absent, discharge areas generally exist where aquifers and potentiometric surfaces intersect the land surface, usually in topographic lows or steep slopes.

- The presence of surface water or springs in topographic lows may indicate a discharge region.

- Aquifers that intersect the shoreline below sea level were determined to discharge offshore where groundwater flow directions and examination of bathymetric surfaces support.

Recharge Estimate using a Water-Mass Balance (Section 4.8)

- The simple water-mass balance equation accounts for all significant inputs and outputs of water into the north Lummi Island system.

- Land cover classes for short grass, medium grass, long grass, and fallow are assumed to have the same evapotranspirative properties. These are assumed to be the same as for grasslands as listed in Dingman (1994)

- Forests classified as mixed deciduous and coniferous are comprised of equal parts deciduous and coniferous. Field observations support this assumption.

- The evapotranspirative properties of red alder are assumed to be the same as for broad leaf forests as listed in Dingman (1994).

- Monthly discharge estimates from Nielson and Armfield are assumed to be fairly accurate. The characteristics of outlet channels for basins within the study area are conducive to the methods used by Nielson and Armfield for the following reasons.

  a. All channels are diverted through culverts under the roads that line the perimeter of the island leaving little ambiguity to the location of the outlet for each basin. Measurements were taken at the outlets of these culverts that generally lie within 100 ft of shoreline.

  b. The basins are small, producing sufficiently low volumes of discharge that can be captured by the constant volume container method.

c. The intermittent and ephemeral nature of these streams makes them responsive to precipitation events. This causes discharge in most channels to be fairly predictable, favoring the measurement routine chosen by Nielson and Armfield.

- Discharge data measured during WY 2003 were not used because they are less complete and considered to be less reliable than data for WY 2004 (Nielson and Armfield, oral communication, 2004).

- The outlet streams monitored by Nielson and Armfield in 2004 represent all known surface water channels in the study area with the exception of one. The exclusion of the west-to-east flowing stream at the southern boundary of the study area is considered appropriate because it probably receives at least half of its water input from the steep bedrock region that lies just south of the study area.

- Estimated runoff in the study area, expressed as a percentage of annual precipitation, is assumed to be consistent from year to year.

Recharge Estimate Using a Chloride-Mass Balance (Section 4.9)

- Using the chloride mass balance method to estimate aquifer recharge assumes that atmospheric deposition is the only source of chloride in groundwater. Sources of chloride in groundwater other than seawater intrusion are discussed in Section 2.8.

- Use of the value for the variable FWD, obtained from another study (Orr et al., 2002), makes the assumption that FWD on north Lummi Island for any given year is close to the average of the two years of measured FWD on Lopez Island.

Survey Groundwater Chemistry and Assess Seawater Intrusion (Section 4.10)

Chemical Approach

- Groundwater sampling in spring 2003 that was not conducted at tide stage +4 feet or higher does not significantly influence water chemistry results over those collected in fall 2002. This sampling criteria was dropped from spring sampling for the following reasons.

- Field work in fall 2002 revealed that many sites have storage tanks, making the effort to sample during high tide irrelevant. While samples were drawn from a location before water treatment, there were many sites where samples could not be drawn before entering a storage tank.

- The majority of wells did not have elevated chloride concentrations during fall 2002 sampling, making this criteria irrelevant for most wells.

- A tidal effects study of three wells completed below sea level (Whatcom County, 1994) gave no indication of changes in chloride concentrations with tide stage.

- The travel time required for seawater-contaminated groundwater to reach the well screen is likely greater than the 5 minute flushing period applied prior to sample collection.

- The influence of cation-exchange processes caused by remnant Pleistocene marine $Na+$ is assumed to be the dominant source of $Na+$ in groundwater. Dissolution of sodium-bearing minerals is assumed to be a minor source.

SOURCES OF ERROR

Domestic Well Data Base(Section 4.1)

Locating well logs is dependent upon the accuracy of information that was used to match them to wells. Some potential sources of error in matching well logs follow.

- Many wells were located based on information from well owners or tenants and neighbors. This information, if outdated or incorrect, could cause wells to be incorrectly matched to wells. In most cases, several pieces of information were referenced to confirm correct well log matching. For example, if a previous property owner's name was used to match a well log to a well, I would cross-reference the water level or quarter/quarter section description from the well log against data I collected during this study.

- Well logs can be incorrectly matched to wells when property owners have drilled more than one well, especially if the wells were drilled over a similar time frame.

- Ten wells with no well logs were assigned to aquifers. Despite the absence of well logs, I am confident that the methods employed ensure that these wells were correctly assigned to respective aquifers.

Horizontal Location and Vertical Elevations (Section 4.1)

- The use of a survey-grade GPS to measure well-head elevations does not ensure that the precision of all measured points meets survey-grade criteria. Many well-head elevation measurements in this study do not meet survey-grade criteria. Nevertheless, the well-head elevation measurements in this study are more precise than those contained in similar hydrgeologic studies that frequently rely on map-grade GPS measurements and topographic map/DEM locations for all wells.

- Numerous GPS baselines solved with errors using Trimble Geomatics Office (TGO) software. Most of the errors cited in TGO (ratio, reference variance, root-mean squared) are the result of poor receiver-satellite connectivity and occupations times that were too short (typically 2 minutes). Another source is the use of only base station. This was later corrected by solving rover data against two other base stations located in Island County, decreasing the number of baselines with errors and improving the precision of those having errors. Examination of GPS residual and root-mean squared (RMS) data in TGO indicates that the vertical precision of most points is less than 1.0 feet and may vary up to 15 feet. This precision is not considered to be survey-grade.

- Mean sea level, as defined by NAVD 88, is about 4 feet above mean tide level in the Puget Sound. This will cause error in determining an aquifer's susceptibility to seawater intrusion based on head distributions that were obtained using NAVD 88 datum.

- A total of 39 wells were located using information from interviews with land owners, field observations, and the Whatcom County Assessor's tax plat map (one was measured using GPS). The coordinates of these wells were obtained from DEM overlay on a topographic map in GIS and GMS. The DEM's are digitized USGS topographic maps and carry any potential errors that these maps may have. The resolution for DEM's is 10x10 meters. Because available DEM's were in the North American Datum 1927 and National Geodetic Vertical Datum 1929 (NGVD 29), coordinate system transformations of these data to NAD 83, NAVD 88 were required. These transformations will introduce additional error into the DEM and topographic maps used to locate wells in GIS and GMS. Wells located using these methods were not used to determine water level elevations, but were used in the development of the stratigraphic model. There was generally less than 3 feet difference between well-head elevations measured using GPS and estimated using DEM.

- The TIN representing land surface elevation in GMS was created from a DEM. To import the DEM into GMS, the 3-D scatter points in the DEM were thinned by a factor of six, introducing additional error that is most obvious at the base of steep slopes.

Bedrock Surface Elevation Model (Section 4.2)

Error in the bedrock surface elevation model is most likely related to incorrect matching of well logs to well locations and interpolation between points where bedrock surface data is limited.

- Incorrectly matching well logs to well locations could change the outcome of the bedrock surface model. The density of well logs incorporated in this study will minimize the effects of a small number of erroneously matched well logs

- Well driller interpretations of rock type will vary by driller and may be different than a geologist's interpretation. Fortunately two companies (Livermore & Sons and Starr Drilling) are responsible for the vast majority of wells drilled on Lummi Island. The distinct color, texture, and density differences between sandstone and greenstone probably minimize interpretation errors.

- In regions with insufficient well log data and where the slope of the bedrock surface changes dramatically over a short distance such as Richards Mountain and Hill 275, use of interpolation methods in GMS could cause bedrock surfaces to be modeled as more subdued or more exaggerated than actual conditions.

- Sandstone is likely underlain by greenstone at most locations (Carroll, 1980; Blake, 2002) and the contact is likely irregular, not flat as modeled. Complex structures in the north half of the study area likely cause greenstone to occur at elevations greater than –261 feet, the depth to which sandstone is modeled. The presence of greenstone within the region modeled as sandstone would influence the hydrogeologic and hydrogeochemical properties of the Sandstone Aquifer.

- The sandstone-greenstone contact in map view is probably not as sharply defined as modeled. Some well logs to the south of this contact and along Seacrest Drive indicate thin units of sandstone on top of greenstone. If these clastic units are Chuckanut sandstone, and not a clastic member of the Fidalgo ophiolite, then the sandstone-greenstone contact would appear more jagged and irregular in plan view than shown.

- Because deep wells completed in Pleistocene deposits were used to determine a minimum depth to the bedrock surface, it is possible that the bedrock surface undulates more dramatically than modeled. One region where the actual bedrock surface might be deeper than modeled is the east-west trending bedrock trough at the southern end of the study area.

- The bedrock surface south of 09S was extrapolated upward, toward sea level due to a lack of data. This may not accurately reflect actual conditions.

- The presence of large boulders within the glacial drift (as seen in field observations) may lead drillers to think they've encountered bedrock. In some cases, they may stop drilling to complete a well in a productive lens that they had already drilled through. This could be the case for wells where drilling stopped after only a few feet of bedrock penetration. Examples are wells 09B and 15O that may not be completed in bedrock.

- The extrapolation of bedrock surface vertices using linear interpolation to the island outline polygon in GMS could lead to error in regions where data is sparse.

- The deep east-west trending bedrock trough in the middle of the study area may extend further to the west than modeled. A well log for an un-located well that lies to the northeast of Village Point (05BB) indicates that the bedrock surface is present at approximately 200 ft below land surface. Insufficient well log data in the vicinity of Village Point are available to resolve this discrepancy.

Pleistocene Stratigraphic Model (Section 42)

Error in the Pleistocene stratigraphic model could originate from poorly-recorded well logs, inaccurate and inconsistent texture descriptions of strata by well drillers, and my interpretations of these descriptions. Incorrectly matching well logs to well locations and wells that were incorrectly located might cause the presence or absence of units in the stratigrpahic model to differ from actual conditions. For these reasons, every attempt was made to avoid basing the presence and extent of strata on data from only one well. Other sources of error follow.

- Because the bedrock surface elevation model was used as the base of the Pleistocene stratigraphic model, error in the bedrock surface model will affect the latter.

- The Pleistocene deposits are described as a gradation of various textures (Easterbrook, 1971; Lapen, 2000) and will not have the same hydraulic properties at all locations. Although the fine-grained material was broadly designated as silt-clay diamction, this material is not diamictic at all places, especially at depths below sea level.

- The modeled sand units were made from preliminary cross sections between well logs in GMS. These sections represent my interpretation of relationships among various strata and are subject to error.

- The TIN's for the top and bottom of each sand unit were interpolated from vertices obtained from the preliminary cross sections. Interpolation methods in GMS might contribute to error, especially where data is sparse.

- The number and distribution of well logs may not be sufficient to define the connectivity between lenses of coarse-grained material. Similar hydraulic head distributions suggest that modeled coarse-grained units are more connected than shown. For example, sand units SU-3 and SU-4 may be connected in the vicinity of 09B.

- The sand unit comprising the Hilltop Deep Aquifer (SU-1) may not be as continuous as shown. Top elevations for this aquifer vary significantly, indicating that it might be comprised of one or more thin sand lenses that may not be hydraulically connected.

- Deeper sand units such as SU-1, SU-3, and SU-4 may be thicker than modeled. The default thickness of 5 feet was used in areas where wells do not fully penetrate sand units and other data were not available. This method may underestimate the thickness of the lowest sand units in places. First, numerous wells are screened in these deeper sand units suggesting that they may be thicker and more productive than the overlying lenses that were used to determine the default thickness of 5 feet. Second, geologic units such as Vashon Advance Outwash and pre-Fraser deposits that lie lower in the stratigraphic column are described in published reports as significantly thick coarse-grained units.

- The extent of the deepest sand units may be underrepresented due to cost of drilling.

- Some sand units were not modeled if they had no wells completed in them, were especially thin, or otherwise were determined to have little hydrogeologic significance. This will affect the geologic map and recharge estimate. For example, the sand unit in the vicinity of Village Point, comprising the Village Point Aquifer, was identified, but not modeled due to limited data. The presence of this unit is suggested by wells 08W, 08G, 05AA. Other areas where logs suggest the presence of sand units that were not modeled are the upper two sand lenses indicated in well logs for 09I and 10G.

- Where there was limited data or where a sand unit appears especially thick, the edges of some units, as seen in cross section, are not modeled as pinch-outs. Instead, the edges of these sand units form abrupt, some times square, contacts with surrounding material.

- Drillers do not always note the presence of water in well logs, especially if they are not convinced that a particular strata will support well completion. This could cause an under-representation of some water bearing units.

- Aquifer volume estimates include some regions of aquifers that are not suitable for domestic water use due to low hydraulic conductivity or poor water quality. This could lead to an overestimation of usable water resources. An example is the upper portion of SU-5, of the Legoe Bay Aquifer, near Legoe Bay. At this location, driller's notes indicate the presence of saltwater and no wells are known to be completed in this portion of the aquifer.

- Some sand units that were combined to form aquifers may not actually be connected, causing an overestimation of the size of some aquifers.

- Legoe Bay and Nugent Aquifers may be connected in the upland regions near 09B.

- Data from the recharge section of this study, published geologic reports, field observations, and water level elevations indicate that many aquifers are probably not confined, but more closely meet the definition of semi-confined, or leaky, aquifers. Schmidt (1978) concluded that insufficient evidence exists to classify any aquifers on north Lummi Island as confined.

- The lateral extent of the two bedrock aquifers was determined by enclosing all wells that are completed in these aquifers. As a result of this, the bedrock aquifer volume estimates do not include saturated bedrock that underlies areas where wells are completed in Pleistocene deposits overlying the bedrock.

- Assuming that potentiometric surface is equal to water table elevation in the Sandstone Aquifer ignores potential confining conditions caused by less permeable facies of the Chuckanut Formation. This could cause an overrepresentation of the saturated volume of this aquifer.

- Assuming that the sandstone aquifer has a bottom elevation of –261 ft at all locations could under/over represent the actual volume of this aquifer and does not account for possibility that underlying greenstone may be folded into the sandstone. Greenstone likely has significantly different hydraulic and hydrogeochemical properties.

Hydraulic Properties (Section 4.4)

Major sources of error for hydraulic properties are related to well construction and well performance test methods and heterogeneities of aquifer material. As with most aspects of this study, the correct matching of well logs to well locations will affect results assigned to each aquifer. The hydraulic properties of some aquifers are based on well performance tests from a limited number of wells.

Sources of error that might favor underestimation of well yield, specific capacity, transmissivity, and horizontal hydraulic conductivity are:

- The exclusion of specific capacity data showing zero drawdown (Table 16) ignores that some wells may be completed in highly productive aquifers (Freeze and Cherry, 1979).

- The inclusion of wells that do not penetrate the entire aquifer thickness may underestimate the capacity of the aquifer to deliver water to the well screen. Most wells in the study area do not fully penetrate aquifers.

- The use of perforations sawed into the well casing, in lieu of a screen, can significantly reduce well production (Freeze and Cherry, 1979). Several study wells have sawed perforations.

- Improperly constructed and developed wells may produce less water than the aquifer can support because the flow of water to the well is inhibited by fine-grained particles surrounding the well screen.

Sources of error that might favor overestimation of well yield, specific capacity, transmissivity, and horizontal hydraulic conductivity are:

- To achieve a desired yield, well performance test pumping rates could be inflated. For example, wells drilled for public water consumption tend to exhibit well yields on logs that are higher than surrounding private wells in the same aquifer. Generally, public water wells are required to exhibit a specified yield that is higher than the yield required for a private well.

- The use of a bailer (used almost exclusively on Lummi Island where cable tool drilling is very common) does not create a constant pumping rate. This allows the water level to periodically recover, confusing the actual time and level of static water (Mace, 2000).

- Using a storage coefficient for confined aquifers (S=.0001) yielded values for transmissivity and hydraulic conductivity that are about one half the values obtained by using a storage coefficient for unconfined aquifers (S=.1).

Water Level Trends (Section 4.5)

Sources of error in determining water levels are mostly from water level measurements that may not be static due to short term effects such as pumping or recovery at a well, the influence from adjacent pumping wells, and tides. The water level measurement procedures used during fieldwork should minimize this error.

- Water levels taken during the 1991-1993 monitoring period as part of an earlier groundwater study (Whatcom County, 1994) frequently have notations that indicate water levels were not static when measured. Though obvious discrepancies were omitted, some of these measurements were incorporated into the well hydrographs.

- The period used for determining correlations between precipitation patterns and seasonal fluctuations in groundwater levels in Whatcom County (1994) is relatively

short; 22 months for water levels and 24 months for precipitation. Fluctuations in water levels are caused by a number of factors including long-term precipitation patterns that precede the 1991-1993 monitoring period.

- Actual water level changes may be larger than those observed between the fall 2002 and spring 2003 monitoring periods. Water levels taken during spring 2003 do not coincide with the highest water levels observed during the 1991-1993 monitoring period that occurred in March.

- The potentiometric maps assume homogeneity of aquifer media. By examination of well logs and geologic conditions, this assumption does not reflect actual conditions. However, since the potentiometric map represents water level distribution across an aquifer, small-scale heterogeneities are minimized.

Groundwater Flow Patterns (Section 4.5)

- Vertical flow is neglected even though it is likely the dominant flow direction, especially in upland regions where recharge is high. Vertical hydraulic conductivity may differ significantly from horizontal conductivity.

- Well head elevation survey errors will be reflected in water level elevations.

- Water level data from 10 wells with no well logs available was used. These wells were assigned to aquifers by comparing well-head elevation and completion depth to the stratigraphic model.

- Heterogeneities within aquifer media will impact groundwater flow patterns and were not considered.

- Limited data at higher elevations in the sandstone caused the modeled groundwater highs to be offset from the topographically highest regions, where it is expected that groundwater head should be highest.

Total Groundwater Storage Capacity (static estimate); (Section 4.6)

- This method overestimates the amount of water actually available for exploitation.

- The hydraulic conductivity of aquifer media is generally too low to allow the movement of water to a well over long distances.

- Significant exploitation of the estimated groundwater quantity would decrease hydraulic head, drying shallow wells and inducing seawater intrusion in wells completed below sea level (78% of all wells).

- Groundwater systems rarely achieve a steady state. Water enters and leaves the system at different rates, causing variations in water table elevation and head distribution with time. Water level monitoring of 38 study area wells (Whatcom County, 1994) demonstrates that water level fluctuations are common.

- Aquifer volumes were calculated based on aquifer solids represented in the stratigraphic model (Section 4.3). This model will have inherent errors from several sources listed in Section 4.3.

- The average effective porosity assigned to each aquifer is dependent upon the dominant texture that I assigned to each aquifer. These textures are my interpretations of driller's notes.

- Assigning average effective porosities does not account for heterogeneities within each aquifer. This is not considered to be a significant source or error. Published values for effective porosity do not vary greatly among similar textures observed in the aquifers of northern Lummi Island and would not significantly change the total groundwater storage capacity estimate.

- The true nature of the bottom surface of the bedrock aquifers is unknown. This study assumes that the bottom of the Sandstone Aquifer is a constant surface located with an elevation of –261 feet. Variations in fracture content among sandstone and greenstone and differences in hydraulic properties of these units cause them to have significantly different groundwater storage capacities. If greenstone is significantly folded into sandstone in the north half of the study area, then this source of error will cause an overestimation of the quantity of groundwater in the Sandstone Aquifer.

- The presence of seawater within aquifers, beneath the freshwater lens, is ignored.

- Some errors may cause an underestimation in the total groundwater storage capacity.

- The areal limits of the Sandstone and Greenstone aquifers were determined by enclosing the regions where wells are completed in these materials. Because no wells are known to be completed in either sandstone or greenstone outside of these limits, does not necessarily mean that the aquifers do not exist there.

- Groundwater is likely present below the designated bottom elevation for the Sandstone and Greenstone aquifers of –261 and –300 feet, respectively.

- Not all water bearing sand units have been modeled. At least one water bearing sand unit, comprising the Village Point Aquifer, was identified but not modeled due to limited data.

- Using this method, I only accounted for groundwater present in aquifer material such as sand and bedrock. It does not account for groundwater stored in the silt-clay diamicton. Though these materials conduct water at a slower rate than the sands and bedrock, they typically will have higher porosities and will store large volumes of groundwater. Though this water is not immediately available for movement to a well, ignoring it will cause an underestimation of the total amount of groundwater in storage.

Identify Recharge and Discharge Areas (Section 4.7)

Major sources of error in identifying recharge and discharge areas are associated with error in the stratigraphic model and potentiometric maps. The stratigraphic model was used to make assumptions about the hydraulic conductivity of geologic material. The groundwater highs and confining conditions delineated through the potentiometric map are subject to error.

Recharge Areas.

- The largest primary recharge area is overlying sandstone. The overall topographic relief within this recharge area is about 200 feet. Not all places enclosed by the primary recharge area are significant to recharge, especially where slope is steep or where relatively impermeable sediments are present.

- The texture and thickness of glacial drift mantling bedrock in the topographically higher regions of the study area are largely unknown due to limited well log data.

- Regions where sand units abut bedrock and receive recharge from the bedrock are inferred from the stratigraphic model and potentiometric surface mapping.

- The hydraulic conductivity of the silt-clay diamicton is not known.

- Potentiometric surfaces mapped for this study were used to determine groundwater highs and confined/unconfined conditions and are subject to error.

- The amount of recharge to the southern part of Nugent Aquifer from the upland region south of the study area (Lummi Mountain) is unknown. This part of the Nugent aquifer likely receives some recharge from the south.

- It is likely that all aquifers receive some recharge from overlying fine-grained units of glacial drift though the relative importance vertical recharge is no known.

<u>Discharge Areas</u>

- The presence of surface water does not necessarily indicate a discharge area. Surface water features may also be caused by runoff and shallow groundwater input to small depressions that are underlain by relatively impermeable material.

- Sand units may be more interconnected than modeled. Instead of discharging offshore or at land surface, some sand aquifers may discharge to a down gradient sand unit through a connection that I did not identify in the stratigraphic model.

Recharge Estimate Using a Water-Mass Balance (Section 4.8)

Of the three variables in the water-mass balance equation that were used to Estimate recharge, only precipitation can be measured directly on an island-wide basis. Error in estimating recharge using this method lies in the estimated values for the output variables evapotranspiration and runoff. For this reason, estimated recharge is presented as a range of values. Specific sources of error are detailed below.

- The Penman-Montheith model was used to estimate potential evapotranspiration (PET), which is always greater than actual evapotranspiration (AET).

- Using a value for AET from the Lake Whatcom watershed (Kelleher, personal communication, 2004) as the lower bound for could introduce error. The Lake Whatcom watershed lies 20 miles to the east and receives significantly more precipitation than north Lummi Island. It is a mountainous region with dramatically different slope, vegetative, and climatic conditions. Additionally, this value was derived from a hydrologic model that will have inherent errors.

- Climatic data used as input to the Penman-Monteith model are from a mainland weather station that lies 8 miles to the east. Climate on north Lummi Island is probably strongly influenced by the surrounding marine waters. Therefore, climatic

conditions in the study area, especially wind and temperature, are probably different than at Bellingham International Airport.

- Exact values for the evapotranspirative properties of vegetation in the study area were not available. Instead, text book values for several species similar to those found on north Lummi Island were used. The properties, maximum leaf conductance and leaf area index, can significantly affect potential evapotranspiration estimates.

- Runoff estimates from discharge data presented by Nielson and Armfield (unpublished) might differ from actual conditions. The authors lacked a means to continuously monitor the discharge from outlet streams. Extrapolation of limited data to produce monthly total discharge estimates may underestimate or overestimate actual discharge.

- Several outlet streams have significant discharge volumes for much of the year. These flows were measured with using a flow meter and engineered channel (either a culvert or existing concrete flume). A margin of error for this method was not estimated.

- Although the discharge monitoring effort of Nielson and Armfield included most of the known outlet channels, it is impossible to directly measure runoff from all sources in the study area.

- The assumption that runoff, expressed as a percentage of annual precipitation, does not vary from year to year could be incorrect. The percent of precipitation that runs off as surface water depends on a variety of climatic variables. Some of these variables include precipitation duration, intensity, and timing. Water Year 2004 was an exceptionally wet year.

- The water-mass balance equation was used to estimate recharge to study area aquifers. However, it does not account for the lateral movement of shallow groundwater that daylights in shoreline bluffs. During field work, I observed some seepage along shoreline bluffs, especially along the interface of geologic materials

with different hydraulic conductivities. The fraction of water lost to shoreline seepage is determined to be insignificant compared to evapotranspiration and runoff.

Recharge Estimate Using a Chloride-Mass Balance (Section 4.9)

- The chloride mass balance equation is most sensitive to changes in the variables FWD and Cg. In the Lopez Island study (Orr et al., 2002), values for FWD and Cg were considerably higher than the Island County study (Sumioka and Bauer, 2003).

- The greatest potential source of error for the chloride mass balance recharge value achieved in the current study is the FWD variable that was not measured.

- This method assumes that chloride in groundwater is from atmospherically-deposited sources. Although precautions were taken to avoid error from elevated concentrations of chloride caused by seawater intrusion, other sources of chloride do exist. Of these, residual chloride from Pleistocene marine inundation of the study area that has not been flushed out of unconsolidated sediments and bedrock is a potential source of error. The contribution of chloride from this and other sources are unknown but could cause recharge estimates to be lower than actual conditions.

- Runoff estimates are also a source of error. Since the same runoff estimates were used for the water-mass balance and chloride-mass balance, these methods are not completely independent.

Survey Groundwater Chemistry and Assess Seawater Intrusion (Section 4.10)

- Variation in water chemistry between fall 2002 and spring 2003 could be partially due to the elimination of the criteria to sample wells completed below sea level at high tide only.

- Use of a 5 minute flushing time starting from when the well pump is energized should be sufficient to draw water from the aquifer to the sample collection port, but may not have occurred for some wells with long, saturated casings and lower capacity pumps.

- Although every effort was made to take samples prior to storage tanks, this was not possible at 11 sites. Values for pH and ORP at these locations were not used in groundwater chemistry trend analysis. Storage tanks are common. It is possible that some samples could have been taken inadvertently from sampling ports after storage or treatment.

- Error associated with field measurements of pH can sometimes cause measurements to be higher than actual pH due to the escape of CO_2 (Fetter, 1980). For this reason, pH was measured immediately after sample collection.

- The use of electrical conductivity can misrepresent total dissolved solids because it does not account for uncharged species dissolved in water (Freeze and Cherry, 1979). In addition, daily calibration of the conductivity dipstick was performed only by checking the instrument against distilled water, and not by calibration solutions. These measurements are intended only to provide a basis for measurements with similar devices.

- Error associated with field measurements of ORP can sometimes cause measurements to be higher than actual ORP due to the introduction of atmospheric oxygen into a sample. To minimize error, ORP was measured immediately after sample collection.

- At some locations where samples were collected after concrete storage tanks, erroneously high concentrations of calcium could occur.

- The use of bleach as a disinfectant in some plumbing systems, wells, and storage tanks could cause elevated concentrations of chloride, that are not associated with the seawater intrusion or the other processes listed above. However, this source of chloride can be identified in wells that were analyzed for major ions.

- Examining groundwater chemistry trends among aquifers assumes that the stratigraphic model represents actual conditions. Conclusions regarding these trends carry much of the error that is associated with the stratigraphic model and identification of aquifers.

- Groundwater chemistry data from wells completed in bedrock that have long open intervals may reflect conditions present along the entire open interval. This could cause error in drawing conclusions regarding groundwater chemistry versus depth.

- The significance of saline waters left over from Pleistocene marine inundation was not quantified. These waters will have the same chemical characteristics as modern seawater but are not indicative of intrusion. Contributions from these older marine waters are likely small but may cause error in my conclusions regarding seawater intrusion.

- Major ion chemistry was not analyzed at every well. Instead, concentrations of some of the major ions (Na^+, Ca^{2+}, Cl^-) were used to draw conclusions regarding groundwater composition (immature, more evolved, highly evolved, intruded) at most wells. This method does not consider concentrations of other major ions which could lead to error in determining groundwater composition.

- Error in well head elevations may be multiplied by a factor of 40 in determining the Gyben-Herzberg predicted interface location.

Table A-1. Monthly climatic data used as input to Penman-Monteith Model north Lummi Island, Washington. Source: National Climatic Data Center, Bellingham International Airport, Water Years 2001-

month WY 2001	average temperature (F^0)	average dew point (F^0)	average wind speed (mph)	average temperature (C^0)	average dew point (C^0)	average wind speed (km/day)
O	50.2	44.6	5.4	10.1	7.0	208.6
N	40.7	34.6	5.6	4.8	1.4	216.3
D	36.8	31.2	6.2	2.7	-0.4	239.5
J	40.1	35	5.7	4.5	1.7	220.2
F	38.1	30.5	6.9	3.4	-0.8	266.5
M	44.1	36.7	7.6	6.7	2.6	293.5
A	47.3	38.1	8	8.5	3.4	309.0
M	52.7	42.9	6.4	11.5	6.1	247.2
J	55.9	47.5	7.2	13.3	8.6	278.1
J	60.5	50.5	8.4	15.8	10.3	324.4
A	61.8	55.4	6.8	16.6	13.0	262.6
S	56.3	51.2	5.2	13.5	10.7	200.8
WY 2002						
O	48.2	43.1	7.1	9.0	6.2	274.2
N	46	40.24	7.7	7.8	4.6	297.4
D	38.8	32.9	9.2	3.8	0.5	355.3
J	39.1	35.7	8	3.9	2.1	309.0
F	39.9	32.7	7.9	4.4	0.4	305.1
M	38.3	30.8	10.1	3.5	-0.7	390.1
A	46.9	39.3	7.6	8.3	4.1	293.5
M	51.3	42.6	6.8	10.7	5.9	262.6
J	59.3	50.6	7.6	15.2	10.3	293.5
J	61.6	53.9	7.3	16.4	12.2	282.0
A	61.7	53.3	6.1	16.5	11.8	235.6
S	56.4	50.5	5.1	13.6	10.3	197.0
WY 2003						
O	47.8	43.3	3.6	8.8	6.3	139.0
N	45.7	39.9	7.1	7.6	4.4	274.2
D	41.7	36.4	8.7	5.4	2.4	336.0
J	43.3	37.9	7.6	6.3	3.3	293.5
F	39.7	34.2	4.9	4.3	1.2	189.3
M	45.2	38.5	9.7	7.3	3.6	374.7
A	48.8	41.7	8.2	9.3	5.4	316.7
M	53	45.8	6.5	11.7	7.7	251.1
J	59.8	51.8	7	15.4	11.0	270.4
J	63.9	54.5	6.8	17.7	12.5	262.6
A	62.8	54.3	6.1	17.1	12.4	235.6
S	58.4	52.2	5.3	14.7	11.2	204.7
WY 2004						
O	52.4	46.8	9	11.3	8.2	347.6
N	40	31.5	8	4.4	-0.3	309.0
D	40.4	34.6	9.1	4.7	1.4	351.5
J	38.6	33.4	8.6	3.7	0.8	332.2
F	41.9	35.7	6.2	5.5	2.1	239.5
M	46.1	38.5	8.3	7.8	3.6	320.6
A	51.5	40.7	5.5	10.8	4.8	212.4
M	54.8	47.5	7	12.7	8.6	270.4
J	60.2	50.8	6.9	15.7	10.4	266.5
J	64.9	55.9	7.5	18.3	13.3	289.7
A	64.8	56.9	7.6	18.2	13.8	293.5
S	58	52	6	14.4	11.1	231.7

Table A-2. Land cover classes and vegetative properties used in Penman-Montheith model, north Lummi Island, Washington. Source: Landsat 4 (Table 3) and Dingman (1994)

land cover class	percent of study area	C_{*leaf} (cm/s)	LAI	Z_{veg} (cm)	notes
coniferous	17.3	0.83	6	2500	assumes 1/2 of mixed forest is coniferous
deciduous	39.2	0.29	6	2500	assumes 1/2 of mixed forest is deciduous
grasses	35.7	0.8	3	50	short, medium, long grasses and fallow
shrub	5.1	0.53	3	800	
urban/rock/water	2.7	-	-	-	
Summary					
forest	56.5				
non-forest	43.5				

C_{*leaf} maximum leaf conductance

LAI   leaf-area conductance

Z_{veg} height of vegetation

Appendix B. Wells used in this study: aquifer, location, well log availability, completion elevation, and use of well in study, north Lummi Island, Washington

well ID	aquifer	confining conditions[1]	easting (m) NAD 83	northing (m) NAD 83	elevation (ft) NAVD 88	locating method	well log	completion elevation[2] (ft)	screened/ saturated open interval[3] (ft)	use in study[4]
04A	Lane Spit	UNC	522657	5397602	13	GPS	y	-35	5	WL/Chem
04AA	Sandstone	UNC	521732	5396765	144	DEM	y	31	55	strat only
04B	Hilltop Deep	CON	522293	5396250	69	DEM	y	-172	5	strat only
04BB	Sandstone	UNK	521741	5396557	91	DEM	y	26	-	strat only
04C	Legoe Bay	CON	522093	5396199	20	GPS	y	-10	5	WL/Chem
04D	Sandstone	UNK	522036	5396930	159	GPS	n	-75	-	WL/Chem
04E	Sandstone	CON	523273	5396230	59	GPS	y	-193	67	WL/Chem
04F	Sandstone	UNK	523247	5396500	33	GPS	n	-104	-	WL/Chem
04G	Legoe Bay	CON	522156	5396203	25	GPS	y	-22	5	WL/Chem
04H	Blizzard	UNC	522181	5397396	173	DEM	y	108	5	strat only
04I	Sandstone	CON	523064	5396806	65	GPS	n	-18	67	WL/Chem
04J	Sandstone	CON	522150	5396632	134	GPS	y	-156	204	WL/Chem
04K	Sandstone	CON	523067	5396873	60	DEM	n	15	29	WL/Chem
04L	Sandstone	CON	522169	5396826	160	DEM	y	-195	256	strat only
04M	Sandstone	UNK	522943	5397140	36	GPS	n	-33	-	WL/Chem
04N	Sandstone	CON	522862	5396973	95	GPS	y	-32	99	WL/Chem
04P	dug well	UNC	522701	5397705	11	GPS	-	2	-	WL/Chem
04Q	Sandstone	CON	523117	5396165	96	GPS	y	-179	227	WL/Chem
04R	Sandstone	UNK	522031	5397288	163	GPS	n	82	-	WL/Chem
04S	Sandstone	UNK	522064	5396619	126	GPS	n	-44	-	WL/Chem
04T	Sandstone	CON	522749	5397329	72	GPS	y	-6	41	WL/Chem
04U	Sandstone	CON	522849	5397057	98	DEM	y	-8	86	strat only
04V	Sandstone	UNC	521873	5396727	141	GPS	y	-12	63	WL/Chem
04W	Sandstone	UNC	522040	5397533	234	GPS	y	112	84	WL/Chem
04X	Sandstone	UNC	522576	5396382	150	GPS	y	35	25	WL
04Y	Centerview	CON	522539	5396917	119	GPS	y	44	5	WL/Chem
04Z	Sandstone	CON	522408	5397636	125	GPS	y	-63	70	WL/Chem

well ID	aquifer	confining conditions[1]	easting (m) NAD 83	northing (m) NAD 83	elevation (ft) NAVD 88	locating method	well log	completion elevation[2] (ft)	screened/ saturated open interval[3] (ft)	use in study[4]
05AA	Village Pt	CON	not located, at Village Pt			DEM	y	< 0	-	strat only
05B	Sandstone	UNC	521457	5397088	212	GPS	y	75	103	WL/Chem
05BB	-	UNK	not located lies NE of Village Pt			DEM	y	< 0	-	strat only
05C	Sandstone	UNC	521363	5396307	79	DEM	y	-289	317	strat only
05E	Sandstone	CON	520590	5397448	51	GPS	y	-107	123	WL/Chem
05G	dug well	UNC	520718	5396642	68	GPS	-	57	-	WL/Chem
05H	Sandstone	UNC	520885	5396512	85	DEM	y	-216	161	strat only
05J	Legoe Bay	UNC	521640	5396450	76	GPS	n	< 0	-	WL/Chem
05L	Legoe Bay	UNC	521582	5396605	117	GPS	y	-64	5	WL/Chem
05M	Legoe Bay	UNK	521692	5396846	157	DEM	y	42	-	strat only
05O	Legoe Bay	UNC	521695	5396474	77	GPS	y	-3	5	WL/Chem
05P	Sandstone	CON	520747	5397484	100	GPS	y	-68	90	WL/Chem
05Q	Sandstone	UNK	520885	5396639	95	DEM	y	-183	-	strat only
05T	Sandstone	UNC	521764	5397104	172	GPS	y	22	103	WL/Chem
05W	Sandstone	CON	521467	5396542	117	GPS	y	-38	5	WL/Chem
05Z	Sandstone	UNC	521173	5397168	226	GPS	y	141	66	WL/Chem
08G	Village Pt	CON	521305	5396212	15	DEM	y	-84	4	strat only
08O	Sandstone	CON	521323	5396147	15	GPS	y	-85	45	WL/Chem
08W	Village Pt	CON	520890	5396172	23	DEM	y	-61	-	strat only
08Z	Legoe Bay	CON	521659	5396148	6	DEM	y	-102	5	strat only
09A	Legoe Bay	CON	522692	5396069	106	GPS	y	-11	5	WL
09B	Legoe Bay	CON	522969	5395686	115	GPS	y	-28	5	WL/Chem
09C	Greenstone	CON	523269	5395185	164	GPS	n	44	-	WL/Chem
09D	Hilltop Deep	CON	523196	5395822	67	DEM	y	-228	5	strat only
09E	Legoe Bay	CON	522739	5395789	100	DEM	y	-57	5	strat only
09F	Legoe Bay	CON	522981	5396062	86	DEM	y	-28	open-ended	strat only
09G	Nugent	CON	523047	5395017	118	GPS	y	-75	5	WL/Chem
09H	-	CON	522618	5395764	69	GPS	n	-112	-	Chem
09I	Nugent	CON	523184	5394920	127	GPS	y	-28	5	WL/Chem
09J	Nugent	CON	523169	5395705	108	GPS	y	-7	10	WL

well ID	aquifer	confining conditions[1]	easting (m) NAD 83	northing (m) NAD 83	elevation (ft) NAVD 88	locating method	well log	completion elevation[2] (ft)	screened/ saturated open interval[3] (ft)	use in study[4]
09K	Legoe Bay	CON	521990	5396087	13	GPS	y	-50	5	WL/Chem
09L	Legoe Bay	CON	522399	5396005	50	GPS	y	-15	10	WL/Chem
09M	Legoe Bay	CON	523267	5395961	26	GPS	y	-50	5	WL/Chem
09P	Legoe Bay	CON	522208	5395881	11	GPS	n	-38	5	WL/Chem
09Q	Nugent	CON	523141	5394565	91	GPS	y	-5	open-ended	WL/Chem
09R	Legoe Bay	CON	522127	5395943	14	GPS	y	-50	open-ended	WL/Chem
09S	Hilltop Deep	CON	522641	5395731	77	GPS	y	-174	4	WL/Chem
09T	Hilltop Deep	CON	523001	5395855	89	DEM	y	-171	5	strat only
09U	Legoe Bay	CON	522315	5395839	21	DEM	y	-59	5	strat only
09V	Nugent	UNC	523304	5395405	108	GPS	y	-22	10	WL
09W	Nugent	CON	523256	5394624	104	DEM	y	-12	5	strat only
09Y	-	CON	522669	5395908	100	DEM	y	15	5	strat only
10A	Hilltop Deep	CON	523999	5395332	7	DEM	y	-195	open-ended	strat only
10B	Greenstone	CON	524231	5394814	109	GPS	y	-61	80.0	WL/Chem
10C	Constitution	CON	523870	5394944	176	GPS	y	113	20	WL/Chem
10D	dug well	UNC	523379	5395069	155	GPS	-	145	-	WL/Chem
10E	Constitution	CON	523758	5395159	163	GPS	y	109	open-ended	WL/Chem
10F	dug well	UNC	523552	5395448	121	GPS	-	114	-	WL/Chem
10G	Greenstone	UNC	523889	5395195	178	GPS	y	-46	47	Chem
10I	Legoe Bay	CON	523517	5395528	123	DEM	y	-59	10	strat only
10J	Greenstone	CON	524286	5394779	78	GPS	y	-51	98	WL
10K	Greenstone	CON	523935	5395081	185	DEM	y	-2	105	strat only
10M	Nugent	UNC	523628	5394696	154	GPS	y	0	open-ended	WL/Chem
10P	Greenstone	CON	523941	5394824	194	DEM	y	-6	151	strat only
10R	Greenstone	UNC	523722	5394767	152	DEM	y	52	76	strat only
10V	Legoe Bay	CON	523356	5395756	62	GPS	y	-61	open-ended	WL/Chem
10X	Legoe Bay	CON	523547	5395448	121	GPS	y	-58	open-ended	WL/Chem
10Y	Greenstone	CON	524264	5394806	91	GPS	y	-4	66	WL
10Z	Greenstone	CON	523397	5395082	159	DEM	y	-11	124	strat only
15A	Nugent	UNC	523608	5393997	118	GPS	y	-44	10	WL/Chem

well ID	aquifer	confining conditions[1]	easting (m) NAD 83	northing (m) NAD 83	elevation (ft) NAVD 88	locating method	well log	completion elevation[2] (ft)	screened/ saturated open interval[3] (ft)	use in study[4]
15C	Nugent	CON	523916	5393970	106	DEM	y	-43	5	strat only
15D	Nugent	CON	523443	5393630	88	GPS	y	-85	open-ended	WL/Chem
15H	Greenstone	UNK	524495	5394504	34	DEM	y	-238	-	strat only
15K	Nugent	CON	524378	5393846	55	GPS	y	-31	5	WL/Chem
15L	Nugent	CON	524034.12	5393832.4	60	GPS	y	-33	5	strat only
15O	Nugent	CON	524452	5394176	123	GPS	y	-25	1	WL/Chem
15P	Nugent	CON	524019	5393809	59	GPS	y	-26	5	WL/Chem
15R	Greenstone	UNK	524447	5394427	101	DEM	y	-199	-	strat only
15S	Nugent	CON	524283	5393954	73	GPS	y	-48	5	WL/Chem
15U	Greenstone	CON	524393	5394479	136	DEM	y	-89	210	strat only
15X	Nugent	CON	523440	5393854	93	DEM	y	-95	5	strat only
15Z	Nugent	CON	523421	5393790	89	DEM	y	-118	open-ended	strat only
16B	Nugent	CON	523304	5394321	87	DEM	y	-87	6	strat only
16K	Nugent	CON	523313	5393963	75	GPS	y	-26	5	WL/Chem
16T	Nugent	CON	523315	5394143	78	DEM	y	-19	5	strat only
16V	Nugent	CON	523323	5393982	73	GPS	y	-24	5	WL/Chem
29C	Sandstone	CON	521021	5399408	34	GPS	y	-45	61	WL/Chem
32A	Sandstone	CON	520937	5398427	217	GPS	y	120	20	WL/Chem
32B	Sandstone	CON	520756	5398491	132	GPS	y	-29	55	WL
32G	Sandstone	CON	521642	5398611	178	DEM	y	78	92	strat only
32H	Loganita	CON	520940	5399010	77	GPS	y	-32	5	WL/Chem
32K	Sandstone	UNK	520699	5398390	122	GPS	n	-66	-	WL/Chem
32L	Sandstone	CON	521227	5399339	30	GPS	y	-90	102	WL/Chem
32M	Sandstone	CON	520990	5398407	199	GPS	y	72	82	WL/Chem
32N	Sandstone	UNC	521125	5398232	259	GPS	y	-37	-	WL/Chem
32P	West Shore	CON	520664	5397984	90	GPS	y	-2	4	WL/Chem
32Q	Sandstone	CON	520939	5398384	168	DEM	y	-47	166	WL/Chem
32R	Loganita	CON	521023	5399091	68	GPS	y	-62	6	WL/Chem
32S	Sandstone	CON	521230	5399123	62	GPS	y	-78	102	WL/Chem
32T	Sandstone	CON	520898	5398456	194	GPS	y	-24	156	WL

well ID	aquifer	confining conditions[1]	easting (m) NAD 83	northing (m) NAD 83	elevation (ft) NAVD 88	locating method	well log	completion elevation[2] (ft)	screened/ saturated open interval[3] (ft)	use in study[4]
32W	Sandstone	UNC	521409	5398588	256	GPS	n	146	-	WL/Chem
32X	Sandstone	UNC	521502	5398691	210	GPS	y	92	72.0	WL/Chem
33A	Sandstone	CON	522251	5398201	72	DEM	y	2	60	strat only
33B	dug well	UNC	522127	5398394	80	GPS	n	66	-	WL/Chem
33D	Sandstone	UNC	521797	5397923	207	GPS	y	81	41	WL/Chem
33F	Lane Spit Deep	CON	522694	5397945	14	GPS	y	-195	15	WL/Chem
33G	Lane Spit	CON	522568	5397843	38	GPS	y	-44	5	WL/Chem
33J	Lane Spit	CON	522724	5397734	7	DEM	y	-66	5	strat only
33M	Sandstone	UNC	521850	5398065	232	GPS	y	56	125	WL/Chem
33N	Sandstone	CON	521813	5397780	240	DEM	y	60	162	strat only
33T	Lane Spit	CON	522620	5397959	12	GPS	y	-49	6	WL/Chem
33W	Sandstone	UNK	522116	5398385	92	GPS	n	-123	-	WL
33X	dug well	UNC	521894	5397566	236	DEM	-	223	-	WL/Chem

1. Aquifer confining conditions at well: unconfined (UNC), confined (CON), unknown (UNK)
2. Completion elevation at bottom of well screen or open borehole (bedrock and gravel-packed wells). Some wells are drilled beyond well screen. Completion elevation determined by measuring total depth at wells with no log available.
3. Screened interval applies to wells in completed in Plesitocene deposits. Saturated open intervals for wells completed in bedrock were determined from water level elevation and completion elevation data.
4. Use of well in study: water level measurement (WL), sampled for water chemistry (Chem), used only in constructing the stratigraphic model (strat only). All wells with well logs were used to create the stratigraphic model (Appendix C).

Appendix C. Interpretations of well driller's reports. Well driller's descriptions of strata encountered during drilling and textural interpretations made from descriptions, north Lummi Island, Washington. Specific interpretations were made directly from the driller's notes contained in well logs. The "broad textural interpretations" were used to construct the stratigraphic model.

well ID	X (m) NAD 83	Y (m) NAD 83	Z (ft) NAVD 88	depth (ft)	driller's descriptions of strata directly from well log	specific textural interpretation	broad textural interpretation
04A	522657	5397602	13	0	gravel	gravel/sand	sand
04A	522657	5397602	9	4	hardpan	hardpan	silt-clay diamicton
04A	522657	5397602	6	7	sand brown	sand	sand
04A	522657	5397602	-5	18	sand blue + water	sand	sand
04A	522657	5397602	-35	48		sand	sand
04AA	521732	5396765	144	0	clay + gravel	gravel clay	silt-clay diamicton
04AA	521732	5396765	107	37	blue clay	clay	silt-clay diamicton
04AA	521732	5396765	103	41	hardpan	hardpan	silt-clay diamicton
04AA	521732	5396765	88	56	decomposed sandstone	sandstone	sandstone
04AA	521732	5396765	85	59	hard sandstone	sandstone	sandstone
04AA	521732	5396765	31	113		sandstone	sandstone
04B	522293	5396250	69	0	top soil	soil	silt-clay diamicton
04B	522293	5396250	68	1	sand, gravel & hardpan	sand w/clay	silt-clay diamicton
04B	522293	5396250	49	20	sand, gravel & blue clay	sand w/clay	silt-clay diamicton
04B	522293	5396250	27	42	sand & gravel (brown)	sand	sand
04B	522293	5396250	22	47	sand, gravel & blue clay	sand w/clay	silt-clay diamicton
04B	522293	5396250	-7	76	sand, muddy (brown)	sand	sand
04B	522293	5396250	-20	89	fine sand & little gravel & (blue clay)	fine sand	silt-clay diamicton
04B	522293	5396250	-158	227		fine sand	silt-clay diamicton
					fine sand & little gravel & very little blue clay		
04B	522293	5396250	-165	234	sand, gravel & water	sand	sand
04B	522293	5396250	-172	241	sand, gravel & blue clay	sand w/clay	silt-clay diamicton
04B	522293	5396250	-173	242		sand w/clay	silt-clay diamicton
04BB	521741	5396557	91	0	top soil	soil	sand

04BB	521741	5396557	90	1	sand + gravel	sand	sand
04BB	521741	5396557	88	3	sand + gravel + hardpan	sand w/ clay	silt-clay diamicton
04BB	521741	5396557	86	5	sand + gravel + little blue clay	sand w/ clay	silt-clay diamicton
04BB	521741	5396557	69	22	sand + gravel + little blue clay soft	sand w/ clay	silt-clay diamicton
04BB	521741	5396557	46	45	boulder	sand w/ clay	silt-clay diamicton
04BB	521741	5396557	37	54	boulder + gravel + broken sandstone + blue clay + water	sand w/ clay	silt-clay diamicton
04BB	521741	5396557	35	56	sandstone	sandstone	sandstone
04BB	521741	5396557	21	70	sandstone	sandstone	sandstone
04C	522093	5396199	20	0	clay + gravel	gravel clay	silt-clay diamicton
04C	522093	5396199	19	24	hardpan + gravel	hardpan	silt-clay diamicton
04C	522093	5396199	16	28	gravel w/water	gravel/sand	sand
04C	522093	5396199	6	30	hardpan	hardpan	silt-clay diamicton
04C	522093	5396199	3	42	heaving sand	sand	sand
04C	522093	5396199	-1	51	grey clay	clay	silt-clay diamicton
04C	522093	5396199	-72	62	hardpan	hardpan	silt-clay diamicton
04C	522093	5396199	-76	63	dry clay	clay	silt-clay diamicton
04C	522093	5396199	-96	230	very fine sand w/water but unable to use	fine sand	sand
04C	522093	5396199	20	250	sealed w/concrete 230-250	fine sand	sand
04E	523273	5396230	59	0	gravel & rocks	gravel/sand	sand
04E	523273	5396230	58	28	clay	clay	silt-clay diamicton
04E	523273	5396230	56	32	hardpan & boulders	hardpaan	silt-clay diamicton
04E	523273	5396230	51	39	hard rock	sandstone	sandstone
04E	523273	5396230	44	52	sandstone + water at unreadable depth	sandstone	sandstone
04E	523273	5396230	37	252	sandstone	sandstone	sandstone
04G	522156	5396203	-78	0	top soil	soil	sand
04G	522156	5396203	25	1	sand, gravel	sand	sand
04G	522156	5396203	25	3	sand, gravel, hardpan	sand/gravel clay	silt-clay diamicton
04G	522156	5396203	23	12	sand, gravel, clay	sand/gravel clay	silt-clay diamicton
04G	522156	5396203	7	26	sand, gravel, clay	sand/gravel clay	silt-clay diamicton
04G	522156	5396203	-13	34	sand, gravel, water	sand	sand

04G	522156	5396203	-38	44	sand, gravel, water	sand	sand
04G	522156	5396203	-84	46	sand, gravel, clay	sand	silt-clay diamicton
04G	522156	5396203	-96	74	sand, gravel, clay	sand	silt-clay diamicton
04G	522156	5396203	25	90	sandstone	sandstone	sandstone
04H	522181	5397396	173	0	topsoil	soil	sand
04H	522181	5397396	172	1	sandy loam	sand	sand
04H	522181	5397396	159	14	clay	clay	silt-clay diamicton
04H	522181	5397396	136	37	clay, sand, gravel	sand w/clay	silt-clay diamicton
04H	522181	5397396	133	40	sand, gravel	sand	sand
04H	522181	5397396	127	46	water, sand, gravel	sand	sand
04H	522181	5397396	108	65	shale	shale	sandstone
04H	522181	5397396	96	77	shale	shale	sandstone
04I	523064	5396806	-19	0	top soil	soil	silt-clay diamicton
04I	523064	5396806	-21	2	hardpan	hardpan	silt-clay diamicton
04I	523064	5396806	-40	16	sandstone	sandstone	sandstone
04I	523064	5396806	-50	82	water	sandstone	sandstone
04I	523064	5396806	-54	83		sandstone	sandstone
04J	522150.35	5396632.1	134	0	top soil	soil	sand
04J	522150.35	5396632.1	133	1	sand and gravel	sand	sand
04J	522150.35	5396632.1	130	4	sand and gravel and hardpan	hardpan	silt-clay diamicton
04J	522150.35	5396632.1	123	11	sand and gravel and blue clay (soft)	sand/gravel clay	silt-clay diamicton
04J	522150.35	5396632.1	96	38	sand and gravel and little clay	sand/gravel clay	silt-clay diamicton
04J	522150.35	5396632.1	62	72	sand and gravel and blue clay (hard)	sand/gravel clay	silt-clay diamicton
04J	522150.35	5396632.1	56	78	sandstone	sandstone	sandstone
04J	522150.35	5396632.1	-76	210	water approx 18 gph	sandstone	sandstone
04J	522150.35	5396632.1	-119	253	shale blue with caving, water app 1 gpm	shale	sandstone
04J	522150.35	5396632.1	-122	256	sandstone	sandstone	sandstone
04J	522150.35	5396632.1	-144	278	water 8+ gpm	sandstone	sandstone
04J	522150.35	5396632.1	-156	290	sandstone and bottom	sandstone	sandstone
04K	523065	5396866	-66	0	top soil	soil	silt-clay diamicton

04K	523065	5396866	-72	2	hardpan		hardpan	silt-clay diamicton
04K	523065	5396866	-100	16	sandstone		sandstone	sandstone
04K	523065	5396866	-103	45			sandstone	sandstone
04L	522169	5396826	160	0	topsoil		soil	silt-clay diamicton
04L	522169	5396826	160	1	dry gravel		gravel/sand	silt-clay diamicton
04L	522169	5396826	140	20	blue clay		clay	silt-clay diamicton
04L	522169	5396826	62	98	grey sandstone		sandstone	sandstone
04L	522169	5396826	-172	332	grey sandstone + water		sandstone	sandstone
04L	522169	5396826	-174	334	grey sandstone		sandstone	sandstone
04L	522169	5396826	-195	355			sandstone	sandstone
04N	522862	5396973	95	0	top soil		soil	sand
04N	522862	5396973	94	1	sand & gravel		sand	sand
04N	522862	5396973	92	3	sand,gravel,hardpan		sand w/clay	silt-clay diamicton
04N	522862	5396973	81	14	sand,gravel,blue clay		sand w/clay	silt-clay diamicton
04N	522862	5396973	78	17	shale (blue)		shale	sandstone
04N	522862	5396973	72	23	sandstone		sandstone	sandstone
04N	522862	5396973	62	33	water app 1 gpm		sandstone	sandstone
04N	522862	5396973	25	70	water app 3 gpm		sandstone	sandstone
04N	522862	5396973	0	95	cave area		sandstone	sandstone
04N	522862	5396973	-22	117	water app 7 gpm		sandstone	sandstone
04N	522862	5396973	-32	127			sandstone	sandstone
04Q	523117	5396165	95	0	top soil		soil	silt-clay diamicton
04Q	523117	5396165	92	5	sand, gravel & hardpan		sand w/clay	silt-clay diamicton
04Q	523117	5396165	87	14	sand & gravel (dry)		sand	sand
04Q	523117	5396165	74	38	sand & clay (brown)		sand w/clay	silt-clay diamicton
04Q	523117	5396165	29	47	sandstone		sandstone	sandstone
04Q	523117	5396165	18	215	water app 30 GPH		sandstone	sandstone
04Q	523117	5396165	11	260	water app 7 GPH		sandstone	sandstone
04Q	523117	5396165	96	275	bottom		sandstone	sandstone
04T	522749	5397329	72	0	top soil & fill		soil	silt-clay diamicton

04T	522749	5397329	69	2	sand & little clay (brown)	sand	silt-clay diamicton
04T	522749	5397329	64	14	sand & little clay (blue)	sand	silt-clay diamicton
04T	522749	5397329	59	17	sandstone (soft)	sandstone	sandstone
04T	522749	5397329	56	28	sandstone (light brown)	sandstone	sandstone
04T	522749	5397329	-8	30	sandstone (grey)	sandstone	sandstone
04T	522749	5397329	-13	43	water approx 1 gpm	sandstone	sandstone
04T	522749	5397329	72	68	water	sandstone	sandstone
04T	522749	5397329	72	78	sandstone	sandstone	sandstone
04U	522849	5397057	98	0	top soil	soil	silt-clay diamicton
04U	522849	5397057	97	1	sand, gravel & little clay	sand w/ clay	silt-clay diamicton
04U	522849	5397057	94	4	sandstone (brown)	sandstone	sandstone
04U	522849	5397057	82	16	sandstone (gray)	sandstone	sandstone
04U	522849	5397057	59	39	sandstone (gray) soft some water	sandstone	sandstone
04U	522849	5397057	58	40	water app 30 gpm	sandstone	sandstone
04U	522849	5397057	-2	100	water	sandstone	sandstone
04U	522849	5397057	-8	106	bottom	sandstone	sandstone
04V	521873	5396727	141	0	clay & gravel	gravel clay	silt-clay diamicton
04V	521873	5396727	141	2	loose gravel	gravel/sand	sand
04V	521873	5396727	139	4	red clay	clay	silt-clay diamicton
04V	521873	5396727	105	11	grey clay	clay	silt-clay diamicton
04V	521873	5396727	93	22	hardpan	hardpan	silt-clay diamicton
04V	521873	5396727	26	24	grey clay & gravel	gravel clay	silt-clay diamicton
04V	521873	5396727	11	78	clay & rocks	clay	silt-clay diamicton
04V	521873	5396727	141	88	sandstone	sandstone	sandstone
04V	521873	5396727	141	153		sandstone	sandstone
04W	522040	5397533	210	0	blk topsoil	soil	silt-clay diamicton
04W	522040	5397533	206	5	decomposed sandstone	sandstone	sandstone
04W	522040	5397533	204	8	sandstone	sandstone	sandstone
04W	522040	5397533	192	93	hard green sandstone	sandstone	sandstone
04W	522040	5397533	183	94	moderate hard sandstone	sandstone	sandstone
04W	522040	5397533	172	97	soft sandstone	sandstone	sandstone

04W	522040	5397533	171	122		sandstone	sandstone
04X	522576	5396382	-80	0	red clay	clay	silt-clay diamicton
04X	522576	5396382	-100	2	loose gravel	gravel/sand	sand
04X	522576	5396382	150	4	hardpan	hardpan	silt-clay diamicton
04X	522576	5396382	150	15	clay & sand	sand clay	silt-clay diamicton
04X	522576	5396382	149	28	hardpan	hardpan	silt-clay diamicton
04X	522576	5396382	147	38	hard clay	clay	silt-clay diamicton
04X	522576	5396382	132	41	hardpan	hardpan	silt-clay diamicton
04X	522576	5396382	70	42	cemented sand	sand	silt-clay diamicton
04X	522576	5396382	10	67	bedrock-sandstone	sandstone	sandstone
04X	522576	5396382	150	115	bedrock-sandstone (dry hole)	sandstone	sandstone
04Y	522539	5396917	119	0	top soil	soil	sand
04Y	522539	5396917	115	3	sand & gravel	sand	sand
04Y	522539	5396917	112	5	sand, gravel & hardpan	sand w/clay	silt-clay diamicton
04Y	522539	5396917	101	14	sand & blue clay (soft)	sand w/clay	silt-clay diamicton
04Y	522539	5396917	71	47	sand, gravel & blue clay	sand w/clay	silt-clay diamicton
04Y	522539	5396917	119	60	sand, gravel & water (muddy)	sand	sand
04Y	522539	5396917	119	69	sand coarse & water	sand	sand
04Y	522539	5396917	111	75		sand	sand
04Z	522408	5397636	112	0	red clay	clay	silt-clay diamicton
04Z	522408	5397636	83	8	grey clay	clay	silt-clay diamicton
04Z	522408	5397636	47	13	conglomerate	conglomerate	sandstone
04Z	522408	5397636	-59	42	hard sandstone	sandstone	sandstone
04Z	522408	5397636	-62	78	moderately hard sandstone	sandstone	sandstone
04Z	522408	5397636	-63	184	hard sandstone w/water	sandstone	sandstone
04Z	522408	5397636	125	187	fractured sandstone	sandstone	sandstone
04Z	522408	5397636	125	188		sandstone	sandstone
05AA	not located, lies in vicinity of			0	clay + sand	sand clay	silt-clay diamicton
05AA	Village Point			61	coarse gravel	gravel/sand	sand
05AA				67	hard dry clay	clay	silt-clay diamicton

05AA				98	coarse gravel + fine sand	gravel/sand	sand
05AA				99	hard grey clay with water and sand	sand clay	sand
05AA				113	pea gravel + rocks w/ clay balls	gravel clay	sand
05AA				121	pea gravel + rocks w/ clay balls	fine sand	sand
05B	521457	5397088	150	0	red clay & gravel	gravel clay	silt-clay diamicton
05B	521457	5397088	148	6	cemented grey clay	clay	silt-clay diamicton
05B	521457	5397088	212	14	soft sandstone	sandstone	sandstone
05B	521457	5397088	212	20	grey/blk sandstone	sandstone	sandstone
05B	521457	5397088	204	145		sandstone	sandstone
05BB	not located, lies in vicinity of			0	red clay + gravel	gravel clay	silt-clay diamicton
05BB	Village Point			12	gravel w/water	gravel/sand	sand
05BB				15	grey clay	clay	silt-clay diamicton
05BB				40	sandy grey clay	sand clay	silt-clay diamicton
05BB				49	grey clay	clay	silt-clay diamicton
05BB				97	clay + cobbles	gravel clay	silt-clay diamicton
05BB				111	black hard clay	clay	silt-clay diamicton
05BB				123	loose gravel w/salt water	gravel/sand	sand
05BB				135	grey clay	clay	silt-clay diamicton
05BB				168	sandy clay	sand clay	silt-clay diamicton
05BB				173	grey clay w/sand	sand clay	silt-clay diamicton
05BB				201	grey clay	clay	silt-clay diamicton
05BB				207	volcanic breccia	greenstone	greenstone
05BB				258		greenstone	greenstone
05C	521363	5396307	79	0	top soil	soil	silt-clay diamicton
05C	521363	5396307	78	1	sand, gravel & hardpan	sand w/clay	silt-clay diamicton
05C	521363	5396307	73	6	sandstone	sandstone	sandstone
05C	521363	5396307	35	44	some water app 10 gpm	sandstone	sandstone
05C	521363	5396307	-146	225	coal seam	sandstone	sandstone
05C	521363	5396307	-147	226	sandstone	sandstone	sandstone
05C	521363	5396307	-156	235	water app 1.5 gpm	sandstone	sandstone
05C	521363	5396307	-261	340	green stone (soft)	greenstone	greenstone

05C	521363	5396307	-270	349	water app 4 gpm	greenstone	greenstone
05C	521363	5396307	-281	360	formation caves	greenstone	greenstone
05C	521363	5396307	-284	363	water app 10 gpm	greenstone	greenstone
05C	521363	5396307	-286	365	formation caves bottom	greenstone	greenstone
05C	521363	5396307	-289	368	bottom green rock (hard)	greenstone	greenstone
05E	520590	5397448	-209	0	brown clay	clay	silt-clay diamicton
05E	520590	5397448	-229	21	sandy clay	sand clay	silt-clay diamicton
05E	520590	5397448	-249	32	decomposed sandstone	sandstone	sandstone
05E	520590	5397448	-309	35	hard blk sandstone	sandstone	sandstone
05E	520590	5397448	51	38	grey moderately hard sandstone	sandstone	sandstone
05E	520590	5397448	51	158		sandstone	sandstone
05H	520885	5396512	85	0	top soil	soil	silt-clay diamicton
05H	520885	5396512	83	2	red clay	clay	silt-clay diamicton
05H	520885	5396512	77	8	grey clay	clay	silt-clay diamicton
05H	520885	5396512	69	16	grey sandstone	sandstone	sandstone
05H	520885	5396512	-216	301	grey sandstone	sandstone	sandstone
05L	521582	5396605	117	0	top soil	soil	sand
05L	521582	5396605	113	2	sand (brown)	sand	sand
05L	521582	5396605	98	18	sand,gravel,blue clay (soft)	sand w/clay	silt-clay diamicton
05L	521582	5396605	83	34	sand,gravel & little blue clay (hard)	sand	silt-clay diamicton
05L	521582	5396605	12	75	sand, gravel washes (brown, hard)	sand	sand
05L	521582	5396605	0	101	sand (brown)	sand	sand
05L	521582	5396605	117	119	fine sand, brown with blue clay seams	fine sand	silt-clay diamicton
05L	521582	5396605	117	123	sand very fine blue & muddy	fine sand	sand
05L	521582	5396605	89	153	sand very fine muddy & water	fine sand	sand
05L	521582	5396605	85	166	sand blue clay	sand w/clay	silt-clay diamicton
05L	521582	5396605	78	168	coarse sand & water	sand	sand
05L	521582	5396605	65	181		sand	sand
05M	521692	5396846	157	0	gravel, sand, clay	undiff GD	silt-clay diamicton
05M	521692	5396846	41	116	gravel, sand, clay	undiff GD	sand

05O	521695	5396474	77	0	top soil	soil	sand
05O	521695	5396474	75	1	gravel	gravel/sand	sand
05O	521695	5396474	64	3	blue clay	clay	silt-clay diamicton
05O	521695	5396474	27	18	S.S.	sand	sand
05O	521695	5396474	6	80	blue clay	clay	silt-clay diamicton
05O	521695	5396474	1	140		clay	silt-clay diamicton
05P	520747	5397484	100	0	sand, dry	sand	sand
05P	520747	5397484	100	67	clay, yellow	clay	silt-clay diamicton
05P	520747	5397484	93	72	sandstone, coarse, gray (water)	sandstone	sandstone
05P	520747	5397484	83	168		sandstone	sandstone
05Q	520885	5396639	95	0	gravel, sand, clay	sand w/clay	silt-clay diamicton
05Q	520885	5396639	43	52	sandstone	sandstone	sandstone
05Q	520885	5396639	14	81	shale	shale	sandstone
05Q	520885	5396639	5	90	conglomerate	conglomerate	sandstone
05Q	520885	5396639	-8	103	sandstone	sandstone	sandstone
05Q	520885	5396639	-46	141	shale	shale	sandstone
05Q	520885	5396639	-50	145	sandstone	sandstone	sandstone
05Q	520885	5396639	-183	278	sandstone	sandstone	sandstone
05T	521764	5397104	172	0	top soil	soil	silt-clay diamicton
05T	521764	5397104	164	2	rocks & soil	sand	silt-clay diamicton
05T	521764	5397104	155	5	hardpan (brown)	hardpan	silt-clay diamicton
05T	521764	5397104	99	21	hardpan (grey)	hardpan	silt-clay diamicton
05T	521764	5397104	72	40	sandstone	sandstone	sandstone
05T	521764	5397104	19	137	sandstone (soft, water)	sandstone	sandstone
05T	521764	5397104	-123	138	sandstone (hard)	sandstone	sandstone
05T	521764	5397104	172	150		sandstone	sandstone
05W	521467	5396542	115	0	top soil	soil	sand
05W	521467	5396542	114	1	sand & gravel	sand	sand
05W	521467	5396542	109	6	sand, gravel & hardpan	sand/gravel clay	silt-clay diamicton

05W	521467	5396542	105	10	sand, gravel & blue clay	sand/gravel clay	silt-clay diamicton
05W	521467	5396542	91	24	sandstone	sanstone	sandstone
05W	521467	5396542	-35	150	some water, large cave area	sandstone	sandstone
05W	521467	5396542	-145	260	blue green shale	shale	sandstone
05W	521467	5396542	-165	280	large cave area	shale	sandstone
05W	521467	5396542	-185	300	large cave area	shale	sandstone
05W	521467	5396542	-245	360	no description	shale	sandstone
05Y	521190	5396685	154	0	top soil	soil	silt-clay diamicton
05Y	521190	5396685	152	2	brown gravel and soft blue clay?	sand w/clay	silt-clay diamicton
05Y	521190	5396685	138	16	brown gravel and soft blue clay?	sand w/clay	silt-clay diamicton
05Y	521190	5396685	131	23	boulder big	sand w/clay	silt-clay diamicton
05Y	521190	5396685	120	34	gravel little blue clay (hard)	gravel/sand	silt-clay diamicton
05Y	521190	5396685	79	75	gravel washes brown hard	gravel/sand	silt-clay diamicton
05Y	521190	5396685	53	101	sand brown	sand	sand
05Y	521190	5396685	39	115	fine sand brown with blue clay seams	sand w/clay	silt-clay diamicton
05Y	521190	5396685	31	123	very fine (sand?) blue (clay?) muddy	sand w/clay	silt-clay diamicton
05Y	521190	5396685	1	153	very fine (sand?) muddy water	fine sand	sand
05Y	521190	5396685	-12	166	blue clay	clay	silt-clay diamicton
05Y	521190	5396685	-14	168	coarse sand and water	sand	sand
05Y	521190	5396685	-27	181	coarse sand and water	sand	sand
05Z	521173	5397168	226	0	sand, clay	sand	silt-clay diamicton
05Z	521173	5397168	224	3	gravel	gravel/sand	sand
05Z	521173	5397168	208	8	clay	clay	silt-clay diamicton
05Z	521173	5397168	192	13	sandstone	sandstone	sandstone
05Z	521173	5397168	151	16	sandstone	sandstone	sandstone
05Z	521173	5397168	125	80	fractured sandstone	sandstone	sandstone
05Z	521173	5397168	107	85			sandstone
08G	521305	5396212	15	0	sand & gravel fill	sand	sand
08G	521305	5396212	10	5	sand & gravel & little clay	sand	silt-clay diamicton
08G	521305	5396212	-4	19	sand & gravel & salt water	sand	sand
08G	521305	5396212	-23	38	sand & salt water	sand	sand

08G	521305	5396212	-26	41	sand fine & salt water	fine sand	sand
08G	521305	5396212	-51	66	sand very fine & muddy	fine sand	sand
08G	521305	5396212	-60	75	sand very fine and blue clay	sand w/clay	silt-clay diamicton
08G	521305	5396212	-78	93	sand & gravel & water	sand	sand
08G	521305	5396212	-84	99	sand & gravel & water	sand	sand
08O	521323	5396147	1	0	blk farm soil	soil	silt-clay diamicton
08O	521323	5396147	-32	2	clay & gravel	gravel clay	silt-clay diamicton
08O	521323	5396147	-45	28	clay & fine sand	sand clay	silt-clay diamicton
08O	521323	5396147	-54	53	decomposed sandstone	sandstone	sandstone
08O	521323	5396147	-60	55	sandstone	sandstone	sandstone
08O	521323	5396147	15	100		sandstone	sandstone
08W	520890	5396172	23	0	s, gr, cl	undiff GD	silt-clay diamicton
08W	520890	5396172	-61	84	s, gr, cl	undiff GD	silt-clay diamicton
08Z	521659	5396148	6	0	loose dry gravel	gravel/sand	sand
08Z	521659	5396148	-11	17	blk sand + clay	sand clay	silt-clay diamicton
08Z	521659	5396148	-12	18	clay + gravel	gravel clay	silt-clay diamicton
08Z	521659	5396148	-39	45	grey clay	clay	silt-clay diamicton
08Z	521659	5396148	-64	70	fine sand + clay	sand clay	silt-clay diamicton
08Z	521659	5396148	-74	80	find sand w/w	fine sand	sand
08Z	521659	5396148	-102	108		fine sand	sand
09A	522692	5396069	60	0	forest overburden	soil	silt-clay diamicton
09A	522692	5396069	-12	4	very hard clay + gravel	gravel clay	silt-clay diamicton
09A	522692	5396069	-64	19	grey clay	clay	silt-clay diamicton
09A	522692	5396069	106	34	very hard clay + gravel	gravel clay	silt-clay diamicton
09A	522692	5396069	106	105	narrow bands of gravel w/water	gravel/sand	sand
09A	522692	5396069	82	117		gravel/sand	sand
09B	522969	5395686	88	0	soil	soil	sand
09B	522969	5395686	42	1	sand, coarse and gravel	sand	sand
09B	522969	5395686	22	13	clay, gravel, blue-boulder	gravel clay	silt-clay diamicton

09B	522969	5395686	117	24	sand, blue and gravel	sand	sand
09B	522969	5395686	117	30	sand, coarse and gravel	sand	sand
09B	522969	5395686	52	70	sand and gravel	sand	sand
09B	522969	5395686	46	108	sand, gravel, and clay, blue	sand w/clay	silt-clay diamicton
09B	522969	5395686	33	118	sand and gravel	sand	sand
09B	522969	5395686	22	138	sandstone, coarse (water 400 gph)	sandstone	sandstone
09B	522969	5395686	-9	143	sandstone, coarse (water 400 gph)	sandstone	sandstone
09D	523196	5395822	67	0	sand, gravel, fill	sand	sand
09D	523196	5395822	63	4	sand, gravel, little clay (brown)	sand	silt-clay diamicton
09D	523196	5395822	26	41	sand, gravel & blue clay	sand w/ clay	silt-clay diamicton
09D	523196	5395822	-47	114	sand, gravel, & blue clay (hard)	sand w/ clay	silt-clay diamicton
09D	523196	5395822	-55	122	sand & blue clay (seepage)	sand w/ clay	silt-clay diamicton
09D	523196	5395822	-59	126	sand & blue clay (soft)	sand w/ clay	silt-clay diamicton
09D	523196	5395822	-88	155	sand & streaks muddy water	sand	sand
09D	523196	5395822	-91	158	set screen to muddy (too muddy?)	sand	sand
09D	523196	5395822	-96	163	sand & firm to hard blue clay	sand w/ clay	silt-clay diamicton
09D	523196	5395822	-196	263	sand & blue clay (hard)	sand w/ clay	silt-clay diamicton
09D	523196	5395822	-223	290	sand very fine	fine sand	sand
09D	523196	5395822	-228	295		fine sand	sand
09E	522739	5395789	100	0	top soil	soil	silt-clay diamicton
09E	522739	5395789	99	1	hardpan, sand, gravel	sand/gravel clay	silt-clay diamicton
09E	522739	5395789	89	11	blue clay	clay	silt-clay diamicton
09E	522739	5395789	53	47	blue clay, sand, gravel	sand/gravel clay	silt-clay diamicton
09E	522739	5395789	3	97	brown clay, sand, gravel	sand/gravel clay	silt-clay diamicton
09E	522739	5395789	-48	148	sand & water	sand	sand
09E	522739	5395789	-57	157	rock	sand	sand
09E	522739	5395789	-58	158	rock	sand	sand
09F	522981	5396062	86	0	topsoil	soil	sand
09F	522981	5396062	85	1	sand & gravel	sand	sand
09F	522981	5396062	78	8	clay (blue-grey)	clay	silt-clay diamicton
09F	522981	5396062	60	26	sand & gravel	sand	sand

09F	522981	5396062	22	64	clay (blue-grey)	clay	silt-clay diamicton
09F	522981	5396062	12	74	sand & gravel	sand	sand
09F	522981	5396062	-27	113		sand	sand
09G	523047	5395017	57	0	clay + sand	sand clay	sand
09G	523047	5395017	-100	3	clay	clay	silt-clay diamicton
09G	523047	5395017	118	185	fine grey sand	fine sand	sand
09G	523047	5395017	118	193		fine sand	sand
09I	523184	5394920	109	0	top soil	soil	sand
09I	523184	5394920	94	1	sand & gravel	sand	sand
09I	523184	5394920	77	4	sand & gravel & hardpan	sand w/clay	silt-clay diamicton
09I	523184	5394920	41	11	sand & gravel & blue clay	sand w/clay	silt-clay diamicton
09I	523184	5394920	24	22	sand & gravel & dry (brown)	sand	sand
09I	523184	5394920	21	33	boulders	sand w/clay	silt-clay diamicton
09I	523184	5394920	10	38	sand & gravel & blue clay	sand w/clay	silt-clay diamicton
09I	523184	5394920	-16	65	big boulder	sand w/clay	silt-clay diamicton
09I	523184	5394920	-22	70	sand & gravel dry	sand	sand
09I	523184	5394920	-34	99	sand & gravel & blue clay	sand w/clay	silt-clay diamicton
09I	523184	5394920	127	111	sand & gravel & dry (brown)	sand	sand
09I	523184	5394920	127	118	sand & gravel & blue clay gradually gets less gravel & very fine sand, wet	sand w/clay	silt-clay diamicton
09I	523184	5394920	110	148	sand & gravel & blue clay	sand w/clay	silt-clay diamicton
09I	523184	5394920	108	149	sand & gravel & water	sand	sand
09I	523184	5394920	92	155	sand & gravel & blue clay	sand w/clay	silt-clay diamicton
09J	523169	5395705	70	0	loose gravel	gravel/sand	sand
09J	523169	5395705	51	6	cemented gravel	gravel/sand	silt-clay diamicton
09J	523169	5395705	39	57	silt clay	clay	silt-clay diamicton
09J	523169	5395705	14	108	fine sand silt w/water	fine sand	sand
09J	523169	5395705	4	115	silt clay	clay	silt-clay diamicton
09J	523169	5395705	108	116		clay	silt-clay diamicton
09K	521990	5396087	13	0	coarse gravel	gravel/sand	sand

09K	521990	5396087	-8	3	coarse gravel, some clay	gravel/sand	silt-clay diamicton
09K	521990	5396087	-19	12	coarse gravel& salt water	gravel/sand	sand
09K	521990	5396087	-22	26	black and green sand & clay (soft)	sand w/clay	silt-clay diamicton
09K	521990	5396087	-25	30	blue clay	clay	silt-clay diamicton
09K	521990	5396087	-145	35	blue clay & some gravel	gravel clay	silt-clay diamicton
09K	521990	5396087	13	59	coarse gravel & sand & water	gravel/sand	sand
09K	521990	5396087	13	63	coarse gravel & sand & water	gravel/sand	sand
09L	522399	5396005	47	0	brown sand gravel	sand	sand
09L	522399	5396005	23	3	brown sand gravel clay	sand w/clay	silt-clay diamicton
09L	522399	5396005	19	45	brown gravel sand	sand	sand
09L	522399	5396005	-31	46	brown sand gravel clay	sand w/clay	silt-clay diamicton
09L	522399	5396005	-40	62	gray sand gravel & water	sand	sand
09L	522399	5396005	-47	65	gray gravel sand silt	sand	silt-clay diamicton
09L	522399	5396005	-76	80	clay	clay	silt-clay diamicton
09L	522399	5396005	50	81			silt-clay diamicton
09M	523267	5395961	26	0	top soil	soil	silt-clay diamicton
09M	523267	5395961	22	2	hardpan (brown)	hardpan	silt-clay diamicton
09M	523267	5395961	11	13	hardpan (grey)	hardpan	silt-clay diamicton
09M	523267	5395961	8	50	sandy clay	sand clay	silt-clay diamicton
09M	523267	5395961	-1	71	water sand (medium)	sand	sand
09M	523267	5395961	-19	76		sand	sand
09Q	523141	5394565	44	0	black surface soil	soil	silt-clay diamicton
09Q	523141	5394565	-85	2	clay & gravel	gravel clay	silt-clay diamicton
09Q	523141	5394565	91	5	grey clay & fine gravel	gravel clay	silt-clay diamicton
09Q	523141	5394565	91	85	hardpan	hardpan	silt-clay diamicton
09Q	523141	5394565	86	95	coarse gravel w/water	gravel/sand	sand
09Q	523141	5394565	77	96		gravel/sand	sand
09R	522127	5395943	-24	0	clay + gravel	gravel clay	silt-clay diamicton
09R	522127	5395943	-33	28	gravel w/ saltwater	gravel/sand	sand
09R	522127	5395943	-201	29	greenish clay	clay	silt-clay diamicton

09R	522127	5395943	-246	43	dry gravel	gravel/sand	sand
09R	522127	5395943	-261	45	clay + sand	sand clay	silt-clay diamicton
09R	522127	5395943	14	56	hardpan	hardpan	silt-clay diamicton
09R	522127	5395943	14	57	grey clay	clay	silt-clay diamicton
09R	522127	5395943	9	59	sand + gravel	sand	sand
09R	522127	5395943	6	62	hardpan	hardpan	silt-clay diamicton
09R	522127	5395943	-79	64		hardpan	silt-clay diamicton
09S	522641	5395731	77	0	red clay & rocks	clay	silt-clay diamicton
09S	522641	5395731	69	8	grey clay w/rocks	clay	silt-clay diamicton
09S	522641	5395731	27	50	soft grey clay	clay	silt-clay diamicton
09S	522641	5395731	24	53	hard clay + gravel	gravel clay	silt-clay diamicton
09S	522641	5395731	-1	78	gravel w/water	gravel/sand	sand
09S	522641	5395731	-2	79	soft grey clay	clay	silt-clay diamicton
09S	522641	5395731	-5	82	hardpan	hardpan	silt-clay diamicton
09S	522641	5395731	-6	83	coarse gravel w/water	gravel/sand	sand
09S	522641	5395731	-7	84	hardpan	hardpan	silt-clay diamicton
09S	522641	5395731	-9	86	fine sand + clay	sand w/clay	silt-clay diamicton
09S	522641	5395731	-28	105	quicksand	sand	sand
09S	522641	5395731	-38	115	hard clay + gravel	gravel clay	silt-clay diamicton
09S	522641	5395731	-42	119	soft clay	clay	silt-clay diamicton
09S	522641	5395731	-45	122	hardpan	hardpan	silt-clay diamicton
09S	522641	5395731	-51	128	soft clay	clay	silt-clay diamicton
09S	522641	5395731	-79	156	dry loose gravel	gravel/sand	sand
09S	522641	5395731	-82	159	soft clay	clay	silt-clay diamicton
09S	522641	5395731	-100	177	hard clay + sand	sand clay	silt-clay diamicton
09S	522641	5395731	-127	204	hard clay + gravel	gravel clay	silt-clay diamicton
09S	522641	5395731	-174	251		gravel clay	sand
09T	523001	5395855	89	0	sand & gravel	sand	sand
09T	523001	5395855	75	14	sand, gravel & blue clay	sand w/clay	silt-clay diamicton
09T	523001	5395855	67	22	sand (brown)	sand	sand
09T	523001	5395855	65	24	sand, gravel & blue clay	sand w/clay	silt-clay diamicton
09T	523001	5395855	46	43	boulder	sand w/clay	silt-clay diamicton

09T	523001	5395855	44	45	sand & gravel (brown)	sand	sand
09T	523001	5395855	11	78	sand, gravel & blue clay	sand w/clay	silt-clay diamicton
09T	523001	5395855	-6	95	sand, gravel & blue clay	sand w/clay	silt-clay diamicton
09T	523001	5395855	-165	254	sand & water	sand	sand
09T	523001	5395855	-171	260	sand & water	sand	sand
09U	522315	5395839	21	0	top soil	sand w/clay	silt-clay diamicton
09U	522315	5395839	20	1	sand, gravel & little clay (brown)	sand w/clay	silt-clay diamicton
09U	522315	5395839	-47	68	sand, gravel & water	sand	sand
09U	522315	5395839	-59	80		sand	sand
09V	523304	5395405	106	0	topsoil	soil	silt-clay diamicton
09V	523304	5395405	104	2	hardpan	hardpan	silt-clay diamicton
09V	523304	5395405	96	36	brown sand/gravel	sand	sand
09V	523304	5395405	85	48	gravel	gravel/sand	sand
09V	523304	5395405	64	115	gravel/sand	gravel/sand	sand
09V	523304	5395405	17	130		gravel/sand	sand
09W	523256	5394624	104	0	topsoil	soil	sand
09W	523256	5394624	102	2	sand + gravel	gravel/sand	sand
09W	523256	5394624	101	3	sand-gravel-hardpan	sand/gravel clay	silt-clay diamicton
09W	523256	5394624	60	44	blue clay + sand	sand clay	silt-clay diamicton
09W	523256	5394624	53	51	blue clay sand + gravel	sand/gravel clay	silt-clay diamicton
09W	523256	5394624	23	81	blue clay + gravel	gravel clay	silt-clay diamicton
09W	523256	5394624	-4	108	sand gravel + water	sand	sand
09W	523256	5394624	-12	116		sand	sand
09Y	522669	5395908	100	0	topsoil	soil	sand
09Y	522669	5395908	98	2	sand, gravel	gravel/sand	sand
09Y	522669	5395908	93	7	sand, gravel	gravel/sand	sand
09Y	522669	5395908	78	22	sand, gravel, clay	sand/gravel clay	silt-clay diamicton
09Y	522669	5395908	73	27	sand, gravel, boulders	gravel/sand	sand
09Y	522669	5395908	70	30	sand, gravel, clay	sand/gravel clay	silt-clay diamicton
09Y	522669	5395908	20	80	sand, gravel, clay, water	gravel/sand	sand

09Y	522669	5395908	15	85			gravel/sand	sand
10A	523999	5395332	7	0	clay & gravel		gravel clay	silt-clay diamicton
10A	523999	5395332	-25	32	blue clay		clay	silt-clay diamicton
10A	523999	5395332	-49	56	grey clay		clay	silt-clay diamicton
10A	523999	5395332	-195	202	sand & cobbles 1"		sand	sand
10A	523999	5395332	-198	205	sand & cobbles 1"		sand	sand
10B	524231	5394814	90	0	hardpan boulders		hardpan	silt-clay diamicton
10B	524231	5394814	65	46	sandstone-green		greenstone	greenstone
10B	524231	5394814	65	118	sandstone-green hard fractured		greenstone	greenstone
10B	524231	5394814	62	170			greenstone	greenstone
10C	523870	5394944	126	0	clay & gravel		gravel clay	silt-clay diamicton
10C	523870	5394944	114	12	soft clay		clay	silt-clay diamicton
10C	523870	5394944	176	15	hard clay		clay	silt-clay diamicton
10C	523870	5394944	176	19	clay & sand		sand clay	silt-clay diamicton
10C	523870	5394944	175	44	trace gravel w/water		clay	sand
10C	523870	5394944	172	44	soft clay		clay	silt-clay diamicton
10C	523870	5394944	161	47	hardpan		hardpan	silt-clay diamicton
10C	523870	5394944	132	50	bedrock-hard		greenstone	sandstone
10C	523870	5394944	126	62			greenstone	sandstone
10E	523758	5395159	107	0	brown clay + gravel		gravel clay	silt-clay diamicton
10E	523758	5395159	91	8	grey clay		clay	silt-clay diamicton
10E	523758	5395159	81	15	clay + gravel		gravel clay	silt-clay diamicton
10E	523758	5395159	163	26	hardpan		hardpan	silt-clay diamicton
10E	523758	5395159	163	28	heaving sand		sand	sand
10E	523758	5395159	155	30	clay + sand		sand clay	silt-clay diamicton
10E	523758	5395159	154	47	fine sand w/water		fine sand	sand
10E	523758	5395159	114	48	grey clay		clay	silt-clay diamicton
10E	523758	5395159	110	49	sand w/water		sand	sand
10E	523758	5395159	95	54	grey clay		clay	silt-clay diamicton

10G	523889	5395195	81	0	clay + rocks	clay	silt-clay diamicton
10G	523889	5395195	5	3	red clay	clay	silt-clay diamicton
10G	523889	5395195	0	27	loose sand	sand	sand
10G	523889	5395195	178	29	red clay	clay	silt-clay diamicton
10G	523889	5395195	178	56	sandy clay	sand clay	silt-clay diamicton
10G	523889	5395195	172	91	flowing sand	sand	sand
10G	523889	5395195	164	106	hard grey clay	clay	silt-clay diamicton
10G	523889	5395195	158	113	grey sandstone	sandstone	sandstone
10G	523889	5395195	33	138	red tinged grey sandstone	sandstone	sandstone
10G	523889	5395195	178	142	greenstone	greenstone	greenstone
10G	523889	5395195	178	173	red tinged blk sandstone	greenstone	greenstone
10G	523889	5395195	176	197	greenstone	greenstone	greenstone
10G	523889	5395195	164	203	blk sandstone	greenstone	greenstone
10G	523889	5395195	161	224	blk sandstone	greenstone	greenstone
10I	523517	5395528	123	0	clay fill	clay	silt-clay diamicton
10I	523517	5395528	121	2	sand, gravel & hardpan	hardpan	silt-clay diamicton
10I	523517	5395528	112	11	sand, gravel & blue clay	sand/gravel clay	silt-clay diamicton
10I	523517	5395528	88	35	sand & gravel (dry)	sand	sand
10I	523517	5395528	75	48	sand & little clay (brown)	sand clay	silt-clay diamicton
10I	523517	5395528	61	62	sand (dry)	sand	sand
10I	523517	5395528	36	87	sand & blue clay	sand clay	silt-clay diamicton
10I	523517	5395528	31	92	sand & gravel (dry)	sand	sand
10I	523517	5395528	16	107	sand, gravel & blue clay	sand/gravel clay	silt-clay diamicton
10I	523517	5395528	-52	175	fine sand with clay lenses & water	sand	sand
10I	523517	5395528	-59	182		sand	sand
10J	524286	5394779	78	0	top soil	soil	sand
10J	524286	5394779	77	1	sand, gravel & boulders (brown)	sand	sand
10J	524286	5394779	74	9	sandy clay (brown)	sand clay	silt-clay diamicton
10J	524286	5394779	67	17	sand, gravel & boulders dark, brown and hard	sand	silt-clay diamicton
10J	524286	5394779	56	31	Shuksan stone very, very hard	greenstone	greenstone
10J	524286	5394779	45	52	water app 5 gph	greenstone	greenstone

10J	524286	5394779	40	118	water app 20 gph	greenstone	greenstone
10J	524286	5394779	13	120	some water app 25 gph	greenstone	greenstone
10J	524286	5394779	8	129		greenstone	greenstone
10K	523935	5395081	185	0	brown sand	sand	sand
10K	523935	5395081	182	3	sand & gravel	sand	sand
10K	523935	5395081	178	7	fine cemented brown sand	fine sand	silt-clay diamicton
10K	523935	5395081	157	28	dry hard clay grey	clay	silt-clay diamicton
10K	523935	5395081	131	54	gravel & clay w/water	sand w/clay	silt-clay diamicton
10K	523935	5395081	129	56	cemented fine sand	fine sand	silt-clay diamicton
10K	523935	5395081	108	77	green sandstone	greenstone	greenstone
10K	523935	5395081	-2	187	green sandstone	greenstone	greenstone
10M	523628	5394696	149	0	very hard clay	clay	silt-clay diamicton
10M	523628	5394696	84	65	cobbles + clay	clay	silt-clay diamicton
10M	523628	5394696	78	71	grey clay	clay	silt-clay diamicton
10M	523628	5394696	65	84	grey sand + clay	sand w/clay	silt-clay diamicton
10M	523628	5394696	54	95	hard grey clay	clay	silt-clay diamicton
10M	523628	5394696	23	126	clay + gravel	gravel clay	silt-clay diamicton
10M	523628	5394696	11	138	coarse gravel w/water	gravel/sand	sand
10M	523628	5394696	8	141	large gravel w/water	gravel/sand	sand
10M	523628	5394696	0	149		gravel/sand	sand
10P	523957	5394824	194	0	top soil	soil	silt-clay diamicton
10P	523957	5394824	193	1	hardpan	hardpan	silt-clay diamicton
10P	523957	5394824	185	9	blue clay	clay	silt-clay diamicton
10P	523957	5394824	182	12	blue clay sand gravel	sand/gravel clay	silt-clay diamicton
10P	523957	5394824	145	49	blue green rock	greenstone	greenstone
10P	523957	5394824	-6	200	blue green rock	greenstone	greenstone
10R	523722	5394767	152	0	clay	clay	silt-clay diamicton
10R	523722	5394767	148	4	hardpan	hardpan	silt-clay diamicton
10R	523722	5394767	141	11	grey clay	clay	silt-clay diamicton
10R	523722	5394767	133	19	decomposed greenstone	greenstone	greenstone

10R	523722	5394767	129	23	hard greenstone	greenstone	greenstone
10R	523722	5394767	52	100	hard greenstone	greenstone	greenstone
10V	523356	5395756	62	0	red clay + gravel	gravel clay	silt-clay diamicton
10V	523356	5395756	53	9	brown clay + gravel	gravel clay	silt-clay diamicton
10V	523356	5395756	48	14	brown clay + gravel	gravel clay	silt-clay diamicton
10V	523356	5395756	46	16	brown clay + fine gravel	gravel clay	silt-clay diamicton
10V	523356	5395756	1	61	clay + sand	sand clay	silt-clay diamicton
10V	523356	5395756	-8	70	grey clay w/water	sand w/clay	sand
10V	523356	5395756	-20	82	cemented fine sand	fine sand	sand
10V	523356	5395756	-40	102	grey clay	clay	silt-clay diamicton
10V	523356	5395756	-56	118	hardpan	hardpan	silt-clay diamicton
10V	523356	5395756	-58	120	pea gravel w/water	gravel/sand	sand
10V	523356	5395756	-60	122	fine sand + clay	sand w/clay	silt-clay diamicton
10V	523356	5395756	-158	220		sand w/clay	silt-clay diamicton
10X	523547	5395448	68	0	clay & gravel	gravel clay	silt-clay diamicton
10X	523547	5395448	53	8	gravel w/water	gravel/sand	sand
10X	523547	5395448	47	9	grey clay	clay	silt-clay diamicton
10X	523547	5395448	37	49	cemented gravel	gravel/sand	silt-clay diamicton
10X	523547	5395448	24	53	clay-narrow bands dry gravel	clay	silt-clay diamicton
10X	523547	5395448	-13	68	50-50 clay & gravel	gravel clay	silt-clay diamicton
10X	523547	5395448	-24	97	hard grey clay	clay	silt-clay diamicton
10X	523547	5395448	-27	173	sand & gravel	sand	sand
10X	523547	5395448	121	178		sand	sand
10Y	524263	5394806	91	0	yellow clay	clay	silt-clay diamicton
10Y	524263	5394806	79	24	decomposed greenstone	greenstone	greenstone
10Y	524263	5394806	63	29	very hard greenstone	greenstone	greenstone
10Y	524263	5394806	58	75	moderately hard greenstone	greenstone	greenstone
10Y	524263	5394806	46	95		greenstone	greenstone
10Z	523397	5395082	159	0	sand, clay	sand w/clay	silt-clay diamicton
10Z	523397	5395082	153	6	sand, clay	sand w/clay	silt-clay diamicton

10Z	523397	5395082	146	13	hardpan	hardpan	silt-clay diamicton
10Z	523397	5395082	119	40	conglomerate	conglomerate	sandstone
10Z	523397	5395082	113	46	greenstone	greenstone	greenstone
10Z	523397	5395082	-11	170	greenstone	greenstone	greenstone
15A	523608	5393997	178	0	top soil	soil	sand
15A	523608	5393997	177	1	sand & gravel	sand	sand
15A	523608	5393997	175	3	sand,gravel,hardpan	sand w/clay	silt-clay diamicton
15A	523608	5393997	166	12	sand & gravel	sand	sand
15A	523608	5393997	135	43	sand,gravel & blue clay, soft	sand w/clay	silt-clay diamicton
15A	523608	5393997	86	92	sand, gravel, blue clay, hard	sand w/clay	silt-clay diamicton
15A	523608	5393997	72	106	fine sand & gravel muddy water	fine sand	sand
15A	523608	5393997	16	162	very fine muddy sand	fine sand	sand
15A	523608	5393997	12	166		fine sand	sand
15C	523916	5393970	106	0	topsoil	soil	sand
15C	523916	5393970	105	1	sand & gravel	gravel/sand	sand
15C	523916	5393970	100	6	sand, gravel & hardpan	hardpan	silt-clay diamicton
15C	523916	5393970	91	15	sand, gravel & blue clay gradually gets less clay	sand/gravel clay	silt-clay diamicton
15C	523916	5393970	53	53	sand & blue clay (soft)	sand clay	silt-clay diamicton
15C	523916	5393970	20	86	sand brown little clay	sand clay	sand
15C	523916	5393970	15	91	sand & gravel (dry)	gravel/sand	sand
15C	523916	5393970	11	95	sand & blue clay	sand clay	silt-clay diamicton
15C	523916	5393970	-18	124	sand & muddy water	sand	sand
15C	523916	5393970	-24	130	sand & blue clay	sand clay	silt-clay diamicton
15C	523916	5393970	-32	138	boulders	sand clay	silt-clay diamicton
15C	523916	5393970	-35	141	sand & blue clay	sand clay	silt-clay diamicton
15C	523916	5393970	-38	144	sand coarse & water	sand	sand
15C	523916	5393970	-43	149		sand	sand
15D	523443	5393630	88	0	clay + gravel	gravel clay	silt-clay diamicton
15D	523443	5393630	83	5	rocks	gravel/sand	silt-clay diamicton
15D	523443	5393630	81	7	red clay	clay	silt-clay diamicton

15D	523443	5393630	76	12	grey clay	clay	silt-clay diamicton
15D	523443	5393630	48	40	hardpan	hardpan	silt-clay diamicton
15D	523443	5393630	41	47	narrow bands of clay & hardpan	clay	silt-clay diamicton
15D	523443	5393630	-27	115	flowing mud	sand	sand
15D	523443	5393630	-44	132	hardpan	hardpan	silt-clay diamicton
15D	523443	5393630	-71	159	sand & gravel	sand	sand
15D	523443	5393630	-84	172		sand	sand
15H	524495	5394504	34	0	clay + rocks	sand/gravel clay	silt-clay diamicton
15H	524495	5394504	-28	62	clay + sand	sand clay	silt-clay diamicton
15H	524495	5394504	-40	74	decomposed sandstone	greenstone	greenstone
15H	524495	5394504	-42	76	hard blk sandstone	greenstone	greenstone
15H	524495	5394504	-139	173	moderately soft sandstone	greenstone	greenstone
15H	524495	5394504	-238	272		greenstone	greenstone
15K	524378	5393846	56	0	top soil	soil	sand
15K	524378	5393846	55	1	sand & gravel	sand	sand
15K	524378	5393846	42	14	sand, gravel & blue clay	sand w/clay	silt-clay diamicton
15K	524378	5393846	34	22	sand & brown clay	sand w/clay	silt-clay diamicton
15K	524378	5393846	1	55	sand & brown clay & water seepage	sand w/clay	silt-clay diamicton
15K	524378	5393846	-18	73	sand & water	sand	sand
15K	524378	5393846	-31	86		sand	sand
15L	524034	5393832	60	0	top soil	soil	sand
15L	524034	5393832	58	2	sand	sand	sand
15L	524034	5393832	57	3	sand & little clay (brown)	sand	silt-clay diamicton
15L	524034	5393832	50	10	sand, gravel & blue clay	sand w/clay	silt-clay diamicton
15L	524034	5393832	45	15	boulder	sand w/clay	silt-clay diamicton
15L	524034	5393832	32	28	sand, gravel & blue clay (hard)	sand w/clay	silt-clay diamicton
15L	524034	5393832	-18	78	sand, gravel & blue clay (very hard)	sand w/clay	silt-clay diamicton
15L	524034	5393832	-22	82	sand, water, muddy very dark (brown)	sand	sand
15L	524034	5393832	-27	87	coarse sand & water	sand	sand
15L	524034	5393832	-33	93		sand	sand

15O	524452	5394176	123	0	red clay + gravel	gravel clay	silt-clay diamicton
15O	524452	5394176	111	12	grey clay + gravel	gravel clay	silt-clay diamicton
15O	524452	5394176	70	53	grey clay + gravel	clay	silt-clay diamicton
15O	524452	5394176	55	68	blue clay	clay	silt-clay diamicton
15O	524452	5394176	49	74	brown clay	clay	silt-clay diamicton
15O	524452	5394176	39	84	red clay & sand	sand clay	silt-clay diamicton
15O	524452	5394176	26	97	grey clay	clay	silt-clay diamicton
15O	524452	5394176	-11	134	clay & sand	sand clay	silt-clay diamicton
15O	524452	5394176	-22	145	soft sandstone	sandstone	sandstone
15O	524452	5394176	-25	148	gravel & broken rock	sandstone	sandstone
15P	524019	5393809	59	0	top soil	soil	sand
15P	524019	5393809	58	1	sand	sand	sand
15P	524019	5393809	55	4	sand, gravel & little clay (brown)	sand	silt-clay diamicton
15P	524019	5393809	50	9	sand, gravel & blue clay	sand w/clay	silt-clay diamicton
15P	524019	5393809	37	22	sand & blue clay (hard)	sand w/clay	silt-clay diamicton
15P	524019	5393809	-8	67	sand & water muddy	sand	sand
15P	524019	5393809	-19	78	sand & gravel & water	sand	sand
15P	524019	5393809	-26	85		sand	sand
15R	524447	5394427	101	0	top soil	soil	silt-clay diamicton
15R	524447	5394427	100	1	cemented gravel boulders	hardpan	silt-clay diamicton
15R	524447	5394427	39	62	conglomerate rock	greenstone	greenstone
15R	524447	5394427	-17	118	clay sand green	greenstone	greenstone
15R	524447	5394427	-25	126	sandstone hard	greenstone	greenstone
15R	524447	5394427	-50	151	clay sand green	greenstone	greenstone
15R	524447	5394427	-53	154	sandstone hard	greenstone	greenstone
15R	524447	5394427	-74	175	clay sand green	greenstone	greenstone
15R	524447	5394427	-199	300		greenstone	greenstone
15S	524283	5393954	73	0	top soil	soil	silt-clay diamicton
15S	524283	5393954	71	2	sand/gravel/hardpan	sandf w/clay	silt-clay diamicton
15S	524283	5393954	55	18	sand/gravel/blue clay	sand w/clay	silt-clay diamicton
15S	524283	5393954	35	38	sand & brown clay	sand w/clay	silt-clay diamicton

15S	524283	5393954	10	63	sand/brown clay/water (very muddy)	sand w/clay	silt-clay diamicton
15S	524283	5393954	-36	109	sand coarse and water	sand	sand
15S	524283	5393954	-48	121		sand	sand
15U	524393	5394479	136	0	broken rock	greenstone	greenstone
15U	524393	5394479	134	2	gray hard rock	greenstone	greenstone
15U	524393	5394479	-69	205	fractured gray rock	greenstone	greenstone
15U	524393	5394479	-89	225		greenstone	greenstone
15X	523440	5393854	93	0	topsoil	soil	silt-clay diamicton
15X	523440	5393854	92	1	sand, gravel & hardpan	hardpan	silt-clay diamicton
15X	523440	5393854	79	14	sand, gravel & blue clay gradually gets less gravel	sand/gravel clay	silt-clay diamicton
15X	523440	5393854	-70	163	sand, gravel & blue clay (hard)	sand/gravel clay	silt-clay diamicton
15X	523440	5393854	-85	178	sand, gravel & little water (muddy)	gravel/sand	sand
15X	523440	5393854	-89	182	sand gravel & water	gravel/sand	sand
15X	523440	5393854	-95	188		gravel/sand	sand
15Z	523421	5393790	89	0	red clay + rocks	gravel clay	silt-clay diamicton
15Z	523421	5393790	73	16	hard grey clay	clay	silt-clay diamicton
15Z	523421	5393790	-48	137	hard sandy clay	sand clay	silt-clay diamicton
15Z	523421	5393790	-60	149	hardpan	hardpan	silt-clay diamicton
15Z	523421	5393790	-68	157	hard clay	clay	silt-clay diamicton
15Z	523421	5393790	-111	200	coarse sand w/water	sand	sand
15Z	523421	5393790	-116	205	coarse gravel	gravel/sand	sand
15Z	523421	5393790	-118	207	fine sand	fine sand	sand
16B	523304	5394321	87	0	overburden	soil	silt-clay diamicton
16B	523304	5394321	84	3	brown clay w/ sand	sand clay	silt-clay diamicton
16B	523304	5394321	75	12	gray clay w/ gravel	gravel clay	silt-clay diamicton
16B	523304	5394321	1	86	flowing mud	clay	sand
16B	523304	5394321	-3	90	soft clay	clay	silt-clay diamicton
16B	523304	5394321	-11	98	hardpan	hardpan	silt-clay diamicton
16B	523304	5394321	-27	114	flowing mud	clay	sand

338

16B	523304	5394321	-31	118	gray sand	sand	sand
16B	523304	5394321	-34	121	gray sand	sand	sand
16B	523304	5394321	-43	130	cemented sand	sand	sand
16B	523304	5394321	-81	168	coarse sand	sand	sand
16B	523304	5394321	-87	174		sand	sand
16K	523313	5393963	75	0	top soil	soil	sand
16K	523313	5393963	73	2	sand & gravel	sand	sand
16K	523313	5393963	71	4	sand & gravel & hardpan	sand w/clay	silt-clay diamicton
16K	523313	5393963	63	12	sand & little clay (brown)	sand w/clay	silt-clay diamicton
16K	523313	5393963	52	23	sand & blue clay (soft)	sand w/clay	silt-clay diamicton
16K	523313	5393963	31	44	sand & blue clay (soft)	sand w/clay	silt-clay diamicton
16K	523313	5393963	-16	91	sand & little gravel & water	sand	sand
16K	523313	5393963	-26	101	blue clay	clay	silt-clay diamicton
16K	523313	5393963	-27	102	blue clay		silt-clay diamicton
16T	523315	5394143	78	0	topsoil	soil	sand
16T	523315	5394143	77	1	sand & gravel (brown)	sand	sand
16T	523315	5394143	74	4	sand, gravel & hardpan	hardpan	silt-clay diamicton
16T	523315	5394143	64	14	sand (brown) & little clay	sand clay	silt-clay diamicton
16T	523315	5394143	61	17	sand & blue clay	sand clay	silt-clay diamicton
16T	523315	5394143	57	21	sand, gravel & blue clay	sand/gravel clay	silt-clay diamicton
16T	523315	5394143	-14	92	sand, gravel clay & water	sand/gravel clay	sand
16T	523315	5394143	-18	96	sand, gravel & blue clay	sand/gravel clay	silt-clay diamicton
16T	523315	5394143	-38	116		sand/gravel clay	silt-clay diamicton
16V	523323	5393982	73	0	top soil	soil	sand
16V	523323	5393982	72	1	sand & gravel (brown)	sand	sand
16V	523323	5393982	69	4	sand, gravel & hardpan	sand w/clay	silt-clay diamicton
16V	523323	5393982	59	14	sand (brown) & little clay	sand	silt-clay diamicton
16V	523323	5393982	56	17	sand & blue clay	sand w/clay	silt-clay diamicton
16V	523323	5393982	52	21	sand, gravel & blue clay	sand w/clay	silt-clay diamicton
16V	523323	5393982	-20	92	sand, gravel clay & water	sand w/clay	sand
16V	523323	5393982	-24	96	sand, gravel & blue clay	sand w/clay	silt-clay diamicton

16V	523323	5393982	-44	116		sand w/clay	silt-clay diamicton
29C	521021	5399408	34	0	top soil	soil	silt-clay diamicton
29C	521021	5399408	33	1	hardpan	hardpan	silt-clay diamicton
29C	521021	5399408	31	3	sand & gravel	sand	sand
29C	521021	5399408	26	8	sand/gravel/blue clay	sand w/clay	silt-clay diamicton
29C	521021	5399408	19	15	sand/gravel brown	sand	sand
29C	521021	5399408	12	22	sandstone (WATER AT 76' AND 85')	sandstone	sandstone
29C	521021	5399408	-69	103		sandstone	sandstone
32A	520937	5398427	217	0	brown clay till	clay	silt-clay diamicton
32A	520937	5398427	200	17	hard grey till	clay	silt-clay diamicton
32A	520937	5398427	198	19	weathered brown sandstone	sandstone	sandstone
32A	520937	5398427	182	35	grey shale	shale	sandstone
32A	520937	5398427	179	38	fine grain sandstone	sandstone	sandstone
32A	520937	5398427	160	57	medium grain sandstone	sandstone	sandstone
32A	520937	5398427	148	69	soft grey shale	shale	sandstone
32A	520937	5398427	123	94	soft blue caving shale	shale	sandstone
32A	520937	5398427	113	104		shale	sandstone
32B	520756	5398491	132	0	brown packed sand + gravel	sand	sand
32B	520756	5398491	114	18	brown gravel + sand	gravel/sand	sand
32B	520756	5398491	99	33	silty gravel + sand	gravel/sand	sand
32B	520756	5398491	82	50	sandy brown clay till	sand clay	silt-clay diamicton
32B	520756	5398491	46	86	clay + gravel till	gravel clay	silt-clay diamicton
32B	520756	5398491	29	103	sandy grey clay till	sand clay	silt-clay diamicton
32B	520756	5398491	26	106	coarse grain sandstone	sandstone	sandstone
32B	520756	5398491	15	117	medium grain sandstone	sandstone	sandstone
32B	520756	5398491	-11	143	hard fine grain sandstone	sandstone	sandstone
32B	520756	5398491	-17	149	coarse grain sandstone	sandstone	sandstone
32B	520756	5398491	-29	161		sandstone	sandstone
32G	521642	5398611	178	0	topsoil	soil	silt-clay diamicton
32G	521642	5398611	177	1	clay	clay	silt-clay diamicton

340

32G	521642	5398611	172	6	sandstone (water bearing)	sandstone	sandstone
32G	521642	5398611	78	100	H2O at 25' and 90-95'	sandstone	sandstone
32H	520940	5399010	77	0	sand+ gravel	sand	sand
32H	520940	5399010	72	5	blue clay little sand (soft)	sand clay	silt-clay diamicton
32H	520940	5399010	55	22	sand + gravel little clay (brown)	sand	silt-clay diamicton
32H	520940	5399010	49	28	sand + gravel dry	sand	sand
32H	520940	5399010	32	45	sand + gravel little clay (brown)	sand	silt-clay diamicton
32H	520940	5399010	25	52	sand + gravel dry	sand	sand
32H	520940	5399010	3	74	sand + blue clay	sand w/clay	silt-clay diamicton
32H	520940	5399010	-3	80	sand + water	sand	sand
32H	520940	5399010	-11	88	sand + gravel + water	sand	sand
32H	520940	5399010	-32	109	sand + gravel + blue clay	sand w/clay	silt-clay diamicton
32L	521227	5399339	30	0	top soil	soil	silt-clay diamicton
32L	521390	5399232	27	3	brown clay and gravel	gravel clay	silt-clay diamicton
32L	521390	5399232	20	10	sandstone	sandstone	sandstone
32L	521390	5399232	-90	120		sandstone	sandstone
32M	520990	5398407	199	0	sand, gravel, boulders and little hardpan	sand	silt-clay diamicton
32M	520990	5398407	187	12	sand, gravel, boulders and blue clay	sand w/clay	silt-clay diamicton
32M	520990	5398407	171	28	sandstone (blue)	sandstone	sandstone
32M	520990	5398407	166	33	shale (blue) hard	shale	sandstone
32M	520990	5398407	154	45	sandstone (light brown)	sandstone	sandstone
32M	520990	5398407	129	70	some water approx 1 gpm	sandstone	sandstone
32M	520990	5398407	129	70	sandstone	sandstone	sandstone
32M	520990	5398407	77	122	sandstone (soft)	sandstone	sandstone
32M	520990	5398407	31	168	sandstone (hard)	sandstone	sandstone
32M	520990	5398407	31	168	more water approx 5 gpm	sandstone	sandstone
32M	520990	5398407	-21	220	lots of water	sandstone	sandstone
32M	520990	5398407	-28	227	bottom	sandstone	sandstone
32N	521125	5398232	259	0	overburden	soil	silt-clay diamicton
32N	521125	5398232	251	8	decomposed sandstone	sandstone	sandstone

32N	521125	5398232	242	17	moderately hard sandstone	sandstone	sandstone
32N	521125	5398232	186	73	fractured areas w/ much sand	sandstone	sandstone
32N	521125	5398232	159	100	highly fractured area	sandstone	sandstone
32N	521125	5398232	106	153	soft sandstone	sandstone	sandstone
32N	521125	5398232	-36	295		sandstone	sandstone
32P	520664	5397984	90	0	red clay	clay	silt-clay diamicton
32P	520664	5397984	83	7	grey clay	clay	silt-clay diamicton
32P	520664	5397984	73	17	fine sand & clay	sand w/clay	silt-clay diamicton
32P	520664	5397984	33	57	gravel trace water	gravel/sand	sand
32P	520664	5397984	32	58	clay & sand	sand clay	silt-clay diamicton
32P	520664	5397984	23	67	grey clay	clay	silt-clay diamicton
32P	520664	5397984	14	76	fine sand w/water	fine sand	sand
32P	520664	5397984	2	88	fine sand grey w/water	fine sand	sand
32P	520664	5397984	-2	91	coarse sand (heaves)	sand	sand
32P	520664	5397984	-4	93		sand	sand
32Q	520950	5398404	177	0	top soil & roots	soil	silt-clay diamicton
32Q	520950	5398404	175	2	hardpan, gravel & boulders	hardpan	silt-clay diamicton
32Q	520950	5398404	159	18	blue clay + gravel	gravel clay	silt-clay diamicton
32Q	520950	5398404	145	32	blue shale-soft	shale	sandstone
32Q	520950	5398404	133	44	sandstone grey	sandstone	sandstone
32Q	520950	5398404	126	51	water 2 gpm	sandstone	sandstone
32Q	520950	5398404	42	135	water 5 gpm	sandstone	sandstone
32Q	520950	5398404	-1	178	blue shale-soft	shale	sandstone
32Q	520950	5398404	-6	183	sandstone grey	sandstone	sandstone
32Q	520950	5398404	-18	195	caving sandstone water	sandstone	sandstone
32Q	520950	5398404	-21	198	sandstone	sandstone	sandstone
32Q	520950	5398404	-38	215	sandstone	sandstone	sandstone
32R	521023	5399091	68	0	farm soil	soil	silt-clay diamicton
32R	521023	5399091	65	3	clay & gravel	gravel clay	silt-clay diamicton
32R	521023	5399091	31	37	brown clay & gravel	gravel clay	silt-clay diamicton
32R	521023	5399091	8	60	80% clay w/gravel	gravel clay	silt-clay diamicton

32R	521023	5399091	-15	83	brown fine sand	fine sand	sand
32R	521023	5399091	-17	85	clay & gravel	gravel clay	silt-clay diamicton
32R	521023	5399091	-32	100	clay & fine sand	sand clay	silt-clay diamicton
32R	521023	5399091	-44	112	coarse gravel w/water	gravel/sand	sand
32R	521023	5399091	-48	116	moderate brown gravel	gravel/sand	sand
32R	521023	5399091	-58	126	grey clay & sand	sand clay	silt-clay diamicton
32R	521023	5399091	-62	130		sand clay	silt-clay diamicton
32S	521227	5399127	66	0	clay & gravel	gravel clay	silt-clay diamicton
32S	521227	5399127	63	3	sandstone	sandstone	sandstone
32S	521227	5399127	31	35	fractured sandstone w/water	sandstone	sandstone
32S	521227	5399127	30	36	moderately hard sandstone	sandstone	sandstone
32S	521227	5399127	-32	98	hard & soft sandstone	sandstone	sandstone
32S	521227	5399127	-74	140	(water in narrow bands b/t 80-140')	sandstone	sandstone
32T	520898	5398456	194	0	clay + sand	sand clay	silt-clay diamicton
32T	520898	5398456	190	4	clay	clay	silt-clay diamicton
32T	520898	5398456	133	61	soft sandstone	sandstone	sandstone
32T	520898	5398456	-24	218		sandstone	sandstone
32X	521502	5398691	211	0	farm soil	soil	silt-clay diamicton
32X	521502	5398691	208	3	hard dry clay	clay	silt-clay diamicton
32X	521502	5398691	200	11	soft sandstone	sandstone	sandstone
32X	521502	5398691	188	23	moderately hard sandstone	sandstone	sandstone
32X	521502	5398691	93	118		sandstone	sandstone
33A	522251	5398201	72	0	dirt	clay	silt-clay diamicton
33A	522251	5398201	50	22	rock	sandstone	sandstone
33A	522251	5398201	2	70	rock	sandstone	sandstone
33D	521797	5397923	207	0	top soil (description from old #2 well)	soil	silt-clay diamicton
33D	521797	5397923	204	3	gravel & clay	gravel clay	silt-clay diamicton
33D	521797	5397923	180	27	clay	clay	silt-clay diamicton
33D	521797	5397923	176	31	sandstone	sandstone	sandstone

33D	521797	5397923	126	81	clay & shale	shale	sandstone
33D	521797	5397923	117	90	sandstone (showing water)	sandstone	sandstone
33D	521797	5397923	110	97	sandstone	sandstone	sandstone
33D	521797	5397923	81	126	sandstone (inferrred from managers notes)	sandstone	sandstone
33F	522694	5397945	14	0	top soil	soil	sand
33F	522694	5397945	13	1	sand	sand	sand
33F	522694	5397945	0	14	sand, gravel & blue clay soft	sand w/clay	silt-clay diamicton
33F	522694	5397945	-49	63	sand fine with blue clay firm	sand w/clay	silt-clay diamicton
33F	522694	5397945	-72	86	sand fine with blue clay harder	sand w/clay	silt-clay diamicton
33F	522694	5397945	-89	103	sand fine with blue clay & thin muddy streaks	sand w/clay	silt-clay diamicton
33F	522694	5397945	-94	108	sand fine with some gravel gradually gets less gravel	fine sand	sand
33F	522694	5397945	-140	154	boulder (very hard)	clay	silt-clay diamicton
33F	522694	5397945	-181	195	very muddy sand & gravel & lots of blue clay & water	sand w/clay	sand
33F	522694	5397945	-195	209	sand gravel & blue clay	sand w/clay	silt-clay diamicton
33G	522573	5397847	28	0	top soil	soil	sand
33G	522573	5397847	27	1	sand & gravel	sand	sand
33G	522573	5397847	24	4	sand, gravel & hardpan	sand w/clay	silt-clay diamicton
33G	522573	5397847	13	15	sand, gravel & blue clay	sand w/clay	silt-clay diamicton
33G	522573	5397847	-16	44	sand, gravel, some clay, brown & some water	sand w/clay	sand
33G	522573	5397847	-22	50	sand, gravel & little blue clay soft	sand	silt-clay diamicton
33G	522573	5397847	-28	56	sand, gravel & little blue clay	sand	silt-clay diamicton
33G	522573	5397847	-44	72	sand fine with clay seams & water	sand w/clay	sand
33G	522573	5397847	-54	82		sand w/clay	sand
33J	522724	5397734	7	0	gravel	gravel/sand	sand
33J	522724	5397734	-14	21	grey clay	clay	silt-clay diamicton
33J	522724	5397734	-17	24	gravel silt	fine sand	silt-clay diamicton
33J	522724	5397734	-48	55	sand/gravel	sand	sand

33J	522724	5397734	-66	73	sand/gravel	sand	sand
33M	521850	5398065	232	0	clay & gravel	gravel clay	silt-clay diamicton
33M	521850	5398065	228	4	grey clay	clay	silt-clay diamicton
33M	521850	5398065	217	15	decomposed sandstone	sandstone	sandstone
33M	521850	5398065	214	18	soft sandstone	sandstone	sandstone
33M	521850	5398065	205	27	hard sandstone	sandstone	sandstone
33M	521850	5398065	187	45	fractured sandstone, sluffed badly	sandstone	sandstone
33M	521850	5398065	185	47	sandstone	sandstone	sandstone
33M	521850	5398065	56	176		sandstone	sandstone
33N	521813	5397780	240	0	top soil	gravel/sand	silt-clay diamicton
33N	521813	5397780	237	3	gravel cobbles clay band	gravel/sand	silt-clay diamicton
33N	521813	5397780	201	39	bedrock conglomerate	conglomerate	sandstone
33N	521813	5397780	186	54	sandstone	sandstone	sandstone
33N	521813	5397780	60	180	sandstone	sandstone	sandstone
33T	522620	5397959	12	0	gravel & clam shells	beach gravel	sand
33T	522620	5397959	10	2	clay & gravel	gravel clay	silt-clay diamicton
33T	522620	5397959	3	9	grey clay & rocks	clay	silt-clay diamicton
33T	522620	5397959	-26	38	very fine sand	fine sand	sand
33T	522620	5397959	-27	39	grey clay & rocks	clay	silt-clay diamicton
33T	522620	5397959	-43	55	fine sand	fine sand	sand
33T	522620	5397959	-49	61		fine sand	sand

Appendix D. Results of water chemistry analyses, north Lummi Island, Washington, fall 2002-spring 2003. (*) unable to take sample before storage tank

Fall 2002

well ID	aquifer	Cl⁻ (mg/L)	Na⁺ (mg/L)	Ca²⁺ (mg/L)	temperature (C⁰)	pH	specific conductance (mS)	TDS (mg/L)	salinity (g/L)	ORP mV	date (mmddyy/hhmm)
10C	Constitution	11	15	13	-	7.9	122	90	0.1	95	100802/1402
10E	Constitution	9	6	6	10.5	7.6	144	50	0.1	89	100802/1455
05G	dug well	14	13	9	13.8	7	185	80	0.1	55	092802/1526
33B	dug well	17	21	25	10.6	7.5	312	130	0.1	140	103102/1440
33X	dug well	15	13	7	10.1	-	192	-	0.1	-	092102/1548
04P	dug well	84	23	48	12.6	-	576	222	0.3	NA	092102/1622
09H	dug well	19	59	9	12.3	8.5	454	190	0.2	68	090102/1447
10D	dug well	16	13	8	12.7	6.8	212	80	0.1	168	100302/1335
10F	dug well	14	20	19	12.0	7	272	110	0.1	94	100802/1513
09C	Greenstone	38	17	56	9.4	7.7	578	220	0.3	81	110702/1652
10B	Greenstone	17	64	2	8.1	8.4	322	130	0.2	119	103102/1205
10G*	Greenstone	11	69	3	11.4	9	335	140	0.2	57	101302/1539
09S	Hilltop Deep	24	61	9	8.2	7.8	429	170	0.2	133	103102/1310
04A	Lane Spit	15	16	15	11.1	7.6	278	120	0.1	-66	090102/1751
33G*	Lane Spit	12	13	22	11.6	8.2	301	120	0.1	77	101302/1452
33T	Lane Spit	16	15	21	11.1	8.1	320	120	0.2	-117	101302/1346
33F	Lane Spit Deep	-	-	-	-	-	-	-	-	-	-
04G*	Legoe Bay	-	-	-	-	-	-	-	-	-	-
05J	Legoe Bay	20	32	13	10.1	9.2	300	120	0.1	100	101702/1617
05L*	Legoe Bay	26	40	21	12.2	8.2	384	160	0.2	105	101002/1211
05O	Legoe Bay	19	30	9	12.0	8.3	305	120	0.1	112	100102/1341
09K	Legoe Bay	17	25	25	12.5	8.1	358	140	0.2	130	100102/1739
09L	Legoe Bay	16	19	32	10.5	9	401	160	0.2	112	101702/1531
09M	Legoe Bay	13	19	25	12.5	8.3	382	150	0.2	49	090102/1401
09P	Legoe Bay	22	17	25	9.3	8.4	396	140	0.2	90	102402/1409
09R	Legoe Bay	23	57	9	9.5	7.2	442	180	0.2	-283	110702/1556
10V	Legoe Bay	24	21	40	14.1	7.9	563	210	0.3	136	091402/1737
10X	Legoe Bay	14	26	20	10.9	8.3	370	150	0.2	-90	100802/1520

well ID	aquifer	Cl⁻ (mg/L)	Na⁺ (mg/L)	Ca²⁺ (mg/L)	temperature (C⁰)	pH	specific conductance (mS)	TDS (mg/L)	salinity (g/L)	ORP mV	date (mmddyy/hhmm)
04C	Legoe Bay	21	19	26	12.1	7.5	378	140	0.2	131	091402/1845
09B	Legoe Bay	10	12	31	9.9	-	355	140	0.2	102	102402/1459
32H	Loganita	19	14	9	9.3	7.3	262	110	0.1	112	092202/1528
32R	Loganita	-	-	-	-	-	-	-	-	-	-
09G*	Nugent	194	85	52	10.3	8.2	979	370	0.5	95	102402/1258
09I	Nugent	21	21	39	10.3	9	509	200	0.2	85	101702/1422
09Q	Nugent	13	22	26	11.6	8	380	150	0.2	71	090102/1650
10M	Nugent	11	12	36	9.6	7.6	362	140	0.2	150	092302/1712
15A	Nugent	12	42	12	11.8	8	313	130	0.2	77	090202/1709
15D	Nugent	16	39	14	8.0	9.7	427	170	0.2	130	102402/1023
15K	Nugent	13	12	6	11.7	7.3	289	110	0.1	122	090102/1603
15P	Nugent	17	18	27	12.0	8	355	140	0.2	87	100302/1410
15S	Nugent	16	11	33	7.8	7.1	343	140	0.2	156	103102/1015
16K	Nugent	28	37	12	10.3	8.4	401	150	0.2	104	100302/1431
16V	Nugent	-	-	-	-	-	-	-	-	-	-
15O	Nugent	30	14	31	11.1	8.1	394	130	0.2	-47	091402/1802
04D	Sandstone	32	139	1	12.8	9.4	583	260	0.3	57	100102/1848
04E	Sandstone	24	69	35	11.8	7.7	550	210	0.3	-116	090102/1341
04F	Sandstone	-	-	-	-	-	-	-	-	-	-
04I	Sandstone	20	100	6	10.2	8.4	495	200	0.2	20	100802/1839
04J	Sandstone	45	157	1	9.7	9.8	701	280	0.3	64	102402/1155
04K	Sandstone	20	38	33	10.4	7.8	452	180	0.2	70	100802/1817
04M	Sandstone	19	81	17	10.1	7.9	493	200	0.2	-100	101002/1746
04N	Sandstone	112	72	49	11.0	7.5	746	250	0.4	30	092802/1351
04Q*	Sandstone	-	-	-	-	-	-	-	-	-	-
04R	Sandstone	18	67	10	10.8	8.2	486	190	0.2	72	092802/1241
04S	Sandstone	21	128	1	13.6	9	539	230	0.3	102	100102/1543
04T	Sandstone	21	29	39	10.5	7.9	463	180	0.2	42	101002/1709
04V	Sandstone	21	119	0	12.1	9.3	503	210	0.2	71	100802/1232
04W	Sandstone	15	53	42	8.6	-	548	200	0.3	-	092102/1902
04Z	Sandstone	17	36	38	13.3	7.5	438	170	0.2	123	090202/1807

well ID	aquifer	Cl⁻ (mg/L)	Na⁺ (mg/L)	Ca²⁺ (mg/L)	temperature (C⁰)	pH	specific conductance (mS)	TDS (mg/L)	salinity (g/L)	ORP mV	date (mmddyy/hhmm)
05B	Sandstone	22	76	14	10.4	8.4	301	170	0.2	88	100302/1749
05E	Sandstone	27	78	5	11.4	7.1	397	150	0.2	130	091402/1624
05P	Sandstone	35	51	17	14.3	7.6	415	160	0.2	108	100102/1605
05T*	Sandstone	13	75	22	10.5	-	499	200	0.2	116	102402/1603
05W*	Sandstone	-	-	-	-	-	-	-	-	-	-
05Z	Sandstone	17	55	9	12.5	8.7	316	130	0.2	73	100302/1605
08O	Sandstone	3231	1345	568	12.6	8.2	11000	>10,000	6.3	128	101702/1726
29C	Sandstone	87	200	54	11.4	7.6	1264	450	0.6	45	100302/1601
32A*	Sandstone	18	46	26	10.5	9	438	160	0.2	130	101702/1808
32K	Sandstone	128	151	38	9.8	9	1030	380	0.5	128	101702/1906
32L*	Sandstone	32	92	37	10.3	7.6	654	260	0.3	74	100802/1611
32M	Sandstone	18	16	50	9.9	8	420	160	0.2	135	100302/1232
32N	Sandstone	15	20	41	11.3	7.8	383	160	0.2	102	101002/1534
32Q	Sandstone	16	18	45	9.5	7.6	409	160	0.2	110	101002/1451
32S	Sandstone	20	67	23	9.3	8.1	476	180	0.2	85	110702/1725
32W	Sandstone	10	28	34	13.5	7.3	381	150	0.2	124	092802/1624
32X	Sandstone	15	37	30	12.6	7.6	400	160	0.2	120	100102/1230
33D	Sandstone	37	27	47	8.7	-	557	-	0.3	-	092102/1516
33M	Sandstone	36	52	68	9.2	-	753	270	0.4	-	092102/1441
32P	West Shore	23	21	17	10.0	7.3	320	120	0.2	126	101002/1257
04Y	Centerview	33	74	13	11.0	7.8	456	180	0.2	88	090202/1442

Spring 2003

well ID	aquifer	Cl⁻ (mg/L)	Na⁺ (mg/L)	Ca²⁺ (mg/L)	temperature (C⁰)	pH	specific conductance (mS)	TDS (mg/L)	salinity (g/L)	ORP mV	date (mmddyy/hhmm)
10C	Constitution	9	16	9	12	8.2	211	80	0.1	134	051303/1808
10E	Constitution	6	6	4	12	7.2	124	40	0.1	144	051303/1634
05G	dug well	-	-	-	-	-	-	-	-	-	-
33B	dug well	15	2	0	13	6.7	313	100	0.1	185	051303/1119
33X	dug well	-	-	-	-	-	-	-	-	-	-
04P	dug well	953	307	172	15	-	3145	1040	1.6	51	060903/1957
09H	dug well	18	59	6	11	8.3	471	170	0.2	127	052203/1639
10D	dug well	12	12	8	12	7.2	210	70	0.1	150	051303/1535

348

well ID	aquifer	Cl$^-$ (mg/L)	Na$^+$ (mg/L)	Ca^{2+} (mg/L)	temperature (C^0)	pH	specific conductance (mS)	TDS (mg/L)	salinity (g/L)	ORP mV	date (mmddyy/hhmm)
10F	dug well	18	24	29	11	7.4	432	170	0.2	131	051403/1455
09C	Greenstone	33	17	43	11	7.8	519	180	0.2	123	052203/1446
10B	Greenstone	11	69	0	12	8.9	310	100	0.1	96	052203/1552
10G*	Greenstone	-	-	-	15	8.5	335	120	0.2	102	051303/1707
09S	Hilltop Deep	22	65	5	12	-	-	130	0.2	88	061603/1557
04A	Lane Spit	14	20	8	11	7.9	293	120	0.1	-22	052203/1159
33G*	Lane Spit	9	14	10	16	-	301	100	0.1	105	060903/1555
33T	Lane Spit	13	16	14	12	-	321	100	0.2	-18	060903/1645
33F	Lane Spit Deep	13	13	9	12	-	308	90	0.1	-0.001	070603/1935
04G*	Legoe Bay	16	18	16	13	-	357	120	0.2	151	053003/1425
05J	Legoe Bay	21	31	8	12	-	305	90	0.1	74	062603/1603
05L*	Legoe Bay	21	38	16	12	8.4	386	120	0.2	81	060303/1717
05O	Legoe Bay	-	30	6	14	-	300	110	0.1	73	062603/1638
09K	Legoe Bay	15	20	17	13	8.3	372	130	0.2	72	060303/1739
09L	Legoe Bay	14	20	26	11	8	421	140	0.2	84	062603/1342
09M	Legoe Bay	14	20	23	12	8.2	400	140	0.2	105	052203/1357
09P	Legoe Bay	14	18	19	12	-	354	120	0.2	59	052903/1827
09R	Legoe Bay	20	55	6	13	-	442	150	0.2	-189	061103/1424
10V	Legoe Bay	23	21	29	13	8.2	601	220	0.3	124	052903/1408
10X	Legoe Bay	12	25	10	12	8.3	378	150	0.2	21	051403/1448
04C	Legoe Bay	19	21	17	11	-	379	120	0.2	137	053003/1350
09B	Legoe Bay	9	12	23	12	8.2	343	130	0.2	145	051303/1928
32H	Loganita	17	15	7	-	-	-	-	-	-	060103/1400
32R	Loganita	16	93	29	12	-	607	220	0.3	31	053003/1705
09G*	Nugent	95	77	41	12	-	908	280	0.5	21	052903/1446
09I	Nugent	20	21	32	9	7.6	536	180	0.3	34	060203/1259
09Q	Nugent	14	22	17	10	-	407	120	0.2	-11	052903/1514
10M	Nugent	12	12	30	10	8.1	350	150	0.2	156	051403/1145
15A	Nugent	13	41	8	14	8.1	320	130	0.2	107	051403/1556
15D	Nugent	16	39	8	12	-	384	110	0.2	65	052903/1705
15K	Nugent	13	12	3	11	7.7	284	120	-	163	051403/1232

349

well ID	aquifer	Cl⁻ (mg/L)	Na⁺ (mg/L)	Ca²⁺ (mg/L)	temperature (C⁰)	pH	specific conductance (mS)	TDS (mg/L)	salinity (g/L)	ORP mV	date (mmddyy/hhmm)
15P	Nugent	17	18	20	11	8.1	356	150	0.2	148	051403/1321
15S	Nugent	13	11	27	12	-	351	110	0.2	104	060903/1827
16K	Nugent	16	30	7	11	-	399	100	0.2	97	052903/1637
16V	Nugent	15	-	-	11	-	377	110	0.2	117	052903/1620
15O	Nugent	5	14	25	10	8.2	392	10	0.3	-48	060203/1422
04D	Sandstone	35	143	0	13	9.5	623	190	0.3	51	060303/1605
04E	Sandstone	21	48	28	10	7.5	565	180	0.3	-46	052803/1159
04F	Sandstone	58	201	4	11	-	977	290	0.5	-101	061903/1444
04I	Sandstone	16	104	3	10	8.2	528	170	0.3	47	052803/1607
04J	Sandstone	63	171	0	11	9.3	785	240	0.4	-9	060303/1452
04K	Sandstone	17	37	26	11	7.7	462	160	0.2	83	052803/1523
04M	Sandstone	19	84	15	10	7.7	536	180	0.3	-39	052803/1431
04N	Sandstone	129	76	45	12	-	838	250	0.4	2	052903/1742
04Q*	Sandstone	56	177	4	15	-	827	300	0.4	32	061903/1530
04R	Sandstone	19	68	7	12	8.2	484	150	0.2	92	051303/1313
04S	Sandstone	22	130	0	12	9.5	555	160	0.3	42	060303/1518
04T	Sandstone	13	30	36	10	7.7	496	160	0.2	10	052803/1630
04V	Sandstone	19	123	0	13	9.6	514	160	0.3	-103	060303/1622
04W	Sandstone	16	52	36	11	7.4	542	190	0.3	141	051303/1228
04Z	Sandstone	18	36	32	11	7.5	439	240	0.2	137	051303/1155
05B	Sandstone	21	70	12	10	7.8	424	140	0.2	147	060303/1321
05E	Sandstone	21	62	4	11	-	367	140	0.2	125	053003/1749
05P	Sandstone	36	NA	NA	19	-	442	160	0.2	92	070603/1739
05T*	Sandstone	12	NA	NA	11	7.5	545	190	0.3	151	060303/1224
05W*	Sandstone	17	125	0	13	9.1	529	200	0.3	99	052203/1715
05Z	Sandstone	19	58	7	12	8.7	337	100	0.2	49	60303/1350
08O*	Sandstone	3578	1288	>516	15	-	10650	>10,000	6.1	81	060903/1723
29C	Sandstone	65	148	39	12	7.7	1010	340	0.5	-25	060203/1553
32A*	Sandstone	15	47	22	10	8.1	398	150	0.2	147	052203/1835
32K	Sandstone	49	127	18	12	8.1	728	270	0.4		052203/1826
32L*	Sandstone	33	46	29	14	7.2	464	170	0.2	142	051303/1033

350

well ID	aquifer	Cl⁻ (mg/L)	Na⁺ (mg/L)	Ca²⁺ (mg/L)	temperature (C⁰)	pH	specific conductance (mS)	TDS (mg/L)	salinity (g/L)	ORP mV	date (mmddyy/hhmm)
32M	Sandstone	14	17	42	10	-	444	120	0.2	33	060903/1321
32N	Sandstone	12	20	31	10	-	402	120	0.2	-19	060903/1102
32Q	Sandstone	-	18	37	10	-	407	140	0.2	157	053003/1509
32S	Sandstone	18	49	21	11	-	408	-	0.2		051203/1414
32W	Sandstone	9	20	20	14	-	314	90	0.2	129	060903/1402
32X	Sandstone	66	39	22	12	-	404	110	0.2	104	060903/1451
33D	Sandstone	52	29	46	10	-	623	210	0.3	-20	061103/1512
33M	Sandstone	34	35	152	10	-	1212	400	0.6	-107	061103/1554
32P	West Shore	21	21	10	13	-	324	100	0.2	40	060903/1156
04Y	Centerview	37	77	8	13	8.1	458	150	0.2	107	051303/1428